2013

APPLICATION OF PYROLYSIS-GC/MS TO THE STUDY OF BIOMASS AND BIOMASS CONSTITUENTS

Anne E. Ware
University of Kentucky, aeha226@uky.edu

Recommended Citation

APPLICATION OF PYROLYSIS-GC/MS TO THE STUDY OF BIOMASS AND
BIOMASS CONSTITUENTS

DISSERTATION

A dissertation submitted in partial fulfillment of the
requirements for the degree of Doctor of Philosophy in the
College of Arts and Sciences
at the University of Kentucky

By
Anne Elizabeth Ware

Lexington, Kentucky

Co-Directors: Dr. Mark Crocker, Adjunct Associate Professor of Chemistry
and Dr. John Selegue, Professor of Chemistry

Lexington, Kentucky

2013

ABSTRACT OF DISSERTATION

APPLICATION OF PYROLYSIS-GC/MS TO THE STUDY OF

BIOMASS AND BIOMASS CONSTITUENTS

Fast pyrolysis, the rapid thermal decomposition of organic material in the absence of oxygen, is a process that can be used to convert biomass into liquid fuels and chemicals. When performed at the micro-scale, pyrolysis is useful for characterizing biomass structure, as well as determining the pyrolysis products that can be generated from specific biomass feedstocks. Indeed, microscale pyrolysis coupled with on-line analysis of the pyrolysis vapors by GC/MS, so-called pyrolysis-GC/MS (Py-GC/MS), is a technique that can be used to characterize the structure and composition of the various components of lignocellulosic and microalgal biomass based on their pyrolysate distributions. Pyrolysates produced also provide insight into the range of products that can be expected when biomass feedstocks are subjected to thermal decomposition processes.

This dissertation focuses on the Py-GC/MS analysis of lignocellulosic biomass such as sorghum and *Scenedesmus* sp. microalgae, in addition to high-lignin feedstocks such as walnut shells, coconut shells, olive pits and peach pits. The differences in the pyrolysate distributions among these biomass types are correlated with differences in the structure and composition of the biopolymers, mainly cellulose, hemicellulose and lignin, present in the biomass. Py-GC/MS analysis of lignin extracted from endocarp feedstocks is also emphasized. In addition to biomass and extracted lignin, sinapyl (S) and coniferyl (G) alcohol have been analyzed by Py-GC/MS in order to understand the relationship between the corresponding pyrolysates and sinapyl/coniferyl ratios of lignin present in lignocellulosic biomass.

KEYWORDS: Pyrolysis-GC/MS, lignin, biomass, endocarp, microalgae

APPLICATION OF PYROLYSIS-GC/MS TO THE STUDY OF
BIOMASSAND BIOMASS CONSTITUENTS

By

Anne Elizabeth Ware

Dr. Mark Crocker
Co-Director of Dissertation

Dr. John Selegue
Co-Director of Dissertation

Dr. Dong-Sheng Yang
Director of Graduate Studies

12/04/2013

TO MY FAMILY

ACKNOWLEDGEMENTS

Table of Contents

LIST OF TABLES

LIST OF FIGURES

Chapter 1. General Introduction

The long-term availability of fossil fuels and the environmental concerns associated with their use have provided an impetus for research directed towards the production of fuels and chemicals from biomass. Specific issues contributing to these concerns include increases in world population and energy consumption as well as the production of greenhouse gases and pollutants from the combustion of fossil fuels. According to the U.S. Census Bureau, the world population currently exceeds 7 billion and the U.S. Energy Information Administration (EIA) reported a total primary energy consumption worldwide of over 510 quadrillion Btu in 2010, showing an increase of over 100 quadrillion Btu since 2000.[1] Fuels are consumed for transportation, generation of electricity, heating, materials production and many other reasons. Fossil fuels, including petroleum, natural gas and coal, provide a large proportion of the energy supplied, particularly to industrialized nations. However, reliance on fossil-based resources is not restricted to energy production. The EIA reported that 191 million barrels of liquid petroleum gas and natural gas liquids were used as feedstock to produce plastic materials and resins in 2010 in the U.S. alone.[2] Utilization of alternative and renewable sources of energy and materials will be necessary to meet the high demands for the latter from an increasing population. It is also imperative that renewable sources of fuels and chemicals be utilized in order to alleviate the depletion of fossil fuel reserves and reduce our dependency on them as a source of both fuels and chemicals.

Renewable biomass and plant-derived materials can be used to produce energy in the form of heat and electricity and can also be used as feedstocks to produce chemicals and other materials. Because plants consume carbon dioxide during photosynthesis, plant-derived materials and biomass are considered to be carbon neutral with respect to combustion or utilization as an energy feedstock.[3,4] Lignocellulosic biomass, being composed primarily of lignin, cellulose and hemicellulose, includes trees, grasses and many other terrestrial plants. This type of biomass has been used for energy and heat production by combustion throughout the entirety of human history.[3] Non-lignocellulosic biomass, such as microalgae, are typically composed of lipids, proteins and carbohydrates. This type of biomass has been the subject of recent investigations regarding its utilization as a source of energy and chemicals.[5,6] The composition and structure of various types of biomass, and how these characteristics determine the products generated from thermal decomposition of the biomass, are discussed in the subsequent chapter.

While biomass can be used as fuel directly, it can also be converted to liquid fuels and chemicals by thermochemical processing. Converting biomass to liquid products is advantageous because the liquids have higher volumetric energy density and are more versatile, cheaper and easier to process, ship and distribute than the dried, ground biomass feedstock.[3,7,8] The liquid products may also be used directly as fuel in boilers and engines to generate electricity.[7-9] Many thermochemical methods used to convert biomass and its constituents into other products, particularly liquids, are being investigated and optimized. Potentially useful methods for converting biomass and its components into fuels and other materials include gasification, hydrothermal liquefaction, pyrolysis and catalytic upgrading.[10] The objectives of the research described in this dissertation focus on the pyrolysis of biomass. Pyrolysis processes can be used to convert biomass into a wide variety of useful chemicals and fuels. Fast pyrolysis processes, which are particularly suited to the production of liquids from biomass, are discussed in this chapter. The subsequent chapter focuses on the micro-scale pyrolysis of biomass coupled to GC/MS for analysis of the condensable vapors generated.

1.1 Fast Pyrolysis Processes Used to Convert Biomass into Other Products

Fast pyrolysis is the rapid thermal decomposition of an organic material in an oxygen-deficient atmosphere. Fast pyrolysis of biomass generates a solid, liquid and a "non-condensable" gas fraction. The gas fraction includes compounds such as carbon monoxide, carbon dioxide and methane and can account for approximately 10-25 wt% of products from biomass pyrolysis.[8] These gases can be used as fuel gases or recycled into pyrolysis reactors.[8] The solid fraction, known as "biochar," contains amorphous carbon (char) and nonvolatile compounds such as partially decomposed biopolymers, large polycyclic aromatic hydrocarbons (PAHs) and ash. Bio-char may also account for 10-25 wt% of converted biomass. Char from the solid fraction can be combusted for heat or energy production or used for soil amendment.[8,11] Mineral nutrients from the biomass can also be recovered from the biochar.[11,12] The liquid fraction, constituting up to approximately 70 wt% of pyrolysis products from biomass, is known as "bio-oil" or "pyrolysis oil" and it contains a diverse range of compounds that collectively have a heating value about half that of conventional fuel oil.[7,8] The liquid fraction may be used as a precursor for fuel or chemical production or it can be combusted for the production of energy in the form of electricity.[8,9] The types and distribution of the products generated from the pyrolysis of biomass are dependent on the feedstock and the operating parameters of the pyrolysis process.[8,13]

Many types of reactors and parameters can be employed to pyrolyze biomass at rapid rates and each technique is capable of producing different liquid components and yields.[8] Fast pyrolysis processes with high heating rates and vapor residence times of approximately 2 s are typically used in an effort to maximize the amount of liquid produced. In order to achieve high liquid yield, high temperatures and rapid heat transfer rates must be combined with short vapor residence and cooling times.[8,13]

Fast pyrolysis reactor configurations include fluidized bed, entrained flow, ablative and vacuum systems, as well as many other approaches.[8,13] Fluidized bed reactors are a well-understood technology and are simple to construct and operate.[7] These reactor configurations utilize dried, small particle-sized (< 3 mm) biomass feedstocks and sometimes a fluid medium such as sand that allow for efficient heat transfer. Biomass is fed into the reactor where it is heated (temperatures typically range from 400 ⁰C to 600 ⁰C) and fluidizing gas (typically N_2) is used to carry products through the reactor. Condensation units can be used to condense aerosols into liquids, filters (typically cyclones) are used to collect bio-char, and gaseous products can be collected and/or recycled back to the reactor. Fluidized bed and other pyrolysis reactors vary in size and operational principles and careful design of hydrodynamics is important in order to produce a consistent and optimal range of products.[7,8] Waste heat from the surplus gas in most reactors can be used to dry feedstocks and burning of char products can produce some of the energy required to heat the reactor. Hence, careful design and operation of pyrolysis systems can provide energy efficient processes that yield potentially useful products from biomass. Figure 1.1 shows a simplified schematic of a fluidized bed pyrolysis unit.
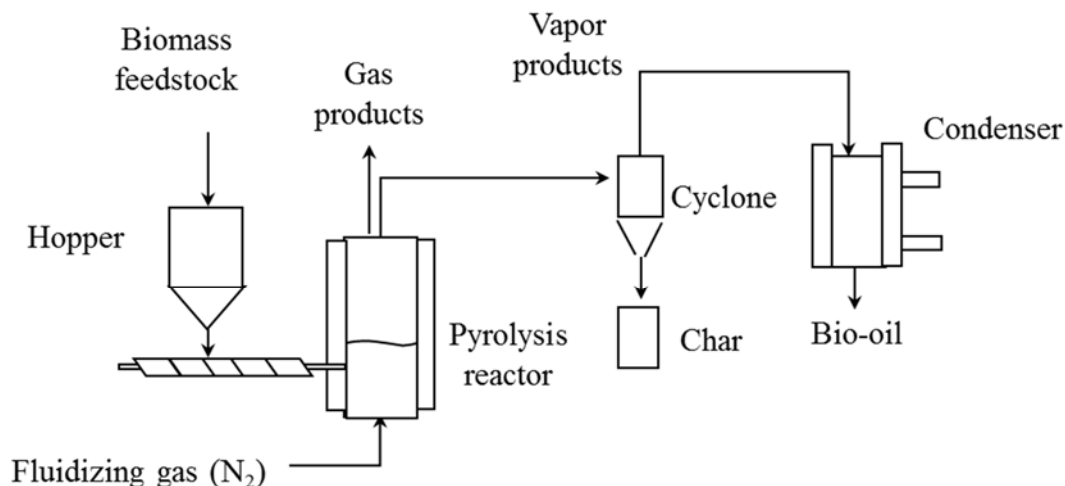
Figure 1.1 Schematic of a fluidized bed fast pyrolysis unit. Biomass enters the heated reactor with the aid of a hopper where it contacts heated fluid media (e.g., sand) that is fluidized using an inert gas, which is often heated. Gas products leave the reactor and can be returned to the reactor or combusted as fuel to supply heat energy for the pyrolysis process. Char and ash can be separated using a cyclone filter and vapors are condensed in a condenser. Condensed vapors (bio-oil) can then be combusted to supply energy to drive the pyrolysis process, shipped and/or or upgraded to generate other products.

Fast pyrolysis systems vary in size ranging from Dynamotive's 200 ton/day plant[7,8,14] to microscale Pyrolysis-Gas Chromatography/Mass Spectrometry (Py-GC/MS) pyroprobes, discussed in Section 1.4, that use sample sizes of less than 1 mg. The size and operation parameters are chosen depending on the types of products desired and their intended uses. Large scale pyrolysis reactors are used to produce bio-oil, food flavorings, charcoal and producer gases and smaller units are used for research purposes and for characterizing biomass and polymers.[8,9]

1.2 Properties of Pyrolysis Oil and Dependence on Feedstock

The liquid produced from the fast pyrolysis of biomass has been characterized by a vast amount of research that has been reviewed by Bridgwater and Mohan; the following provides a summary of their reviews.[7-9,13] Bio-oil is typically brown, has a smoky odor and contains hundreds of compounds ranging in size and abundance that result from decomposition of the biopolymers present in biomass.[8,13] Table 1.1 summarizes some of the properties of bio-oil obtained from typical lignocellulosic feedstocks.[8] Bio-oil typically has a water content of approximately 20

wt%, a pH of approximately 3, a higher heating value (HHV) of around 18 MJ/kg and it is miscible with methanol and acetone but it is not miscible with hydrocarbon fuels.[8,13] Bio-oil is chemically unstable because it contains a diverse range of compounds that can react together to produce water, tars and other organic compounds over a wide range of temperatures and conditions. Hence, distillation is not practiced and storage and transportation of bio-oil must be carefully controlled.[8] Despite these characteristics, bio-oil shows potential for use as a fuel[9] or as a feedstock for the production of fuel by means of catalytic upgrading processes, as reviewed by Huber et al.[15] It may also be used in catalytic processes to produce other valuable compounds. Because bio-oil is a liquid with a volumetric energy density greater than the dried biomass feedstock from which it came, costs and complications associated with transportation and processing (such as stirring and pumping) are minimized in comparison to ground biomass feedstocks.[3,7]

Table 1.1 Typical properties of lignocellulosic-derived bio-oil. Values reported are obtained from reviews by Bridgwater, Mohan and Huber.[3,8,13,15]

Property	Value
Elemental Analysis	
C	56 wt%
H	6 wt%
O	38 wt%
N	<0.1 wt%
Higher heating value (HHV)	16-20 MJ/kg
pH	2-3
Moisture content	20 wt%
Density	1.1 g/cm^3

Compounds produced from pyrolysis, particularly those present in bio-oil, are commonly referred to as "pyrolysates." The types and the relative abundance of these compounds influence the properties of pyrolysis oil and they vary depending on the reactor type, the pyrolysis conditions used and the biomass feedstock. The pyrolysates originate from decomposition of compounds present in biomass. Lignocellulosic biomass, such as wood and grasses, is primarily composed of hemicellulose, cellulose and lignin. Hemicellulose is an amorphous polysaccharide composed of various sugar units and cellulose is a polysaccharide of β(1→4) linked D-glucose units. Lignin is

an amorphous polymer composed of phenylpropanoid monomers, monolignols, derived from coniferyl, sinapyl and coumaryl alcohol. The structure and composition of lignin is discussed in the subsequent chapter. Upon pyrolysis, hemicellulose and cellulose generate anhydrosugars, furans, and small oxygenated compounds such as hydroxypropanone and acetic acid that are present in bio-oil.[16,17] The lignin fraction of biomass produces phenols and other aromatic compounds during pyrolysis.[18,19] Common compounds generated from pyrolysis of lignocellulosic biomass and their sources and potential applications are shown in Table 1.2. Potential applications include flavors or reagents that can be used for a wide variety of applications, including production of polymers, resins and other synthetic materials. However, few commercial processes exist for the development of materials from bio-oil components outside of the flavor industry. The relative abundance of the pyrolysates present in bio-oil depends on the relative abundance and structures of the biopolymers present in biomass as well as the pyrolysis conditions. For example, biomass that contains more lignin may produce more lignin-based pyrolysates. The structure and abundance of the biopolymers present in biomass varies according to species, age, growing conditions, the part of the plant, nutrient supplies and other factors.[20,21] Obviously, fractionation of biomass and subsequent pyrolysis of the constituents will yield compounds associated with the fraction pyrolyzed.[19] Hence, fractionation of biomass can be used to produce certain compounds from pyrolysis of its separate components.

Table 1.2. Common compounds present in lignocellulosic-derived bio-oil. Potential applications have been reviewed by Czernik and others.[8,9]

Compound	Source	Potential Application
hydroxyacetaldehyde	Holocellulose	Flavor industry
acetic acid	Holocellulose	Reagent
furfural	Holocellulose	Reagent
levoglucosan	Holocellulose	Reagent
1,4:3,6-dianhydro-α/β-d-glucopyranose	Holocellulose	
eugenol	Lignin	Flavors/Fragrances
syringol	Lignin	
vanillin	Lignin	Flavors/Fragrances
syringaldehyde	Lignin	
phenol	Lignin	Reagent, plastics
2-methoxy-4-methylphenol	Lignin	Flavors
2,6-dimethoxy-4-methylphenol	Lignin	

Non-lignocellulosic biomass, such as microalgae, can also be used as a pyrolysis feedstock.[22-26] Microalgae are primarily composed of lipids, proteins and some carbohydrates.[27] Lipids present in microalgae can constitute up to 50 wt% (dry) of the biomass with the remainder being carbohydrates, proteins and ash.[6] Free fatty acids, triglycerides, phospholipids, steroids and other terpene-derived compounds (such as phytol in chlorophyll) are the main types of lipids found in many microalgal species, as well as lignocellulosic biomass. Carbohydrates, including glucose, mannose and other sugars, are present in the form of oligomers, polymers and monosaccharides in microalgae.[27-29] Like lignocellulosic biomass, pyrolysis of microalgae produces compounds associated with the various components present in the biomass. The relative abundance of each of the components depends on the species of microalgae as well as growing conditions and nutrient supplies.[23,27]

Pyrolysis of the lipids produces long-chain (fatty) acids, aldehydes and alcohols as well as saturated and unsaturated linear hydrocarbons.[30-32] Aromatic compounds can also be produced from Diels-Alder cyclization of unsaturated lipids.[31] Lipids present in microalgae and their resulting pyrolysates have higher heating values[23] and these compounds are more amenable to the

production of fuel and fuel-like precursors by upgrading processes than lignocellulosic components and their pyrolysates. Pyrolysis of the proteins present in microalgae generates a wide variety of nitrogenous species such as indoles, pyrrolidones, amines and amides that result from cracking and cyclization mechanisms that occur during pyrolysis.[33-36] Like lignocellulosic biomass, algae can also be fractionated in order to obtain separate extracts, such as lipids, which can be further processed for production of specific chemicals.[5]

Overall, pyrolysis of biomass generates products characteristic of the starting feedstocks. This is not only important to consider when selecting a feedstock for the production of pyrolysis oil or gases with certain properties or chemical components, but can also be useful for characterizing biomass constituents.[18,32] The relative abundance of lignin in lignocellulosic biomass and its individual monomer types can be reflected in the composition and distribution of pyrolysates present in bio-oil.[37,38] Microalgae feedstocks of varying lipid and protein composition can be screened for high heating value potential according to the pyrolysates generated.[32] Moreover, mutations resulting in lignification or other biopolymer alterations may also be reflected in products obtained from biomass pyrolysis. Hence, the simultaneous characterization of biomass structure and determination of its potential for conversion into other products makes pyrolysis a valuable analytical tool.

1.3 Chemical and Physical Mechanisms Leading to Pyrolysis Products

Pyrolysis of biomass is an endothermic process that involves physical and chemical transformations. The physical transformations have been described in reviews by Mohan[13] and Sinha using simple heat transfer explanations.[39] Haas et al. have used microscopy techniques to analyze the physical changes in biomass that occur during pyrolysis.[40] Figure 1.2 shows a schematic of the physical processes that occur during pyrolysis of a single particle. The process begins with the transfer of heat from a source to the outside of the biomass particle causing the temperature of the particle to increase. Next, primary pyrolysis reactions such as dehydration and thermolysis (homolytic cleavage) occur, producing gases, liquids, volatiles and char. Heat is transferred from the outside of the particle to the inside of the particle through the hot liquids, volatile compounds and gases. Simultaneously, the cooler portions of the biomass may cool some volatiles, causing them to condense back into liquids. The condensed compounds may then undergo secondary pyrolysis reactions. The heating of the inside of the biomass particle is followed by primary pyrolysis reactions that produce more gases, volatiles and char. Again, secondary reactions and condensation can occur and may be controlled by heat transfer within the

particle, the residence time of the volatiles and the ability of the particle to expand as gases and volatiles are released.

1.) < 200 °C   2.) 200 °C – 300 °C   3.) 300 °C – 500 °C   4.) 500 °C

H_2O

CO, CO_2, CH_4, condensable vapors

Condensable vapors

Chars and liquids remaining, gases are still produced at high temperatures
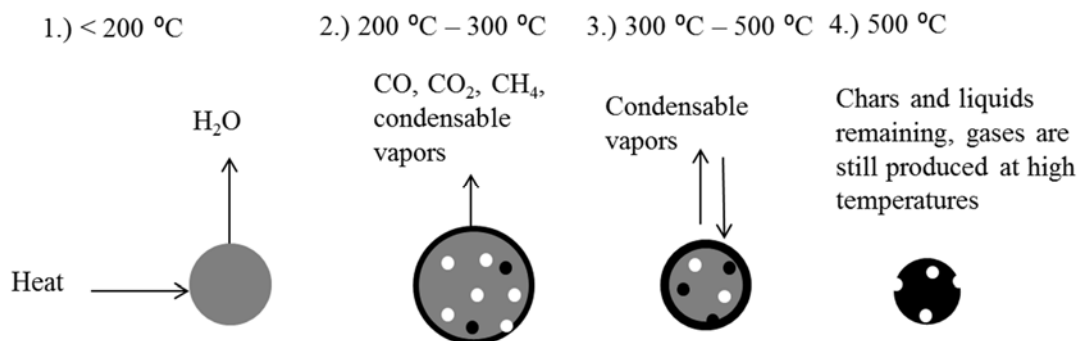
Heat

Figure 1.2. Schematic of physical processes of pyrolysis.[13,39] **Biomass is grey, gases/voids are white, chars and liquids are black. 1. The particle is heated and moisture is removed. 2. As the temperature of the particle increases, the particle expands, releasing gases and condensable vapors, and begins forming char. 3. The temperature increases and some vapors condense on the particle as the size of the particle decreases; more vapors, gases and chars are generated. 4. Solids and liquid products of thermally decomposed biomass remain at the final temperature. Gases will continue to be produced and liquids will react further if the particle maintains the higher temperature or if the temperature increases.**

Specific reactions associated with pyrolysis processes include homolytic cleavage (homolysis or thermolysis), dehydration and rearrangement mechanisms that result in depolymerization, cracking, repolymerization and general decomposition of biopolymers in biomass.[16,17,41-43] Collectively, these reactions are commonly referred to as "thermochemical processes" and many can occur simultaneously over a period of less than 2 s in fast pyrolysis systems. Condensed bio-oil may also undergo additional reactions over extended periods of time leading to increases in viscosity and average molecular weight.[8,44] Many reactions have been used to explain the changes that occur in bio-oil during aging processes and are reviewed by Diebold.[44] For example, alcohols may react with organic acids during aging to form esters and water. Aldehydes may also react together to produce polyacetals. However, the formation of many compounds is still not understood given the complexity of bio-oil and the many possible mechanisms that can produce various compounds. Many factors, such as inorganic and char content and storage temperature

and container materials may also play roles in the kinds and amounts of compounds generated during bio-oil aging.[45]

Mechanisms and kinetics associated with pyrolysis of the carbohydrate or saccharide fractions in biomass have been investigated by Patwardhan et al.[16,43] and others[17,46] in order to elucidate the origin and formation of carbohydrate-based pyrolysates. Pyrolysis of carbohydrates involves the depolymerization of polysaccharides by cleavage of the glycosidic bonds and these processes are accompanied by dehydrations, ring opening mechanisms and cracking reactions. Figure 1.3 shows the formation of several pyrolysates that originate from the carbohydrate, particularly cellulose, fraction in biomass.
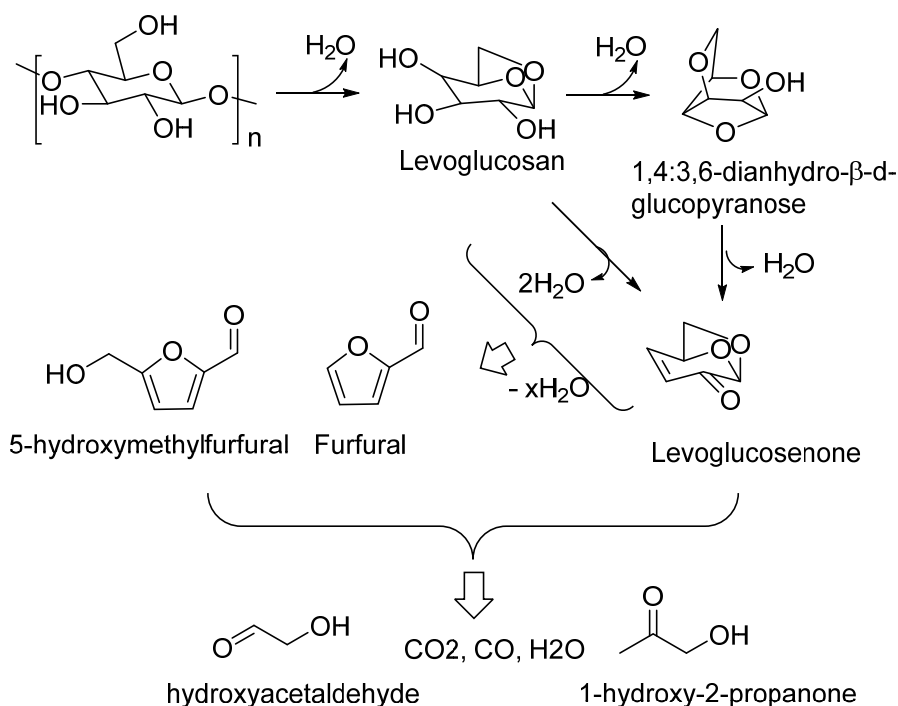
Figure 1.3. Formation of certain pyrolysates from cellulose and carbohydrates.

Pyrolysis of the lignin fraction in lignocellulosic biomass has been researched as a means of converting lignin into useful products and as a way to characterize the structure and composition of the lignin being investigated. Lignin, being an amorphous, irregular polymer made from three types of monomers, has many types of bonds capable of undergoing homolytic cleavage, dehydrations and isomerizations during pyrolysis.[41,42,47-50] The bonds connecting the aromatic monomers have lower bond dissociation energies than the bonds present in the aromatic framework.[51] Hence, homolytic cleavage and other reactions involving the bonds connecting the

monomers are the dominant reactions driving the decomposition of lignin during pyrolysis. Therefore, pyrolysates in the liquid fraction usually contain some distribution of aromatic compounds with identities reflecting the distribution of monomers and the types of bonds linking them. The monomers, coumaryl, coniferyl and sinapyl alcohol, have zero, one, and two methoxy substitutions, respectively. Depending on the pyrolysis conditions, the methoxy groups may be largely unaffected and the distribution of pyrolysates from each of the monomers in the liquid fraction may reflect the relative abundance of the monomers in the starting feedstock.[52] Therefore, it is possible to measure the sinapyl/coniferyl (S/G or S:G) ratio in lignin polymers based on pyrolysate distributions.[38,52] However, demethoxylation processes can occur and different monomers may be more or less likely to form char or nonvolatile products associated with the solid fraction of the pyrolysis products.[53-55] Additionally, the presence of inorganic components in biomass may influence pyrolysate distributions.[56] The coexistence of the various polymers within biomass may also influence pyrolysis mechanisms and product distributions relative to those obtained from separated components.[57,58] Therefore, structural characterization of lignin based on pyrolysate distribution in the condensable vapor fraction should be undertaken with caution or supplemented with other analyses such as NMR spectroscopy or oxidative techniques. Figure 1.4 shows the formation of representative pyrolysates from the lignin fraction of biomass.[41,50] Further discussion on the formation and types of pyrolysates generated from lignocellulosic biomass in relation to its structure and composition is provided in Chapter 2.
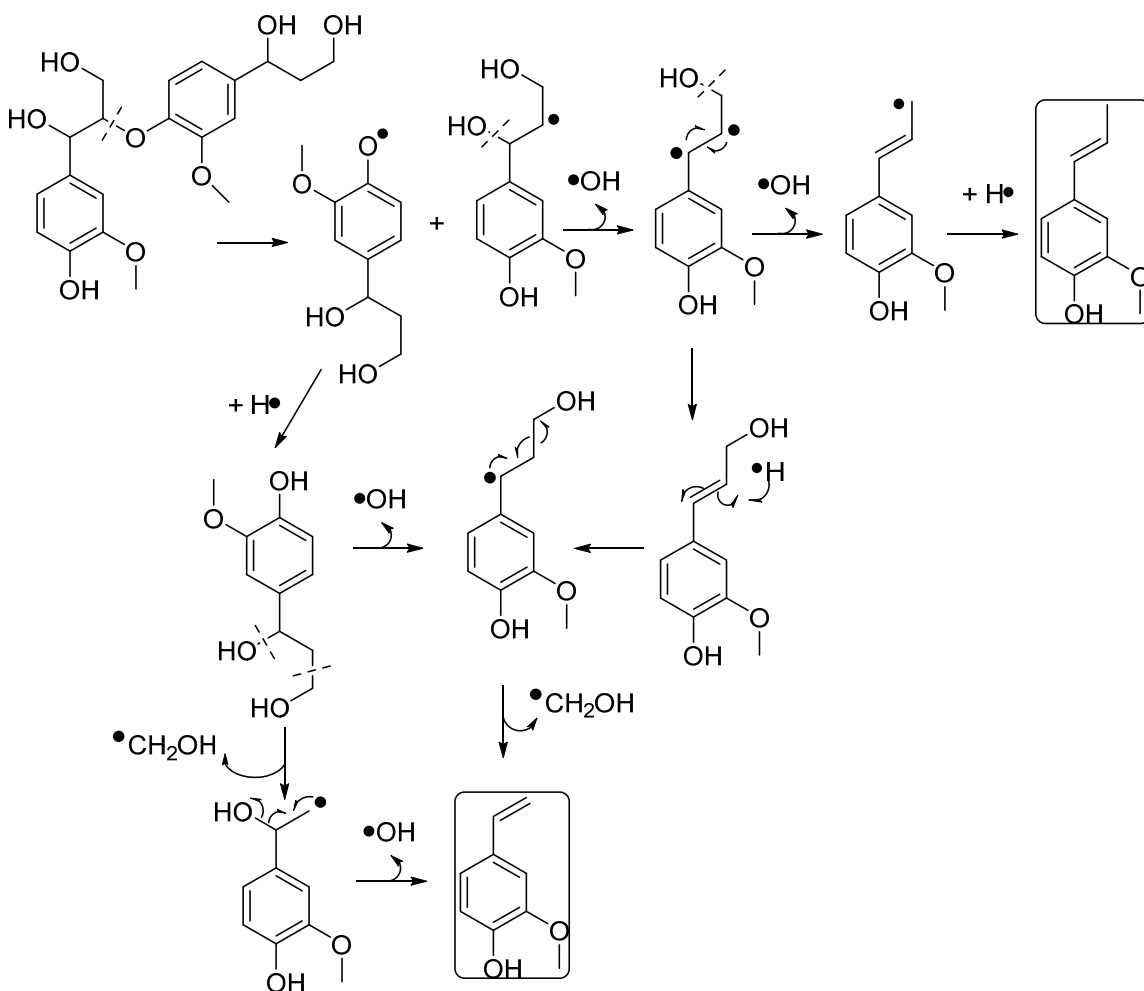
**Figure 1.4. Several radical mechanisms that can occur to form lignin-based pyrolysates.
When a lignin dimer of coniferyl monomers linked by a β-O-4 bond undergoes pyrolysis the
bonds with the lowest bond dissociation energies undergo homolysis to produce free
radicals. The mechanisms shown have been hypothesized to generate the products indicated
but many other reactions may occur to produce the same products. During pyrolysis, many
other reactions also occur simultaneously to produce a diverse range of aromatic
compounds from the lignin polymer.**

Like other organic feedstocks, the pyrolysis of lipids present in high lipid feedstocks such as
microalgae involves the homolytic cleavage of bonds as well as dehydrations, isomerizations and
many other reactions.[30,31] Generally speaking, lipid pyrolysis is straightforward because of the
linear structure of many of the lipids and has been thoroughly investigated. Figure 1.5 shows the
identities and formation of many types of pyrolysates obtained from pyrolysis of lipids such as

fatty acids and triglycerides. The formation of these products has been reviewed by Maher et al.[31] These products are important because they are similar in composition to hydrocarbon fuels and/or consist of high heating value products that can be used as or converted into fuels. If the lipids have not been fractionated from the whole biomass then they may also react with proteins to form fatty amides and other compounds.

Protein pyrolysis also involves homolytic cleavage of bonds, dehydrations and isomerizations as well as inter and intra-molecular cyclization reactions of the amino acids.[33-35] The types of pyrolysates formed depend on the amino acids present in the proteins and the pyrolysis conditions. Particular amino acid residues have not been reported in algal bio-oil, but the occurrence of certain pyrolysates indicates the presence of certain residues, e.g. imidazole, in bio-oil may have originated from histidine. Proteins also react with sugars through a complex set of Maillard reactions that can also occur during thermal processes.[59] These reactions are also known as "non-enzymatic browning reactions" and are responsible for many compounds that lead to the brown color and the smells associated with pyrolysis oil. Pyrazines, for example, are believed to originate from Maillard reactions that occur during pyrolysis.
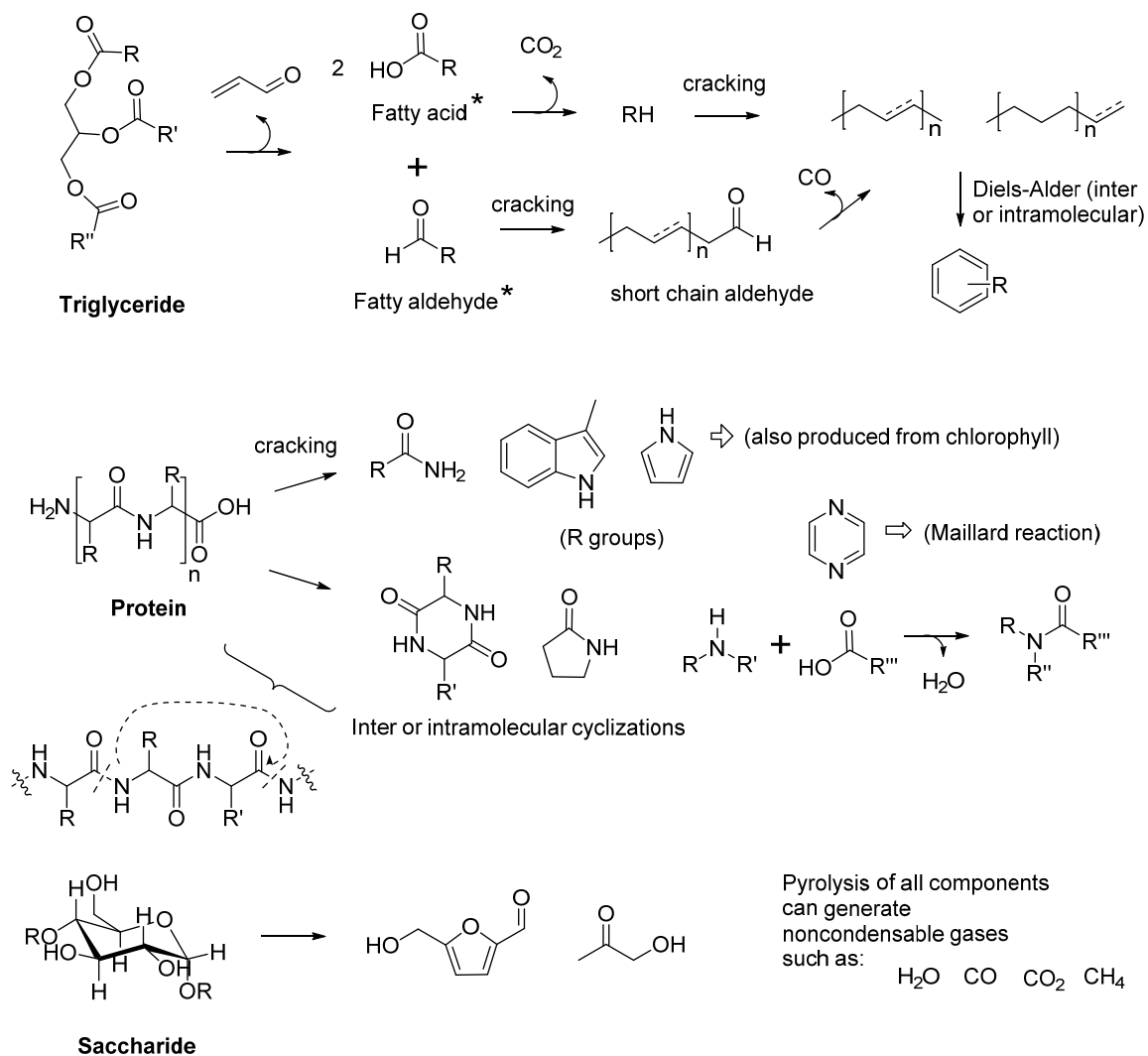
Figure 1.5 Example pyrolysates formed from triglycerides, proteins, saccharides and fatty acids. Cracking reactions involve homolysis of bonds and may include rearrangements such as hydride shifts. *Fatty acids and aldehydes formed from triglyceride decomposition shown may be radicals. Dotted double bonds indicate the possible presence of olefins.

Other compounds in biomass, particularly in microalgae, such as chlorophylls, carotenes and steroids, produce characteristic compounds upon pyrolysis.[32,60] Chlorophyll (a, b and d) produces phytol and terpenoid compounds and each type of chlorophyll can produce pyrroles.[61] Vitamin E and carotenes may be present in biomass and can also produce terpenes and phytol-related compounds upon pyrolysis. Sterols have also been detected in pyrolysates from microalgae.[32] Depending on the plant, its age and environment, other compounds may be present that may appear in pyrolysis products. These compounds may include alkaloids and anthocyanins, many of which can be removed by pretreatment processes.

14

Many other factors play roles in the distribution of pyrolysates and products from biomass pyrolysis. Pyrolysis of whole biomass and separate fractions may yield differences in pyrolysate distributions due to changes induced in the biopolymers during extraction processes.[19,55,62,63] As discussed with microalgae pyrolysis, separate biomass components may react together to produce compounds that may not be produced during pyrolysis of separated fractions. In addition, the presence of metals such as potassium and sodium may influence the occurrence of certain reactions leading to differences in product distributions.[64,65] The particle size and the moisture content of the biomass will also influence the type and amount of pyrolysates generated.[66] However, if particle size, moisture content, heating rates and other operating and pretreatment parameters are consistent, pyrolysis can be used as a tool for comparing biomass structure, composition and potential for producing certain chemicals.

1.4 Pyrolysis-Gas Chromatography/Mass Spectrometry (Py-GC/MS)

Pyrolysis-Gas Chromatography/Mass Spectrometry (Py-GC/MS) is a technique that uses a microscale pyrolysis unit to pyrolyze organic material on a micro- to milligram scale. Various forms of Py-GC/MS exist and the reactor configurations and parameters for analysis can be optimized for the types of samples and the information sought. While reactors are sometimes constructed by researchers, commercial models are available from companies such as CDS Analytical and Frontier Laboratories. Biomass is typically analyzed by Py-GC/MS by subjecting it to pyrolysis in a quartz tube or boat cell inside a heated chamber or a metal coil (such as platinum), the latter offering maximum heating rates and heat transfer to the biomass particles. The product vapors then pass through heated filters or sorbent media or go directly to the GC through a heated transfer line to prevent condensation of vapors. The pyrolysis units are purged with an inert gas, He, which is also the carrier gas for the GC/MS. Carrier gas flow rates are typically on the order of 50 mL/min, allowing for rapid transfer of pyrolysates from source to GC. Combined with the use of sorbent media or short transfer lines, Py-GC/MS in the presence of GC carrier gas can allow for analysis of the primary pyrolysates formed. However, some condensation and secondary reactions are difficult to avoid, although good reproducibility is usually achievable providing there are no cold spots or leaks within the unit.

Figure 1.6 shows CDS Analytical's 5200 Pyrolysis-GC/MS Pyroprobe that utilizes a Pt coil to heat samples at rates of up to 1000 °C/s. Samples (less than 1 mg) are placed in a quartz cell packed with quartz wool and inserted into the Pt coil probe. The probe is then inserted into a

chamber that is purged with He and heated during pyrolysis to prevent condensation. During pyrolysis, the Pt coil heats the sample to the desired temperature and carrier gas transports the vapors to the GC inlet. GC column selection is based on the type of analytes expected from a given source. DB-5 columns are useful for most applications and more polar DB1701 columns can be particularly useful for biomass pyrolysis.[8] The mass spectrometer typically uses an electron impact (EI-MS) source and is equipped with a quadrupole that is capable of performing selective ion monitoring.

Figure 1.6 CDS Analytical 5200 Pyroprobe unit and Pt coil.

Py-GC/MS has been used to analyze the composition and structure of biomass and its separated constituents.[19,38,52,67] The distribution of pyrolysates generated reflects the relative amount of the constituents from which they originate in the starting feedstock. For example, lignocellulosic biomass that contains more sinapyl monomers than coniferyl monomers in the lignin may produce more sinapyl-based pyrolysates than coniferyl-based pyrolysates. Extracted lignin can be analyzed by Py-GC/MS to determine the presence of carbohydrates remaining in the lignin. Py-GC/MS can also be used to evaluate differences in structure and composition between lignin in biomass and extracted lignin.[18,19] Lignin model compounds have been analyzed in order to understand the origin of certain pyrolysates and mechanisms associated with their formation.[68] The pyrolysates produced also provide information about the types of compounds that would appear in bio-oil from a given feedstock. Since Py-GC/MS uses small sample sizes, requires

minimal sample preparation and provides rapid analysis of a feedstock, it is a useful technique for screening biomass intended for use as a pyrolysis feedstock on larger scales.

In summary, Py-GC/MS is capable of rapidly analyzing biomass and its constituents in order to understand their structure, composition and resulting pyrolysates. It is useful for understanding starting materials and the fundamental thermochemical conversion processes associated with transforming renewable feedstocks into other chemicals. Further discussion of Py-GC/MS analysis of biomass and its constituents is provided in Chapter 2.

1.5 Scope of Dissertation

The main objective of the research described in this dissertation is to gain an understanding of the structure and composition of biomass from different sources using pyrolysis-GC/MS. Biomass constituents, such as extracted lignin, as well as lignin monomers were studied using pyrolysis techniques in order to understand the origin of various pyrolysates and obtain quantitative information from Py-GC/MS analysis of biomass and its components. Other techniques, such as thermogravimetric analysis and FTIR were also used to understand biomass composition and to provide a fuller understanding of the Py-GC/MS data.

The second chapter of this dissertation describes the general structure and composition of lignocellulosic and microalgal biomass. The relationship between the composition of biomass and its resulting pyrolysates as analyzed by Py-GC/MS is discussed.

The pyrolysis of coniferyl alcohol and sinapyl alcohol as well as mixtures of the two compounds is discussed in the third chapter. The Py-GC/MS analysis of these two lignin monomers provided a means to calibrate the instrument to measure sinapyl/coniferyl ratios in lignin as well as provide an understanding of the types of pyrolysates expected from lignin and lignocellulosic biomass.

In the fourth chapter, characterization of high-lignin feedstocks (i.e., walnut shells and coconut shells) and lignin extracts using Py-GC/MS and other techniques is discussed. Emphasis is placed on the differences in pyrolysate distributions seen between different endocarp species and the lignins extracted using different extraction procedures.

The fifth chapter describes the use of Py-GC/MS to analyze the differences in pyrolysate distributions seen between wild type and mutated sorghum plants. The differences in pyrolysate distributions from different parts of sorghum plants are also discussed.

The sixth chapter focuses on the pyrolysis of *Scenedesmus* sp. microalgae. Py-GC/MS analysis of the microalgae is discussed as well as the characterization of products obtained from pyrolysis in a larger-scale, fluidized bed reactor.

Concluding remarks are included in the seventh chapter.

The most common abbreviations used throughout this dissertation can be found in Appendix 1. Supplementary tables can be found in Appendix 2 and Appendix 3 contains supplementary figures.

Chapter 2. Biomass Structure and Composition

Biomass is organic material of recent biological origin. In this context, biomass refers to plants and microalgae as well as materials derived from these feedstocks. Both plants and microalgae consume water and CO_2 in the presence of light to produce O_2 and chemical energy in the form of carbohydrates through the process of photosynthesis. A wide variety of other compounds, such as lipids, lignin and proteins are also synthesized by plants to serve various purposes. Lignocellulosic biomass such as trees and herbaceous plants consist of mostly cellulose and lignin whereas biomass such as microalgae are composed primarily of lipids, sugars and proteins. Biomass and its constituents are a renewable source of carbon and can be used directly as fuel or processed to generate other fuels and chemicals. Utilization of biomass and its components as fuel is considered to be carbon neutral because biomass fixes atmospheric CO_2 in the form of sugars as it grows.[1,2] Hence, there is no net production of CO_2 when biomass is combusted as a fuel.

The types of fuels and chemicals that can be generated and the necessary processing associated with a given biomass source are dependent on the type of biomass. The structure and composition of biomass varies according to species, genetic traits, age, environmental conditions and the part of the plant. Fractionation processes, such as pulping of lignocellulosic biomass, may also have an effect on the structure and composition, and hence application, of the processed biomass components.[3] These factors influence the potential of a given biomass source to generate particular materials and fuels as well as the economics associated with cultivation and processing.[1,4,5] For example, certain types of lignocellulosic biomass, discussed below and in Chapter 1, can be used as a source of cellulose for paper, as a source of sugars for the production of ethanol and butanol[6] and for many other chemicals and materials. High-lipid biomass feedstocks, such as microalgae, can be used to generate biofuels from lipid components present in the biomass.[7,8] All forms of biomass can also be gasified, pyrolyzed and combusted to create other useful chemicals and to produce energy.

The purpose of this chapter is to provide fundamental information regarding the structure and composition of several types of biomass. It is important to properly characterize the structure and composition of biomass in order to understand how they relate to the conversion of biomass to particular materials and to ensure efficient utilization of biomass for specific applications. Emphasis is placed on lignin, its structural changes induced by extraction processes and lignin-

based pyrolysates. Techniques used to analyze lignocellulosic biomass and lignin structure are discussed with emphasis on Pyrolysis-GC/MS.

2.1 Lignocellulosic Biomass Structure and Composition

Lignocellulosic biomass is biomass with cell walls that are composed primarily of lignin, cellulose and hemicellulose.[1,9,10] Lignocellulosic biomass also contains smaller quantities of lipids in the forms of fatty acids, triglycerides and terpenes. Proteins, lecithins, alkaloids, pectin, starches and other compounds are also present in various types of lignocellulosic biomass. Most terrestrial plants, including trees, grasses and other vegetation are lignocellulosic in nature. The amount of lignin, cellulose and hemicellulose in lignocellulosic biomass varies according to plant species, the age and the particular part of the plant, the environment and growing conditions.[1,11] Typically, lignocellulosic biomass is composed of approximately 40% cellulose, 20% hemicellulose and 20% lignin, the remainder being proteins, lipids, inorganic ash and other compounds.[1] Figure 2.1 depicts the main components of lignocellulosic biomass.
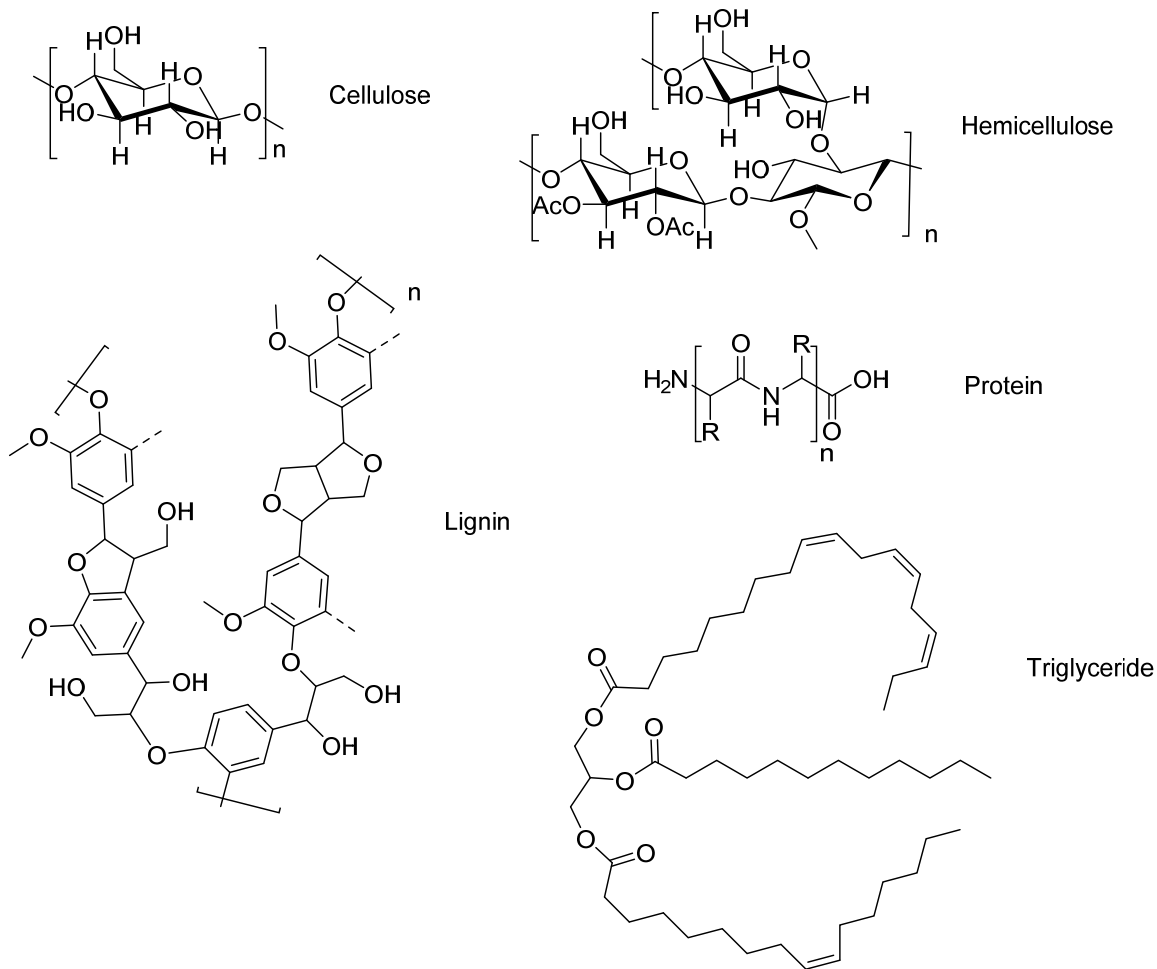
Figure 2.1. Common components present in lignocellulosic biomass.

Lignin is one of the most abundant natural polymers on earth.[12,13] It is an irregular, aromatic polymer synthesized from three monomers, sinapyl (S), coniferyl (G) and coumaryl (H) alcohols.[12] Figure 2.2 shows the structures of the monomers and several of the most abundant linkages found in lignin structures. The relative amount of the different monomers (S:G ratios) and linkages depends on the type of plant, the part of the plant, its age, growing conditions, etc.[11,14] For example, lignin from hardwood trees is composed of approximately equal parts sinapyl and coniferyl alcohol with trace amounts of coumaryl alcohol.[13-15] Softwood trees are typically about 90 % coniferyl monomers with approximately 10% sinapyl units and trace amounts of coumaryl alcohol.[12] Herbaceous or grassy plants usually contain larger quantities of the coumaryl alcohol monomer, often in the form of coumarate.[16-18]

Coumaryl alcohol   Coniferyl alcohol   Sinapyl alcohol
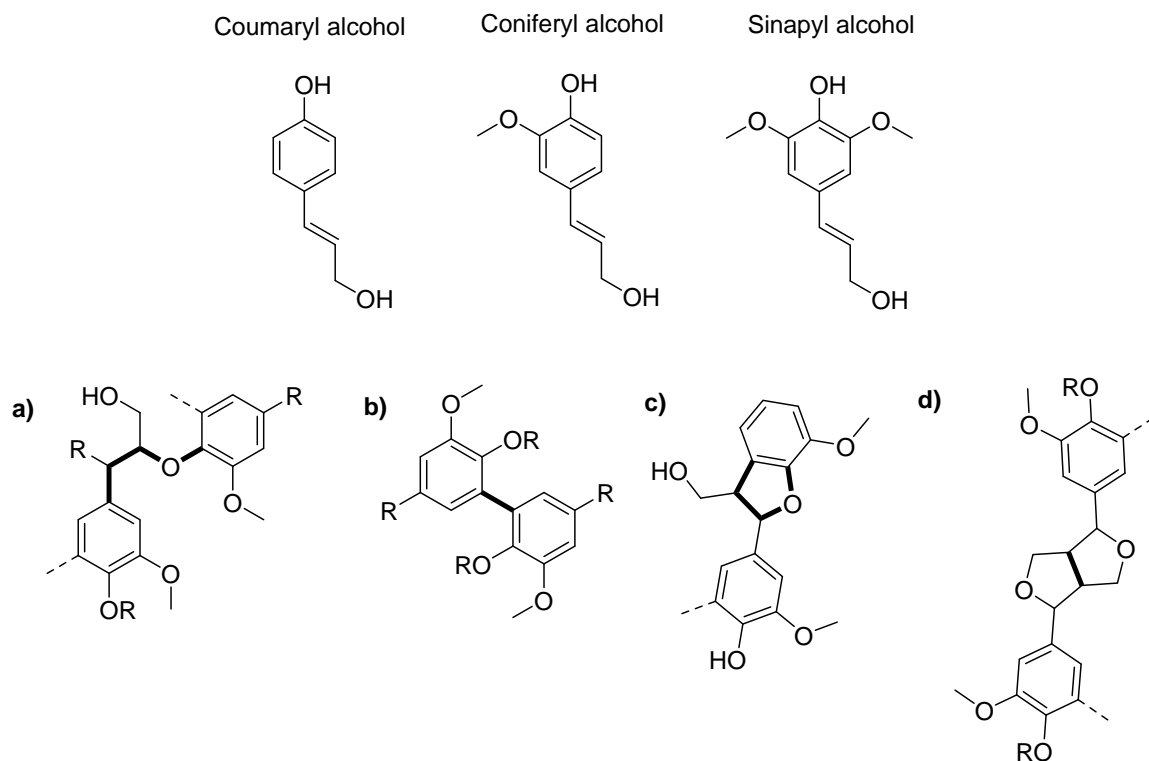
Figure 2.2. Lignin monomers and common linkages. a) β-O-4 bond, b) 5-5 bond, c) α-O-4 or β-5 bond, d) β-β bond.

The most abundant linkage in lignin is the β-O-4 bond, which may constitute up to 60% of the linkages present (Figure 2.2a).[12,19] Other common linkages in lignin shown in Figure 2.2 include α-O-4/β-5, β-β and 5-5 bonds. The relative abundance of the linkages is dependent on biomass type and monomeric abundances. For example, sinapyl-rich lignin (high S:G) is less cross-linked or branched because the presence of the additional methoxy group at the 5 position prevents the formation of 5-5 bonds.[12] Depending on the relative abundance of lignin and of the various linkages and the S:G monomer ratios, biomass displays different degradability and conversion properties.[4,5,20,21] For example, maize cell wall residues showed different degradability efficiencies by cellulase/amyloglucosidase that correlated with differing β-O-4 bond and monomer abundances within the lignin polymer.[4] Lignin also has a higher heating value than the carbohydrate fraction of the biomass and hence biomass with more lignin typically possesses higher heating values.[22,23] Hence, understanding the relative distribution of monomers and linkages may help in the screening of biomass for particular properties and applications.

Lignin helps provide a defensive barrier and structural rigidity to the plant and is covalently bound to the saccharides present in biomass cell walls.[24,25] Lignin-carbohydrate complexes

(LCCs), the structures in which lignin is bound to saccharides, are not well understood or characterized. It is believed that lignin is bound to mostly hemicelluloses through phenyl glycoside bonds, esters and benzyl ethers.[26] Figure 2.3 shows several proposed lignin-carbohydrate complex structures; a) and b) have been suggested to be present in poplar wood, as determined by heteronuclear single quantum coherence (HSQC) NMR spectroscopy.[27]
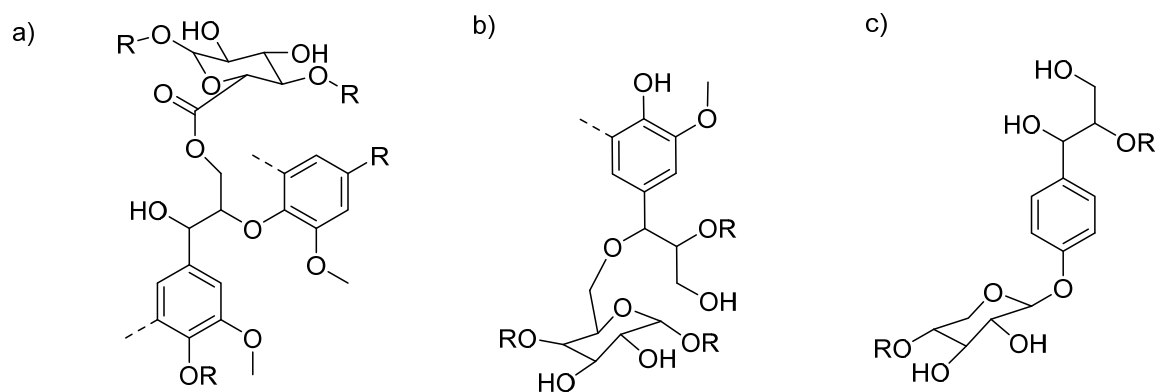
Figure 2.3. Proposed lignin-carbohydrate complex structures.[26,27]

2.2 Techniques for Determining Lignocellulosic Biomass Structure and Composition

There are many techniques used to determine the structure and composition of biomass. Determination of cellulose content, crystallinity and degree of polymerization, as well as analysis of the total saccharide profile, including hemicellulose sugars, can be performed using a variety of techniques and is well understood.[2,28-30] While holocellulose structure, composition and analysis play important roles in understanding biomass fractionation and utilization, in-depth discussion of this part of lignocellulosic biomass is beyond the scope of this dissertation. Attention is focused on lignin composition, structure and analysis for the purposes of the research discussed herein.

Techniques used to determine lignin composition and structure include chemical degradations as well as spectroscopic and thermal methods. The accepted method for determination of the total lignin content in biomass yields lignin referred to as "Klason lignin."[28,31] Klason lignin is the insoluble material remaining after biomass has been treated with H_2SO_4 under certain conditions. The residue is also known as "acid insoluble lignin" and the liquor contains a small fraction of acid soluble lignin. Klason lignin techniques have shown that herbaceous biomass typically contains between 7 and 15 wt% lignin whereas woody biomass can contain up to 25 and 30 wt%

Klason lignin content.[32] The structure of the isolated Klason lignin is undoubtedly changed during the extraction process but is still dependent on the biomass from which it originated.[33,34] Klason lignin is virtually insoluble in most solvents and the properties and structures of this lignin from various biomass sources have been analyzed using a variety of techniques (discussed in Section 2.4), including thermogravimetric analysis (TGA) and Pyrolysis-GC/MS.[33,34]

The characterization of the monomers present in lignin has been achieved by oxidative techniques including nitrobenzene and permanganate oxidation, as reviewed by Catherine in Lignin and Lignans.[19] Nitrobenzene oxidation (NBO) procedures are performed using biomass or extracted lignin dissolved in alkaline solutions (2M NaOH) heated to temperatures in excess of 160 $^{\circ}$C. Benzaldehydes and benzoic acids from corresponding sinapyl, coniferyl and coumaryl monomers are theoretically produced in distributions relative to their monomeric abundance in the lignin structure. The yield of products and their relative distributions should be characteristic of the lignin present in biomass, however NBO techniques suffer from several disadvantages. Variations in reaction time and temperature, as well as interferences from nitrobenzene derivatives, analytical difficulties and incomplete reactions lead to discrepancies in quantitative analysis of the products generated.[14,35] Also, different types of lignin have different reactivities due to the fact that S-rich lignins have less crosslinking (or condensed) bond structures relative to G rich lignins.[36] This can lead to an overestimation of the S:G ratios determined for a given biomass sample. Incomplete extraction and subsequent analysis of isolated lignin may yield results that do not reflect the actual monomeric distribution within the original biomass. This can occur because not all bonds (particularly condensed or C-C bonds) linking lignin together and to the holocellulosic fraction may be broken during the extraction process and the extracted lignin may not contain a representative distribution of linkage and monomer types.

Permanganate oxidation techniques, reviewed by Catherine in Lignin and Lignans,[19] are also performed in high pH solutions and utilize isolated lignin that has undergone peralkylation of the phenolic hydroxyl groups. Permanganate and hydrogen peroxide are used to oxidize the alkylated lignin to produce mono-, di- and tri-carboxylic acids, which can be analyzed by capillary electrophoresis,[37] high performance liquid chromatography (HPLC) or GC (after derivatization or esterification). KMnO$_4$ techniques have played important roles in lignin monomer analysis and determination of free phenolic groups but also suffer from several limitations. This oxidation technique is an intensive, multistep process that has low throughput and can also suffer from similar reproducibility issues as NBO.[14]

Thioacidolysis is a very important and heavily utilized technique for determination of the relative bond distributions and monomeric abundance in lignin.[4,19,38] Ethanethiol and boron trifluoride etherate are used to cleave the β-O-4 bonds in lignin to yield thioethylated monomers and dimers. Product yields are related to the amount of arylglycerol units involved in β-O-4 bonds, whereas the remaining lignin mass is attributed to monomers connected by carbon-carbon bonds, or "condensed units." The "degree of condensation" of lignin polymers is important for characterizing how lignin structure varies across biomass sources and how processing conditions can change the structure of lignin present in or derived from biomass. Thioacidolysis can also provide information about the identity of the free phenolic units in lignin. Figure 2.4 shows the structures of different monomers generated from various thioacidolysis processing techniques of lignin.[19]
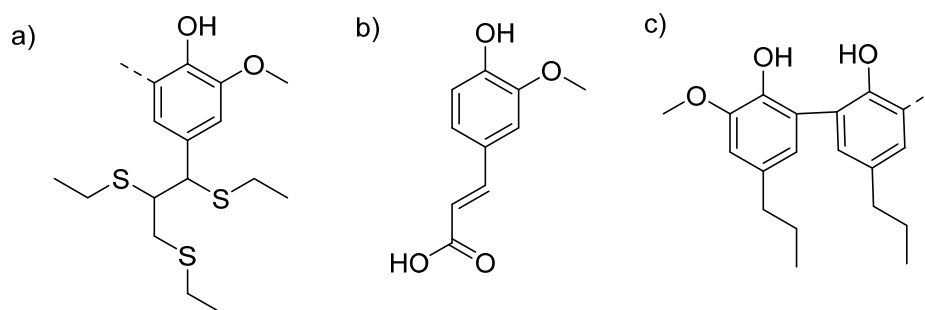
Figure 2.4. Thioacidolysis techniques are capable of generating monomers that reflect the structure of lignin and are reviewed in Catherine's section in Lignin and Lignans.[19] General thioacidolysis produces thioethylated monomers such as a) that have varying methoxyl substitutions indicated by the dashed lines. Diazomethane-methylated lignin thioacidolysis can show the presence of b) ferulic acid in lignin. Thioacidolysis followed by Raney nickel desulfurization of lignin can be used to isolate lignin dimers such as c) to help determine the degree of condensation in lignin.

Derivatization followed by reductive cleavage (DFRC) is another technique that produces lignin monomers by cleavage of β-O-4 bonds.[19] This technique uses acetyl bromide, zinc dust and an acetylation step to produce acetylated monomers in the form of hydroxycinnamyl alcohols with methoxy substitutions corresponding to the H, G and S monomers. DFRC has been used to reveal that *p*-coumarates are attached to *γ* positions on lignin side chains. This method is not as widely

used as thioacidolysis because it does not necessarily cleave all β-O-4 bonds and quantitative analysis of the products formed is difficult.

Spectroscopic methods are also important for determination of lignin content as well as identifying and characterizing lignin monomers and their linkages. Fourier transform infrared spectroscopy (FTIR) in the mid-IR region provides information about the functional groups in lignin. Spectra are commonly collected by transmittance of radiation through a KBr pellet containing lignin or by reflectance techniques such as attenuated total reflection (ATR). FTIR has been used to quantify the presence of lignin in biomass and pulps and to characterize its structure and composition.[11,39,40] For example, the S/G ratio in lignin samples can be determined by comparing the bands corresponding to ring breathing of the S and G monomers.[14,36,41] Specifically, FTIR has shown that hardwoods such as white oak typically have higher S content than softwoods such as loblolly pine.[14] This technique is also useful for characterizing the changes in lignin structure that occur during processing and isolation.[42] For example, FTIR analysis of lignin obtained from formic acid pulping of corn cob showed an increase in the intensity of bands at 1718 and 1604 cm^{-1} in comparison to milled lignin, indicating the lignin linkages had been esterified during the pulping process. Table 2.1 shows common vibrational frequencies in FTIR spectra of lignin samples[39,40] and their functional group assignments.

Table 2.1. Common bands present in FTIR spectra of lignin and their assignments.

Wavenumber (cm^{-1})^a	Assignment
3440 vs	O-H stretch
2880-2940 m	C-H methyl stretch
2850 w	(O-CH$_3$) C-H stretch
1715-1735 vs	C=O stretch, unconjugated ketone, carboxylic acid and ester
1670 w	C=O ring conjugated
1645 w	C=C ring
1600, 1510 vs	Aryl ring stretch
1465 vs	C-H deformation
1425, 1458, 1375, 1367 m	(O-CH$_3$) C-H deformation
1330 m	C-O with aryl ring breathing
1252, 1270 vs	C=O with aryl ring breathing
1140, 1130, 1035, 1050 s	C-H aromatic deformation

^{a} Intensities: w = weak, m = medium, s = strong, vs = very strong.

Nuclear magnetic resonance (NMR) is another important spectroscopic technique that can be used to quantitatively and qualitatively analyze the composition and structure of native lignin in biomass and isolated lignin.[43] NMR spectra contain signals that correspond to atoms in unique chemical environments. ^{13}C and ^{1}H NMR are used to understand the functionalities of these atoms and their neighbors based on the chemical shift (measured in ppm) of the peaks present in the spectra. Chemical structures of unknown compounds can be interpreted using 2-dimensional NMR techniques. For example, heteronuclear single quantum coherence spectroscopy (HSQC) shows carbon-hydrogen connectivity on a 2-D spectrum containing a proton spectrum on one axis and a carbon spectrum on the other axis. Since each "distinct" proton and carbon within a molecule will produce a peak at a characteristic ppm shift, a structural map of an unknown molecule can be constructed from ^{1}H, ^{13}C and HSQC spectra. Table 2.2 shows generalized chemical shifts that correspond to particular protons and carbons that can be found in lignin structures as reported in the literature (for example, see the review by Wen et al.[44]). The values reported are approximate and depend on the degree of acylation of the lignin structure as well as the solvent used to dissolve the lignin.[44]

Table 2.2. Chemical shift assignments of peaks in NMR spectra of lignin (in DMSO-d$_6$).

^{1}H chemical shift (ppm)	^{13}C chemical shift (ppm)	Structure assignment
0-2.5	20-40	Aliphatic, side chains
3.5	55	Methoxy groups (-O-CH$_3$)
4.5	80	β-C, H (β-O-4)
4.5-6	75	α-C, H (β-O-4)
6.5-8	100-140	Aromatic C, H
6.7	104	Ar-C$_{2,6}$-H$_{2,6}$ S monomer
7.0	110	Ar-C$_2$-H$_2$ G monomer
7.6	153	α-C, H cinnamyl aldehyde

NMR has been used to characterize the structure of lignin both isolated and within biomass in its native form.[45-47] Various bond types in lignin and biomass have been identified and their relative abundances have also been measured semi-quantitatively.[27] Lignin-carbohydrate complex structures have also been analyzed by NMR techniques as shown in Figure 2.3.[27] Monomer distributions (S:G ratios) can be analyzed as well as lignin acylation and condensation degrees by NMR analysis.[25] Perturbation of lignin biosynthetic pathways has also been traced by comparison of NMR analysis of wild type and genetically modified biomass.[48] For example, in a study by Pu et al.,[48] genetically engineered alfalfa lignins displayed increased signals corresponding to H monomers. NMR can also be utilized to measure changes in the structure of lignin and model compounds after application of chemical degradation or oxidative techniques.[49] Overall, NMR has proven to be an informative technique but, due to the diverse, irregular nature of the lignin polymer, is limited by resolution. Solution-state NMR is limited by the solubility of biomass and lignin in appropriate solvents.

Pyrolysis-GC/MS is a thermochemical technique that provides structural and compositional information based on biomass pyrolysate distributions and is discussed in Section 2.5. Fast pyrolysis of lignocellulosic biomass, as discussed in the preceding chapter, produces condensable vapors (bio-oil) consisting of products that are indicative of the composition and structure of biomass and lignin. The relative abundance of lignin-based pyrolysates in lignocellulosic bio-oil is related to the amount of lignin in the biomass. The distribution of pyrolysates is related to the monomer composition and bond type occurrence present in the lignin polymer. Holocellulosic-based pyrolysates may also reflect the relative abundance and types of saccharides in biomass.

Many other techniques are used to understand the structure, composition and reactivity of lignin and biomass. Size-exclusion chromatography, thermogravimetric analysis and differential scanning calorimetry are other techniques commonly used to analyze the molecular weight distribution and thermal decomposition processes associated with biomass and its constituents, respectively.[25,50,51] Overall, biomass and lignin characterization is essential for understanding the differences between biomass types and the consequences of cultivation, pretreatment and conversion processes on biomass and its constituents. Obviously, biomass structure and composition can vary drastically. These differences may influence the degradability of biomass or influence its conversion into sugars and ethanol.[4,5,21] From this it follows that in order to properly utilize biomass as a feedstock for fuels and chemicals, it is important to properly characterize the composition and structure of its constituents.

2.3 Lignin Extraction and Isolation

Cleavage and hydrolysis of the bonds connecting lignin to saccharides are important for fractionation of biomass into its individual components. Lignin can be isolated using acidic or alkaline methods by cleaving and hydrolyzing bonds in polysaccharides and lignin carbohydrate complexes. The Klason method, discussed in Section 2.1, isolates lignin by hydrolyzing the holocellulosic fraction of biomass. Extraction and isolation methods also include pulping processes that use a variety of organic and inorganic chemicals. Lignin extraction and pulping processes induce changes in the lignin structure such that it may not resemble its native form; i.e., isolated lignins may not always be representative of the whole.[3,47,52] Table 2.3 lists various methods used to extract or isolate lignin and the parameters and reagents associated with each of the techniques.[19,53] Figure 2.5 shows representative reactions that may occur, resulting in changes to the lignin structure during extraction processes such as ethanol Organosolv processes.

Table 2.3. Processes used to extract or isolate lignin.

Technique	Reagents	Time/Temperatures	Commercial Process or Purpose
Klason	H_2SO_4	<5 h, 120 °C	Total lignin content
Kraft pulping	NaOH, Na_2S	2 h, 150-180 °C	Pulp production
Sulfite pulping	$(Mg^{2+}/Ca^{2+})(SO_3^{2-}/HSO_3^-)$	130-160 °C	Pulp production
Organosolv	C_1-C_4 alcohol	<3 h, 180 °C	Fractionation/pulping
Organic acid	Formic/acetic	3h, 90 °C	Fractionation
Milling (Björkman)	Dioxane, water	varies	Protolignin research

Solvoytic cleavage of β-O-4 linkage in the presence of an acid

Solvoytic cleavage of α-O-4 linkage in the presence of an acid

Interchain condensation of e- rich carbon on other lignin molecule

(Ethanol Organosolv)
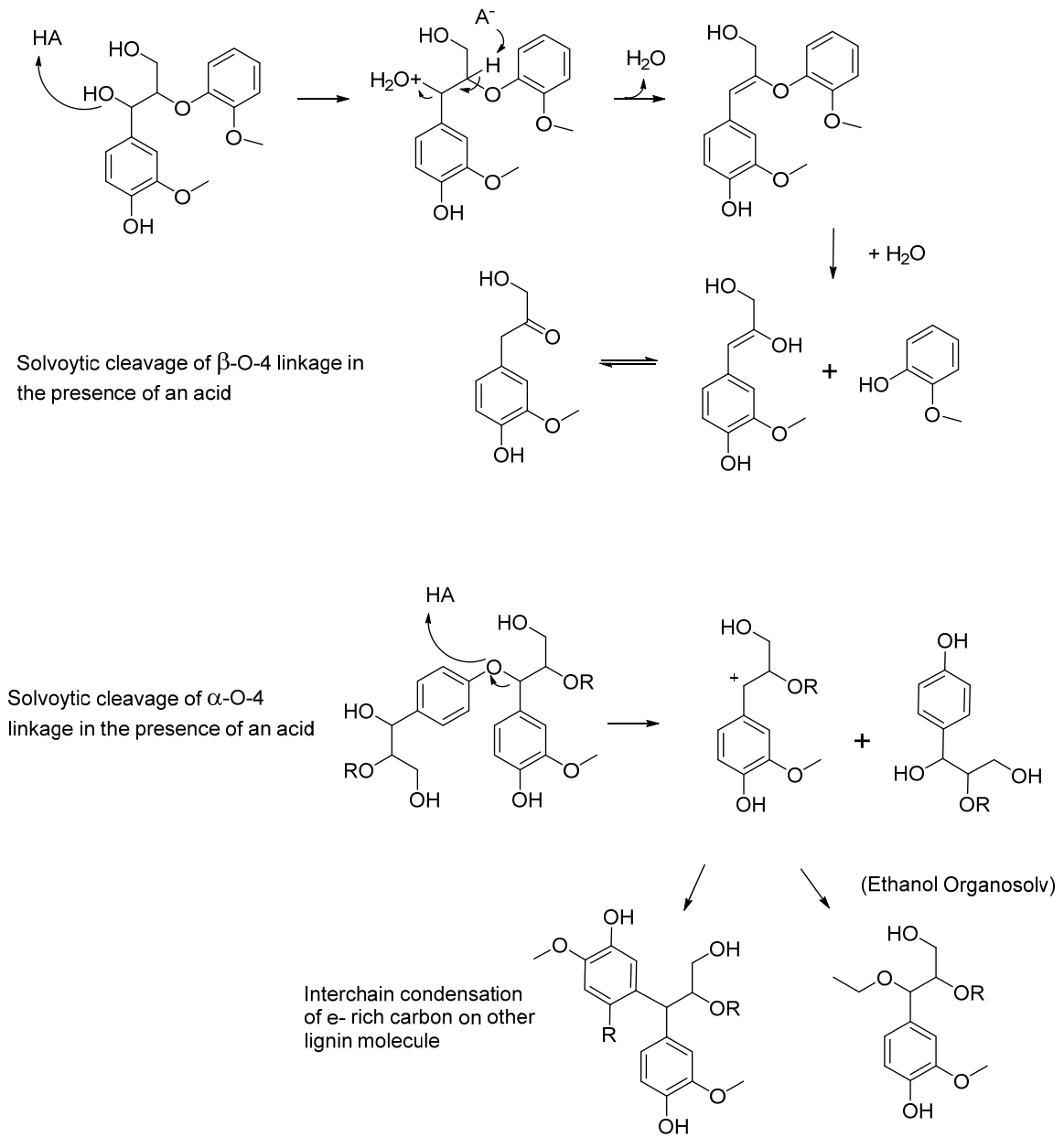
Figure 2.5. Changes induced in lignin structure during extraction, those shown above focus on an Organosolv extraction using ethanol in the presence of acid. Reactions involve both cleavage of bonds and condensation reactions to form new bonds within the lignin structure.[3,54]

The Kraft process, which is used to produce pulp from lignocellulosic biomass to create paper and other products, generates lignin as a byproduct. This process uses high pHs and moderate temperatures and utilizes the lignin byproduct as fuel to generate heat to drive the process. Chakar et al.[55] have reviewed the reactions that occur during the Kraft pulping process and the effects on lignin structure. Another pulping process, sulfite pulping, is conducted over various pH regimes using sulfite or bisulfite with either magnesium or calcium as the counterion.[12] The final lignin product contains benzylic sulfonate groups and is known as lignosulfonate.

Organosolv processes utilize organic solvents such as ethanol or butanol mixed with water to fractionate biomass into its individual cellulose, hemicellulose and lignin components. Some Organosolv processes incorporate the use of formic acid, acetic acid, inorganic acids and/or hydrogen peroxide.[42,47,56-62] These processes have important ramifications for the utilization of biomass components because they generate sulfur-free lignin and separate streams of hemicellulose and cellulose and can change the structure of the lignin[3,46,47,54] as shown in Figure 2.5. Reactions that occur during Organosolv extractions include hydrolysis, dehydration, isomerization, condensation as well as many other reactions. The final lignin products, while different from their original structure, are dependent on the biomass feedstock.[33,34]

Milling processes in the presence of chemicals such as dioxane (Björkman method) can also be used to rupture lignocellulosic bonds to produce lignin products. Milling produces milled wood lignin (MWL or ML) that is believed to retain the most resemblance to the native lignin structure within the original biomass.[53] However, this technique does not yield pure lignin as it still has many carbohydrates incorporated in its structure. Also, the lignin composition and structure first depend on the biomass but are also influenced by the processes employed to isolate it.[33] Depending on the biomass and processing conditions, some lignins may have more potential for conversion into certain products; hence, extracted lignins must be properly characterized in order to efficiently utilize them for the production of other materials.

2.4 Microalgal Biomass Structure and Composition

Microalgae are another form of photosynthetic biomass but are not lignocellulosic in composition. Microalgae have received attention in the context of biofuels and renewable materials processes because these organisms can be used to mitigate CO_2, have high areal productivity and do not require agricultural land for cultivation.[63-66] In addition to these advantages, microalgae composition is also conducive for the production of high heating value products[67] and fuel-like hydrocarbons because of its potential for having high lipid content. Like lignocellulosic biomass, pyrolysis and other thermochemical conversion processes can be used to convert microalgae to liquid fuels and chemicals. However, engineering and cultivation challenges need to be overcome before microalgae can be efficiently utilized for fuels and other materials. Specifically, correlations between growing conditions and strain selections to produce algae with particular compositions need to be understood and developed.[68,69] For example, it has been found that heterotrophic *Chlorella protethecoides* produced bio-oil of greater value in comparison to that which was grown autotrophically.[68]

Microalgal biomass is composed of microscopic algae cells (typically about 10 μm) that primarily consist of lipids, proteins and saccharides.[70] Figure 2.6 shows images of *Scenedesmus* sp. microalgae grown at the University of Kentucky Center for Applied Energy Research. The relative abundance of the constituents in microalgal biomass is dependent on the species, nutrient supplies as well as age and environmental factors.[68,71] Many microalgae genera have been the focus of renewable energy and nutritional research. However, the characterization of the components in microalgae cells and the factors that influence the abundance of and the types of components in microalgae is limited. This dissertation emphasizes primarily *Scenedesmus*, *Chlorella*, and *Nannochloropsis* genera because of the suitability of these types of microalgae for the production of renewable materials and the information available pertaining to their composition. The composition of several other types of microalgae is also briefly addressed.
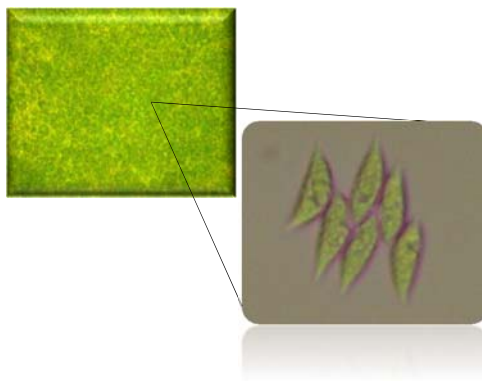
Figure 2.6. *Scenedesmus* **sp. microalgae.**

Lipids in microalgae exist mostly as triglycerides, fatty acids and phospholipids containing fatty acid moieties ranging from 10 to 20 carbons with 1 to 3 double bonds.[72,73] The lipid content of microalgae can be determined by extracting lipids from the biomass using a technique such as the Bligh and Dyer method.[74] In this process, dried microalgae cells are ground and lipids are extracted into an organic solvent layer using a chloroform/methanol/water solvent system. The lipids that are extracted contain a mixture of free fatty acids and triglycerides. The lipids can then be converted to fatty acid methyl esters by esterification followed by transesterification processes to convert the fatty acids and then triglycerides, respectively. The products can then be analyzed by GC/MS to determine the fatty acid profiles. Terpenes, lipopolysaccharides, hydrocarbons and steroids may also be present in microalgae species.[69] The abundance of lipids in microalgae is dependent on the species of the organism but is also influenced by the nutrient supply and culturing conditions, which can be optimized to produce algae displaying high lipid content.[68,71] For example, microalgae that have been starved of nitrogen nutrients have shown increased cellular lipid content.[71] Microalgae may contain between 10 and 40 wt% lipids that have the potential to be converted into fuels and which help to improve the yield and heating value of bio-oil obtained from the thermochemical processing of microalgae.[65,70]

Microalgae species may also contain large amounts (30 wt% or more) of proteins.[70] The amount of proteins present can be determined using standard techniques such as the Bradford[75] or Lowry[76] methods. The types of amino acids in the proteins can also be analyzed by standard techniques such as the method developed by Moore and Stein.[70] One study showed that the most abundant amino acids in both *Chlorella vulgaris* and *Nannochloropsis oculata* microalgae are glutamic acid, alanine and leucine.[77] In another study, glutamatic acid and aspartic acid were found to be the most abundant amino acids in 16 microalgae species.[70] The presence of proteins

in microalgae poses challenges for upgrading processes intended to convert microalgae and its constituents into fuels. However, the high protein and nitrogen content may also be beneficial if the algae are intended for use in nutritional or fertilizer applications.

Saccharides and amino sugars are also present in microalgae, constituting 10-30 wt% of the biomass.[70,78] Saccharides may occur as oligomers such as pectin and can be quantified and classified using standard techniques such as the Dubois method[29] or ASTM E1758.[30] *Scenedesmus* species are composed primarily of glucose, mannose and galactose saccharides, whereas *Chlorella* species contain mostly glucosamine, glucose and mannose.[78,79] Other components of microalgae include pigments such as chlorophyll and carotenoids. For example, *Scenedesmus* species have been found to contain the antioxidant carotenoid, lutein.[80] Despite the developed techniques for determining the composition of algal biomass, more research is still needed to understand the factors that influence the composition of many microalgal species. Like lignocellulosic biomass, microalgal biomass may vary in its potential to generate valuable products based on its structure and composition. Hence, characterization of microalgal biomass components and their potential for conversion into other products is imperative for efficient utilization of microalgae as a renewable source of fuels and/or chemicals.

2.5 Pyrolysis-Gas Chromatography/Mass Spectrometry as a Means to Elucidate Biomass Structure and Composition

Pyrolysis of biomass generates solids, gases and condensable compounds composed of pyrolysates that are associated with particular components of the biomass. The relative abundance of the pyrolysates is indicative of the relative amount of components present in the biomass. Pyrolysis-GC/MS is a rapid, microscale pyrolysis technique that can be used to monitor the relative abundance of condensable pyrolysates formed from pyrolysis of biomass and its constituents. The relative abundance of these pyrolysates may also influence the properties of the bio-oil obtained and hence influence its application for particular uses. Therefore, Py-GC/MS can be used to infer information about the composition of a feedstock as well as the potential products it can generate upon thermochemical processing. Table 2.4 lists many biomass pyrolysates analyzed by Py-GC/MS

.

Table 2.4. Common pyrolysates analyzed in biomass by Py-GC/MS.

Compound	Origin
phenol	lignin
2-methoxyphenol	G-lignin
2-methoxy-4-methylphenol	G-lignin
2-methoxy-5-(1-propenyl) phenol (trans)	G-lignin
vanillin	G-lignin
2-methoxy-4-propylphenol	G-lignin
3-(4-hydroxy-3-methoxyphenyl)-2-propenal	G-lignin
coniferyl alcohol	G-lignin
4-methylsyringol	S-lignin
4-ethylsyringol	S-lignin
4-vinylsyringol	S-lignin
2,6-dimethoxy-4-(2-propenyl)phenol	S-lignin
2,6-dimethoxy-4-(1-propenyl)phenol	S-lignin
4-hydroxy-3,5-dimethoxybenzaldehyde	S-lignin
4-propylsyringol	S-lignin
2,6-dimethoxyphenol (syringol)	S-lignin
furfural	holocellulose
2-methyl-2-cyclopenten-1-one	holocellulose
acetic acid	holocellulose
1-hydroxy-2-propanone	holocellulose
furfural	holocellulose
1,2-cyclopentanedione	holocellulose
5-methyl-2-furancarboxaldehyde	holocellulose
palmitic acid	lipid
stearic acid	lipid
hexadecanamide	lipid
pentadecene	lipid
indoles	protein
pyrroles	protein/chlorophyll

Py-GC/MS has been widely used to study the structure and composition of lignocellulosic biomass and its separated components. It has also been used to understand the mechanisms and kinetics associated with the thermal decomposition of biomass. Whole biomass, separated components and various model compounds of biomass components have all been analyzed by Py-GC/MS to explain the origin and formation of pyrolysates. Most studies have focused on lignocellulosic biomass and its components whereas few studies have focused on Py-GC/MS analysis of microalgae species. Py-GC/MS studies have been supported by other techniques used to study biomass structure and composition. Chemical degradation techniques, spectroscopic analysis and thermogravimetric analysis have all shown that Py-GC/MS analysis can give consistent information about biomass composition.

Py-GC/MS techniques may be used to analyze primary pyrolysates from biomass, which can be compared to products from large-scale pyrolysis reactors. Py-GC/MS configurations, discussed in Chapter 1, vary according to the structure of the unit and the type of heating source. The configuration of the pyrolysis reactor may influence the general pyrolysis of the feedstocks. For example, Pt heating coils may provide better heat transfer to samples inside quartz cells and minimize secondary pyrolysis reactions. Pyrolysates can also be rapidly transferred to and trapped/filtered through sorbent media as they are formed prior to GC/MS analysis in order to analyze primary pyrolysates. Heating coils with sorbent tube configurations usually have longer transfer line lengths from the pyrolysis unit to the GC/MS, which may hinder analysis of primary products. Heated chambers with shorter transfer lines mounted directly to GC/MS inlets can also be used to analyze pyrolysates from biomass. These configurations may not have efficient heat transfer in comparison to coils but are usually constructed with shorter transfer lines. However, the actual differences between Py-GC/MS techniques based on unit configurations have not been reported in the literature.

Py-GC/MS analysis of biomass in this context is reviewed on a case-by-case basis because configurations for analysis as well as temperatures and pyrolysis times vary. Gases, volatile and semi-volatile pyrolysates analyzed are considered to be primary products. Primary pyrolysates generated provide information about the structure of biomass and potential components found in bio-oil but may not necessarily reflect the final composition of bio-oil. Secondary pyrolysis reactions that occur upon condensation of bio-oil may lead to differences in the pyrolysates observed from Py-GC/MS analysis of biomass and the components present in bio-oil. However, some units with longer transfer lines may allow secondary reactions to occur and cold spots in

any unit may cause products to condense during transfer to the GC/MS. Additionally, non-volatile and solid or char products that are not capable of GC/MS analysis are not analyzable by Py-GC/MS methods.[81] Hence, Py-GC/MS techniques are limited by analysis of the transferrable vapor products.

Py-GC/MS of whole biomass has been used to analyze thermal decomposition products from many types of biomass such as sugar cane bagasse, wheat straw, switchgrass, *Miscanthus*, pine, eucalyptus and *Nannochloropsis* microalgae.[32,81-87] Pyrolysates monitored were indicative of the presence of the various components present in each of the biomass species. *Miscanthus*, for example, produces furfural, hydroxy-propanone and other small oxygenates that are generated by pyrolysis of the holocellulosic fraction of the biomass. Lignin-based pyrolysates from lignocellulosic biomass include guaiacol and syringol with various substitutions at the aromatic 4-position. Herbaceous lignocellulosic biomass (such *Miscanthus* and kenaf) pyrolysis also produces large amounts of 4-vinylphenol, originating from coumarate in the lignin polymer,[18] which is not as abundant in woody lignocellulosic biomass types. Figure 2.7 shows a comparison of select pyrolysates from several whole biomass sources as analyzed by Py-GC/MS and reported in Greenhalf et al.[32]
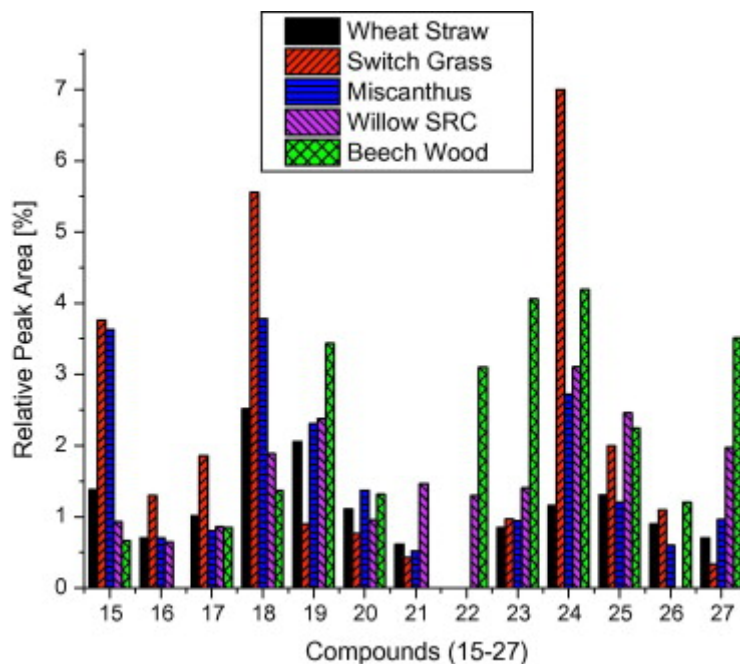
Figure 2.7. Relative peak area comparison of key pyrolysis products from wheat straw, switch grass, miscanthus, willow SRC and beech wood. (15) 3-Methyl-benzaldehyde; (16) 3-methoxycatechol; (17) 4-ethyl-2-methyl-phenol; (18) 2-methoxy-4-vinylphenol; (19) 2,6-dimethoxy-phenol; (20) vanillin; (21) 1,2,4-trimethoxybenzene; (22) 1,4:3,6-dianhydro-α-d-glucopyranose; (23) 2-methoxy-6-(2-propenyl)-phenol; (24) levoglucosan; (25) 3′5′-dimethoxyacetophenone; (26) syringaldehyde; and (27) 2,6-dimethoxy-4-(2-propenyl)-phenol. Reprinted from:[32] Greenhalf, C. E.; Nowakowski, D. J.; Harms, A. B.; Titiloye, J. O.; Bridgwater, A. V., A comparative study of straw, perennial grasses and hardwoods in terms of fast pyrolysis products. *Fuel* 2013, *108*, 216-230 with permission from Elsevier.

Analysis of the non-condensable gases, CO, CO_2, and C_1-C_3 hydrocarbons is also possible using Py-GC/MS and has been performed by Boateng et al. using switchgrass and Bermudagrass as feedstocks.[86,88] Switchgrass physiological maturity influenced gas yields when pyrolysis was conducted under 900 ^{0}C; results indicated that more mature plants produced a higher yield of non-condensable products.[86] Different Bermudagrass genotypes were found to produce no significant differences in the non-condensable fraction.[88] However, different genotypes of *Miscanthus* have been shown to generate different pyrolysate distributions in the condensable fraction due to variations in the structure and composition of the biomass types.[85] *Miscanthus* biomass of different genotypes harvested at the same time showed significant differences in the pyrolysates originating from the holocellulose within the biomass.[85] Wheat straw whole biomass and its corresponding milled wood lignin (MWL) has been analyzed by Py-GC/MS and results

were compared to NMR analysis.[87] Data from the Py-GC/MS analysis showed similar S:G ratios (being 0.5) of the lignin in the whole wheat straw biomass as in the MWL, which also agreed with S:G ratios determined by NMR techniques.[87]

Py-GC/MS has also been supported by studies comparing pyrolysis products from biomass in larger scale reactors. Pyrolysates from spruce and beech pyrolyzed in a larger scale reactor were similar to those analyzed by Py-GC/MS analysis of various biomass feedstocks in a study by Azeez et al.[89] Figure 2.8 shows an overlay of a pyrogram obtained from Py-GC/MS analysis of beech with a chromatogram of the corresponding bio-oil from a fluidized bed pyrolysis unit. Py-GC/MS has also been utilized to screen for catalyst activities intended for bio-oil upgrading processes using feedstocks such as sawdust.[90,91] The influence of inorganic compounds on the pyrolysis of switchgrass and poplar has also been studied using Py-GC/MS.[92-94] Inorganic compounds have shown to decrease yields of levoglucosan and condensable vapor yields.
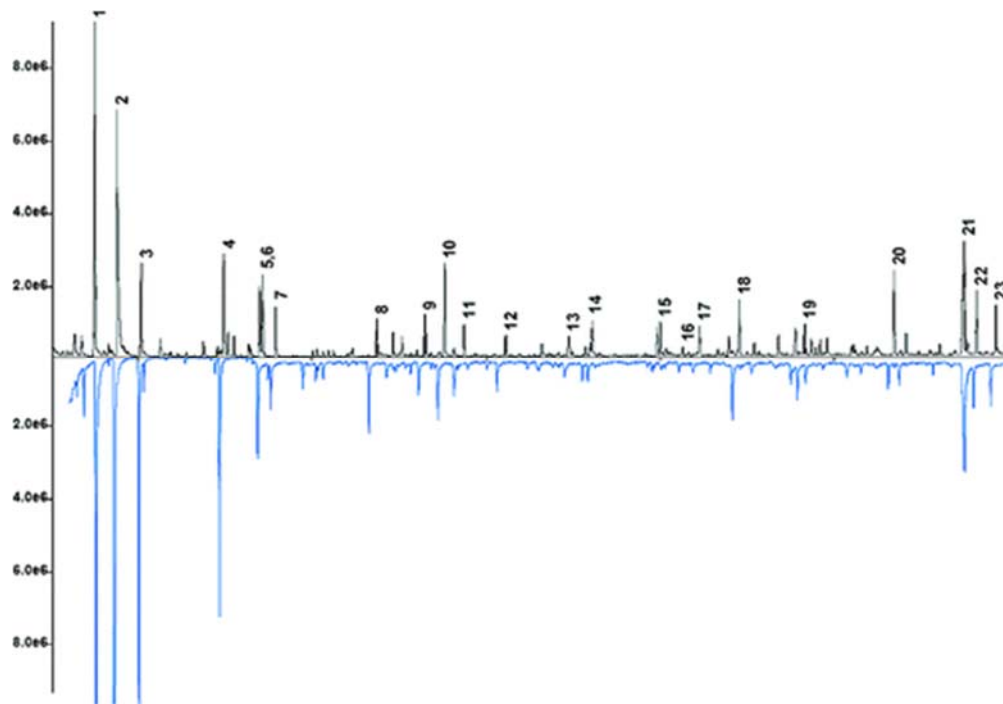
Figure 2.8. Overlay of GC/MS chromatograms obtained from bio-oil (below) and Py-GC/MS of beech: 1, hydroxyacetaldehyde; 2, acetic acid; 3, acetol (hydroxypropanone); 3-hydroxy 4- propionaldehyde; 5, prob. oxopropanoic acid methylester; 6, butanedial; 7, 2-furaldehyde; 8, 2-hydroxy-2-cyclopentene-1-one; 9, 2(5H)furanone; 10, 3-hydroxy-5,6-dihydro-(4H)-pyran-4-one; 11, 2-hydroxy-3-methyl-2- cyclopenten-1-one; 12, guaiacol; 13,

Several types of lignocellulosic biomass have also been analyzed by Py-GC/MS for determination of the abundance of sinapyl and coniferyl monomers present within the lignin polymers. Eucalyptus has been found to generate more sinapyl-based pyrolysates than coniferyl-based pyrolysates, indicating this type of biomass has a high S:G ratio, being about 2.7.[83,84,95] Nitrobenzene oxidation of eucalyptus samples and forages have yielded similar S:G values to those obtained by comparing the relative distributions of certain pyrolysates generated by Py-GC/MS.[83,84,95] Spruce (*Picea abies* L.) was found to produce very few sinapyl-based pyrolysates and a high amount of coniferyl-based pyrolysates.[89] Kenaf, jute, sisal and abaca were found to have S:G ratios of 5.4, 2.0, 4.3 and 4.7, respectively, by Py-GC/MS analysis.[18] These plants were also found to contain acetylated lignin units using Py-GC/MS.

Separate components of lignocellulosic biomass have also been studied using Pyrolysis-GC/MS. Py-GC/MS studies of cellulose and dextran have been performed in order to elucidate the mechanisms and kinetics (discussed in Chapter 1.3) associated with the thermolysis of these polysaccharides in biomass.[96-98] Lignin extracted from various types of biomass has also been studied using Py-GC/MS in order to understand its thermolysis, structure, monomeric composition and the differences in these characteristics between the native and extracted lignin.[81,99-102] Lignin extracted using various techniques from different biomass sources was subjected to Py-GC/MS and thermogravimetric analysis in a study by Brebu et al.[34] Py-GC/MS data suggested that lignins from hardwood biomass types generated similar pyrolysates even if the lignin extraction techniques were different. Kim et al. extracted lignin from poplar wood using assorted techniques and Py-GC/MS analysis indicated some differences in the pyrolysate distributions of the lignins examined.[33] Lignin extracted using an ionic liquid generated pyrolysates originating from the ionic liquid, indicating the ionic liquid was not completely removed or it was chemically associated with the lignin. Milled lignin generated more acetic acid upon pyrolysis, indicating there were more acetyl groups, possibly from the hemicellulose or the

lignin side chains. Klason, ionic liquid and organosolv lignins also showed fewer pyrolysates with oxygenated side chains in comparison to milled wood lignins. This may be the result of structural changes induced during lignin isolation or changes in how the lignin decomposes to produce volatile, condensable pyrolysates.

Lignin isolated from industrial black liquor was analyzed by Py-GC/MS and bond dissociation energies were used to explain the formation of radicals that lead to the pyrolysates observed.[102] Lignin model compounds have also been studied using Py-GC/MS and other microscale pyrolysis techniques in effort to elucidate the mechanisms of lignin pyrolysis (discussed in Chapter 1.3) and explain the origin of various pyrolysates. Lignin model monomers, dimers with β-O-4 linkages and various other synthesized lignin models have been analyzed by Py-GC/MS and other microscale pyrolysis-mass spectrometry techniques.[101,103-108] Figure 2.9 shows the initiation mechanisms associated with the homolysis of the weakest bonds in the lignin linkages as studied by Hu et al. using industrial black liquor lignin.[102] Similar mechanisms can be used to explain thermolysis of lignin, model polymers and lignin present in whole biomass.
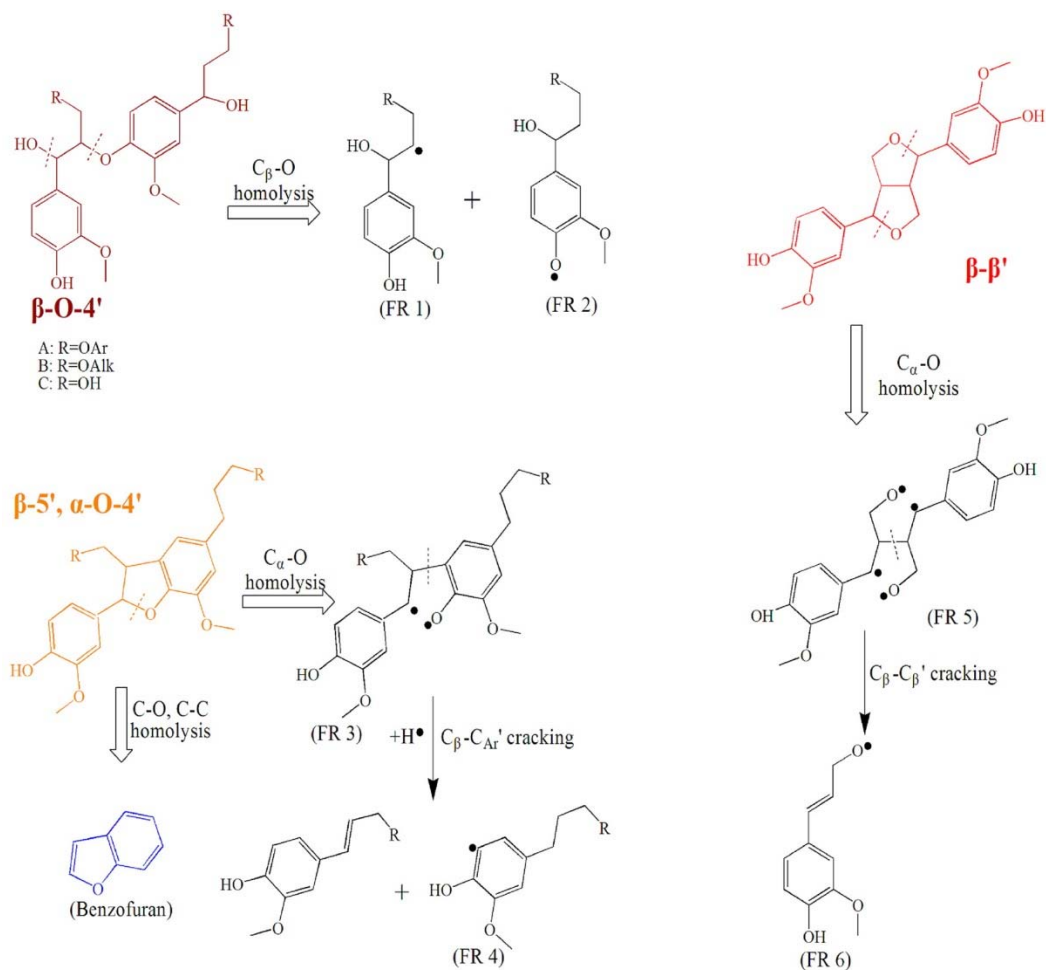
Figure 2.9. Cleavage mechanism for β–O–4, β–5, α–O–4, and β–β bonds in lignin. Reprinted with permission from Hu, J.; Shen, D.; Xiao, R.; Wu, S.; Zhang, H., Free-Radical Analysis on Thermochemical Transformation of Lignin to Phenolic Compounds. *Energy & Fuels* **2013,** *27*, **285-293. Copyright © 2010, American Chemical Society.[102]**

Py-GC/MS has also provided useful information about the composition of components in microalgae. For example, *Chlamydomonas reinhardtii* and *Botryococcus braunii* were phenotypically compared based on their hydrocarbon pyrolysate distributions.[69] *Chlamydomonas* produced more palmitic acid and less stearic acid than *Botryococcus*, which provided information about the biosynthetic pathways of lipids in the microalgae and the potential for the algae to produce certain lipid-based products. Other algae pyrolysis products analyzed in this study included fatty acid esters, sterols and other hydrocarbons. These products are important because they give the microalgae greater potential as a biofuel feedstock in comparison to lignocellulosic feedstock, particularly for producing hydrocarbon fuels such as diesel or biodiesel.

Nannochloropsis microalgae have also been analyzed using Py-GC/MS in order to obtain the relative protein, carbohydrate and lipid content of the biomass.[82] The Py-GC/MS analysis of the components in *Nannochloropsis* correlated strongly with standard protein, carbohydrate and lipid content determination. While the relative content of the biomass components correlated with other techniques and could be calculated using regression lines, raw values obtained from Py-GC/MS did not yield accurate values of protein, carbohydrate and lipid content. This may have been the result of preferential formation of certain pyrolysates in the vapor phase. Hence, comparison to other techniques was necessary to determine accurate values of biopolymers in biomass using Py-GC/MS.

Py-GC/MS analysis of *Schizochytrium limacinum* was performed at various temperatures in order to determine the optimal parameters for maximum production of certain pyrolysates.[109] Alkenes, alkanes and aromatic hydrocarbons were produced from lipids, whereas furans were produced from carbohydrates. Nitrogenous species formed from proteins were also detected in the pyrolysis products of *Schizochytrium limacinum*.[109] Maximum volatile pyrolysis product yields (67.7 wt%) occurred at 700 ^{0}C but lower temperatures were suggested to be more suitable for larger applications to avoid the formation of polycyclic aromatic hydrocarbons (PAHs).

Py-GC/MS has provided a wealth of information about the structure and composition of whole biomass as well as isolated biomass components. Catalyzed and uncatalyzed thermal decomposition of biomass and its components has been monitored by Py-GC/MS, providing valuable insight into the types of products generated by thermochemical processing of biomass. Mechanisms and kinetics associated with the pyrolysis of biomass have also been revealed using Py-GC/MS. In conclusion, Pyrolysis-GC/MS can simultaneously analyze the structure of the starting biomass feedstock and the potential products it can generate upon thermochemical processing.

Chapter 3. Pyrolysis-GC/MS of Sinapyl and Coniferyl Alcohol

Note – This chapter was reprinted from:

Harman-Ware, A. E.; Crocker, M.; Kaur, A. P.; Meier, M. S.; Kato, D.; Lynn, B., Pyrolysis–GC/MS of sinapyl and coniferyl alcohol. *Journal of Analytical and Applied Pyrolysis* **2013**, *99*, 161-169.[1]

The article appears in this dissertation with permission from Elsevier.

Section 3.2.4 Determination of S:G Ratios of Lignin by Capillary Electrophoresis references the aforementioned journal article. The content in this section was not performed by the author and is beyond the scope of this dissertation.

3.1 Introduction

Lignin is a complex, irregular polymer that provides structural integrity in plants and accounts for up to 40% weight (dry) in softwoods, hardwoods, and herbaceous plants.[2,3] The three-dimensional lignin structure is made in plants by free radical polymerization of three monomeric subunits: *p*-coumaryl alcohol, coniferyl alcohol and sinapyl alcohol. These lignols are incorporated into lignin in the form of the phenylpropanoids *p*-hydroxyphenyl (H), guaiacyl (G), and syringyl (S), respectively.[4,5] Depending on the part of the plant, the type of plant and its environment, the lignin structure may vary in the amounts of the different monomeric subunits present.[5,6] For example, hardwood lignin contains roughly 1:1 sinapyl:coniferyl (S:G) monomeric units whereas softwood lignin contains these units in an approximate 1:9 (S:G) ratio.[2] The S:G ratio and the abundance of lignin within biomass are important values in the pulping industry because of their influence on sugar recovery from biomass.[7,8] The relative abundance of the lignin and these two monomers may also influence the products formed during pyrolysis of biomass which can influence the potential production of fuel and other chemicals from pyrolysis oil.[9,10]

The S:G ratio in lignin can be determined using techniques that involve oxidative depolymerization of lignin or the whole biomass using nitrobenzene or potassium permanganate.[4,11-15] However, these techniques require intensive sample preparation prior to chromatographic analysis, the results are not always considered reliable[6] and relative product formation is dependent on the reaction time, temperature and reagent concentration.[11] Alternatively, pyrolysis-GC/MS (Py-GC/MS) provides a high throughput technique for analysis of polymers and biomass that utilizes small sample sizes and requires little to no sample preparation. Several studies have focused on the use of Py-GC/MS as a technique to analyze

lignin composition and structure in biomass.[12,13,16-19] The pyrolysis of lignin model compounds, as well as lignin extracted from biomass, has also been studied using Py-GC/MS and other analytical techniques such as FTIR.[9,20-30] Additionally, determination of the S:G ratios of lignin in biomass using Py-GC/MS has been compared to nitrobenzene oxidation techniques.[12,13,16] Nunes and co-workers[12] pyrolyzed eucalyptus wood and measured the relative formation of certain pyrolysates in order to establish S:G ratios of the lignin in the starting biomass. They found that the S:G ratios obtained using certain marker compounds formed during pyrolysis agreed with S:G ratios obtained by nitrobenzene oxidation of the biomass. Lima et al.[13] conducted a similar study using different marker pyrolysates that also correlated to nitrobenzene oxidation S:G ratios. Mann et al. studied the variation in the S:G ratio of lignin in switchgrass grown in different conditions by comparing pyrolysis product mass intensities of certain sinapyl marker compounds to coniferyl markers.[5] Izumi and Kuroda used Py-MS spectra of lignin model polymers to correlate marker ion mass intensity S:G ratios to the molar S:G ratios in the synthesized polymers.[31] Recently, Asmadi and co-workers[32] pyrolyzed mixtures of syringol and guaiacol in order to understand the reactivities of the aromatic nuclei in hardwood lignins.

Despite recent research, Py-GC/MS has not been utilized to pyrolyze the sinapyl alcohol and coniferyl alcohol monomers alone or in simple mixtures together in order to understand the origin of certain pyrolysates and examine S:G ratios using monomers as standards. For example, sinapyl alcohol and its marker compounds may undergo demethoxylation during pyrolysis.[32] Hence, the area % contributed by certain sinapyl and coniferyl alcohol marker pyrolysates may or may not be demonstrative of, or provide a linear correlation with, the molar S:G ratio. The goal of this investigation was to use Py-GC/MS to pyrolyze sinapyl and coniferyl alcohols as well as various mixtures of the two in order to find which, if any, pyrolysate combinations exhibit a linear correlation between molar S:G ratios and sum area % S:G ratios from marker pyrolysates. Consequently, the extent of the demethoxylation of sinapyl alcohol and its markers was monitored and the analysis was able to explain the origin of certain pyrolysates, as well as calibrate for S:G ratios in biomass using sinapyl and coniferyl alcohol mixtures as standards. The S:G ratio of peach pit lignin was also determined using unique marker pyrolysates from Py-GC/MS. The S:G ratio from Py-GC/MS analysis was compared to the S:G ratio obtained from capillary electrophoresis of products from $KMnO_4$ oxidation of the peach pit lignin.

3.2 Materials and Methods

3.2.1 Reagents

Sinapyl alcohol (technical grade, Sigma Aldrich) was dissolved 1:10 in methanol and analyzed for purity using the same GC/MS method as described in the pyrolysis experiment. Toluene was the only impurity detected and was removed via purification of the sinapyl alcohol in a methanol/hexane solvent system. The sinapyl alcohol was dissolved in methanol, this mixture was washed with hexane and the hexane layer was removed. The sinapyl alcohol in methanol was then analyzed via GC/MS and found to contain no impurities. The methanol was removed from the sinapyl alcohol via rotary evaporation leaving behind the purified sinapyl alcohol which was used in the pyrolysis experiments. Coniferyl alcohol (98%, Sigma Aldrich) was also analyzed for purity via GC/MS prior to pyrolysis experiments and found to contain no impurities. Lignin extracted from peach pits was also pyrolyzed for use as a reference.

3.2.2 Pyrolysis-GC/MS

Experiments were performed using a Pyroprobe Model 5200 (CDS Analytical, Inc.) connected to an Agilent 7890 GC with an Agilent 5975C MS detector. The pyroprobe was operated in trap mode under He atmosphere. Pyrolysis was conducted at 650 °C (1000 °C/s heating rate) for 20 s. The valve oven and transfer lines were maintained at 325 °C. The column used in the GC was a DB1701 (60 m × 0.25 mm × 0.25 µm) and the temperature program was as follows: 45 °C for 3 min, ramp to 280 °C at 4 °C/min and hold for 10 min. The flow rate was set to 1 mL/min using He as the carrier gas. The inlet and auxiliary lines were both maintained at 300 °C and the MS source was set at 70 eV. The GC-MS was calibrated for a number of phenolic compounds including phenol, 2-methoxyphenol, 2-methoxy-4-methylphenol, 2,6-dimethoxyphenol, vanillin, syringaldehyde and 2-methoxy-4-vinylphenol. Pyrolysis products were analyzed according to retention time and mass spectra data obtained from a NIST library.

1 mg of coniferyl and sinapyl alcohol were each separately pyrolyzed in triplicate in order to monitor each monomer's pyrolysate profile. Next, 0.1, 0.4, 0.9 and 1.7 molar ratios of sinapyl:coniferyl alcohol were prepared and 1 mg of each sample was pyrolyzed in triplicate. Marker compounds for each monomer were chosen according to those compounds produced in highest abundance and compared to marker compounds chosen in previous studies[12], as well as marker compounds selected based on pyrolysis of 1 mg of lignin extracted from peach pits. S:G

ratios were calculated by summing the area % of the selected sinapyl marker compounds and dividing by the sum of the area % of the coniferyl marker compounds.

3.2.3 Extraction of Lignin from Peach Pits

Ground peach pits were degummed via overnight Soxhlet extraction using acetone. Lignin was extracted by stirring 10 g of degummed biomass with 200 ml of 85% formic acid containing 0.2% HCl in a shaker bath for 24 h at 65 °C. The solution was then filtered and the liquid filtrate containing lignin and hemicellulose was removed on a rotary evaporator to recover formic acid. Next, water was added to dissolve the hemicellulose present, which also caused the lignin to precipitate. The mixture was then centrifuged, decanted, and filtered to collect lignin, which was dried overnight in an oven at 80 °C. The dried lignin was pyrolyzed using the same method as described for the monomer pyrolysis.

3.2.4 Determination of S:G Ratios of Lignin by Capillary Electrophoresis

The procedure for $KMnO_4$ oxidation of lignin was performed according to the method described by Gellerstedt.[33] The procedure is beyond the scope of this dissertation but is detailed in Harman-Ware et al.[1]

3.3 Results and Discussion

3.3.1 Individual Monomer Pyrolysis

Pyrolysis of sinapyl and coniferyl alcohols was conducted at 650 °C in order to maximize the transfer of volatiles to the GC inlet. Lower temperatures resulted in condensation and carry over effects within the instrument and higher temperatures result in further cracking, hence 650 °C provided a reasonable balance for the current study. Also, due to carryover complications, area %, as opposed to absolute area, was utilized as the dependent variable. This helps to eliminate inconsistent areas due to variable sample sizes and product carryover, and it was found that the contribution of the area for a given peak was similar between experiments. Several structures of positively identified pyrolysates formed from coniferyl alcohol are displayed in Figure 3.1. Table 3.1 provides a list of positively identified pyrolysates from coniferyl alcohol.
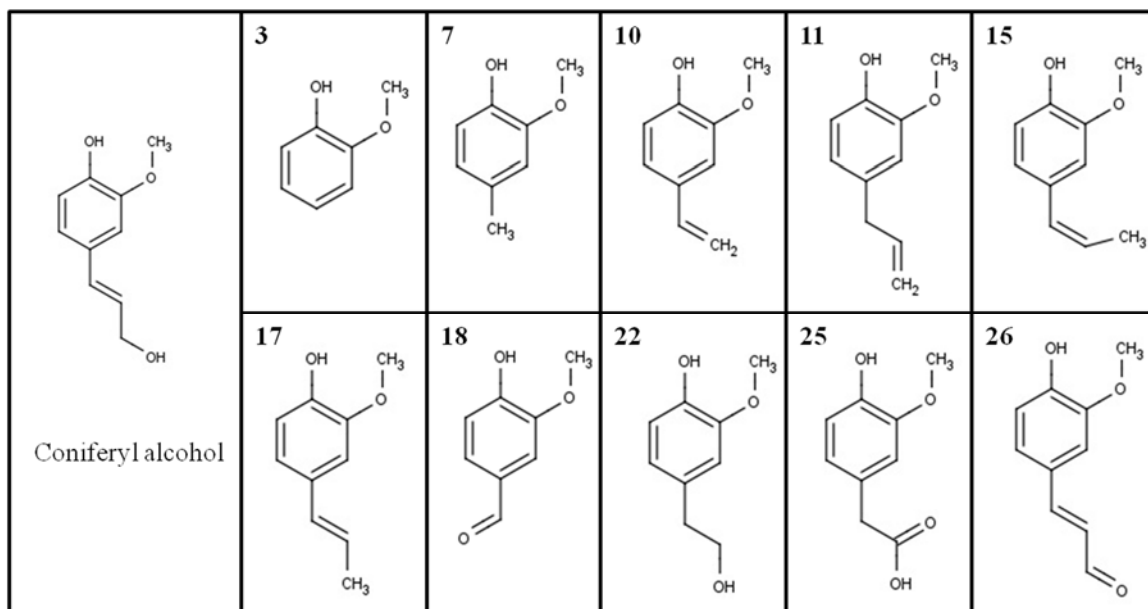
Figure 3.1. Selected pyrolysates formed from the pyrolysis of coniferyl alcohol at 650°C.

The most abundant compounds produced are 3-(4-hydroxy-3-methoxyphenyl)-2-propenal, *trans*-isoeugenol, vanillin, 2-methoxy-4-propylphenol, and homovanillic acid. As shown in Table 3.1, several other compounds containing the guaiacol structure are produced. 3-Methoxy-2-naphthalenol and dehydrodiconiferyl alcohol, larger compounds than the coniferyl alcohol starting material, were observed in the pyrograms in very small quantities. The presence of other compounds, such as 2-methoxy-3-methylphenol, indicates the occurrence of isomerization reactions. The formation of these products has been explained on the basis of radical, cleavage, dehydration and various other reaction pathways that may occur during pyrolysis.[20,25-27,32] Exact mechanisms of formation are beyond the scope of this work, but may be important when considering mechanisms of polymer vs. monomer pyrolysis. However, products formed are similar to those observed in previous studies of lignin and lignin model compound pyrolysis.[9,12,13,15-29]

Table 3.1. Pyrolysates formed from coniferyl alcohol pyrolysis at 650 °C.

Compound Number	Retention Time (min)	Compound	Average Chromatogram Area %	Standard Deviation (absolute)
1	10.4	toluene	0.15	0.05
2	25.5	phenol	0.04	0.04
3	26.2	2-methoxyphenol	1.32	0.27
4	27.2	2-methylphenol	0.12	0.01
5	28.5	4-methylphenol	0.06	0.01
6	28.8	2-methoxy-3-methylphenol	0.07	0.02
7	30.0	2-methoxy-4-methylphenol	2.61	0.49
8	30.2	2,4-dimethylphenol	0.26	0.03
9	32.8	4-ethyl-2-methoxyphenol	0.43	0.06
10	34.7	2-methoxy-4-vinylphenol	3.08	0.34
11	35.5	eugenol	1.97	0.23
12	35.9	2-allylphenol	0.07	0.02
13	36.0	1,2-benzenediol	0.71	0.11
14	37.0	2-methoxy-5-(1-trans-propenyl)phenol	0.08	0.01
15	37.3	cis-isoeugenol	1.26	0.13
16	38.5	4-methyl-1,2-benzenediol	1.38	0.79
17	39.0	trans-isoeugenol	6.58	0.70
18	39.8	vanillin	8.14	1.12
19	41.5	2-methoxy-4-propylphenol	6.08	0.94
20	41.7	2-methoxy-1,4-benzenediol	1.13	0.63
21	42.1	1-(4-hydroxy-3-methoxyphenyl)ethanone	0.68	0.03
22	43.8	homovanillyl alcohol	0.31	0.06
23	44.8	dehydrodiconiferyl alcohol	1.33	0.18
24	46.4	3-methoxy-2-naphthalenol	0.40	0.13
25	47.0	homovanillinic acid	5.27	0.71
26	50.7	3-(4-hydroxy-3-methoxyphenyl)-2-propenal	11.61	0.95
	50.1	coniferyl alcohol	29.62	2.86

Several pyrolysates formed from sinapyl alcohol pyrolysis are shown in Figure 3.2. Table 3.2 provides a list of pyrolysates generated from sinapyl alcohol. The most abundant compounds produced include 2,6-dimethoxy-4-vinylphenol, 4-hydroxy-3,5-dimethoxybenzaldehyde, 2,6-dimethoxy-4-(1-propenyl)phenol, 4-propylsyringol and 4-methylsyringol.
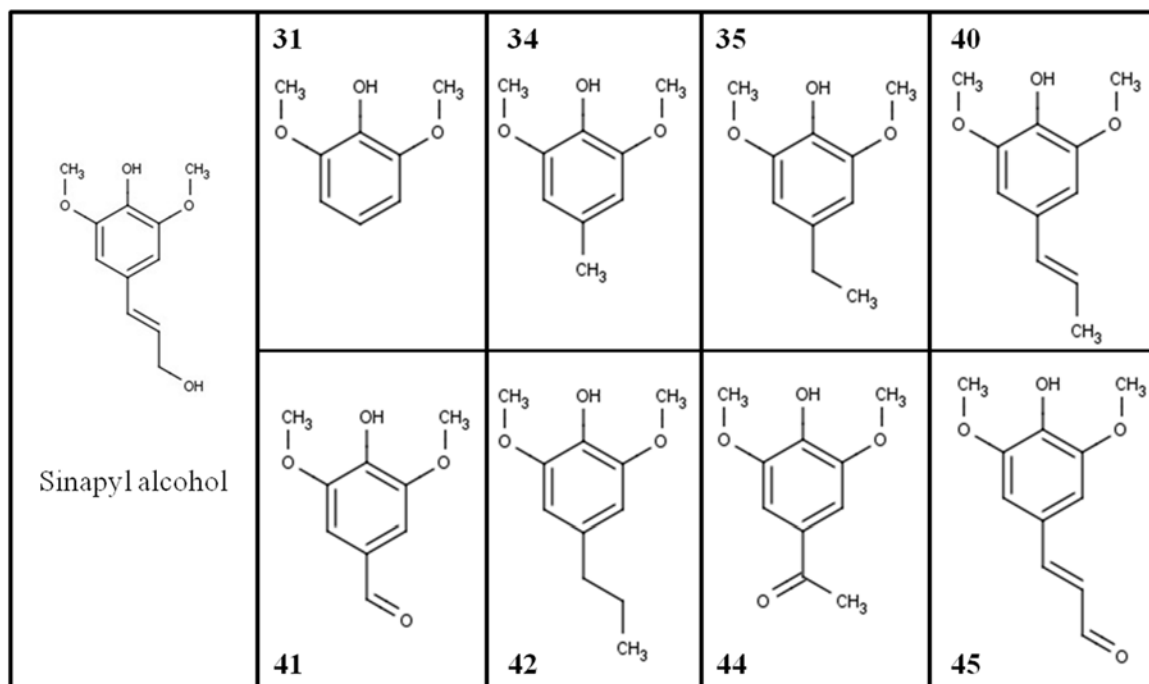
Figure 3.2. Selected pyrolysates formed from sinapyl alcohol pyrolysis at 650 °C.

The Py-GC/MS results indicated that in our system, demethoxylation of sinapyl alcohol does occur at 650 °C, but not to a statistically significant extent. The sum of the area percent of demethoxylated products was approximately 0.6%. The formation of these pyrolysates could be accounted for when calculating the S:G ratio using the sum of the area % of the marker compounds in order to obtain area percent S:G ratios that more closely resemble the molar S:G ratio. However, provided the ratios of the sum area percent of the marker compounds chosen exhibit a linear response with respect to the molar S:G ratio, the demethoxylation adjustment would also follow a linear correlation.

Table 3.2. Pyrolysates formed from pyrolysis of sinapyl alcohol at 650 °C.

Compound Number	Retention Time (min)	Compound	Chromatogram Area %	Standard Deviation
2	25.4	phenol	0.07	0.02
3	26.2	2-methoxyphenol	0.09	0.01
4	27.2	2-methylphenol	0.04	0.01
27	27.8	2,6-dimethylphenol	0.04	0.01
28	28.6	3-methylphenol	0.03	0.01
6	28.8	2-methoxy-3-methylphenol	0.12	0.01
7	29.9	2-methoxy-4-methylphenol	0.06	0.00
8	30.1	2,4-dimethylphenol	0.04	0.01
29	31.0	2,4,6-trimethylphenol	0.05	0.01
30	34.6	3-methoxy-1,2-benzenediol	0.84	0.09
31	36.5	2,6-dimethoxyphenol	4.83	0.33
32	37.2	4-methyl-1,2-benzenediol	0.11	0.05
33	37.5	3,4-dimethoxyphenol	0.75	0.12
17	38.8	trans-isoeugenol	0.02	0.01
34	39.3	4-methylsyringol	5.50	0.37
35	41.4	4-ethylsyringol	0.79	0.11
36	43.2	4-vinylsyringol	9.16	0.15
37	43.8	2,6-dimethoxy-4-(2-propenyl)phenol	5.46	0.42
38	44.3	3,4,5-trimethoxybenzaldehyde	0.02	0.03
39	45.2	2,6-dimethoxy-4-(1-propenyl)phenol (Z)	4.33	0.33
40	46.9	2,6-dimethoxy-4-(1-propenyl)phenol (E)	19.84	0.58
41	47.8	4-hydroxy-3,5-dimethoxybenzaldehyde	19.75	1.94
42	48.9	4-propylsyringol	9.03	1.47
43	49.0	3,5-dimethoxycinnamic acid	1.56	0.16
44	49.4	1-(4-hydroxy-3,5-dimethoxyphenyl)ethanone	1.03	0.09
44	51.4	3,5-dimethoxy-4-hydroxycinnamic acid	0.29	0.10

Table 3.2 (continued)

45	56.6	3,5-dimethoxy-4-hydroxycinnamaldehyde	2.04	0.73
46	56.3	sinapyl alcohol	0.93	0.16

3.3.2 Monomer Mixtures

Pyrolysates formed from pyrolysis of the mixtures of the sinapyl and coniferyl alcohols are shown in Table 3.3. The products formed from the mixtures appear to represent the sum of the pyrolysates from the individual alcohols with practically no new products being formed from the reactions between the individual alcohols and their corresponding pyrolysates. However, the trends for the formation of some of the products indicate that the coexistence of the two alcohols alters the product distribution during pyrolysis. For example, as the relative amount of coniferyl alcohol decreases, the relative amounts of trans-isoeugenol and vanillin should also decrease; however, the area percentages do not follow a linear regression. This may indicate that coexistence of the two monomers has an influence on their reactivity and/or the reactivity of the decomposition products. Previous studies have shown that coexistence of guaiacol and syringol has an effect on the overall pyrolysis process, which may alter the product distributions.[32] Hence, the selection of particular marker compounds is important when establishing the S:G ratio via pyrolysate area percent comparisons since particular compounds may be more or less abundant given the starting S:G ratio. Therefore, it may prove to be more accurate to include as many marker compounds for each monomer as possible.

Table 3.3. Pyrolysates produced from the pyrolysis of mixtures of sinapyl and coniferyl alcohol at 650 °C. Values reported are obtained from total ion chromatogram area %. Values in parenthesis are absolute standard deviations.

Compound Number	Retention Time (min)	Compound	Area % (S:G = 0.1)	Area % (S:G = 0.4)	Area % (S:G = 0.9)	Area % (S:G = 1.7)
1	10.4	toluene	0.13 (0.02)	0.08 (0.01)	0.07 (0.02)	0.13 (0.04)
2	25.5	phenol	0.05 (0.01	0.05 (0.00)	0.05 (0.010)	0.12 (0.02)
3	26.2	2-methoxyphenol	1.36 (0.27)	0.99 (0.20)	0.86 (0.05)	1.09 (0.09)
4	27.2	2-methylphenol	0.10 (0.02)	0.08 (0.02)	0.06 (0.00)	0.10 (0.01)
5	28.5	4-methylphenol	0.05 (0.02)	0.03 (0.01)	0.02 (0.00)	0
6	28.8	2-methoxy-3-methylphenol	0.08 (0.02)	0.08 (0.01)	0.08 (0.01)	0.09 (0.05)
7	30.0	2-methoxy-4-methylphenol	2.18 (0.32)	1.55 (0.36)	1.13 (0.09)	1.69 (0.3)
8	30.2	2,4-dimethylphenol	0.21 (0.02)	0.14 (0.04)	0.09 (0.01)	0.16 (0.04)
	30.5	3,5-dimethoxytoluene	0.04 (0.01)	0.03 (0.00)	0.03 (0.00)	0.04 (0.01)
29	31.0	2,4,6-trimethylphenol	0.02 (0.00)	0.02 (0.00)	0.02 (0.00)	0.05 (0.00)
9	32.8	4-ethyl-2-methoxyphenol	0.39 (0.07)	0.32 (0.07)	0.24 (0.03)	0.31 (0.04)
10	34.7	2-methoxy-4-vinylphenol	5.64 (0.81)	3.09 (0.26)	3.89 (0.27)	3.48 (0.32)
11	35.4	eugenol	2.19 (0.31)	1.24 (0.17)	1.34 (0.11)	1.40 (0.34)
12	35.9	2-allylphenol	0.19 (0.03)	0.08 (0.01)	0.05 (0.00)	0.11 (0.04)
31	36.4	2,6-dimethoxyphenol	0.53 (0.16)	1.12 (0.02)	1.67 (0.22)	4.38 (1.07)
15	37.2	cis-isoeugenol	1.67 (0.22)	1.04 (0.26)	1.10 (0.07)	1.19 (0.33)
33	37.4	3,4-dimethoxyphenol	0.06 (0.05)	0.20 (0.04)	0.25 (0.10)	0.69 (0.45)
17	38.9	trans-isoeugenol	8.79 (1.10)	5.71 (0.34)	6.35 (0.41)	8.18 (1/63)
34	39.2	4-methylsyringol	0.63 (0.17)	1.25 (0.09)	1.86 (0.41)	6.28 (1.11)
18	39.7	vanillin	3.43 (1.21)	1.95(0.072)	1.37 (0.29)	4.28 (0.39)
	40.7	1,2-dimethoxy-4-(2-propenyl)benzene	0.09 (0.02)	0	0	0

Table 3.3 (continued)

19	41.3	2-methoxy-4-propylphenol	2.15 (0.52)	1.37 (0.62)	0	2.15 (0.47)
20	41.6	2-methoxy-1,4-benzenediol	0.48 (0.13)	0	0.15 (0.11)	0
21	42.1	1-(4-hydroxy-3-methoxyphenyl)ethanone	0.24 (0.07)	0.14 (0.05)	0.11 (0.01)	0.16 (0.00)
36	43.1	4-vinylsyringol	1.56 (0.48)	2.81 (0.03)	5.01 (0.72)	12.76 (2.16)
37	43.5	2,6-dimethoxy-4-(2-propenyl)phenol	0.71 (0.30)	1.26 (0.16)	2.51 (0.52)	6.20 (0.38)
22	43.7	homovanillyl alcohol	0.12 (0.03)	0.06 (0.02)	0.12 (0.08)	0
39	45.0	2,6-dimethoxy-4-(1-propenyl)phenol (Z)	0.48 (0.17)	0.94 (0.12)	2.13 (0.76)	3.95 (0.55)
40	46.7	2,6-dimethoxy-4-(1-propenyl)phenol (E)	3.30 (1.02)	5.79 (0.26)	10.19 (1.09)	15.88 (1.19)
25	47.0	homovanillinic acid	3.99 (0.31)	3.28 (0.26)	2.86 (0.07)	0.14 (0.14)
41	47.5	4-hydroxy-3,5-dimethoxybenzaldehyde	2.68 (0.86)	1.39 (0.47)	1.88 (0.64)	0.76 (0.42)
42	48.7	4-propylsyringol	0.32 (0.13)	0.82 (0.86)	1.03 (0.28)	0.35 (0.17)
	50.0	coniferyl alcohol	31.10 (7.30)	35.56 (4.97)	28.39 (7.97)	3.10 (0.94)
26	50.5	3-(4-hydroxy-3-methoxyphenyl)-2-propenal	6.52 (2.71)	8.79 (0.16)	6.80 (0.81)	0.10 (0.09)
	56.1	sinapyl alcohol	0.18 (0.08)	0.77 (0.44)	0.62 (0.30)	0.13 (0.01)
43	56.5	3,5-dimethoxy-4-hydroxycinnamaldehyde	0.52 (0.15)	0.72 (0.35)	0.11 (0.01)	0.80 (0.53)

S:G ratios were calculated by summing the area % of certain sinapyl alcohol pyrolysates and dividing by the sum of the area percent of certain coniferyl alcohol pyrolysates. There are many marker groups that can be constructed, hence, the reported marker pyrolysates were chosen as examples according to abundance and standard deviation of area percent contributions. The first set of marker compounds (M1) used the 13 most abundant coniferyl alcohol pyrolysates and the 10 most abundant uniquely sinapyl alcohol pyrolysates that had relatively low standard deviations and did not include the starting products. Other marker compound groups were derived from M1 in order to try and minimize the number of products being considered. Table 3.4 shows the marker compound groups chosen for comparison. For example, the marker compounds in M3 were selected based on the major pyrolysates created during peach pit lignin pyrolysis.

Table 3.4. Marker compound groups chosen for calibration of molar S:G ratio using sum area % S:G ratios.

Marker compound group #	Sinapyl (S) pyrolysates	Coniferyl (G) pyrolysates
M1	2,6-dimethoxyphenol 4-methylsyringol 4-vinylsyringol 4-propylsyringol 2,6-dimethoxy-4-(2-propenyl)phenol 2,6-dimethoxy-4-(1-propenyl)phenol (Z) 2,6-dimethoxy-4-(1-propenyl)phenol (E) 4-hydroxy-3,5-dimethoxybenzaldehyde 3,5-dimethoxycinnamic acid	2-methoxyphenol 2-methoxy-4-methylphenol 4-ethyl-2-methoxyphenol 2-methoxy-4-vinylphenol eugenol 2-methoxy-4-(1-propenyl)phenol (Z) 2-methoxy-4-(1-propenyl)phenol (E) vanillin 2-methoxy-4-propylphenol 1-(4-hydroxy-3-methoxyphenyl)ethanone homovanillic acid homovanillic alcohol 3-(4-hydroxy-3-methoxyphenyl)-2-propenal
M2	4-vinylsyringol	2-methoxy-4-vinylphenol vanillin
M3 (peach pit lignin)	2,6-dimethoxyphenol 4-methylsyringol 4-vinylsyringol 2,6-dimethoxy-4-(2-propenyl)phenol 2,6-dimethoxy-4-(1-propenyl)phenol (Z) 2,6-dimethoxy-4-(1-propenyl)phenol (E) 4-hydroxy-3,5-dimethoxybenzaldehyde	2-methoxyphenol 2-methoxy-4-methylphenol 2-methoxy-4-vinylphenol 4-ethyl-2-methoxyphenol 2-methoxy-4-propylphenol eugenol 2-methoxy-4-(1-propenyl)phenol (Z) 2-methoxy-4-(1-propenyl)phenol (E) vanillin 4-hydroxy-3-methoxyacetophenone

Table 3.4 (continued)

M4	2,6-dimethoxyphenol 4-methylsyringol 4-propylsyringol 4-vinylsyringol	2-methoxyphenol 2-methoxy-4-methylphenol 2-methoxy-4-vinylphenol 2-methoxy-4-(1-propenyl)phenol (Z) 2-methoxy-4-(1-propenyl)phenol (E)
M5	2,6-dimethoxyphenol	2-methoxy-4-vinylphenol
M6	4-hydroxy-3,5-dimethoxybenzaldehyde	2-methoxy-4-vinylphenol

Figure 3.3 shows the plots constructed from the S:G sum area % of M1, M2 and M3 marker compounds vs. molar S:G ratios. M1 provides a linear correlation between S:G sum area percent and molar S:G. However, since the slope is not exactly one; the sum area % ratios do not accurately reflect the actual molar S:G ratios. Additionally, the plot does not pass through the origin, i.e., a S:G ratio greater than 0 would be obtained even if there were no sinapyl alcohol in the sample. This would also be the case if accounting for the possible demethoxylation of sinapyl markers during pyrolysis; i.e. some coniferyl marker area percent needs to be considered as having developed from the demethoxylation of sinapyl alcohol. There would always be some G-marker pyrolysate contribution towards sinapyl alcohol and hence a positive S:G ratio if the demethoxylation reaction occurred to a significant extent. Our findings indicate that demethoxylation does not occur in our pyrolysis system to an extent that would greatly affect the measurement of the molar S:G ratio. Therefore, there is no need to adjust pyrolysate distribution to account for demethoxylation. M1 is the marker group that contained the largest amount of marker compounds for each monomer and was predicted to provide the most reasonable linear correlation and accuracy. Of all of the marker groups, M1 provided a line with a slope close to 1, a y-intercept close to 0, and a reasonable correlation coefficient. If the line is forced through the origin, the equation for M1 becomes y= 1.2547x with $R^2 = 0.9889$.
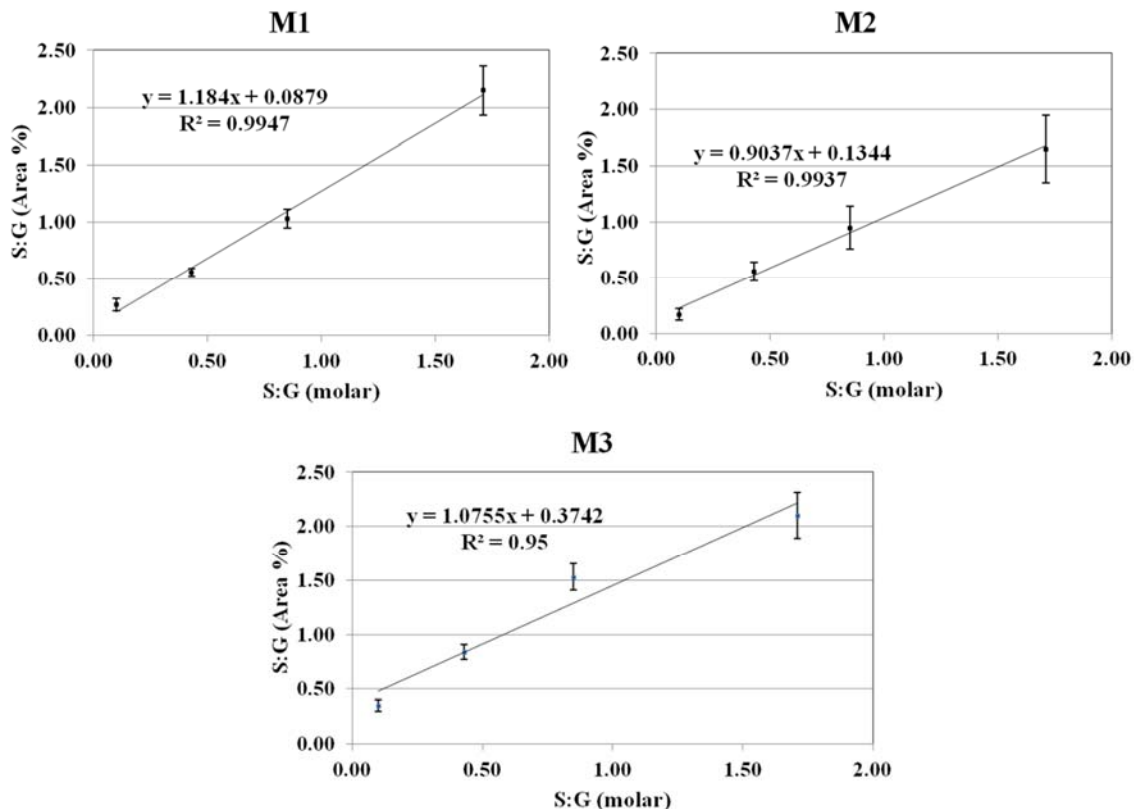
Figure 3.3. Sum area percent S:G ratio vs. molar S:G for marker compound groups M1, M2 and M3.

The other marker compound groups contained fewer markers for each monomer. The plot for M2 shows a similar R^2 in comparison to M1 but the deviation of each data point is higher. In this case, the slope of the calibration curve is also not exactly 1 and the intercept is still positive, indicating a lower limit for the molar S:G ratio of 0.13. When this line is forced through the origin, the slope of the line becomes 1.0118 and the R^2 is 0.9708. Hence, it is reasonable to say that there is a direct linear correlation between molar S:G ratio and the sum area % S:G ratio for the markers in M2. Notably, M2 contains only one marker compound representing sinapyl alcohol and two marker compounds representing coniferyl alcohol. However, given the pyrolytic profile of the particular sample being analyzed, it may be more accurate to use as many markers for each monomer as possible. For example, lignin pyrolysates produced from switchgrass may be different than those produced from coconut shells. Hence, markers for each monomer chosen should be a fair representation of the pyrolytic profile of the biomass being analyzed. If switchgrass produces insignificant quantities of a particular marker, its contribution may be minimal. However, the same marker may be produced in higher abundance from coconut shells and should be accounted for when determining S:G ratios. Utilizing as many markers for the

given biomass helps to eliminate errors that may occur when accounting for a few pyrolysates for each monomer.

M3, the marker group selected according to the results of peach pit lignin pyrolysis, has a slope that is 0.005 greater than M1 and the R^2 is slightly smaller than for M1 but it still shows a reasonable linear correlation. However, this line has a larger *y*-intercept of 0.3742; hence, it would not be useful for deriving very small S:G ratios. Using this equation, the S:G ratio in peach pit lignin was found to be 0.13. Results from the capillary electrophoresis of peach pit lignin oxidation products gave an S:G of 0.16. Hence, the pyroprobe and capillary electrophoresis of $KMnO_4$ oxidation products yield similar S:G values. Overall, the marker compounds chosen for M1, M2 and M4 provide the best linear fit and closer correlation for measuring molar S:G ratios according to the sum area percent of the selected marker compounds than marker compound groups M5 and M6. As noted above, the marker compound group M3 also exhibits a reasonable linear correlation with molar S:G ratios due to its slope and R^2 being close to one; however, it may not be appropriate for samples with small S:G ratios due to its large y-intercept.

M4, M5 and M6 plots of S:G area percent vs. molar S:G are shown in Figure 3.4. M4 is the most accurate marker compound group in this figure and was selected based on marker compounds used by Nunes et al; these marker compounds were shown to correlate to S:G ratios obtained by nitrobenzene oxidation.[12] This curve, while the slope is not exactly 1, still displays a reasonable linear relationship between sum area percent S:G ratios and molar S:G ratios. After adjusting S:G ratios using this calibration curve, molar S:G values obtained are very similar to sum area percent S:G ratios. In contrast, M5 and M6 plots demonstrate how the area percent S:G ratio of some compound groups do not accurately represent the molar S:G ratio or provide acceptable linear relationships with respect to the relative production of the compounds in mixtures. This indicates that competing pathways occur during pyrolysis that cause marker compounds to form other pyrolysates, the formation of which needs to be accounted for when comparing one monomer to another. Therefore it is important to account for as many marker pyrolysates as possible, depending on their relative abundance.
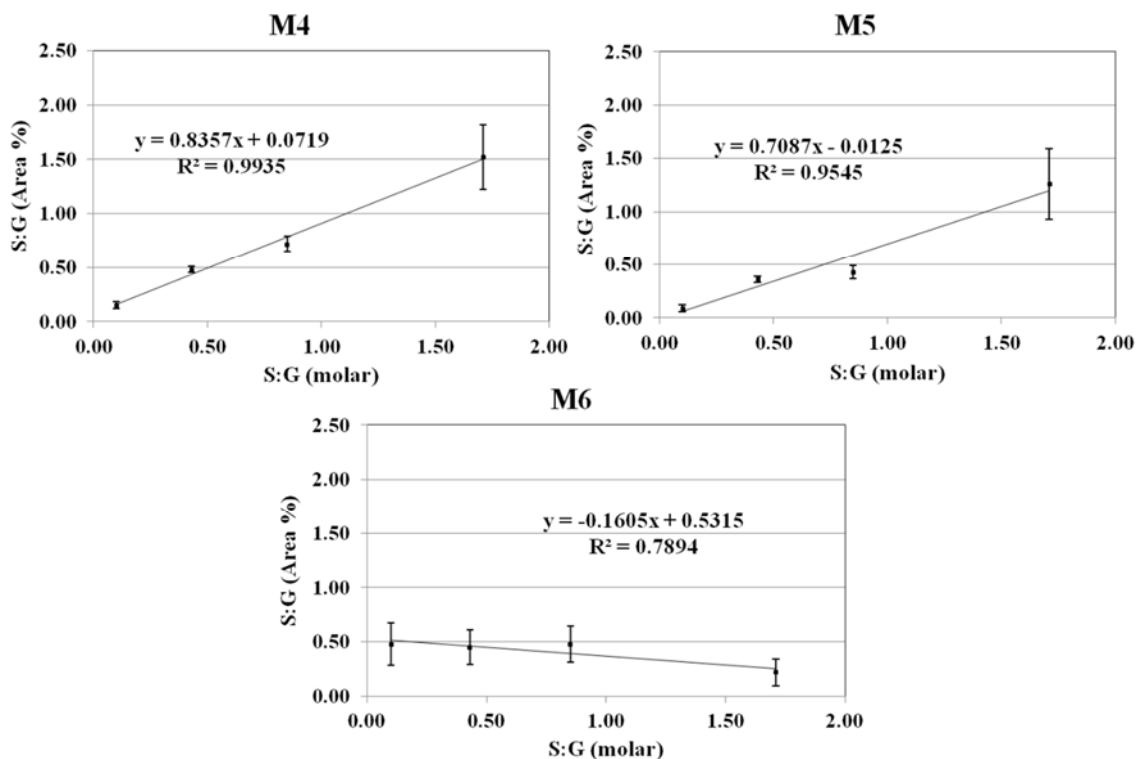
Figure 3.4. Sum area percent S:G ratio vs. molar S:G for marker compound groups M4, M5 and M6.

Given the number of pyrolysates produced from each alcohol, a large amount of marker compound groups can be assembled for calibration of molar S:G ratios. Hence, having the pyrolysate profiles of the mixtures of sinapyl and coniferyl alcohols makes it possible to construct unique calibration curves according to particular marker compounds that may appear during pyrolysis of certain types of biomass. For example, marker compounds chosen to analyze S:G ratios in switchgrass may not be suitable for application to alfalfa pyrolysis given the relative abundances of the pyrolysates produced. Since different marker compound groups show different calibration curves, it would be better to first analyze the biomass pyrolysate profile for the most abundant pyrolysates and use an appropriate S:G calibration curve.

It should also be noted that factors such as biomass particle size and the presence of inorganic species in biomass may influence the amount and types of products formed during pyrolysis.[34,35] The relative amounts of lignin-based pyrolysates may also be influenced by the types and abundances of the various bonds within the lignin polymers.[30] The reactor and parameters used in pyrolysis experiments will also influence different product distributions. Hence, caution should

be taken when extrapolating conclusions based on calibrations of models. Calibrations should be applied to unique systems as opposed to being adapted from other reported results.

3.4 Conclusions

To facilitate measurement of the S:G ratio of lignin in biomass, pyrolysis-GC/MS calibration curves were obtained by plotting S:G sum area % ratios from certain marker pyrolysates originating from sinapyl and coniferyl alcohol against the molar sinapyl:coniferyl alcohol ratio. The equations describing the calibration curves changed depending on the pyrolysates chosen in the marker compound groups, and some curves showed improved linearity over others, particularly those groups containing a larger number of marker compounds. Demethoxylation of sinapyl alcohol occurred, indicating that not all of the guaiacyl-related compounds originate from the coniferyl monomer. However, demethoxylation only occurred to a very minor extent; hence, correction of the S:G ratio is not necessary. Depending on the abundance of the various lignin pyrolysates in different types of biomass, it may be necessary to construct calibration curves using unique marker compound groups. Having the pyrolysate profiles of sinapyl alcohol, coniferyl alcohol, and various mixtures of the two makes it possible to construct S:G ratio calibration curves using a variety of marker compounds from each alcohol. To validate the calibrations, the S:G ratio of peach pit lignin was determined using Py-GC/MS and found to agree with the S:G ratio obtained from capillary electrophoresis of $KMnO_4$ oxidation products from the peach pit lignin.

Chapter 4. Characterization of Endocarp Biomass and Lignin Extracted by Different Techniques using Pyrolysis and Spectroscopic Methods

4.1 Introduction

The development of renewable sources of fuel and chemicals from biomass is being investigated world-wide in order to alleviate our dependency on non-renewable fossil fuels. Thermochemical methods, such as pyrolysis, offer a means of converting biomass into liquid products (pyrolysis oil) which can be upgraded into valuable chemicals and fuels.[1-4] The properties of pyrolysis oil, otherwise known as bio-oil, are dependent on the composition of the starting feedstock and the pyrolysis conditions applied.[5-8] Pyrolysis of many types of biomass such as switchgrass, eucalyptus and algae, as well as biomass components such as lignin extracted from lignocellulosic feedstocks,[5,9-13] has been investigated. Lignin, the second most abundant natural polymer after cellulose, constitutes up to 40 wt% of lignocellulosic biomass and more than half of its energy content.[1,14] However, lignin has traditionally been regarded as a waste product from the pulping industry and has been underutilized, despite its potential to produce valuable products including aromatic hydrocarbons. Of late, there has been increased interest in the utilization of lignin for the production of chemicals and other bio-products using thermochemical methods such as pyrolysis. Indeed, lignin extracted in pulping plants, as well as high-lignin biomass such as waste nut shells, shows great potential as a feedstock for biofuel production from thermochemical processing. For example, a recent study by Mendu et al. elucidated the potential energy contribution that high-lignin endocarp feedstocks (e.g., coconut shell) could provide to poverty-stricken nations.[15]

Effective pretreatment processes are required to efficiently utilize whole biomass intended for the production of bio-products. Many methods are currently used to separate the biopolymer fractions in biomass for specific applications, particularly in the pulping industry. For example, organosolv and Kraft processes have been thoroughly researched and developed for delignification of biomass.[16,17] A promising alternative to these processes is formic acid pulping. Successful separation of biomass, such as beech, corncob, eucalyptus and bagasse, into its separate cellulosic, hemicellulosic and lignin fractions, with minimal hydrolysis of the remaining cellulose, has been achieved by formic acid pulping under a variety of relatively mild conditions.[18-23] The formic acid can be recovered for reuse and the process generates sulfur-free lignin that can be further processed. However, the lignin extracted from formic acid pulping has received little attention in terms of characterization and utilization. Moreover, formic acid pulping

of high-lignin biomass such as nut shells, particularly for the purpose of lignin extraction, has not been adequately studied to date.

Of the analytical methods available to characterize biomass and its lignin extracts, Pyrolysis-GC/MS (Py-GC/MS) has emerged as both a powerful and convenient technique.[9,13,24,25] This analysis quantifies the products formed from the thermal decomposition of biomass and hence provides information about both the composition and structure of the biomass, as well as its resulting bio-oil composition. Py-GC/MS has previously been used to analyze pyrolysates formed from lignocellulosic biomass,[26] extracted lignin[9] and high-lignin endocarp biomass as well as its formic acid-extracted lignin,[24] Other techniques, such as NMR and thioacidolysis have been used to support Py-GC/MS analysis as a means to characterize milled wood lignin isolated from coconut coir.[27] However, endocarp lignin isolated using sulfuric acid has not been characterized by Py-GC/MS, nor has the amount of lignin that can be extracted using formic acid been quantified. Moreover, while high-lignin feedstocks such as the stones and shells of fruits and nuts are important byproducts of the food industry, to date they have received little attention as a source of fuel and chemicals.[28] Although several studies concerning the pyrolysis of coconut shells[29,30] and various nut shells[31] have been performed, thorough analysis and understanding of the pyrolysis of these feedstocks is still lacking.

The goal of this investigation was to compare the pyrolysate distributions and TGA profiles of biomass from four high-lignin drupe endocarp biomass types, black walnut shell (*Juglans nigra)*, olive pits (*Olea europaea*), peach pits (*Prunus persica*), and coconut shells (*Cocos nucifera*) with that of lignin extracted using two techniques based on sulfuric acid and formic acid. Differences in lignin yield, weight loss curves and pyrolysate distributions from the two extractions provide insight into the abundance, structure and composition of the lignin within the biomass, as well as changes induced by the extraction process. FTIR and heteronuclear single quantum coherence (HSQC) NMR analysis of the extracted lignins also provide structural and compositional information that supplement the Py-GC/MS results.

4.2 Materials and Methods

4.2.1 Chemicals

All chemicals and reagents used were of analytical grade or higher. Authentic samples of organic compounds were obtained as applicable from Sigma-Aldrich (St Louis, MO, USA), FMC BioPolymer (Philadelphia, PA, USA), Fisher Scientific (Pittsburgh, PA, USA), Riedel-de Haën (Seelze, Germany) and BDH Merck Ltd (Poole, UK).

4.2.2 Sulfuric Acid Technique for Determination of Klason Lignin Content

The biomass analyzed included black walnut shell (*Juglans nigra)*, coconut shell (*C. nucifera*), peach pit (*P. persica*) and olive pit (*O. europaea*). Fresh endocarp biomass from these sources was isolated by physical removal from the remaining pericarp and mesocarp tissue prior to aqueous washing. Pure endocarp biomass was ground to a particle size of < 1 mm using an Arthur H Thomas Co. scientific grinder (Philadelphia, PA, USA). Samples were then degummed using ethanol and acetone to remove extractives and dried overnight at 80 °C prior to extraction and analysis.[24] Acid-soluble and acid-insoluble lignin content (Klason lignin) was determined according to NREL laboratory analytical procedures (LAP).[32] Briefly, 300 mg of biomass was hydrolyzed in 3 mL of 72% H_2SO_4 for 1 h at 30 °C. The H_2SO_4 concentration was diluted to 4% in water and the mixture heated at 120 °C for 1 h. The acid-soluble lignin content was spectrophotometrically determined at 320 nm. Acid-insoluble lignin was calculated based on dry weight and ash content was determined using thermogravimetric analysis (TGA). Each sample was analyzed for lignin content in triplicate. For comparison of the mass of extractable lignin, walnut shell lignin was also extracted in 4% H_2SO_4 at 65 °C for 24 h instead of 120 °C for 1 h. Walnut shell Klason lignin content was also determined using sulfuric acid according to ASTM D1106.[33]

4.2.3 Lignin Extractions using 85% Formic Acid

Lignin was extracted from each sample by stirring 1 g of degummed biomass with 20 ml of 85% formic acid containing 0.2% HCl (35% assay) in a sealed vessel for 24 h at 65 °C. The mixture was then filtered, the solid residue was washed with formic acid and the liquid filtrate containing lignin and hemicellulose was rotary evaporated to recover formic acid. Next, water was added to the residue remaining after evaporation to dissolve hemicellulose present, leaving behind a lignin precipitate. The water mixture was then centrifuged, decanted, and filtered to collect lignin which was washed with water and dried overnight in an oven at 80 °C. The pulp residue remaining from

the initial extraction step was also dried overnight in an oven at 80 °C. This procedure was repeated three times for each biomass sample. For comparison of total lignin recovered, walnut shell was also subjected to formic acid extractions for 3 h at 90 °C and 120 °C. These extraction temperatures were chosen in effort to extract the maximum amount of lignin without hydrolyzing cellulose. A 24 h, 65 °C extraction of walnut shell lignin was also monitored over time by taking a 10 µL sample of the supernatant formic acid and diluting in 2 mL of formic acid/HCl. The diluted sample was then analyzed by UV/Vis spectroscopy from 800 to 280 nm in a Cary-Varian 300 Bio UV/Vis spectrophotometer equipped with a temperature controlled Peltier sample block (Varian).

4.2.4 Pyrolysis-GC/MS

Experiments were performed using a Pyroprobe Model 5200 (CDS Analytical, Inc.) connected to an Agilent 7890 GC with an Agilent 5975C MS detector. The pyroprobe was run in trap mode under He atmosphere. Pyrolysis was conducted at 650 °C (1000 °C/s heating rate) for 20 s. The valve oven and transfer lines were maintained at 325 °C. The column used in the GC was a DB1701 (60 m × 0.25 mm × 0.25 µm) and the temperature program was as follows: 45 °C for 3 min, ramp to 280 °C at 4 °C/min and hold for 10 min. The flow rate was set to 1 mL/min using He as the carrier gas. The inlet and auxiliary lines were both maintained at 300 °C and the MS source was set at 70 eV. The GC-MS was calibrated for a number of phenolic compounds including phenol, 2-methoxyphenol, 2-methoxy-4-methylphenol, 2,6-dimethoxyphenol, vanillin, syringaldehyde and 2-methoxy-4-vinylphenol. Pyrolysis products were analyzed according to retention times and mass spectra data obtained from a NIST library.

A 1 mg aliquot of the ground (45-150 µm) biomass, pulp residue or lignin samples was analyzed in a quartz cell packed with quartz wool. Samples were heated to 100 °C for 10 s in the probe prior to analysis in order to remove any residual water. Prior to sample analysis, blank experiments were performed in order to validate the cleanliness of the system. After sample analysis, methanol was run as a sample to remove any condensed products inside the pyroprobe. Methanol and blank experiments were repeated as necessary until the system was clean.

4.2.5 Thermogravimetric Analysis (TGA)

Thermogravimetric analysis (TGA) was performed under N_2 (50 mL/min) using a TA Discovery TGA. Ground lignin extract (5-10 mg) was used, with the temperature being ramped from ambient temperature at 10 °C/min to 1000 °C. Determination of ash content in biomass and sulfuric acid lignin was performed using the same temperature ramp under air at 25 mL/min. Ash content was taken to be the final weight percent remaining at 1000 °C.

4.2.6 FTIR and NMR Spectroscopy

FTIR spectra of ground, dried sulfuric and formic acid-extracted lignin samples were obtained using a Nicolet 6700 spectrometer equipped with an attenuated total reflectance (ATR) accessory containing a diamond crystal. Spectra were collected from 600 to 4000 cm^{-1}, 32 scans being taken at a resolution of 4 cm^{-1}.

For heteronuclear single quantum coherence nuclear magnetic resonance spectroscopy (HSQC NMR) analysis of formic acid-extracted lignins, 100 mg of lignin was dissolved in 0.60 mL of DMSO-d_6. Sulfuric acid-extracted lignins and whole biomass were not analyzed because of their low solubility in DMSO-d_6. NMR spectra were collected at 60 °C on a Varian Inova 600 MHz equipped with a pulsed field gradient probe. The spectral widths were 6595 and 33195 Hz for the ^1H and ^{13}C dimensions, respectively. Data sets of 120 transients and 208 increments were recorded and processed using a Gaussian function corresponding to 35 ms in the ^1H dimension and 8.5 ms in the ^{13}C dimension. DMSO (at 25 °C) was used as the chemical shift reference (δ_C/δ_H, 39.51/2.50). It should be noted that analysis of each of these lignins is limited by the solubility of the lignin in DMSO-d_6. The samples were centrifuged and residual solids that were trapped in the NMR cap were not analyzed by NMR.

4.3 Results and Discussion

4.3.1   Mass Recovery of Lignin Extracted from Endocarp using Sulfuric and Formic Acid

Acid-soluble and acid-insoluble lignin and ash content for each sample were determined according to NREL LAP[32] (sulfuric acid) and are reported in Figure 4.1. The results agree with previous analyses[24] of the same endocarp materials and are considered to be the maximum amount of extractable lignin. NREL sulfuric acid lignin content for walnut shell also agreed with ASTM D1106 lignin determination, which is likewise based on the use of sulfuric acid.
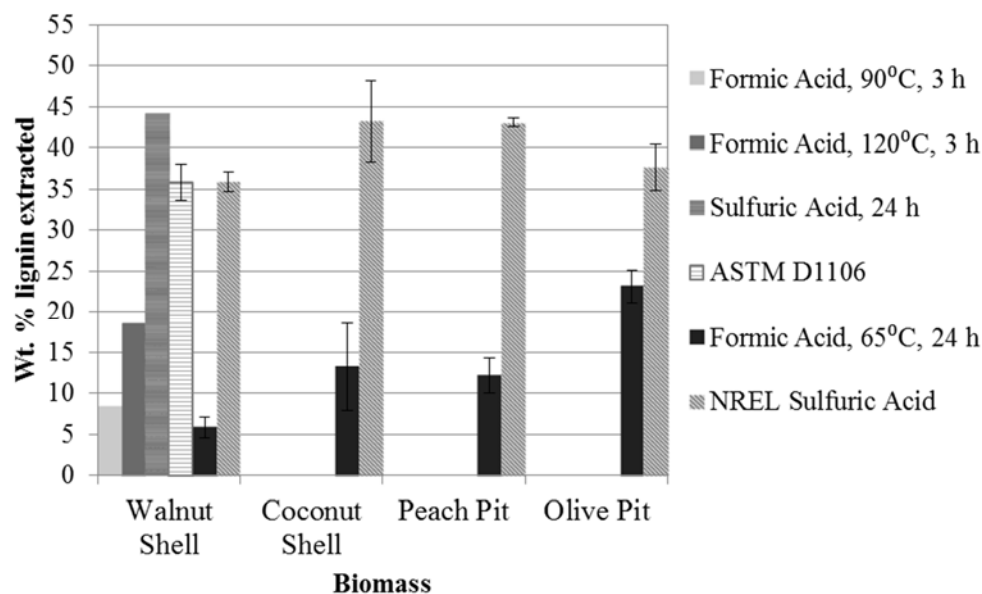
Figure 4.1. Wt% of lignin extracted from endocarp using different acid extraction techniques. Bars represent standard deviations for 3 experiments.

In contrast, treatment of each of the biomass samples with 85% formic acid for 24 h at 65 °C extracted only a fraction of the amount of lignin extracted by sulfuric acid. Moreover, the amount of lignin extracted using formic acid did not correlate with the total lignin content determined using sulfuric acid. Figure 4.2 shows the UV/Vis spectra of the supernatant formic acid sampled from a walnut shell lignin extraction over a 24 h period. Absorbance at 320 nm was chosen as the reference for lignin and appeared to reach a maximum in the time interval 18 -24 h. These results suggest that the maximum amount of lignin extractable by formic acid occurred within 24 h under these conditions. However, the absorbing chromophores (with unique molar absorptivities) may have been changing in concentration over time; hence, quantitative analysis by UV/Vis may lack precision.

The difference between the amount of lignin extracted using formic acid and sulfuric acid for each biomass sample is likely due to the variation in the structure of lignin and its bonding network with the holocellulosic fraction of the biomass. Lignin analysis of more than one type of biomass was performed in order to see whether the lignin extracted from different sources using the same techniques produced the same pyrolysate distribution, indicating similar lignin

structures. Results discussed below (see Section 4.3.3) confirm that the formic and sulfuric acid extraction techniques yield lignin that is unique to the biomass from which it is extracted.

The data also suggest that formic acid extraction parameters were not optimal for isolating lignin from endocarp (Figures 4.1 and 4.2). For comparison, lignin was extracted from walnut shells in formic acid at 90 °C and 120 °C for 3 h. Although the amount of lignin extracted slightly increased with increasing temperature, the amount of remaining solid residue decreased by more than expected due to hydrolysis of the carbohydrate fraction. Moreover, the amount of lignin extracted using formic acid at 120 °C was only about half of the total lignin in the feedstock.
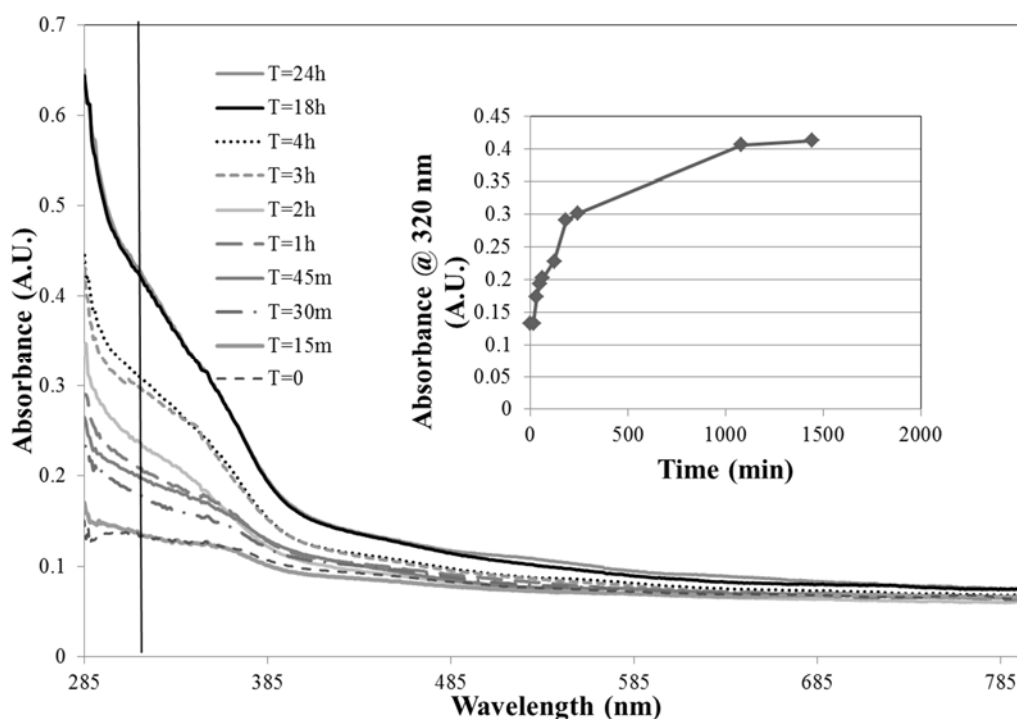
Figure 4.2. UV/Vis spectra of the diluted supernatant formic acid sampled during lignin extraction from walnut shell at 65 °C over 24 h. Inset: absorbance at 320 nm vs. time.

4.3.2 Whole Biomass Pyrolysis

Tables 4.1 – 4.4 show the amounts, based on relative total ion chromatogram peak areas, of select pyrolysates produced from the pyrolysis of the whole biomass samples and their respective lignin extracts and residues. Note that only the most abundant compounds are reported (standard deviations being reported for the most abundant of these compounds). Other numerous compounds were evident in the pyrograms that were excluded due to their small quantities and

high standard deviations (see Supplementary Tables 4.1 –4.4 in Appendix 2 for further details) although their area % contributions were included in the totals in Tables 4.1 -4.4. Pyrograms obtained from pyrolysis of each biomass type and the corresponding lignins are shown in Figures 4.3 –4.6, while Table 4.5 shows the sum area percent S:G ratios based on pyrolysate distributions that were determined for each of the biomass types and corresponding fractions.

Notable differences in the lignin-based pyrolysate distributions are seen between the different types of whole biomass endocarp and their respective lignin and residue fractions. For example, pyrolysis of walnut shells and peach pits (Tables 4.1 and 4.2, pyrograms in Figures 4.3 and 4.4) produced mostly 2-methoxy-4-vinylphenol and 2-methoxy-4-(1-propenyl)phenol, both of which originate from the coniferyl monomer. These findings indicate that walnut shells and peach pits have low S:G ratios in the lignin polymer. On the other hand, the most abundant coconut shell pyrolysates included 2-methoxy-4-vinylphenol and 2,6-dimethoxyphenol (Tables 4.3, pyrogram in Figure 4.5), indicative of a higher S:G ratio based on pyrolysates than the walnut shells and peach pits.

Table 4.1. Walnut shell pyrolysates from whole biomass and extracted lignin.

Compound Number	Retention Time (min)	Compound	Whole Biomass Area %	Formic Acid Lignin Area %	Sulfuric Acid Lignin Area %
1	8.63	acetic acid	4.85 (± 0.47)	0.10	0.09
	13.44	acetic acid ethenyl ester	1.48 (± 0.09)	0.00	0.00
2	15.50	furfural	1.75 (± 0.06)	0.48	0.91
	19.80	1,2-cyclopentanedione	1.62 (± 0.08)	0.01	0.03
3	22.80	4-hydroxy-5,6-dihydro-2H-pyran-2-one	1.92 (± 0.11)	0.20	0.07
	23.65	2-hydroxy-3-methyl-2-cyclopenten-1-one	1.72 (± 0.07)	0.00	0.00
4	24.71	phenol	0.96	3.25 (± 1.37)	1.27 (± 0.41)
5	25.35	2-methoxyphenol	5.06 (± 0.21)	9.62 (± 2.61)	4.58 (± 0.95)
	26.46	2-methylphenol	0.56	1.80 (± 1.05)	1.60 (± 0.65)
	27.72	4-methylphenol	0.67	2.89 (1.02)	1.54 (± 0.38)
6	29.01	2-methoxy-4-methylphenol	3.87 (± 0.48)	10.51 (± 2.57)	7.76 (± 2.36)
	29.37	2,4-dimethylphenol	0.47	2.00 (± 1.27)	2.27 (± 0.90)
	32.31	4-ethyl-2-methoxyphenol	1.56 (± 0.28)	3.05 (± 0.65)	2.41 (± 0.60)
7	33.76	2-methoxy-4-vinylphenol	12.61 (± 0.23)	10.59 (± 1.39)	3.65 (± 0.15)
	34.55	eugenol	2.80 (± 0.15)	1.80 (± 0.58)	0.34
	35.39	1,2-benzenediol	0.00	0.52	1.50 (± 0.70)
8	35.48	2,6-dimethoxyphenol	2.71 (± 0.23)	3.82 (± 0.54)	3.22 (± 0.38)
	36.31	2-methoxy-4-(1-propenyl)phenol (Z)	2.33 (± 0.23)	2.03 (± 0.63)	1.41 (± 0.46)
	37.80	4-methyl-1,2-benzenediol	0.00	0.00	1.53 (± 0.76)
9	37.90	2-methoxy-4-(1-propenyl)phenol (E)	12.50 (± 0.26)	6.73 (± 3.66)	4.35 (± 0.67)
10	38.30	4-methylsyringol	1.16	2.66 (± 0.72)	2.58 (± 0.50)

Table 4.1 (continued)

11	38.65	vanillin	3.54 (± 0.83)	3.47 (± 1.59)	4.25 (± 1.50)
	41.05	4-hydroxy-3-methoxyacetophenone	1.00	0.79	1.71 (± 1.56)
12	42.15	4-vinylsyringol	1.57 (± 0.41)	0.38	0.88
		Sum identified compounds	78.37 (± 0.56)	76.56 (± 5.32)	56.51 (± 1.53)
		Sum lignin-based pyrolysates	61.61 (± 1.12)	75.70 (± 4.94)	55.07 (± 2.13)
		Sum sinapyl-based pyrolysates	7.14 (± 0.96)	8.39 (± 0.60)	8.50 (± 2.35)
		Sum coniferyl-based pyrolysates	47.61 (± 0.54)	50.73 (± 2.74)	32.05 (± 1.51)
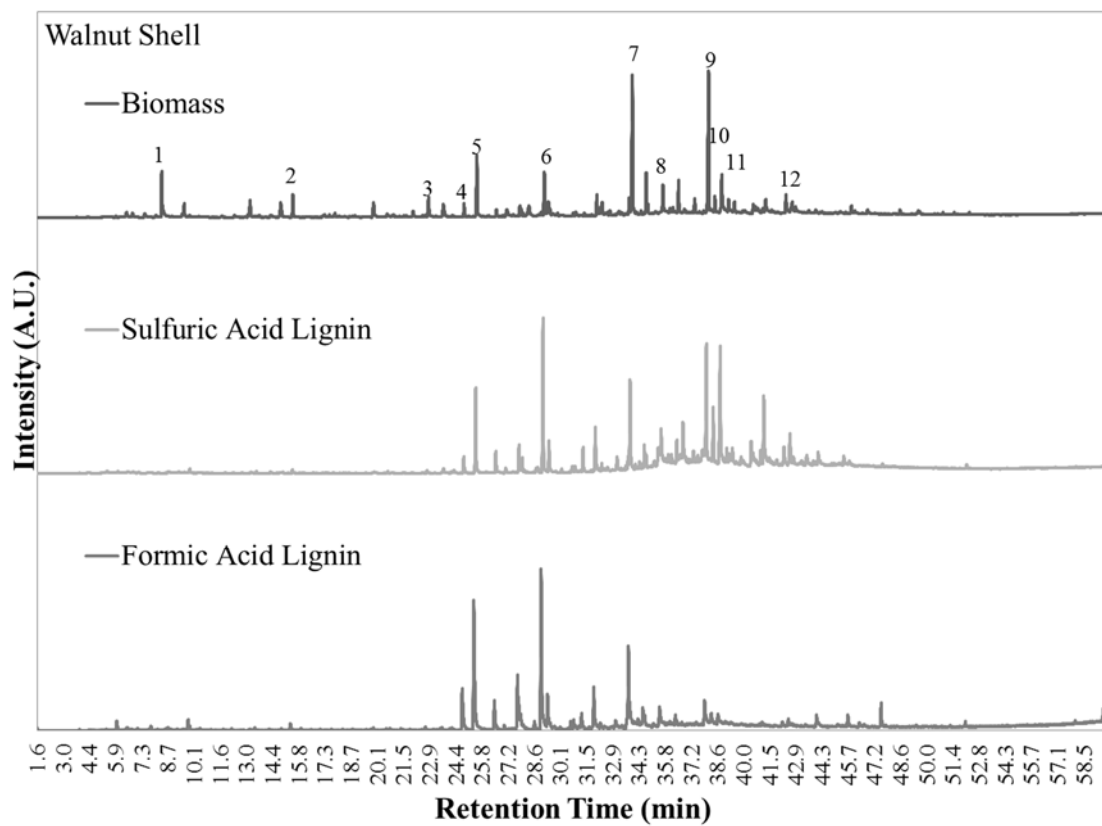
Figure 4.3. Pyrograms obtained from pyrolysis of walnut shell and corresponding lignin fractions.

Table 4.2. Peach pit pyrolysates from whole biomass and extracted lignin.

Compound Number	Retention Time (min)	Compound	Whole Biomass Area %	Formic Acid Lignin Area %	Sulfuric Acid Lignin Area %
1	8.63	acetic acid	1.87 (± 0.66)	0.92	0.14
	13.44	acetic acid ethenyl ester	1.90 (± 0.06)	0.00	0.00
2	15.50	furfural	1.89 (± 0.21)	1.35	1.20
3	22.80	4-hydroxy-5,6-dihydro-2H-pyran-2-one	4.23 (± 0.34)	1.41	0.00
	23.65	2-hydroxy-3-methyl-2-cyclopenten-1-one	2.16 (± 0.27)	0.00	0.12
4	24.71	phenol	0.74	0.77	2.00 (± 0.60)
5	25.35	2-methoxyphenol	3.08 (± 0.38)	3.70 (± 0.05)	7.50 (± 1.81)
	26.46	2-methylphenol	0.49	0.59	2.67 (± 1.03)
	27.72	4-methylphenol	1.20	0.67	1.52 (± 0.36)
	27.90	2-methoxy-3-methylphenol	0.23	0.23	1.74 (± 0.65)
6	29.01	2-methoxy-4-methylphenol	4.89 (± 0.85)	5.63 (± 0.86)	10.09 (± 1.54)
	29.37	2,4-dimethylphenol	0.87	0.90	3.63 (± 1.24)
	32.20	3-methyl-2,4(3H,5H)-furandione	1.61 (± 0.16)	0.00	0.00
	32.31	4-ethyl-2-methoxyphenol	1.67 (± 0.04)	1.32	3.36 (± 0.87)
7	33.76	2-methoxy-4-vinylphenol	10.35 (± 1.71)	4.67 (± 1.08)	3.23 (± 1.23)
	34.55	eugenol	2.77 (± 0.26)	2.01 (± 0.63)	0.33
8	35.48	2,6-dimethoxyphenol	2.51 (± 0.61)	4.71 (± 0.84)	3.60 (± 0.91)
	36.31	2-methoxy-4-(1-propenyl)phenol (Z)	2.12 (± 0.04)	2.21 (± 0.33)	0.77
9	37.90	2-methoxy-4-(1-propenyl)phenol (E)	9.21 (± 1.97)	7.38 (± 0.97)	2.71 (± 1.40)
10	38.30	4-methylsyringol	2.96 (± 0.76)	6.11 (± 1.35)	2.69 (± 1.19)
11	38.65	vanillin	2.89 (± 1.80)	6.55 (± 2.23)	2.82 (± 2.04)
	41.05	4-hydroxy-3-methoxyacetophenone	0.00	1.56 (± 0.95)	1.08

Table 4.2 (continued)

12	42.15	4-vinylsyringol	0.60	1.70 (± 0.94)	0.43
	42.56	1-(4-hydroxy-3-methoxyphenyl)acetone	0.22	2.17 (± 1.37)	0.41
	42.68	2,6-dimethoxy-4-(2-propenyl)phenol	0.30	1.60 (± 0.92)	0.17
		Sum identified compounds	72.30 (± 2.94)	66.07 (± 2.52)	58.69 (± 2.89)
		Sum lignin-based pyrolysates	52.19 (± 3.93)	61.82 (± 6.03)	56.43(± 2.25)
		Sum sinapyl-based pyrolysates	7.54 (± 1.43)	17.43 (± 5.08)	7.54 (± 2.57)
		Sum coniferyl-based pyrolysates	38.43 (± 3.77)	38.26 (± 1.87)	32.93 (± 1.01)
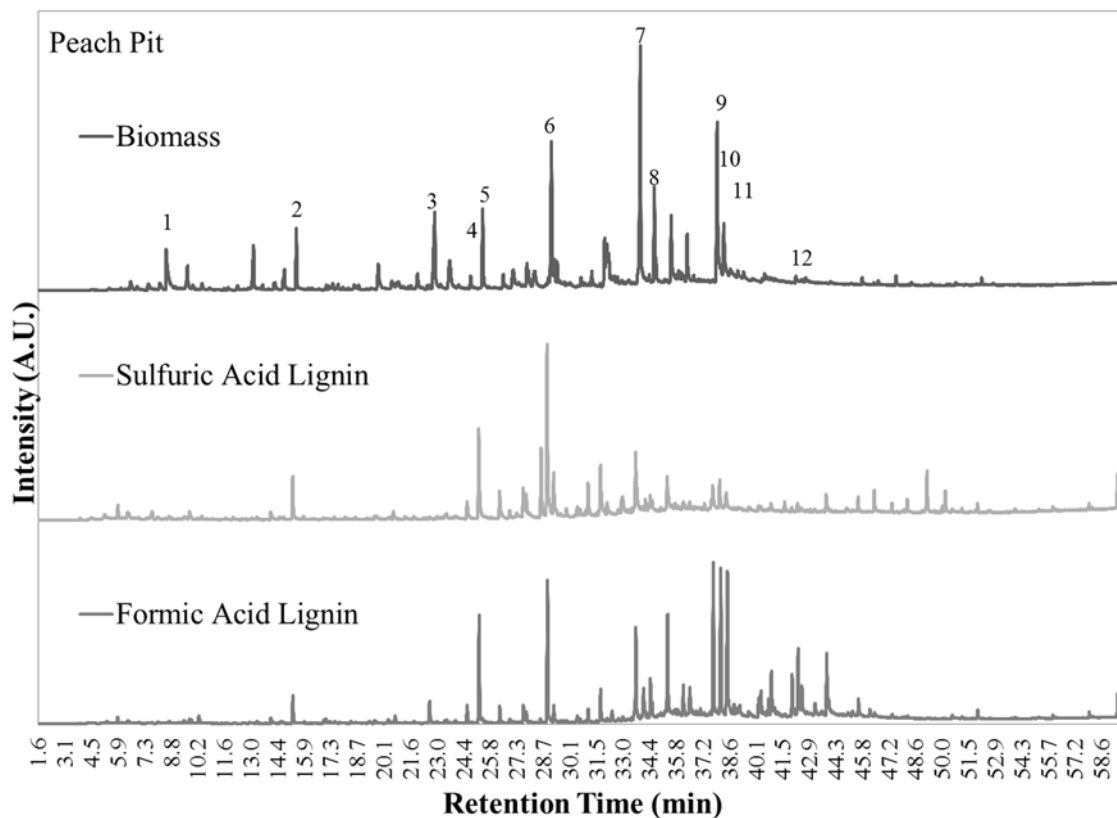
Figure 4.4. Pyrograms obtained from pyrolysis of peach pit and corresponding lignin fractions.

Coconut shell pyrolysis also produced more phenol than the other endocarp samples. According to pyrolysis studies of sinapyl and coniferyl alcohol monomers,[25] phenol was not produced from the pyrolysis of either of these monomers in any appreciable amount by demethoxylation. Hence, it most likely originates from the coumaryl monomer in the lignin polymer, which may be acylated or esterified or occur as *p*-hydroxybenzoate. Coumarate monomers, which are commonly found in herbaceous biomass,[34] may produce large amounts of 4-vinylphenol upon pyrolysis. Coconut shell pyrolysis did not produce this compound in significant amounts, which suggests that the source of the phenol was not from coumaryl monomers present as coumarate. NMR spectra, discussed in section 4.3.7, indicate that the majority of the coumaryl monomer (H-monomer) occurs as p-hydroxybenzoate. The presence of *p*-hydroxybenzoate in coconut coir has been elucidated by NMR in other studies, where phenol was also generated in high abundance according to Py-GC/MS analysis.[27] Olive pit pyrolysates (shown in Table 4. 4 and pyrogram in Figure 4.6) included large amounts of 2,6-dimethoxyphenol and 4-vinylsyringol, and like coconut

75

shells, generated more sinapyl-based pyrolysates relative to peach pit and walnut shell pyrolysates.

Consistent with the presence of hemicellulose and cellulose, the endocarp biomass produced more low molecular weight oxygenates during pyrolysis than the lignin extracts. Carbohydrate-based pyrolysates such as acetic acid, furfural, hydroxypropanone, dehydrated sugars and cyclopentenones were identified, of which acetic acid was the most abundant (with the exception of peach pit pyrolysis). In addition, carbohydrate-based pyrolysates such as methylfurans and levoglucosan were observed for the various samples, although these proved difficult to quantify due to peak coelutions and inconsistent production during pyrolysis. Inconsistencies could be due to secondary cracking of these compounds, char formation or condensation in the unit prior to analysis.[35]

Table 4.3. Coconut shell pyrolysates from whole biomass and extracted lignin.

Compound Number	Retention Time (min)	Compound	Whole Biomass Area %	Formic Acid Lignin Area %	Sulfuric Acid Lignin Area %
1	8.63	acetic acid	4.68 (± 0.19)	1.36 (± 0.19)	0.00
2	15.50	furfural	1.64 (± 0.04)	1.49 (± 0.45)	1.24
3	22.80	4-hydroxy-5,6-dihydro-2H-pyran-2-one	2.70 (± 0.11)	1.15	0.02
4	24.71	phenol	6.43 (± 0.34)	9.42 (± 2.69)	12.71 (± 3.09)
5	25.35	2-methoxyphenol	2.33 (± 0.06)	4.26 (± 0.91)	3.27 (± 0.68)
	26.46	2-methylphenol	0.47	1.33	5.98 (± 2.88)
	27.72	4-methylphenol	0.36	0.58	1.53 (± 0.47)
	27.90	2-methoxy-3-methylphenol	0.16	4.88 (± 0.48)	0.87
6	29.01	2-methoxy-4-methylphenol	1.70 (± 0.06)	0.95	3.83 (± 0.53)
	29.37	2,4-dimethylphenol	0.24	0.35	1.72 (± 0.71)
	32.31	4-ethyl-2-methoxyphenol	0.72	1.78 (± 0.27)	1.40
7	33.76	2-methoxy-4-vinylphenol	7.23 (± 0.33)	5.67 (± 1.22)	3.14 (± 0.63)
8	35.48	2,6-dimethoxyphenol	11.94 (± 0.28)	11.93 (± 1.45)	9.16 (± 2.90)
	36.31	2-methoxy-4-(1-propenyl)phenol (Z)	0.83	1.62 (± 0.06)	0.77
9	37.90	2-methoxy-4-(1-propenyl)phenol (E)	5.44 (± 0.01)	4.38 (± 1.01)	1.98 (± 0.71)
10	38.30	4-methylsyringol	5.62 (± 0.09)	8.14 (± 1.28)	9.09 (± 3.17)
11	38.65	vanillin	1.49 (± 0.20)	2.12 (± 1.42)	1.59 (± 0.95)
	40.48	4-ethylsyringol	1.89 (± 0.12)	1.40	2.07 (± 0.78)
12	42.15	4-vinylsyringol	6.46 (± 0.34)	1.17	1.36
	42.68	2,6-dimethoxy-4-(2-propenyl)phenol	2.35 (± 0.36)	0.92	0.44
	45.71	2,6-dimethoxy-4-(1-propenyl)phenol (E)	3.89 (± 0.24)	0.44	0.19

Table 4.3 (continued)

Sum identified compounds	81.11 (± 0.57)	74.24 (± 2.51)	67.56 (± 2.60)
Sum lignin-based pyrolysates	66.03 (± 0.411	69.68 (± 3.06)	65.16 (± 2.80)
Sum sinapyl-based pyrolysates	33.59 (± 0.29)	24.46 (± 0.60)	22.54 (± 8.03)
Sum coniferyl-based pyrolysates	23.03 (± 0.31)	24.32 (± 3.34)	17.13 (± 2.99)
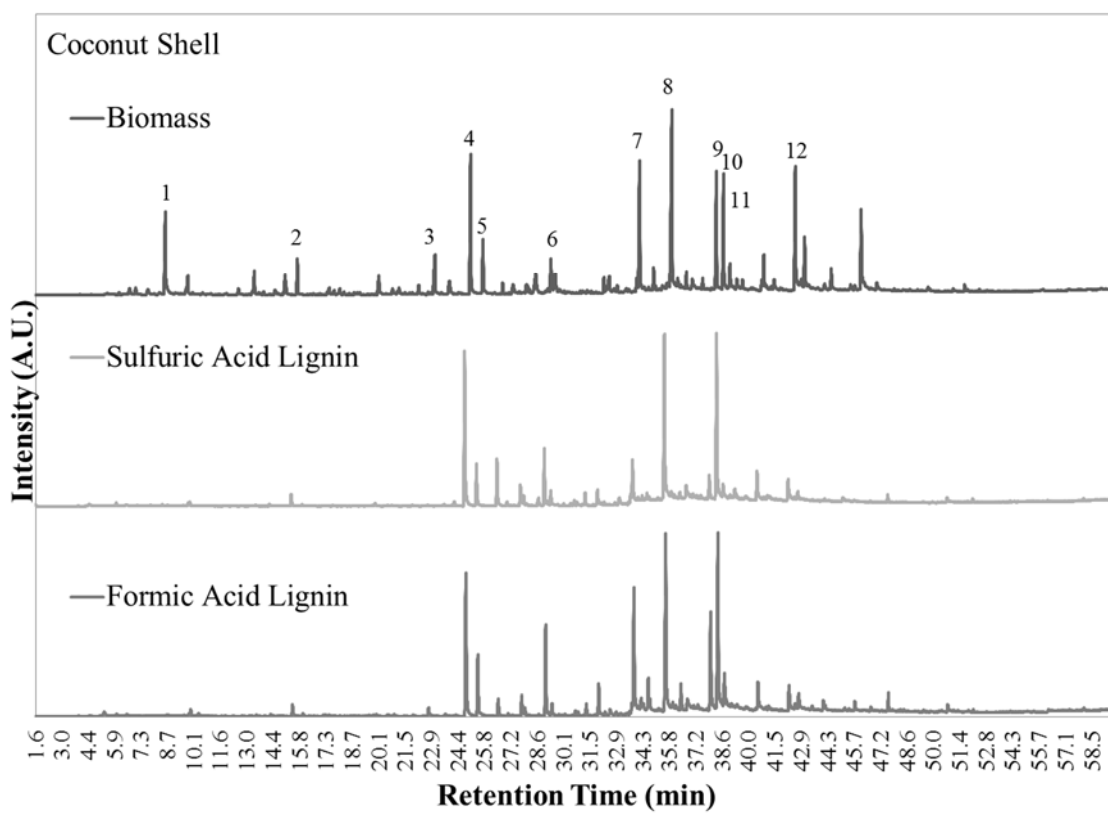
Figure 4.5. Pyrograms obtained from pyrolysis of coconut shell and corresponding lignin fractions.

Table 4.4 Olive pit pyrolysates from whole biomass and extracted lignin.

Compound Number	Retention Time (min)	Compound	Whole Biomass Area %	Formic Acid Lignin Area %	Sulfuric Acid Lignin Area %
1	8.63	acetic acid	4.66 (± 0.34)	0.17	0.08
	9.84	1-hydroxy-2-propanone	1.54 (± 0.04)	0.06	0.00
	13.44	acetic acid ethenyl ester	1.62 (± 0.20)	0.00	0.00
2	15.50	furfural	1.88 (± 0.10)	1.36	0.88
3	22.80	4-hydroxy-5,6-dihydro-2H-pyran-2-one	2.84 (± 0.13)	0.36	0.11
5	25.35	2-methoxyphenol	3.71 (± 0.46)	4.96 (± 1.22)	4.13 (± 0.78)
6	29.01	2-methoxy-4-methylphenol	2.19 (± 0.09)	6.66 (± 1.17)	5.76 (± 1.53)
	29.37	2,4-dimethylphenol	0.32	0.85	1.68 (± 0.02)
	32.31	4-ethyl-2-methoxyphenol	0.85	1.71 (± 0.46)	1.98 (± 0.46)
7	33.76	2-methoxy-4-vinylphenol	8.01 (± 0.56)	4.81 (± 0.79)	2.54 (± 0.31)
	34.55	eugenol	1.38	1.79 (± 0.13)	0.99
8	35.48	2,6-dimethoxyphenol	10.58 (± 0.42)	11.12 (± 2.74)	9.86 (± 1.26)
	36.31	2-methoxy-4-(1-propenyl)phenol (Z)	1.15	1.75 (± 0.29)	0.89
9	37.90	2-methoxy-4-(1-propenyl)phenol (E)	8.11 (± 0.21)	6.06 (± 0.67)	2.79 (± 0.03)
10	38.30	4-methylsyringol	4.45 (± 0.33)	10.06 (± 0.90)	8.64 (± 1.71)
11	38.65	vanillin	2.30 (± 0.41)	4.35 (± 0.66)	2.64 (± 0.36)
	40.48	4-ethylsyringol	2.08 (± 0.03)	1.62(± 0.55)	1.52 (± 0.51)
12	42.15	4-vinylsyringol	9.28 (± 0.67)	1.38	0.72
	42.68	2,6-dimethoxy-4-(2-propenyl)phenol	2.18 (± 0.10)	1.73 (± 1.10)	0.35
	45.71	2,6-dimethoxy-4-(1-propenyl)phenol (E)	2.19 (± 0.10)	0.56	0.11

Table 4.4 (continued)

Sum identified compounds	81.44 (± 0.95)	69.95 (± 4.82)	57.53 (± 1.58)
Sum lignin-based pyrolysates	64.63 (± 0.46)	67.70 (± 4.29)	53.23(± 2.89)
Sum sinapyl-based pyrolysates	31.60 (± 0.82)	27.40(± 1.84)	21.33 (± 2.99)
Sum coniferyl-based pyrolysates	29.36 (± 0.61)	34.21 (± 4.70)	23.06 (± 1.77)
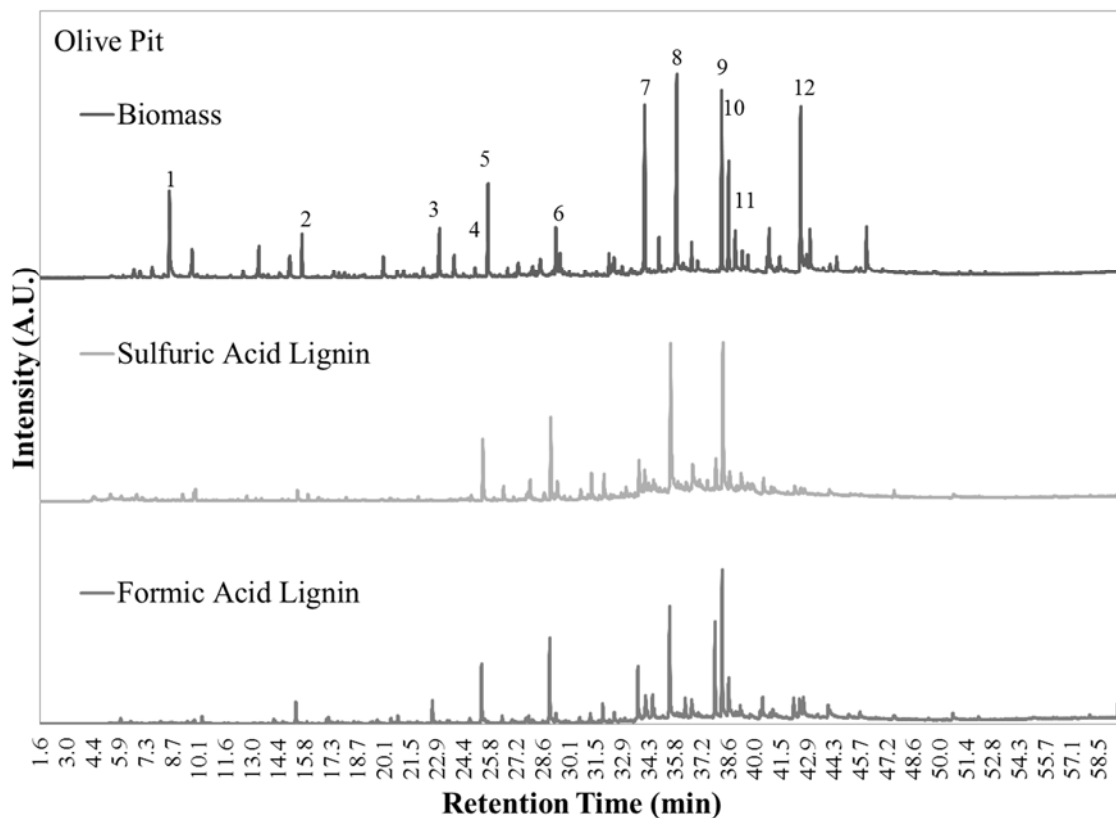
Figure 4.6. Pyrograms obtained from pyrolysis of olive pit and corresponding lignin fractions.

4.3.3 Pyrolysis of Lignin Isolated using Sulfuric Acid and Formic Acid

Figure 4.7 shows a generalized mechanism for the formation of products during formic acid extraction of lignin and subsequent pyrolysis of the lignin fraction. Actual mechanisms for each step have been researched and explained using both lignin and model compounds, although many pathways remain unknown or are speculative.[16,25,36-43] In the first step of the extraction, lignin and hemicellulose-based saccharides are separated (mostly by hydrolysis) from polysaccharides in cellulose and unreacted/not solubilized lignin. After filtering the solid residue, formic acid is evaporated from the filtrate, leaving behind lignin and some hemicellulose-derived compounds. Water is used to wash water-soluble hemicellulose-based compounds from the extracted lignin. The final lignin product is then pyrolyzed to produce phenolics and other volatile and semi-volatile products that would appear in the bio-oil fraction. Solid and non-condensable gas products are also generated. The formation of the pyrolysates from various monomers, dimers and lignin compounds has been investigated,[25,36-40,43] while mechanisms and parameters

influencing their formation and distribution from pyrolysis has also been reviewed by Amen-Chen et al.[41] Each step of the process is influenced by the native structures and composition of the polymers in the biomass and is subject to secondary reactions. For example, 5-5 bonds between coniferyl monomers may not be efficiently extracted using dilute acid techniques and may remain in the cellulosic fraction. Furthermore, a representative distribution of the lignin monomers (sinapyl, coniferyl and coumaryl alcohol) may not be reflected in the extracted lignin due to the differences in the cleavage of certain bonds between the monomers. The resulting extracted lignin, possibly only representing a portion of the total lignin, may then pyrolyze to produce a different distribution of lignin-based products compared to the original lignin in the biomass. For this reason, a comparison of the distribution of S- and G-based pyrolysates of whole biomass lignin and extracted lignin is of interest (*vide infra*). Moreover, lignin may undergo condensation reactions during the extraction process,[16,44,45] which can further influence the structure of the extracted lignin and its corresponding pyrolysate distributions.
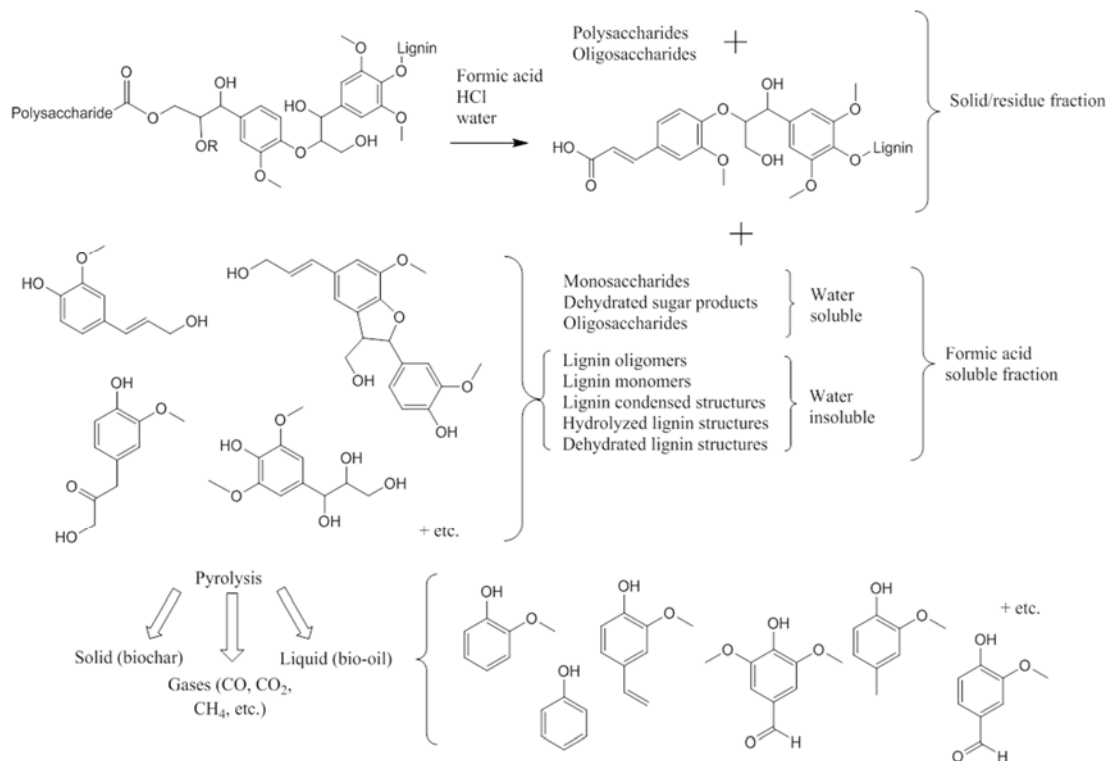
Figure 4.7. Generalized mechanism outlining examples of lignin-based products obtained from the formic acid lignin extraction process and from pyrolysis of the derived lignin.

Klason lignin, on the other hand, is isolated using sulfuric acid, which facilitates hydrolysis of cellulose and hemicellulose to leave behind insoluble lignin. Pyrolysates generated from the lignin fractions obtained from each of the biomass types using the NREL (sulfuric acid) protocol and the 65 °C, 24 h formic acid extraction method are shown in Tables 4.1 -4.4, the corresponding pyrograms being shown in Figures 4.3 –4.6. Repeated analysis of samples from the same extraction showed standard deviations for the pyrolysates to fall within the standard deviations of those from different extractions. Fewer pyrolysates were successfully identified from the sulfuric acid-derived lignins compared to the biomass and formic acid lignin fractions. Unidentified compounds likely included lignin-based pyrolysates containing sulfur, lignin-based dimers and small molecules resulting from decomposition of these compounds. The most abundant pyrolysates from the sulfuric acid lignins differed among the different types of biomass, indicating that sulfuric acid did not isolate or generate similar lignin from different species. This indicates that the lignin differs among biomass samples, and that these differences are expressed in the lignin extracts, even if the lignin has undergone changes during the sulfuric acid isolation

process. A small amount of sulfur dioxide, originating from residual sulfate or generation of lignosulfonate compounds, was also seen in the pyrograms of the sulfuric acid-extracted lignin but was not quantified due to peak coelutions and inconsistent production. Formic acid lignin pyrolysate distributions were also biomass-dependent and showed slight differences from the whole biomass pyrolysates. Finally, it is worth noting that pyrolysis of the lignin fractions typically yielded small quantities of furfural and acetic acid, indicating that the lignin fractions contained carbohydrate contaminants albeit that lignin pyrolysis may also generate some acetic acid.

4.3.3.1 Walnut Shell and Peach Pit Lignin Pyrolysates

As shown in Table 4.1 and Figure 4.3, walnut shell sulfuric acid lignin, like the biomass, produced mostly 2-methoxy-4-vinylphenol, 2,6-dimethoxyphenol, 2-methoxy-4(1-propenyl)phenol, vanillin and more 2-methoxyphenol and 2-methoxy-4-methylphenol. The majority of the products originate from coniferyl alcohol monomers, most of which were likely bound by β-O-4 linkages in the original biomass polymer. However, the isolation process likely led to the breakage of many bonds and possibly reformation of other bonds within the polymer.[16,20,23] Hence, the relative distribution of these major pyrolysates differs between the whole biomass and the sulfuric acid lignin. For example, whole biomass produced predominantly 2-methoxy-4-vinylphenol and 2-methoxy-4-(1-propenyl)phenol, whereas the sulfuric acid lignin generated more 2-methoxyphenols with lighter groups at the 4-position. The same pattern was observed for S-based pyrolysates and it was also apparent in the formic acid-extracted lignin. This indicates that some breakage of the β-O-4 and α-O-4 linkages, and possibly β-5 and β-β bonds, occurred during lignin extraction and pyrolysis causing cracking, dehydration, etc., of the groups at the 4-position and leading to smaller molecules in the isolated lignin pyrolysis products. On the other hand, 5-5 bonds, which only occur between coniferyl and/or coumaryl monomers, are less likely to be broken during the extraction process and some may even still remain in the bio-char after pyrolysis.[42]

Walnut shell sulfuric acid lignin pyrolysates showed a slightly higher apparent S:G ratio (0.27 ± 0.06) than the biomass (0.15 ± 0.02) and formic acid lignin (0.17 ± 0.02) S:G ratios. These small differences are not statistically significant ($p > 0.05$) but could be explained based on the possibility that G-monomers condensed during the extraction process with the subsequent formation of char and non-volatile products during pyrolysis.[42] Detector responses of the different compounds may also vary slightly such that changes in relative abundance could reflect slight

differences in area % S:G ratios. In other words, S:G ratios may be similar based on mass but the shifts in pyrolysate distributions may cause a change in the measured area % S:G ratios. However, differences in the distribution of pyrolysate abundances are still evident, suggesting structural variations. It should also be noted that, unlike the sulfuric acid method, only a fraction of the total lignin was extracted using formic acid. Consequently, the formic acid lignin may have not been representative of the whole, even if the S:G ratio was similar.

Peach pit sulfuric acid lignin showed a similar apparent S:G ratio as the biomass (lignin: 0.23 ± 0.07, biomass: 0.20 ± 0.05), where the formic acid lignin pyrolysates showed a slightly higher apparent S:G ratio (0.46 ± 0.12), although the S:G ratios determined for peach pits were statistically similar (p > 0.05). As mentioned for walnut shells, this could be due to the lack of bond breakage/hydrolysis between coniferyl monomers during the formic acid extraction, i.e., these monomers may have been joined by 5-5 bonds. The cleavage of β-O-4 and/or β-β bonds linking the sinapyl monomers during the formic acid extraction process would then appear to produce higher S-content in the lignin extract. Like the other samples, the lignin extracts showed a larger production of monomer pyrolysates with smaller groups at the 4-position in comparison with the whole biomass.

4.3.3.2 Coconut Shell and Olive Pit Lignin Pyrolysates

Coconut shell sulfuric acid lignin generated large amounts of 2-methoxyphenol, 2-methylphenol, 2-methoxy-4-vinylphenol, 4-methylsyringol and more phenol and 2,6-dimethoxyphenol. These are similar to the most abundant pyrolysates generated from the biomass and formic acid lignin but differ in their relative distributions. Phenol was produced in high abundance, especially from the sulfuric acid lignin in comparison to the formic acid lignin and biomass. This characteristic was unique to the coconut shell and its corresponding lignin, likely originating from coumaryl monomers. Overall, similarities in pyrolysates generated from each extract provide a fair representation of the biomass as a whole in the case of coconut shells. Minor differences in relative pyrolysate distributions and abundance were evident though, indicating that the composition of the resulting bio-oil may vary.

As shown in Table 4.5, the apparent S:G ratio of the coconut shell sulfuric acid lignin was similar to that obtained from the whole biomass, while the sulfuric acid ratio was slightly higher than, although not statistically different from, that observed from formic acid lignin. In contrast, the formic acid lignin from coconut shells showed a slightly lower S:G ratio (1.01 ± 0.15) that was

statistically different from the biomass S:G ratio (1.46 ± 0.03). This observation suggests that many of the linkages that connect sinapyl monomers were not broken during the formic extraction process and remained in the biomass fraction, and/or the types of linkages connecting the sinapyl monomers may have undergone condensation reactions more readily during extraction or pyrolysis, which would be the opposite case from walnut shell and peach pit lignins.

Table 4.5. Apparent S:G ratios determined for each biomass and extraction fraction based on sum area percent ratios of sinapyl and coniferyl alcohol-based pyrolysates.

Sample Type	Walnut Shell	Coconut Shell	Peach Pit	Olive Pit
Whole Biomass	0.15 (± 0.02)	1.46 (± 0.03)	0.20 (± 0.05)	1.08 (± 0.04)
Formic Acid Lignin	0.17 (± 0.02)	1.01 (± 0.15)	0.46 (± 0.12)	0.80 (± 0.12)
Sulfuric Acid Lignin	0.27 (± 0.06)	1.32 (± 0.33)	0.23 (± 0.07)	0.92 (± 0.16)
Residue after Formic Acid Extraction	0.26 (± 0.05)	1.47 (± 0.02)	0.38 (± 0.01)	0.65 (± 0.02)

Olive pit sulfuric acid lignin and formic acid lignin pyrolysates showed similarities with the whole biomass pyrolysates as well. The biomass and corresponding lignin extracts produced similar most-abundant pyrolysates and area % S:G ratios were similar (1.08 ± 0.04, 0.80 ± 0.12, 0.92 ± 0.16, respectively, $p > 0.05$), being higher than walnut shell and peach pit. Interestingly, the formic acid process was also able to extract the most lignin from olive pits. Together, these observations suggest the majority of both S and G monomers were bound by a higher abundance of reactive linkages, such as β-O-4 and α-O-4 bonds, making formic acid extraction more efficient and resulting in similar pyrolysate distributions.

4.3.4 Pyrolysis of Pulp Residues from Formic Acid Extractions

Pyrolysis-GC/MS analysis of the residues remaining after formic acid extraction was performed in order to compare the distribution of pyrolysates and account for differences between the whole biomass and formic acid-extracted lignins. Table 4.6 shows the most abundant, positively identified pyrolysates generated from residues obtained from each biomass type. A more comprehensive list of all pyrolysates observed from each residue is provided in Supplementary Table 4.5 in Appendix 2. As expected, the residues showed a decrease in lignin-based pyrolysates relative to carbohydrate-based products in comparison to the whole biomass. There were also significant differences in the types of products generated, particularly from the holocellulosic fraction, between the biomass and the formic acid residue. In general, residues generated more 2,3-anhydro-*d*-mannosan, 5-(hydroxymethyl)furfural, 1,6-anhydro-β-D-glucopyranose (levoglucosan) and other sugar-related compounds. This implies that the formic acid treatment resulted in the partial hydrolysis of the holocellulosic fraction, thereby rendering the sugars more susceptible to decomposition into these pyrolysates. Presumably, many of these species are not generated from the whole biomass due to the ordered structure of the polymers which upon thermal decomposition, may generate nonvolatile products including char. There were also many products that were not positively identified. Library search results suggest that most of the unidentified compounds were structural isomers of cyclic alcohols and furans, likely derived from carbohydrates and sugar moieties.

Table 4.6. Pyrolysates obtained from the pyrolysis of endocarp pulp residues from formic acid extractions (extractions at 65 ^{0}C, 24h).

Retention Time (min)	Compound	Walnut shell residue	Coconut shell residue	Peach pit residue	Olive pit residue
15.04	furfural	2.02 (± 0.16)	1.58 (± 0.22)	1.70 (± 0.65)	2.58 (± 0.61)
19.40	1,2-cyclopentanedione	0.81	0.76	0.54	1.72 (± 0.55)
22.40	4-hydroxy-5,6-dihydro-2H-pyran-2-one	2.84 (± 0.87)	1.84 (± 0.57)	1.40 (± 0.86)	1.15
23.22	2-hydroxy-3-methyl-2-cyclopenten-1-one	0.48	0.83	0.47	1.48 (± 0.60)
24.42	phenol	0.51	4.12 (± 0.87)	0.34	0.67
25.00	2-methoxyphenol	2.39 (± 0.19)	1.81 (± 0.44)	2.58 (± 0.57)	3.09 (± 0.20)
29.01	2-methoxy-4-methylphenol	3.88 (± 0.48)	2.04 (± 0.25)	4.29 (± 0.59)	1.50 (± 0.46)
29.39	3,5-dihydroxy-2-methyl-4H-pyran-4-one	0.07	2.14 (± 0.55)	0.37	0.90
32.20	2,3-anhydro-d-mannosan	0.86	0.65	0.95	1.73 (± 0.16)
32.73	1,4:3,6-dianhydro-α-*d*-glucopyranose	0.81	0.82	1.12	2.14 (± 0.20)
33.43	2-methoxy-4-vinylphenol	5.34 (± 1.34)	4.06 (± 0.87)	3.94 (± 1.22)	1.83 (± 0.23)
34.19	eugenol	1.41 (± 0.09)	0.61	1.62 (± 0.81)	0.41
34.73	5-(hydroxymethyl)furfural	2.65 (± 1.27)	3.66 (± 1.73)	1.30 (± 0.30)	7.53 (± 0.58)
35.11	2,6-dimethoxyphenol	1.17	4.74 (± 0.47)	1.49 (± 0.28)	3.58 (± 0.19)
35.95	2-methoxy-4-(1-propenyl)phenol (Z)	1.35 (± 0.09)	0.94	1.08	0.65
36.95	4-(2-propenyl)phenol	2.57 (± 1.64)	0.00	0.00	0.00
37.56	2-methoxy-4-(1-propenyl)phenol (E)	5.64 (± 1.21)	3.14 (± 0.55)	4.75 (± 0.76)	2.19 (± 0.29)
37.94	4-methylsyringol	1.65 (± 0.42)	6.41 (± 0.92)	1.99 (± 0.23)	1.99 (± 0.62)
38.30	vanillin	4.03 (± 0.28)	1.83 (± 0.34)	3.58 (± 0.69)	1.48 (± 0.28)
40.00	4-ethylsyringol	1.55 (± 0.38)	0.78	1.19	0.60
40.67	4-hydroxy-3-methoxyacetophenone	1.31 (± 1.04)	0.68	2.01 (± 0.32)	0.95

Table 4.6 (continued)

41.80	4-vinylsyringol	1.32 (± 0.44)	4.68 (± 0.13)	1.62 (± 0.21)	1.48 (± 0.34)
42.13	1-(4-hydroxy-3-methoxyphenyl)acetone	3.65 (± 0.69)	1.39 (± 0.21)	3.71 (± 1.05)	2.10 (± 0.71)
42.33	2,6-dimethoxy-4-(2-propenyl)phenol	1.03	2.85 (± 0.50)	1.30 (± 0.17)	0.60
43.39	4-((1E)-3-hydroxy-1-propenyl)-2-methoxyphenol T	1.46 (± 0.09)	0.53	1.91 (± 0.18)	0.60
43.77	2,6-dimethoxy-4-(1-propenyl)phenol (Z)	0.50	1.36 (± 0.16)	1.12	0.55
44.80	1,6-anhydro-β- *d*-glucopyranose	2.47 (± 2.00)	1.51 (± 0.49)	3.62 (± 0.68)	3.02 (± 1.61)
45.04	3-methoxy-2-naphthalenol	0.80	0.00	1.01	0.55
45.37	2,6-dimethoxy-4-(1-propenyl)phenol (E)	1.52 (± 0.03)	5.25 (± 0.99)	2.77 (± 0.73)	1.19
45.98	4-hydroxy-3-methoxy-phenylacetylformic acid	0.73	0.13	1.58 (± 0.51)	0.00
	Sum identified compounds	67.00 (± 5.08)	68.38 (± 1.68)	63.65 (± 3.16)	58.57 (± 1.22)
	Sum lignin-based pyrolysates	48.69 (± 1.19)	50.43 (± 3.60)	49.39 (± 0.27)	28.36 (± 4.97)
	Sum sinapyl-based pyrolysates	9.05 (± 1.90)	26.47 (± 2.11)	13.04 (± 0.73)	10.45 (± 1.74)
	Sum coniferyl-based pyrolysates	34.64 (± 1.36)	17.97 (± 1.39)	34.29 (± 0.74)	16.10 (± 3.17)

The most abundant lignin-based walnut shell residue pyrolysates were similar to those produced from pyrolysis of the whole biomass and the apparent S:G ratio of the residue was not statistically different ($p > 0.05$). The lignin extracted from the biomass using formic acid showed a similar S:G ratio based on pyrolysate distributions, indicating that the bonds broken in the formic acid extraction yielded a monomer distribution similar to that of biomass. Peach pit residue lignin-based pyrolysis products show a slightly higher S:G ratio (Table 4.5) than the biomass ($p < 0.05$) although it was not significantly different from the S:G ratio of the formic acid lignin ($p > 0.05$). However, it would be expected that the residues from walnut shell and peach pits would create pyrolysates reflecting a slightly lower S:G ratio than the biomass because the formic acid lignin pyrolysates showed a higher apparent S:G ratio than the biomass. The fact that this is not the case may be due to condensation of coniferyl-based monomers and corresponding pyrolysates.

Coconut shell residue pyrolysates generated in highest abundance were similar to those from the whole biomass, but their relative distributions were significantly different. The lignin-based pyrolysate distributions from the residue also differed from the other two lignin fractions and, like the biomass, generally created heavier/large pyrolysates with larger groups at the 4-position in the aromatic rings. Despite these differences, the apparent S:G ratio of the residue was similar to the whole biomass based on the sum area % pyrolysates from each monomer. However, since the formic acid lignin pyrolysates showed a lower S:G ratio than the whole biomass, it would be expected that the residue would have a higher S:G ratio than the biomass. Coconut shell holocellulose-based pyrolysates were similar in abundance and distribution to the other biomass residue types, except for higher production of 3,5-dihydroxy-2-methyl-4H-pyran-4-one. Like the other samples, an increase in holocellulose-based pyrolysates relative to the lignin-based pyrolysates was seen for the residue and many more types of holocellulose-based pyrolysates were seen from the residue.

Olive pit residue produced even fewer lignin-based pyrolysates than the other residue samples. This agrees with the fact that the formic acid extracted more lignin from the olive pits than the other biomass samples. The S:G ratios determined based on pyrolysate distributions (Table 4.5) for the formic acid lignin, whole biomass and sulfuric acid lignin were all similar ($p > 0.05$) with formic acid lignin being only slightly lower. Hence, it would be expected that the pyrolysates from the formic acid residue would be similar or that the S:G ratio would be slightly higher than the formic acid lignin S:G ratio. However, residue pyrolysates appear to produce S:G ratios slightly lower than those from the biomass and formic acid lignin. This is a similar observation to

that seen for the coconut shell (which also had higher S:G ratios) where the residues produced fewer sinapyl-based products than expected. As for low S:G biomass (walnut shells and peach pits), it may be the case that the remaining, non-extractable lignin oligomers favored condensation of the most abundant monomers during pyrolysis, leading to more volatile products from the less abundant monomer.

4.3.5 Thermogravimetric Analysis of Biomass and Lignin

Thermogravimetric analysis (TGA) of the endocarp biomass samples showed similar weight loss curves and derivative-weight loss curves (DTG) for the samples with similar S:G ratios. Figure 4.8 shows the TGA and DTG plots for the walnut shell (low S:G) and coconut shell (high S:G) and their respective lignin fractions. The TGA and DTG plots from peach pits (low S:G, not shown) look similar to walnut shell whereas olive pits (high S:G, not shown) look similar to coconut shells. The DTG plots indicate that there is a difference in the kinetics of the slow pyrolysis between the two types of biomass. The DTG peak corresponding to hemicellulose[46] pyrolysis occurs at a lower temperature, 284 ^{0}C, for the high S:G biomass and decomposes at a higher rate than that of the low S:G biomass, for which the maximum occurs at 294 ^{0}C. These differences indicate structural and composition differences in the hemicellulosic fraction of the biomass. It is also possible that linkages between the hemicellulosic fraction and the lignin lead to differences in the thermal decomposition mechanisms. Distributed activation energy models have been used to elucidate the activation energies, frequency factors and reaction orders associated with the thermal decomposition of the components in biomass.[46-48] While determination of these values is beyond the scope of this work, the DTG data suggest that the thermal decomposition of the different biomass types and lignin fractions proceeds with different activation energies, reaction orders and/or frequency factors. The higher decomposition rate and lower temperature of the hemicellulose peak for the high S:G ratio biomass may indicate a lower activation energy and/or increase in frequency factor for decomposition of hemicellulose in this type of biomass. The DTG peak observed at 353 ^{0}C from each biomass sample corresponds to cellulose decomposition and the broad shoulder from approximately 200 ^{0}C to 700 ^{0}C corresponds to lignin decomposition.[46] Each of the biomass types also formed char that remained at 900 ^{0}C and totaled approximately 20 wt% of the original mass.
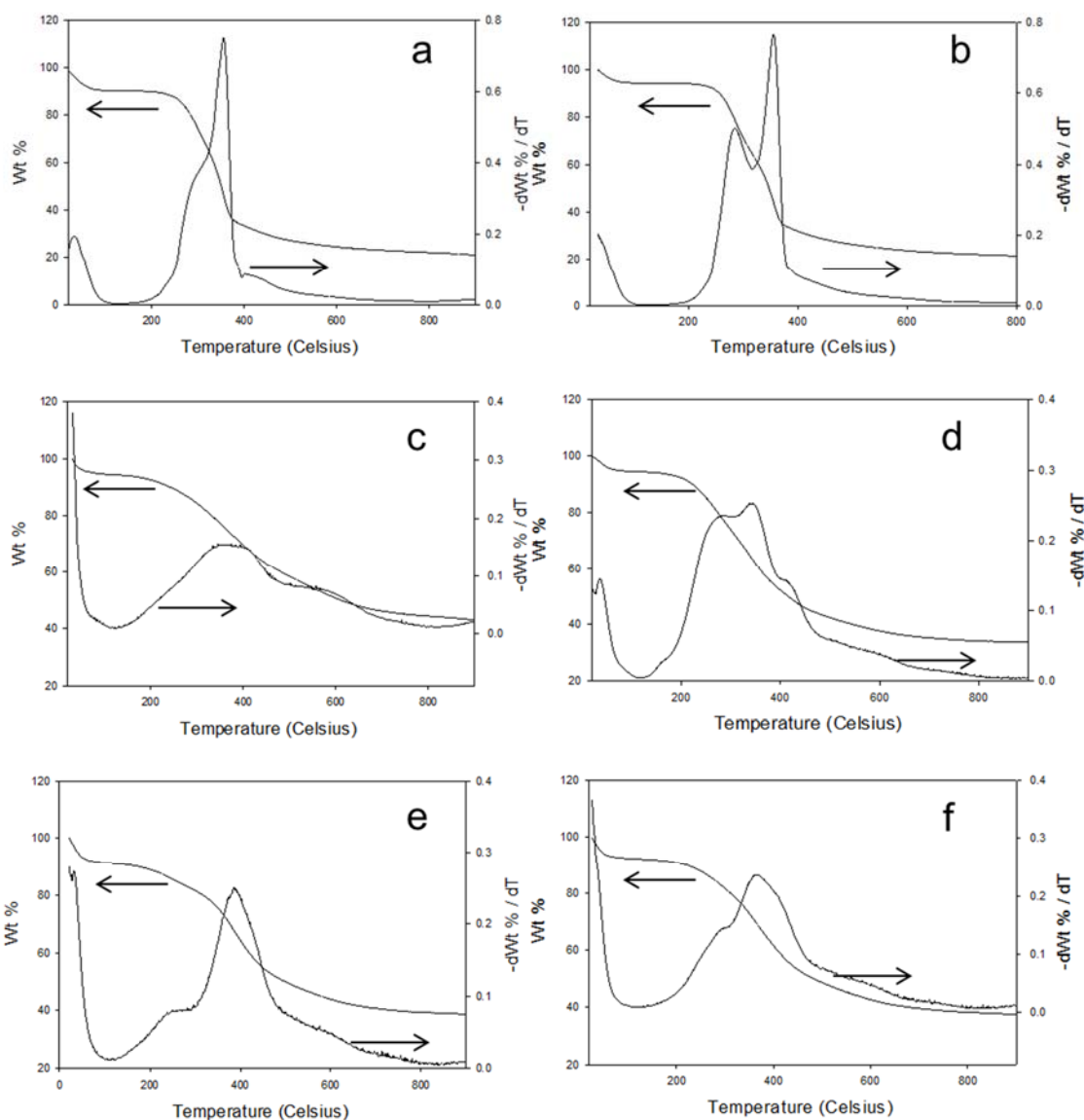
Figure 4.8. TGA and DTG profiles of a) walnut shell whole biomass, b) coconut shell whole biomass, c) walnut shell formic acid lignin, d) coconut shell formic acid lignin, e) walnut shell sulfuric acid (NREL or Klason) lignin, f) coconut shell sulfuric acid (NREL or Klason) lignin.

TGA and DTG plots of the lignin extracts are different for each type of lignin from each biomass type. These differences indicate that the lignin extracted by different techniques exhibits different reaction kinetics during slow pyrolysis. The differences in decomposition kinetics may be the result of compositional and structural variation between the lignin samples. Since the kinetics of

93

thermal decomposition varies between lignin extracted by different techniques and biomass types, different pyrolysate distributions would be expected. Residual char at 900 ^{0}C totaled between 33 and 43 wt% of the original mass of the lignin samples and was higher for three of the four NREL extracted lignin samples in comparison to the formic acid lignin.

4.3.6 FTIR Analysis of Extracted Lignin

FTIR analyses of the lignins extracted from the biomass using the different extraction techniques were compared in order to elucidate compositional differences between the high and low S:G ratio lignin types. Vibrations corresponding to hydroxyl (O-H) stretching were observed at 3370 cm^{-1} for all lignin samples. All lignin samples also had peaks at 1592 cm^{-1} and 1508 cm^{-1} corresponding to aromatic vibrations, as well as vibrational stretches for C-H between 2930 and 2940 cm^{-1} and peaks at 1268 cm^{-1} from C-O stretching. FTIR spectra (coconut shell lignins and walnut shell lignins, shown in supplementary Figure 4.1 and 4.2 in Appendix 3) show differences between the formic acid and sulfuric acid extracts. All formic acid lignin samples have stronger peaks at 1713 cm^{-1} than the corresponding sulfuric acid lignin. This peak may correspond to carbonyls (C=O) in the lignin structure but may also include residual formic acid in the lignin. Walnut shell, olive pit and peach pit sulfuric acid lignins showed higher intensity bands at 1029 cm^{-1} than the formic acid lignin, possibly resulting from the presence of S=O in the lignin samples, although this was not observed in the case of the coconut shell lignins. Both coconut shell and olive pit lignin extracts showed stronger bands corresponding to syringyl absorbances[49] at 1326 cm^{-1} as well as stronger bands corresponding to O-CH$_3$ deformations at 1430 and 1450 cm^{-1} when compared to the walnut shell and peach pit lignins. Hence, FTIR analysis of the lignins agreed with Py-GC/MS analysis indicating the coconut shell lignins had higher S:G ratios than the walnut shell lignins. Overall, the FTIR data are representative of lignin spectra reported in the literature.[43,49,50]

4.3.7 NMR of Formic Acid Extracted Lignins

HSQC NMR spectra of the four formic acid-extracted lignins are shown in Figure 4.9. Table 4.7 shows the shifts of the main signals present in the spectra and their structural assignments. Peak assignments were made by comparison to spectra reported in the literature.[51-54] Figures 4.9a and d show spectra from the coconut shell and olive pit formic acid lignins, respectively. In comparison to the walnut shell and peach pit lignins, these lignins produced a higher intensity of correlation signals at approximately 104.0/6.7 ppm (δ_C/δ_H), originating from the aromatic C-H at the 2- and 6- positions in syringyl-based units (S monomers), as well as 107.0/7.1 ppm from the C-H at the 2- and 6- positions in S monomers with carbonyls on the α position in the linkages. These results agree with the relative magnitudes of S:G ratios determined from Py-GC/MS analyses of the lignins. Table 4.8 shows the S:G ratios obtained from NMR signal intensity comparisons. The intensities contributing from aromatic S monomers at the 2- and 6- positions and G monomers at the 2- and 5- positions were summed and divided to obtain S:G ratios. NMR S:G ratios agreed closely with those determined by Py-GC/MS for walnut shell, coconut shell and olive pit lignins, and showed reasonable agreement for peach pit lignins. In agreement with the foregoing is the higher intensity of signals at 87.0/5.5 ppm corresponding to the α C-H in β-5 linkages (green circle in Figure 4.9) in the walnut shell and peach pit lignins. Since these lignins contain a lower abundance of S-based monomers, they are more likely to contain more β-5 linkages in than the coconut shell and olive pit lignins.
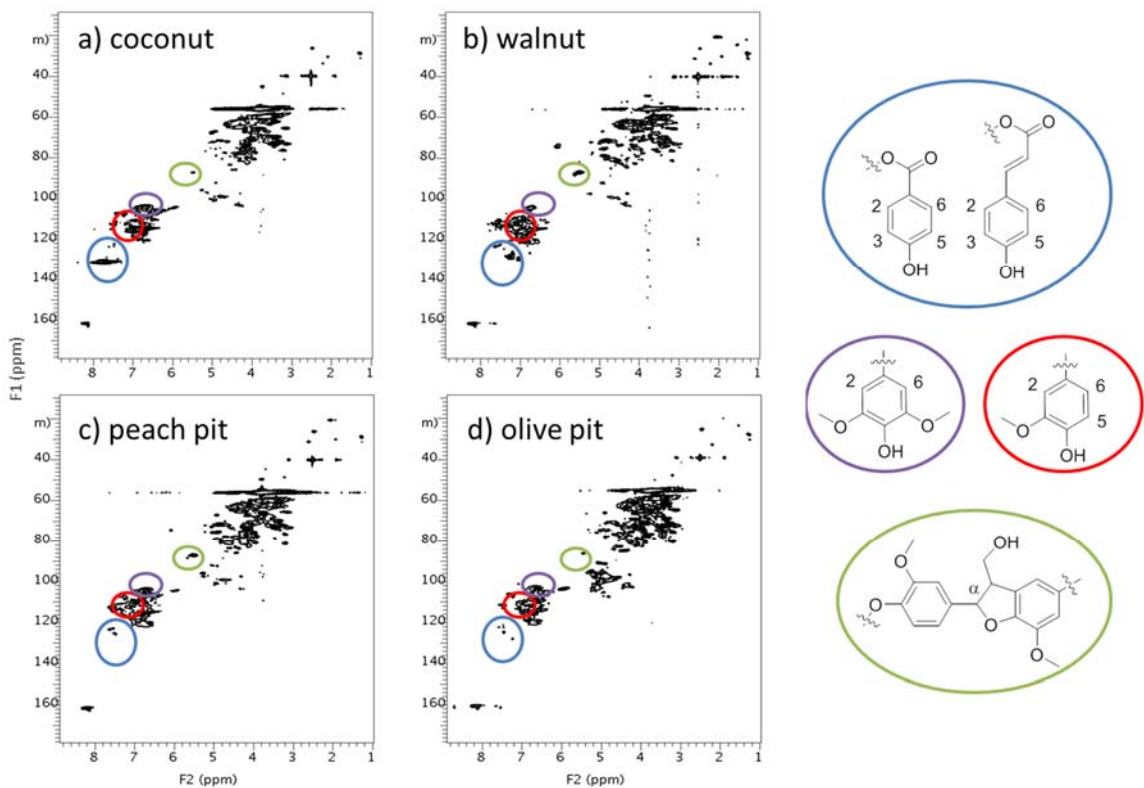
Figure 4.9. HSQC NMR spectra of formic acid extracted lignins, a) coconut shell, b) walnut shell, c) peach pit, d) olive pit.

Coconut shell lignin showed signals at 131.0/7.8 ppm that can originate from the aromatic C-H at the 2- and 6- positions of a *p*-hydroxybenzoate unit present in the polymer.[27] This signal was unique to the coconut shell lignin and explains the large amount of phenol produced from the pyrolysis of the coconut shell and its derived lignins. The coconut shell lignin also had peaks with greater intensity at 118/6.8 ppm and 115/6.7 ppm that may originate from the aromatic 3- and 5- positions on the benzoate and coumaryl/coumarate (H) monomers, respectively. The signal at 118/6.8 ppm likely overlaps with the signals from the aryl 6-position on G monomers and was therefore not used to quantify the amount of G-monomers present in the lignin. Olive pit lignin showed peaks in the 98-103/4.3-4.7 region that likely originate from the C-H in sugar moieties (possibly at the 1-, 2- and 3- positions in pyranose sugars) connected to or not washed from the lignin. The presence of residual sugars in the olive pit lignin (in higher abundance relative to the other lignins) was also confirmed by Py-GC/MS analysis of the formic acid lignin. The presence of saccharides and related compounds may also account for the apparently higher yield of lignin from the formic acid extraction of olive pits.

Table 4.7 Assignments of several of the main ^{13}C-^{1}H cross signals in the HSQC spectra of the formic acid lignins. W= walnut shell, O= olive pit, P= peach pit, C= coconut shell.

Biomass	δ_C/δ_H (ppm)	Assignment
W,O,P,C	55.0/3.5	C-H(β) in β-5
W,O,P,C	55.6/3.1	C-H(β) in β- β
W,O,P,C	55.6/3.8	C-H methoxy
W,O,P,C	59.6/3.4-3.6	C-H(γ) in β-O-4
W,O,P,C	61.5/3.7	C-H(γ) in β-5
W,O,P,C	63.2/4.3-4.5	C-H(γ) in γ-acylated β-O-4
W,O,P,C	72.0/3.8,4.2	C-H(γ) in β- β
W,O,P,C	71.3/4.8	C-H(α) in β-O-4
W,O,P,C	83.0/4.4	C-H(β) in β-O-4, G, H units
W,O,P,C	87.0/5.5	C-H(α) in β-5
W,O,P,C	104.0/6.7	C-H$_{2,6}$ in S units (ether linkage)
O,P,C	107.0/7.1,7.2	C-H$_{2,6}$ in S units Cα => C=O
W,O,P,C	111.0/7.0	C-H$_2$ in G units
W,O,P,C	112.0/7.5	C-H$_6$ in G units Cα = C=O
W,P,C	114.6/6.7	C-H$_{3,5}$ H units
W,O,P,C	114.6/6.8	C-H$_5$ G units
W,O,P,	118.2/6.8	C-H$_6$ G units
P	122.4/7.6	C-H$_2$ G units Cα = C=O
W,O,P	127.2/7.2	C-H$_{2,6}$ H units
C	131.0/7.7,7.9	C-H$_{2,6}$ p-hydroxybenzoate
W,O,P,C	98.6/4.7	C-H$_1$ in phenyl glycoside bond
O,P,C	101.6-102.8/4.3	C-H$_3$ in phenyl glycoside bond

The likely origin of other correlation signals observed in the NMR spectra of the lignins is outlined in Table 4.7. For example, the methoxyl C-H signals for the aromatic monomers occur at 55.6/3.7 ppm. C-H correlations for α, β, and γ positions in the different linkages present in the lignin polymers are also observed for of the formic acid-extracted lignins. There are also signals indicating that the α positions in the linkages contain C=O for both S- and G-monomers in each of the lignin fractions. Comparisons of the intensities of aromatic C-H correlation peaks indicate that more C=O groups occur at the α positions in the linkages amongst G-monomers than S-monomers. Signals from cinnamaldehyde or hydroxycinnamyl alcohol endgroups and spirodienone structures were absent from the spectra, although they have been observed in other lignins. This does not mean these structures were not present in the native lignin given that their absence could be the result of the extraction process (either they were not extracted or reacted to give new structures). Nevertheless, the HSQC NMR spectra provided valuable information that support the Py-GC/MS analysis and explain the origin of certain pyrolysates.

Table 4.8 S:G ratios for formic acid lignins determined by NMR in comparison to S:G ratios determined by Py-GC/MS.

Lignin Origin	NMR S:G	Py-GC/MS S:G
Walnut Shell	0.15	0.17
Coconut Shell	0.99	1.01
Peach Pit	0.69	0.46
Olive Pit	0.81	0.80

4.4 Conclusions

Pyrolysis-GC/MS was used to analyze pyrolysates obtained from peach pits, coconut shells, olive pits and walnut shells and their respective formic and sulfuric acid-extracted lignin and formic acid residue fractions. Results indicate that the formic acid treatment extracted only a fraction of the lignin present and that acid extraction procedures, including that using sulfuric acid, induce limited changes in the lignin structure. The pyrolysate distributions of lignins from different biomass types, extracted using the same formic acid procedure, reveal that the extraction technique does not only yield lignin of particular structure or composition. Indeed, different monomers and distributions of bond linkages are represented in the extracted and isolated lignins that lead to different pyrolysate distributions. TGA similarly showed that the lignin structures and thermal decomposition kinetics are biomass dependent. Pyrolysates that originate from the holocellulosic fraction are also present in the lignin fractions, indicating the extraction techniques typically do not produce pure lignin. However, the likely occurrence of condensation reactions during extraction and/or pyrolysis, leading to nonvolatile, tar and char products, greatly complicates analysis of the changes in lignin composition and structure that occur upon acid extraction from the whole biomass.

According to Py-GC/MS data, coconut shells, olive pits and their respective lignin fractions produced pyrolysate distributions that indicate these feedstocks contained higher amounts of sinapyl monomers relative to coniferyl monomers than peach pits and walnut shells. Coconut shells and corresponding lignin extracts produced more phenol in comparison to the other biomass samples. HSQC NMR spectra of the formic acid-extracted lignins supported the Py-GC/MS analysis of the lignins showing coconut shells and olive pits to contain more S-monomers and elucidated the presence of *p*-hydroxybenzoate structures in coconut shell lignin that can pyrolyze to generate phenol. Overall, the extracted lignin fractions were, to a certain degree,

representative of the corresponding biomass, although distributions of the various pyrolysates provide evidence that the structures and thermal reactivity of the extracted lignins vary from that which are present in the whole biomass.

Chapter 5. Pyrolysis-GC/MS of Wild-Type and Mutant Sorghum

Note – Content included in this chapter was published as an article in the following journal:

Petti, C.; Harman-Ware, A. E.; Tateno, M.; Kushwaha, R.; Shearer, A.; Downie, A. B.; Crocker, M.; DeBolt, S., Sorghum mutant RG displays antithetic leaf shoot lignin accumulation resulting in improved stem saccharification properties *Biotechnology for Biofuels* **2013,** *6*.[1]

Note – Biomass collection, preparation, chemical mutagenesis, saccharification efficiency and sugar analysis were not performed by the author and these methods and techniques are beyond the scope of this dissertation. Content in this chapter was included in the above open access journal article and appears in this dissertation as excerpts, figures and tables with inclusion of additional introductory information and expanded results and discussion with emphasis on thermogravimetric analysis (TGA) and Pyrolysis-GC/MS (Py-GC/MS) data.

5.1 Introduction

The production of renewable fuels and chemicals from biomass has been heavily investigated due to factors such as the depletion of petroleum resources.[2] The utilization of biomass as a source of fuels or chemicals must be researched from many perspectives. Genetic, agricultural, and thermochemical processes must be understood and optimized in order to efficiently utilize biomass for production of chemicals. In particular, understanding the biosynthetic processes that regulate the production, composition and distribution of biopolymers within biomass feedstocks is fundamental towards the generation of crops that may be more amenable towards production of fuels.[3-5] These processes, along with plant maturity, growing conditions and various other factors, may influence the ability to recover sugars, impact the total energy content, and/or have an effect on the thermal decomposition pathways and the type of products obtainable from biomass.[2,6-10]

Lignin content and lignin structure in particular have been shown to influence the saccharification efficiency and energy content of biomass.[11-13] For example, maize cell wall residues showed different degradability efficiencies by cellulase/amyloglucosidase that correlated with differing β-O-4 bond and monomer abundances within the lignin polymer.[11] Also, biomass with higher lignin content possesses higher heating values.[12,13] Many investigations have focused on understanding the genetic and metabolic processes associated with lignin production in order to optimize such biomass properties. Mutations in genes associated with caffeic acid O-methyl transferase

(COMT) and cinnamyl alcohol dehydrogenase (CAD) have been linked to changes in lignin structure and content, which have also resulted in changes in the cellulose digestibility in biomass feedstocks.[14-16] These studies provide insight into the regulation of the phenylpropanoid pathway that generates lignin and how biomass properties might be optimized by understanding the genetic variables associated within.

Characterization of biomass structure and composition is necessary in order to understand the links between genetic variations in biomass and its potential for conversion into fuels and chemicals. Thermochemical decomposition processes such as pyrolysis can provide information about the structure and composition of the original feedstock and is also an important technique for conversion of biomass into fuels and chemicals.[2,8,9,17-20] Pyrolysis is simply the thermal decomposition of organic material in an inert atmosphere. Pyrolysis-GC/MS (Py-GC/MS) is a rapid, micro-scale pyrolysis technique that has been used to study the products formed from the thermal decomposition of various biomass feedstocks and their separated components.[6,7,9,18-30] Pyrolysates are generated from different biopolymers within the biomass and their abundance and distribution provide information about the structure and composition of the starting feedstock. For example, S:G ratios in eucalyptus have been determined using Py-GC/MS.[27] Py-GC/MS has also shown structural variations of lignin in mutant sorghum feedstocks.[14] Thermogravimetric analysis (TGA) can also be used to study the decomposition processes of biomass and its components.[9,21-23,31-34] In this technique, thermal decomposition of biomass is monitored by measuring weight loss over a temperature gradient in an inert atmosphere. Decomposition processes and reaction kinetics vary for individual biomass components and differences in the structure and composition of biomass are reflected in the weight-loss and derivative-weight loss curves. Hence, TGA can provide information about structural variations between biomass types while simultaneously monitoring thermal decomposition properties of biomass.

The goal of this study was to utilize Py-GC/MS and TGA in order to understand the differences in biopolymer structure and composition and resulting decomposition products between wild-type and mutated *Sorghum bicolor* (L.) of the Della variety. Here, the dominant REDforGREEN (RG) mutant was generated through chemical mutagenesis (ethyl methanesulfonate, EMS) in the Della variety. The RG mutant was identified through a phenotypic screen for enhanced red pigmentation in plant tissues. It is demonstrated that the RG mutant displays an antithetic abundance/reduction of lignin in a tissue-specific manner. The pyrolysates formed from decomposition of the biomass provide both structural information about the biomass and

information about the effect of mutations on the biomass thermal decomposition processes and resulting product distributions. Additional studies and information pertaining to this research, including saccharification efficiency of the sorghum, are reported in Petti et al.[1] but are beyond the scope of this dissertation.

5.2 Materials and Methods

5.2.1 Biomass Collection and Preparation

Sorghum bicolor (L.) samples were obtained from the DeBolt research group at the University of Kentucky Department of Horticulture. Biomass samples were cultivated as described in Petti et al.[1] Briefly, plants were sown in soil-less media (MetroMix 360, SunGro Industries Bellevue, WA) in a glasshouse at 24 °C and integrated with soil prior to transplantation to a field maintained under plasticulture. Plants were grown for 3 months and collected for analysis. The biomass was separated into stems and leaves from wild-type sorghum plants and two groups of mutants. Mutations were induced by means of chemical mutagenesis using ethylmethanesulfonate (EMS) as reported by Petti et al.[1] The mutant, referred to as RG, which stands for "REDforGREEN", was identified through a phenotypic screen for enhanced red pigmentation in plant tissues. The samples were dried (10% water according to TGA) and ground (< 1 mm) prior to analysis.

5.2.2 Biomass Analysis

Inductively coupled plasma optical emission spectroscopy (ICP-OES) was used to determine metal content using the procedure reported in Petti et al.[1] Ultimate analysis (ASTM D3176) using a LECO CHN-2000 analyzer was performed to determine C, H, N content of the biomass samples. An ELTRA CS-500 instrument was used to determine S content and O was calculated by difference. A LECO TGA 601 was used in order to determine the total ash and moisture content according to ASTM D3172. A LECO AC500 was used to determine the calorific content of the biomass. Acid-soluble lignin and acid-insoluble lignin were measured using the NREL LAP.[35]

Each biomass sample was analyzed via Pyrolysis-GC/MS (Py-GC/MS) and thermogravimetric analysis (TGA). Pyrolysis-GC/MS experiments were performed using a Pyroprobe Model 5200 (CDS Analytical, Inc.) connected to an Agilent 7890 GC with an Agilent 5975C MS detector. The pyroprobe was operated in trap mode under He atmosphere. Pyrolysis was conducted at 650

°C (1000 °C/s heating rate) for 20 s. The valve oven and transfer lines were maintained at 325 °C. The column used in the GC was a DB1701 (60 m × 0.25 mm × 0.25 μm) and the temperature program was as follows: 45 °C for 3 min hold, ramp to 280 °C at 4 °C/min and hold for 10 min. The flow rate was set to 1 mL/min using He as the carrier gas. The inlet and auxiliary lines were both maintained at 300 °C and the MS source was set at 70 eV. The GC-MS was calibrated for a number of phenolic compounds including phenol, 2-methoxyphenol, 2-methoxy-4-methylphenol, 2,6-dimethoxyphenol, vanillin, syringaldehyde and 2-methoxy-4-vinylphenol. Pyrolysis products were analyzed according to retention time and mass spectra data obtained from a NIST library. TGA was performed on a TA Discovery TGA under 25mL/min of N_2 at a ramp of 10 °C /min to 800 °C followed by a ramp of 20 °C /min to 1000 °C.

5.3 Results and Discussion

5.3.1 Biomass Composition

The elemental composition of the biomass samples are summarized in Tables 5.1 and 5.2. Table 5.1 shows the metal composition of several of the biomass samples. Metals occurring in highest abundance included Ca, Mg, Mn, and Fe. In general, the leaves of the sorghum samples contained a higher total metal content than the stems. It was found that the wild-type leaf tissue exhibited greater metal abundance than observed in RG. The opposite trend was observed in RG stems, where total metal composition was 27015 ppm compared to the WT stem total of 14437 ppm, i.e., the metal content of the WT stem was almost 50% less (Table 5.1). The primary macronutrient K was more abundant in WT leaves than in the RG. The opposite K-trend was highlighted in the stem composition where RG displayed more than the wild-type. Calcium was the most abundant secondary macronutrient in all samples, the RG leaf and stem containing around 50% more Ca than wild-type. Further, the secondary macronutrient Mg was also more prevalent in RG leaves than in wild-type. The complete analysis for C, H, N and O displayed no significant ($p > 0.05$) differences between the RG and wild-type (Table 5.2). The differences seen in the abundance of ash relative to the sum of the metals are most likely due to the presence of Si, which was not determined for the biomass samples. The presence of these metals is important because they influence the potential of the biomass to be utilized as a source of nutrients and they influence the thermal decomposition processes of the biomass.[12,28] Calorific content was highest for the wild-type leaves but was similar for the wild-type stems and the RG leaves and stems.

Table 5.1. Metal composition (ppm) of biomass samples.

Bio-mass	As	Al	B	Ca	Cu	Fe	Mg	Mn	Na	Zn	K	Sum
WTL[a]	2	77	8	8482	13	142	1423	103	53	25	22622	32950
WTS[b]	2	100	4	1099	3	189	952	27	44	10	12007	14437
*RG*L[c]	2	52	28	12459	8	129	3347	170	195	47	13269	29706
*RG*S[d]	3	51	6	2668	6	138	1036	213	61	20	22813	27015

[a.] Wild-type leaves; [b.] wild-type stems; [c.] RG leaves; [d.] RG stems

Table 5.2. Ultimate analysis of biomass samples.

Bio-mass	C (%)	H (%)	N (%)	O (%)	S (ppm)	P (ppm)	Ash (%)	Moisture (%)	Calorific Content (MJ/kg)
WTL[a]	43.72	6.19	2.89	39.96	2141	3699	7.15	5.83	17.978
WTS[b]	42.01	6.59	0.48	48.24	475	1177	2.65	10.82	16.477
*RG*L[c]	43.58	6.07	1.04	43.74	1455	2837	5.46	9.97	16.784
*RG*S[d]	41.18	6.45	1.58	45.08	988	1247	5.63	8.60	16.240

[a.] Wild-type leaves; [b.] wild-type stems; [c.] RG leaves; [d.] RG stems

Acid soluble and acid insoluble lignin content in the wild-type and mutant sorghum samples is shown in Figure 5.1. Both forms of lignin were increased significantly in the leaf tissue of RG compared with wild-type. In contrast, acid insoluble lignin content decreased significantly in the stem of RG compared with wild-type. Acid soluble lignin, which accounts for a small proportion (2-3%) of the total lignin, was unchanged in the RG and wild-type stems. The acid insoluble lignin content of the RG leaf was similar to that of the wild-type stem ($p > 0.05$). Taken together, these results demonstrate that lignin accumulated in an antithetic pattern in the RG biomass. Interestingly, the increase in lignin content did not correlate with the calorific content determined for each of the biomass samples. This may be due to differences in the types of sugars and extractives (not determined) present in the RG and wild-type sorghum. Additionally, the RG stems showed increased saccharification efficiency in comparison to the WT, whereas the leaves

showed a decrease in saccharification efficiency, consistent with changes in lignin content within the biomass. These results may also be influenced by differences in the neutral sugar content of the biomass; thorough discussion of sugar content and saccharification efficiency are beyond the scope of this dissertation but are discussed in Petti et al.[1]
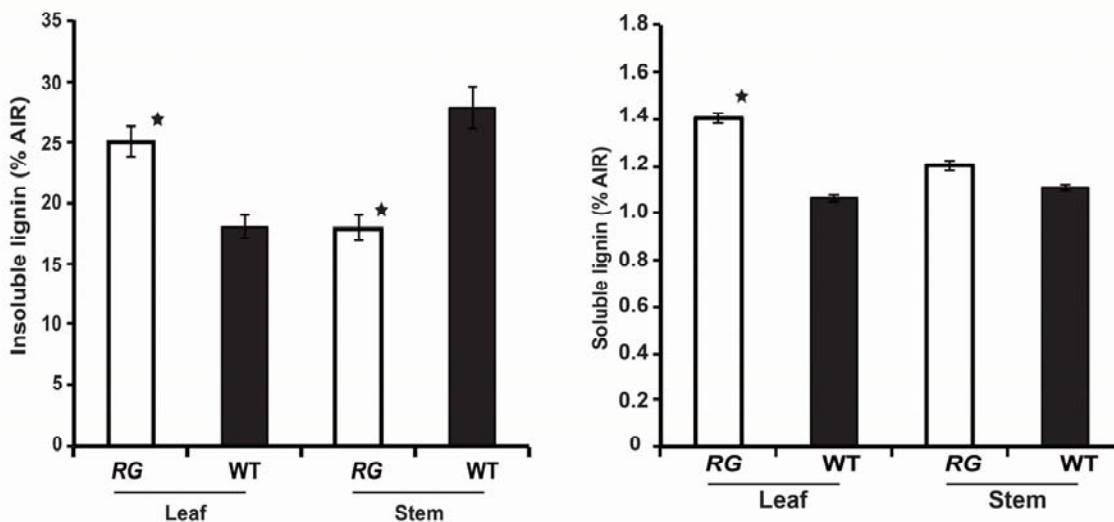
Figure 5.1 Total insoluble lignin and total soluble lignin. Each bar comprises the mean of four biological and four technical replicates. Error bars indicate the standard error from the mean. Significance (p < 0.05) is indicated by a star (★).

As reported in Petti et al.,[1] the cellulose content of the biomass did not differ between wild-type and mutant sorghum, but there were differences in the neutral sugars, which contribute towards the hemicellulosic fraction, present in the biomass. Briefly, rhamnose was significantly greater in the RG leaves than in the WT. Also, arabinose, galactose, and glucose were significantly more abundant in RG than wild-type leaves. In contrast, leaf xylose decreased from 26% in wild-type to 19% in RG. The stem composition also displayed differences from the wild-type. Here, galactose decreased significantly and glucose increased in RG in comparison to the WT. Since lignin is considered to be bound to the hemicellulosic fraction in biomass it is likely that these differences are related to the differences seen in lignin abundance, saccharification efficiency and biomass decomposition products.

5.3.2 Thermogravimetric Analysis

Thermogravimetric analysis of each of the biomass samples was performed; selected weight loss curves and corresponding derivative plots (DTG) being displayed in Figure 5.2. The figure shows how pyrolysis of the leaves differs from the stems for each of the wild-type and mutant sorghum samples. Generally, the leaves pyrolyze over a broader temperature regime than the stems. The leaves display a first weight-loss peak in the DTG plots around 275 °C corresponding to decomposition of hemicellulose, as well as a separate peak at a higher temperature (around 330 °C) corresponding to decomposition of cellulose.[31] However, the stems generally exhibit a higher rate of weight loss around 330 °C, corresponding to the decomposition of the cellulose, than the leaves. This may also be due to the hemicellulose decomposition overlapping with the cellulose given that the hemicellulose does not decompose at the lower temperature in the stems as it does in the leaves. Hence, the cellulose and associated hemicellulose decomposition peak appears sharper and occurs over a narrower temperature regime for the stems. The broad peak of low weight-loss rate occurring in all of the DTG plots from approximately 200 °C to 600 °C corresponds to the decomposition of lignin in the biomass.[31] Lignin in all of the leaf and stem samples appears to decompose at similar rates and temperatures but slight differences in DTG plot shapes are noticeable.
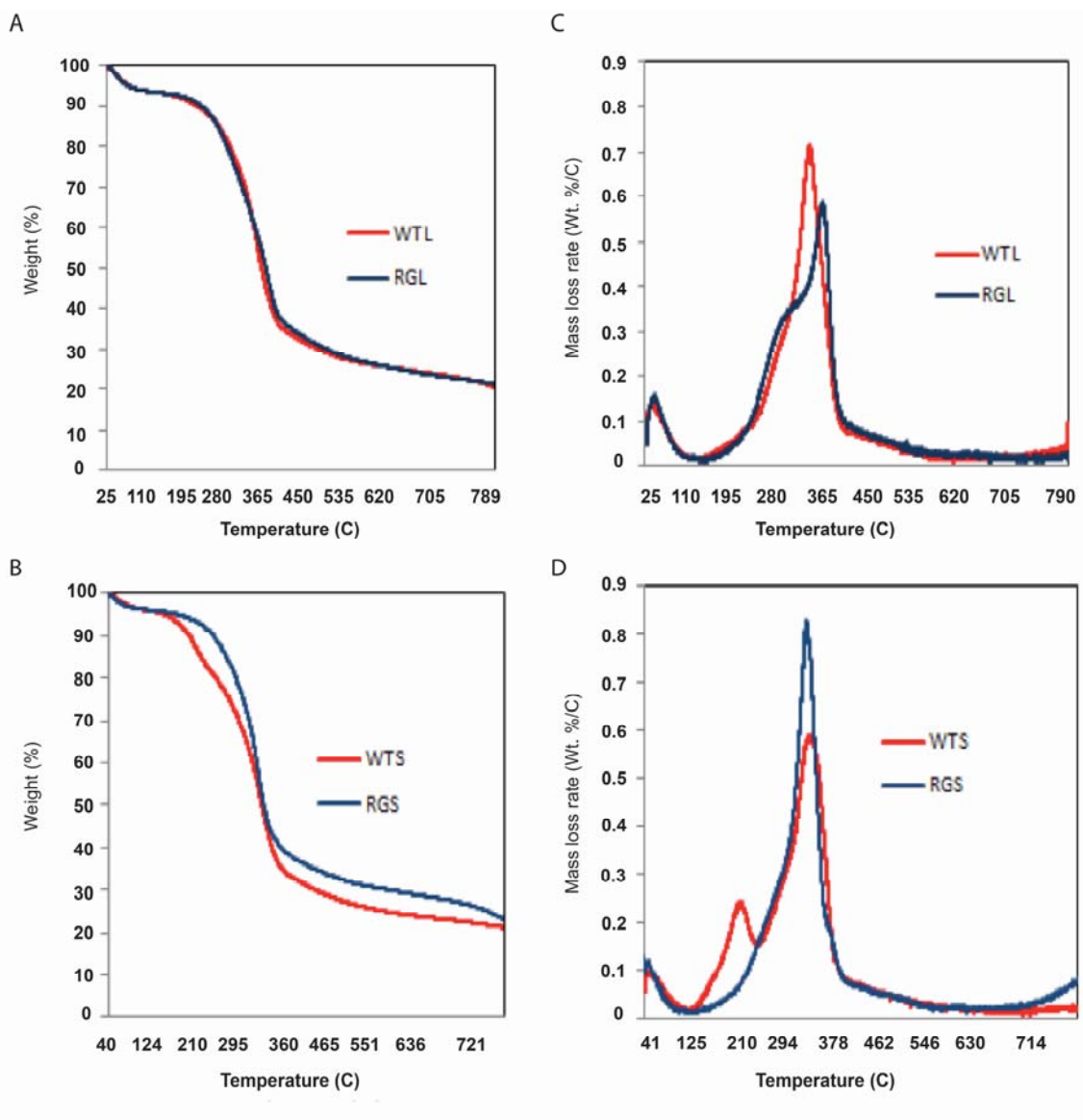
Figure 5.2. Weight-loss curves (A and B, left) and corresponding DTG plots (C and D, right) of the sorghum biomass. DTG values are reported as negative of mass-loss rates. Thermogravimetric analysis plots of leaves are shown in A and C, top, and plots of the stems are shown at the bottom in B and D.

On the basis of TG curves, it is evident that the RG stem pyrolyzed over a more narrow temperature regime than the wild-type feedstock (Figure 5.2B, D). Furthermore, the RG stem displayed approximately 10% less weight loss at 450 °C than the wild-type stem (Figure 5.2B). This can be partially explained by the higher ash content present in the RG stems in comparison to the wild-type. Neither stem nor leaf samples showed greater than 80% weight loss, which may

reflect repolymerization of lignin residue forming "hard coke" [31] in addition to the ash content of the biomass. DTG analysis of leaves showed that RG biomass underwent decomposition at a higher temperature (about 365 °C) compared to wild-type leaves (Figure 5.2C) and also demonstrated a prominent shift in the main cellulosic decomposition peak from 355 to 365 °C. Wild-type leaf tissue showed a single decomposition peak at 355 °C, which was consistent with a cellulose peak. RG leaf decomposition took place at two different temperatures (290-300 °C, 365-375 °C) corresponding to two distinct DTG peaks (Figure 5.2C). The wild-type leaves also showed a higher decomposition rate of cellulose in comparison to the RG leaves. These results suggest that modifying cell wall composition in the RG mutant modestly increased the pyrolysis temperature of the leaf sample. Since lignin content in RG leaves was higher than the wild-type, an increase in decomposition temperature from the holocellulosic fraction would be expected due to possible increase in lignin-carbohydrate bonds and interaction between lignin and holocellulosic biopolymers during decomposition. These results are also consistent with decreased saccharification efficiency in the RG leaves than the wild-type.

In stem analyses, the DTG curves revealed a pronounced peak at 355 °C for both mutant and wild-type (Figure 5.2D) corresponding to the pyrolysis of the cellulose in the plants. The pyrolysis of the hemicellulosic sugars is likely masked within this peak. In contrast to the leaves, the RG stem showed a higher decomposition rate corresponding to the cellulosic peak than the wild-type stem. The higher cellulose decomposition rate in RG stems compared to wild-type stems may result from changes in hemicellulosic sugars that do not show a separate DTG peak. This higher decomposition rate is also consistent with the greater saccharification efficiency for the RG stems in comparison to the wild-type. A decrease in lignin content and hence lignin-carbohydrate bonds may have allowed for higher rates of decomposition seen for the holocellulosic fraction, although a decrease in the pyrolysis temperature was not seen. The wild-type stem also displayed a nominal, uncharacterized pyrolysis peak at 210 °C that was absent from all other samples. Taken together, the RG leaves pyrolyzed over a broader temperature regime than the stems. It is likely that a masked broad peak of low weight-loss rate occurring in all of the DTG plots from approximately 200 °C to 600 °C corresponds to the decomposition of the lignin in the biomass.[31] The lignin in each of the samples (leaves and stems) appears to decompose at similar rates despite differences in the DTG plots.

Differences in the temperatures at which decomposition occurs indicate differences in the kinetics of the decomposition reactions. For example, the higher the temperature at which the maximum rate of weight loss occurs, the higher the expected activation energies associated with the thermal decomposition process, as long as the heating rate is held constant.[31] Other kinetic parameters such as the reaction order (n) and frequency factor (A) may also be the source of differences seen in the decomposition kinetics of the biomass samples. The differences in decomposition profiles results from variations in the composition and structure of components present in biomass. In order to obtain precise activation energy, frequency factor and reaction order values for the different decomposition processes and avoid errors from compensation effects, a thorough analysis of the thermogravimetric behavior at different heating rates needs to be performed. Obtaining these values is beyond the scope of this investigation but the results of thermogravimetric analysis suggest that they will differ. However, differences in biomass composition and structure are still reflected in the thermogravimetric analyses shown in Figure 5.2.

5.3.3 Pyrolysis-GC/MS

Pyrograms obtained from pyrolysis-GC/MS of the biomass samples provide information about the amount and types of pyrolysates generated from the holocellulosic and lignin fractions of the biomass. Peak area percentages from the total ion chromatogram for each compound created during pyrolysis provide a reasonable estimate of the relative abundance of those compounds within the pyrolysis product mixture. While not all compounds were positively identified in the pyrograms, the area percent contribution of the unknown compounds toward the whole pyrogram was still included so that area percent contribution of particular compounds generated during pyrolysis could be monitored relative to the whole pyrolysate distribution as seen in the total ion chromatogram.

Typically, under conditions employed in this work, pyrolysates originating from the holocellulosic fraction of the biomass have shorter retention times (less than 24 min) than those originating from the lignin fraction, although there are several exceptions. Holocellulosic pyrolysates include anhydrosugars, furans, hydroxyacetaldehyde, acetic acid, furfural, 1-hydroxy-2-propanone and other oxygenated hydrocarbons. Pyrolysates originating from the lignin fraction of the biomass include phenol, guaiacol, syringol and related aromatic hydrocarbons. The relative abundance of the lignin-based pyrolysates compared to holocellulose-based pyrolysates is dependent on the relative abundance of each of these polymers within the biomass. The

distribution of the lignin-based pyrolysates will also vary according to the relative abundance of the different lignin monomers (sinapyl, coniferyl and coumaryl alcohols) within the polymer. The relative abundance of different bond types within the lignin polymer may also influence the distribution of lignin-based pyrolysates.

Wild-type sorghum leaves and stems generated pyrograms shown in Figure 5.3 and Py-GC/MS analysis of the pyrolysates is summarized in Table 5.3. The total area percentage of pyrolysates originating from the lignin fraction of the biomass is higher in the stems than in the leaves. The stems also produced more pyrolysates originating from the sinapyl monomer within the lignin polymer. Hence, the S:G ratio of the stems was higher than that of the leaves. Additionally, pyrolysis of the stems produced larger amounts of 4-vinylphenol; most likely resulting from higher coumaryl-lignin content in the stems. The pyrograms show that the relative heights and areas of the peaks from the holocellulose (retention time < 24 min) are lower than those from the lignin (retention time >24 min) for the stem materials in comparison with the leaves. Again, this indicates that the stems have higher lignin content.
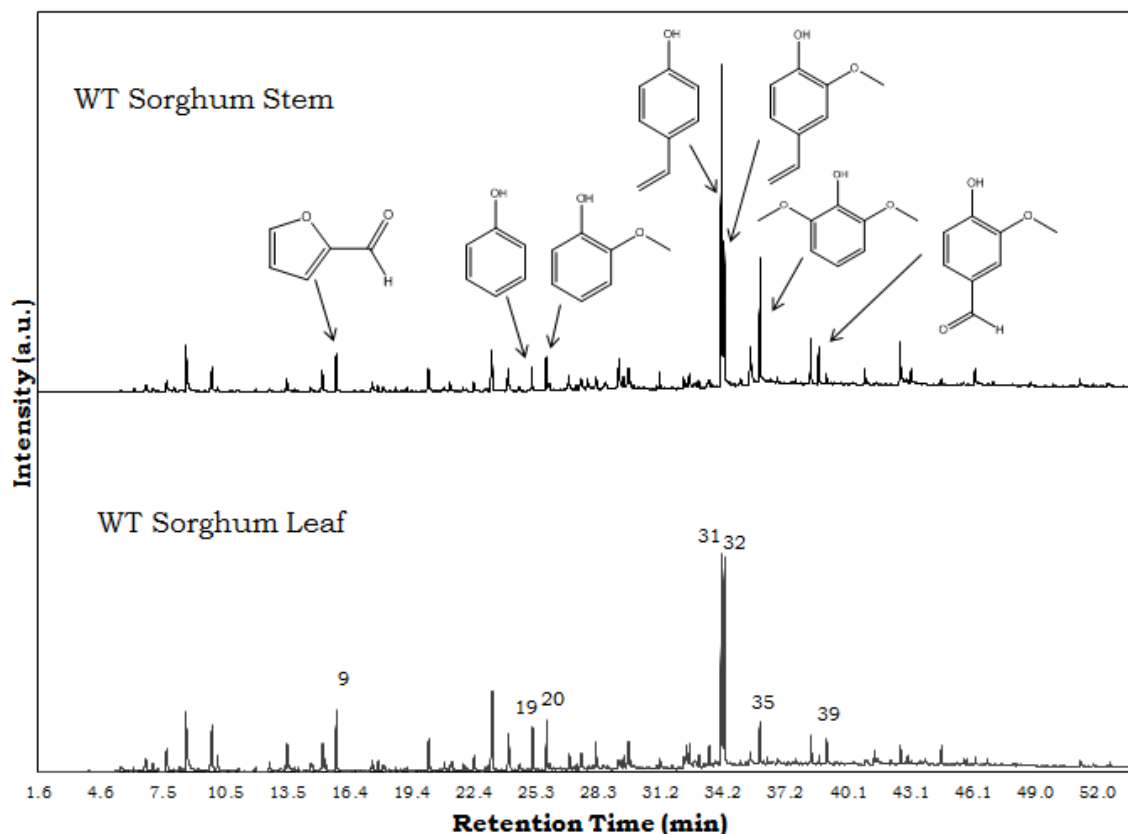
Figure 5.3. Pyrograms of wild-type sorghum leaf and stem. Peak numbers correspond to compounds listed in Table 5.3.

Table 5.3 Wild-type sorghum Py-GC/MS analysis. Area % and sum values reported are averages between 3 samples.

	Retention Time	Compound	WTL[a] Area %	Std. Dev.	WTS[b] Area %	Std. Dev.
1	6.14	2-methylfuran	0.30	0.02	0.27	0.07
2	6.72	2,3-butanedione	1.39	0.13	0.94	0.13
3	7.70	hydroxyacetaldehyde	0.73	0.12	0.74	0.05
4	8.66	acetic acid	2.47	0.47	2.87	0.46
5	9.85	1-hydroxy-2-propanone	3.09	0.25	3.22	0.29
6	10.14	toluene	0.98	0.08	0.33	0.08
7	13.44	acetic acid methyl ester	1.72	0.25	1.59	0.13
8	13.81	o-xylene	0.30	0.03	0.04	0.07

Table 5.3 (continued)

9	15.79	furfural	4.63	0.55	2.41	0.20
10	17.30	2-furanmethanol	0.45	0.07	0.73	0.09
11	18.01	2-methyl-2-cyclopenten-1-one	0.23	0.10	0.10	0.09
12	18.45	2-ethyl-5-methylfuran	0.10	0.08	0.14	0.04
13	19.00	2-cyclopentene-1,4-dione	0.17	0.15	0.22	0.05
14	20.16	1,2-cyclopentanedione	1.30	0.15	1.72	0.03
15	21.20	5-methyl-2-furancarboxaldehyde	0.18	0.16	0.34	0.07
16	21.83	3-methyl-2-cyclopenten-1-one	0.25	0.05	0.19	0.02
17	22.33	2(5H)-furanone	0.77	0.01	0.81	0.08
18	23.97	2-hydroxy-3-methyl-2-cyclopenten-1-one	1.87	0.17	1.55	0.14
19	25.12	phenol	1.48	0.13	1.26	0.13
20	25.79	2-methoxyphenol	1.43	0.09	1.78	0.09
21	26.87	2-methylphenol	0.64	0.04	0.93	0.19
22	27.05	3-ethyl-2-hydroxy-2-cyclopenten-1-one	0.00	0.00	0.24	0.04
23	28.13	4-methylphenol	0.99	0.11	0.57	0.06
24	28.20	3-methylphenol	0.30	0.06	0.33	0.02
25	29.45	2-methoxy-4-methylphenol	0.38	0.01	0.63	0.03
26	29.77	2,4-dimethylphenol	0.23	0.01	0.22	0.02
27	31.18	4-ethylphenol	0.32	0.07	0.45	0.09
28	31.41	benzoic acid	0.00	0.00	0.00	0.00
29	32.33	4-ethyl-2-methoxyphenol	1.00	0.23	0.58	0.10
30	33.52	1,4:3,6-dianhydro-α-d-glucopyranose	0.93	0.11	0.50	0.13
31	34.09	4-vinylphenol	5.46	0.30	9.92	0.79
32	34.23	2-methoxy-4-vinylphenol	6.46	0.15	5.08	0.21
33	34.83	eugenol	0.00	0.00	0.29	0.03
34	35.20	5-hydroxymethyl-2-furancarboxaldehyde	1.58	0.21	4.81	0.81
35	35.92	2,6-dimethoxyphenol	0.84	0.10	3.36	0.50
36	36.78	2-methoxy-4-(1-propenyl)phenol C	0.34	0.09	0.40	0.06
37	38.36	2-methoxy-4-(1-propenyl)phenol T	2.30	0.31	1.65	0.13
38	38.74	4-methylsyringol	0.14	0.16	0.74	0.01
39	39.10	vanillin	0.77	0.05	0.73	0.05
40	39.30	3-hydroxybenzaldehyde	0.15	0.09	0.15	0.16
41	40.00	3-phenyl-2-propenoic acid	0.00	0.00	0.00	0.00
42	41.51	4-hydroxy-3-methoxyacetophenone	0.28	0.07	0.56	0.20
43	42.00	4-hydroxybenzaldehyde	0.83	0.08	1.04	0.03
44	42.28	3,5-dimethoxyphenol	0.00	0.00	0.00	0.00
45	42.62	4-vinylsyringol	1.09	0.06	2.67	0.61

Table 5.3 (continued)

46	42.96	1-(4-hydroxy-3-methoxyphenyl)acetone	0.36	0.03	0.55	0.11
47	43.14	2,6-dimethoxy-4-(2-propenyl)phenol	0.12	0.02	0.84	0.13
48	43.80	1-(2-hydroxyphenylethanone)	0.00	0.00	0.00	0.00
49	44.56	2,6-dimethoxy-4-(1-propenyl)phenol (cis)	0.25	0.01	0.52	0.09
50	46.19	2,6-dimethoxy-4-(1-propenyl)phenol (trans)	0.46	0.05	3.20	0.48
51	47.06	4-hydroxy-3,5-dimethoxybenzaldehyde	0.06	0.10	0.75	0.16
52	48.64	4-hydroxy-3,5-dimethoxyacetophenone	0.36	0.12	0.71	0.29
53	49.07	4-((1E)-3-hydroxy-1-propenyl)-2-methoxyphenol	0.00	0.00	0.62	0.43
54	49.63	4-hydroxy-2-methoxycinnamaldehyde	0.07	0.06	0.62	0.12
55	49.70	3-(4-hydroxy-3-methoxyphenyl)-2-propenal	0.00	0.00	0.91	0.68
56	50.70	3-(4-hydroxy-3-methoxyphenyl)-2-propenoic acid methyl ester	0.13	0.11	0.14	0.06
		Sum Lignin	28.51	1.15	42.58	2.46
		S derivatives	3.32	0.15	12.79	1.62
		G derivatives	13.17	0.58	14.16	1.21
		S:G	0.25	0.02	0.91	0.16

[a.] Wild-type leaves; [b.] Wild-type stems.

Figure 5.4 shows the pyrograms from mutant sorghum leaves and stems and the Py-GC/MS analysis in summarized in Table 5.4. The RG leaves produce more lignin-based pyrolysates than the wild-type leaves, consistent with the lignin content determination. Moreover, RG-leaves produced more sinapyl-derived pyrolysates relative to coniferyl-derived pyrolysates than the wild-type leaves and hence are indicated to have a higher S:G ratio based on the distribution of the pyrolysates. The RG stems also generated more lignin-based pyrolysates than the wild-type stems. While this analysis contradicts the total lignin content determination, it may reflect the differences between the RG and wild-type stems in the preferential formation of char from certain biopolymers. For example, pyrolysis of the sorghum samples may generate varying degrees of char and nonvolatile compounds from the lignin or holocellulosic fractions. Thermogravimetric analysis, Figure 5.1, showed that the pyrolysis of the RG stems left approximately 10 wt% more solid residue at high temperatures than the wild-type stems. This residue (char and nonvolatiles) is likely the cause of the discrepancy seen between the area % contribution of the lignin-based pyrolysates and the lignin content determination. As discussed below, the metal or ash content

present in biomass may also influence the volatile pyrolysate distributions analyzed. In this case, Py-GC/MS analysis may not always agree with lignin content determination.

Py-GC/MS, however, can provide some information about the composition of biomass and the production of certain renewable bio-chemicals produced by thermal decomposition. For example, the mutant stems produced significantly more phenol and 4-vinylphenol (P < 0.05) than the wild-type stems. These pyrolysates are likely the result of increased coumaryl content, likely esterified, in the lignin in the RG stems.[14,19] Higher S:G ratios in stems than in the leaves shown in both wild-type and mutant sorghum are also consistent with S:G analysis of other forms of biomass in the literature.[8] The RG leaves also produced more vanillin, a product used in the flavor industry, upon pyrolysis. Pyrolysates originating from the holocellulosic fractions also differed slightly between the leaves and stems and the wild-type and mutant sorghum. For example, wild-type sorghum leaves generated more acetic acid than the RG sorghum leaves. Generally, the leaves of the sorghum generated higher amounts of furfural than then stems. Again, these pyrolysates may also be influenced by the presence of metals in the biomass. Even if all pyrolysates were influenced by the presence of inorganic metals/ash content, Py-GC/MS analysis is still capable of differentiating biomass components and their subsequent decomposition products. Taken together, these data indicate that the composition and structure of the lignin polymers differed between the RG and wild-type.
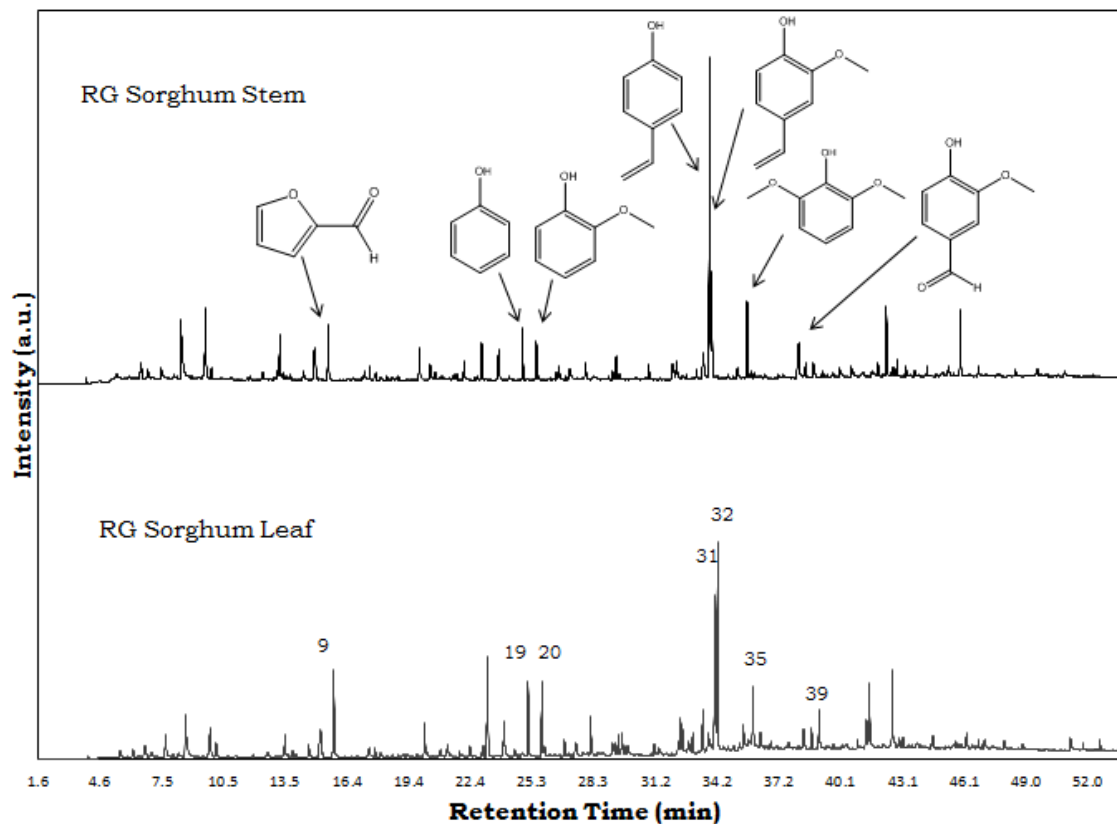
Figure 5.4. Pyrograms produced from RG sorghum stem and leaf. Peak numbers correspond to compounds listed in Table 5.4.

Table 5.4. Mutant sorghum Py-GC/MS analysis. Area % and sum values reported are averages between 3 samples.

	Retention time	Compound	RG Leaf[a] Area %	Std. Dev.	RG Stem[b] Area %	Std. Dev.
1	6.14	2-methylfuran	0.32	0.02	0.05	0.05
2	6.72	2,3-butanedione	0.76	0.02	1.16	0.12
3	7.70	hydroxyacetaldehyde	0.33	0.03	0.90	0.54
4	8.66	acetic acid	1.18	0.32	3.40	0.82
5	9.85	1-hydroxy-2-propanone	1.26	0.01	4.14	0.47
6	10.14	toluene	0.59	0.02	0.69	0.27
7	13.44	acetic acid methyl ester	0.86	0.01	1.47	0.22

Table 5.4 (continued)

8	13.81	o-xylene	0.22	0.01	0.00	0.00
9	15.79	furfural	2.97	0.20	2.65	0.40
10	17.30	2-furanmethanol	0.00	0.00	0.66	0.13
11	18.01	2-methyl-2-cyclopenten-1-one	0.14	0.01	0.11	0.08
12	18.45	2-ethyl-5-methylfuran	0.00	0.00	0.02	0.03
13	19.00	2-cyclopentene-1,4-dione	0.00	0.00	0.07	0.13
14	20.16	1,2-cyclopentanedione	1.08	0.04	1.39	0.08
15	21.20	5-methyl-2-furancarboxaldehyde	0.27	0.02	0.02	0.03
16	21.83	3-methyl-2-cyclopenten-1-one	0.09	0.08	0.33	0.02
17	22.33	2(5H)-furanone	0.52	0.03	1.01	0.13
18	23.97	2-hydroxy-3-methyl-2-cyclopenten-1-one	1.56	0.02	2.02	0.24
19	25.12	phenol	2.19	0.10	2.10	0.27
20	25.79	2-methoxyphenol	2.08	0.10	1.76	0.23
21	26.87	2-methylphenol	0.59	0.04	0.74	0.06
22	27.05	3-ethyl-2-hydroxy-2-cyclopenten-1-one	0.00	0.00	0.22	0.04
23	28.13	4-methylphenol	1.12	0.05	0.62	0.12
24	28.20	3-methylphenol	0.38	0.02	0.41	0.11
25	29.45	2-methoxy-4-methylphenol	0.59	0.03	0.27	0.23
26	29.77	2,4-dimethylphenol	0.27	0.02	0.11	0.10
27	31.18	4-ethylphenol	0.29	0.03	0.83	0.15
28	31.41	benzoic acid	0.37	0.04	0.00	0.00
29	32.33	4-ethyl-2-methoxyphenol	1.09	0.08	1.07	0.69
30	33.52	1,4:3,6-dianhydro-α-d-glucopyranose	1.02	0.00	0.28	0.25
31	34.09	4-vinylphenol	3.44	0.18	18.59	2.24
32	34.23	2-methoxy-4-vinylphenol	5.51	0.09	6.18	0.73
33	34.83	eugenol	0.14	0.12	0.10	0.18
34	35.20	5-hydroxymethyl-2-furancarboxaldehyde	1.98	0.23	0.18	0.13
35	35.92	2,6-dimethoxyphenol	1.38	0.11	3.51	0.31
36	36.78	2-methoxy-4-(1-propenyl)phenol C	0.30	0.05	0.13	0.13
37	38.36	2-methoxy-4-(1-propenyl)phenol T	1.98	0.47	2.52	1.17
38	38.74	4-methylsyringol	0.58	0.04	0.82	0.01
39	39.10	vanillin	2.62	0.14	0.67	0.08
40	39.30	3-hydroxybenzaldehyde	0.25	0.23	0.22	0.10
41	40.00	3-phenyl-2-propenoic acid	0.44	0.08	0.00	0.00
42	41.51	4-hydroxy-3-methoxyacetophenone	2.29	0.17	0.27	0.26
43	42.00	4-hydroxybenzaldehyde	1.87	0.21	0.64	0.44

Table 5.4 (continued)

44	42.28	3,5-dimethoxyphenol	0.58	0.04	0.00	0.00
45	42.62	4-vinylsyringol	2.34	0.15	3.10	0.22
46	42.96	1-(4-hydroxy-3-methoxyphenyl)acetone	0.33	0.03	0.15	0.20
47	43.14	2,6-dimethoxy-4-(2-propenyl)phenol	0.56	0.03	0.91	0.08
48	43.80	1-(2-hydroxyphenylethanone)	2.00	0.24	0.17	0.18
49	44.56	2,6-dimethoxy-4-(1-propenyl)phenol (cis)	0.59	0.12	0.63	0.11
50	46.19	2,6-dimethoxy-4-(1-propenyl)phenol (trans)	1.08	0.06	3.02	0.22
51	47.06	4-hydroxy-3,5-dimethoxybenzaldehyde	0.44	0.06	0.75	0.07
52	48.64	4-hydroxy-3,5-dimethoxyacetophenone	0.57	0.07	0.75	0.06
53	49.07	4-((1E)-3-hydroxy-1-propenyl)-2-methoxyphenol	0.00	0.00	0.04	0.08
54	49.63	4-hydroxy-2-methoxycinnamaldehyde	0.20	0.03	0.32	0.46
55	49.70	3-(4-hydroxy-3-methoxyphenyl)-2-propenal	0.00	0.00	0.13	0.22
56	50.70	3-(4-hydroxy-3-methoxyphenyl)-2-propenoic acid methyl ester	0.27	0.03	0.03	0.05
		Sum Lignin	**41.54**	**0.56**	**53.25**	**2.05**
		S derivatives	**7.54**	**0.29**	**13.49**	**0.32**
		G derivatives	**17.07**	**0.40**	**13.03**	**1.35**
		S:G	**0.44**	**0.02**	**1.04**	**0.09**

[a.] RG leaves; [b.] RG stems.

Differences in metal composition may influence pyrolysis product distribution.[12,23,28] For example, Fahmi et al.[23] found that higher levels of potassium in switchgrass correlated to decreased production of levoglucosan from pyrolysis of the biomass. They suggest that the presence of metals has a catalytic effect that leads to further decomposition of the levoglucosan into hydroxyacetaldehyde and other compounds. Moreover, they found that the metal content of switchgrass had an inverse relationship with the amount of Klason lignin in the biomass. The results presented here demonstrate that this is true for wild-type sorghum; the stems have higher lignin content and lower metal (ash) content whereas the leaves have less lignin and more metals. However, total ash content was similar in the leaves and stems in the RG biomass despite differences in lignin content. The RG stems also contained more K than the RG leaves and the wild-type stems, but was similar to the wild-type leaves. The presence of K may have increased the cracking of holocelulosic products in the mutant stem to generate non-condensable gases

causing an apparent decrease in the production of holocellulosic-based pyrolysates relative to the lignin-based pyrolysates. While the metals were not leached from the biomass prior to pyrolysis (in order to avoid hydrolyzing sugars and removing compounds providing structural information), their presence most likely only shifted the abundance of the various holocellulose-based pyrolysates but not their summed contribution to the pyrograms. The influence of metal content on lignin pyrolysis product formation has been found to be minimal, possibly due to the aromatic nature of the lignin polymer being unable to readily coordinate and/or react with the mineral species.[24] However, thermogravimetric analysis (Figure 5.2) indicates that slow pyrolysis of the mutant stems generates a higher percentage of remaining char/nonvolatiles than the wild-type stems. Therefore it is possible that the variation in the pyrolysates between the wild-type and RG sorghum are the result of a combination of differences in biopolymer structure, composition and metal content, which can lead to differences in the decomposition processes that occur during pyrolysis.

5.4 Conclusions

Chemical mutagenesis was used to induce mutations in *Sorghum bicolor* (L.) of the Della variety. The wild-type plants stems and leaves were separated dried, ground and analyzed for chemical composition and thermal decomposition products. The RG mutant stems have lower lignin content than the wild-type stems and the mutant leaves contain more lignin than the wild-type leaves. Pyrolysates generated from the RG mutants showed an increase in the amount of lignin-based pyrolysates from both stems and leaves in comparison to the wild-type. Even though the RG stems were found to have lower lignin content than the wild-type, the production of higher amounts of lignin-based pyrolysates from the stems may be due to the presence of metals (ash) in the biomass. Additionally, thermogravimetric analysis (TGA) showed that the pyrolysis of the mutant stems left behind more nonvolatile residue than wild-type, which may also explain the differences in the pyrolysate abundances. The mutant leaves and stems also produced higher amounts of sinapyl-derived pyrolysates than the wild-type, suggesting that the mutant lignin has higher S:G ratios. TGA also showed differences in the rate and temperatures at which the wild-type and mutant biomass pyrolyzed. The main decomposition of the mutant leaves occurred at a higher temperature than the wild-type, which may result from the increase in lignin content. The RG stems main decomposition occurred at a higher rate than the decomposition of the wild-type stems. All of these results are consistent with the finding that stems of the RG biomass exhibit increased saccharification efficiency compared to the wild-type stems, with the opposite trend

observed in the leaves. Overall, Py-GC/MS and thermogravimetric analysis of the wild-type and mutant stems and leaves indicated differences in the structure and composition of the biomass, as well as its thermal decomposition behavior.

Chapter 6. Microalgae as a Renewable Fuel Source: Fast Pyrolysis of *Scenedesmus* sp.

Note – This chapter was reprinted from:

Harman-Ware, A. E.; Morgan, T.; Wilson, M.; Crocker, M.; Zhang, J.; Liu, K.; Stork, J.; DeBolt, S., Microalgae as a renewable fuel source: Fast pyrolysis of *Scenedesmus* sp. *Renewable Energy* **2013,** *60*, 625-632.[1]

The article appears in this dissertation with permission from Elsevier.

Note –The experimental content in Section 6.2.2 was not performed by the author and is beyond the scope of this dissertation.

6.1 Introduction

The need for sustainable, renewable energy, as well as the aspiration to lower greenhouse gas emissions and decrease our dependency on fossil fuels, has driven interest and research towards the development of fuels derived from biomass resources. Agricultural crops and their waste, such as soybeans, corn and corn stover, have been extensively researched for use in the production of biofuels such as bioethanol and biodiesel.[2] Cassava, a non-grain feedstock, has also been used as a starch source to produce bioethanol.[3,4] However, production, preparation, transportation, and land supply concerns are associated with some of these resources.[5] Increases in world market food prices and disruption of soil nutrient cycles are also problems associated with the use of food crops and associated wastes for biofuel production. Consequently, there is a strong impetus to develop biofuels that are not based on agricultural food crops.[6] In this context, microalgae species have shown potential as a feedstock for the production of several types of renewable fuels including bioethanol, biodiesel and methane.[2] Microalgae can also be used to remove CO_2 from industrial flue gases and as wastewater treatment for removal of ammonium salts and phosphates, and do not require the use of agricultural land for cultivation.[7,8] Additionally, microalgae have higher areal productivity than traditional, terrestrial biomass sources, typically up to 20 g/m^2/day.[9] Hence, the use of microalgae as a feedstock for the production of biofuels offers many opportunities if challenges in large-scale cultivation, harvesting and conversion to fuels can be overcome.

Fast pyrolysis, the rapid thermal decomposition of organic material in the absence of oxygen, has been investigated as a practical route for the generation of renewable fuels and chemicals from biomass.[10-12] Traditionally, lignocellulosic biomass such as wood from poplar, eucalyptus and other trees, as well as grasses (e.g., switchgrass), has been used as a pyrolysis feedstock. The bio-oil produced from pyrolysis of lignocellulosic materials is complex, unstable and has high viscosity, moisture and oxygen content.[5,11] These properties can be attributed to the non-specific thermal degradation of the lignin and holocellulose in the biomass. The resulting pyrolysis liquid contains hundreds of compounds including aldehydes, cresols and acids. Hence, catalytic upgrading is typically required in order to facilitate utilization of the bio-oil as fuel.[8]

Microalgae have a very different chemical composition from wood and other lignocellulosic feedstocks. Whereas wood is composed mostly of cellulose, hemicellulose and lignin, microalgae can contain substantial amounts of lipids and proteins in addition to carbohydrates.[2] Hence, bio-oil produced from pyrolysis of microalgae can contain different types and amounts of compounds such as linear hydrocarbons and nitrogenous species resulting from pyrolysis of lipids and proteins, respectively. In principle, these differences from lignocellulosic feedstocks may lead to improved properties in the resulting bio-oil, such as higher heating values and reduced tar formation. In addition, biochar obtained from algae pyrolysis may be useful for agricultural purposes. The addition of biochar to soil can improve water-holding capacity, increase nutrient content, and enhance microbial activity.[13-15]

To date, there have been relatively few reports about the pyrolytic characteristics of microalgae. Wu and co-workers[16] studied the effect of temperature and residence time in the pyrolysis of *Chlorella protothecoides* performed in a batch autoclave and found that a maximum oil yield of 52% was obtained after heating at 500 °C for 5 min. The same group also studied the yield and composition of hydrocarbon gases produced during the slow pyrolysis of *C. protothecoides*.[17] A more recent study by Miao and Wu[18,19] examined the production of bio-oil from *C. protothecoides* and *Microcystis aeruginosa* using fast pyrolysis. Interestingly, the yield of bio-oil from heterotrophic *C. protothecoides* was 3.4 times higher than the bio-oil yield obtained from the same algae grown autotrophically, while the bio-oil obtained from the former had lower oxygen content, higher heating value, lower density and lower viscosity than the latter. These results could be attributed to the much higher lipid content of the heterotrophic algae (55.2% versus 14.6%). Campanella *et al.*[20] compared the slow pyrolysis of duckweed to *Scenedesmus sp.* under CO_2 at 300 °C. The *Scenedesmus sp.* afforded a higher yield of pyrolysis oil than the

duckweed, while the microalgae feedstock was also found to have a higher heating value (HHV) of 19 MJ/kg, greater than the HHV of the duckweed (15 MJ/kg). Speciation of the pyrolysis oil produced from the algal feedstock identified 300+ compounds, with similar amounts of hydrocarbons and oxygenates, while acetic was the major product in the aqueous phase.

Babich *et al.*[21] studied the pyrolysis of *Chlorella* algae in a fixed bed microreactor both with and without Na_2CO_3 as a catalyst. Use of Na_2CO_3 resulted in bio-oil with lower acidity and higher heating value than bio-oil produced without the catalyst. Microwave-assisted pyrolysis of *Chlorella* sp. has also been reported.[22] The product was an alkaline bio-oil possessing a relatively low oxygen content (16.5%) and a comparatively high heating value (30.5 MJ/kg). Pan and co-workers[23] pyrolyzed *Nannochloropsis sp.* without and with various amounts of HZSM-5 catalyst at a variety of temperatures. They found the optimal temperature for the yield of bio-oil to be 400 °C. The bio-oil yield and the amount of oxygen in the product decreased with an increase in the amount of catalyst used. Hence, the use of the catalyst caused an increase in the HHV of the bio-oil from 24.6 MJ/kg to 32.7 MJ/kg.

The goal of the current study was to examine the fast pyrolysis of a dried microalgae feedstock, *Scenedesmus* sp., using a bench-scale isothermal spouted bed pyrolysis unit. The bio-oil and biochar produced were analyzed for total acidity, composition, and calorific content. Micro-scale Pyrolysis-GC-MS was also performed in order to provide insights into the nature of the primary products obtained from *Scenedesmus* sp. pyrolysis. A portion of this work has been previously communicated.[24]

6.2 Materials and Methods

6.2.1 Algae Feedstock

The algae feedstock was dried, ground *Scenedesmus* sp. which had been cultured autotrophically in an open pond. 20 gallons of wet algae (11 -16% dry mass) was dried at 60 °C for 24 h. The dried algae clusters (2.9% residual water) were then milled to produce 2 mm particles. The algae feedstock was analyzed for total protein content using the Bradford method[25] and total glucose content using a modified Updegraff method.[26] The Bligh and Dyer method[27] was used to determine the total lipid content. Ultimate analysis was performed according to ASTM D3176; a LECO CHN-2000 instrument was used to determine C, H, N content, an ELTRA CS-500 was used to determine S content and O was calculated by difference. Proximate analysis was

performed according to ASTM D3172 using a LECO TGA 601 in order to determine the total ash, moisture, and volatile content of the algae feedstock.

6.2.2 Spouted Bed Pyrolysis

Pyrolysis was conducted in a bench-scale spouted (fluidized) bed fast pyrolysis reactor. A schematic of the unit is shown in Figure 6.1. Pyrolysis was performed at 480 °C and 100 kPa with a 2 s vapor residence time and total run time of 2 h. The pyrolysis temperature was chosen after trial runs indicated maximum liquid product yields at 480 °C. A screw feeder (Acrison's MD-II Weight Feeder Controller) with an air-locked star rotary valve (Sunco Power Systems) was used as the feeding system and was run at approximately 2.3 kg/h. The biomass was fed into the pyrolysis chamber (draft tube) from the bottom through pneumatic transportation by nitrogen. Prior to mixing with the biomass, the nitrogen (flow rate 8 m^3/h) was heated to 170 °C. The feedstock was introduced into the bottom of the draft tube where it contacted the bed material, 60 mesh sand, and was then heated immediately to 480 °C by the bed material for fast pyrolysis. The spouting stream was redirected downward by the recirculating tube above the draft tube. Here, the sand was separated from the vapors, recycled and heated. The draft tube had a 10 cm ID, the recirculating tube had a 15 cm ID and the whole pyrolysis chamber was 1.8 m tall. The bed height was 254 mm.
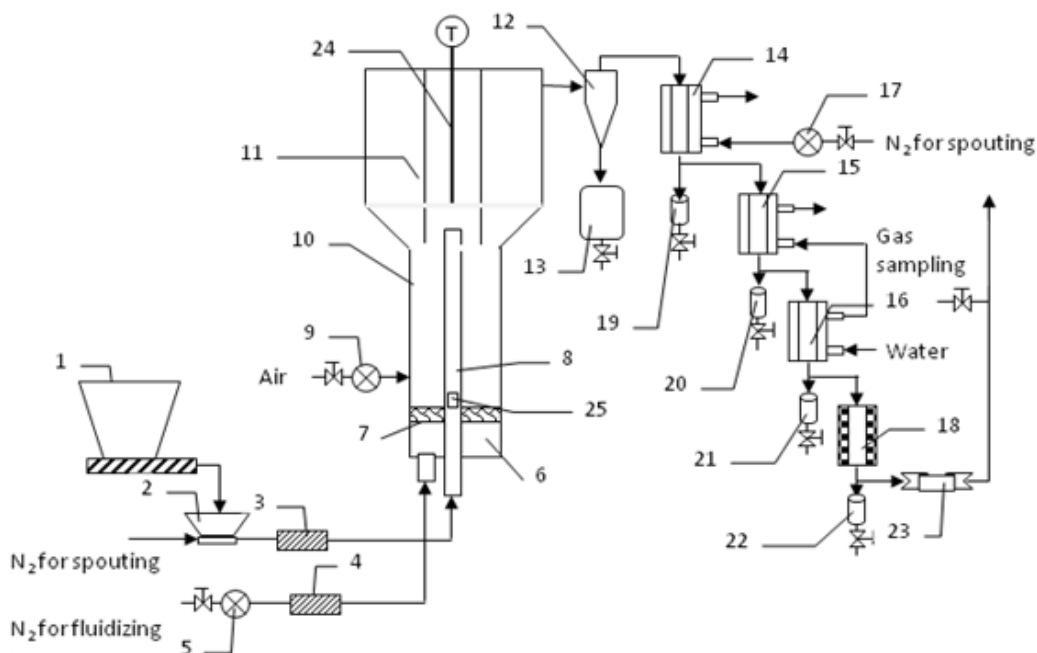
Figure 6.1. Schematic of fast pyrolysis unit. 1. Screw feeder; 2. Rotary valve; 3,4. Tape heater; 5. MFC; 6. Windbox; 7. Distributor; 8. Draft tube; 9. MFC; 10. Main body; 11. Recirculating tube; 12. Cyclone; 13. Char bin; 14-16. Heat exchanger; 17. MFC; 18. Heat exchanger with dry ice; 19-22. Oil container; 23. Filter; 24. Thermocouple; 25. Open window for solids entrainment.

The pyrolysis stream flowing out of the reactor first passed through a high-temperature cyclone (480 °C) where char and ash were separated from the gas. A tape heater was installed on the outside surface to prevent the condensation of bio-oil in the cyclone. After passing the cyclone, four condensers were installed in series to collect bio-oil. The first condenser (C1, corresponding to items 14 for the heat exchanger and 19 for the collection bin in Figure 6.1) was cooled with spouting gas (nitrogen) for heat recovery, the temperature of the gas inside the condenser being measured at 365 °C and 67 °C at the outlet. The second and the third condensers were cooled with tap water and the temperatures were 270 °C and 135 °C, respectively, at their inlets and approximately 10 °C at their outlets. The fourth condenser (C4: heat exchanger 18 and bin 22 in Figure 6.1) used dry ice as a coolant, the temperature at the inlet being approximately 20 °C. After passing through the condensing units, residual gas and vapors were filtered with glass wool, which was kept cool with dry ice at -15 °C. The non-condensable gases in the effluent were compressed, reheated to 170 °C and recycled back into the reactor as fluidizing gas. Oil samples

from the reactor walls and final filter were also collected for mass recovery calculations and analysis. The weight of oil collected was determined by weighing the containers and the glass wool before and after each run. Additionally, the oil condensed on the wall was determined by weighing the parts. The oil captured by glass wool in the filters was extracted with acetone for further analysis. All oil products were stored in a refrigerator. The char in the cyclone was also collected and weighed. The coke deposited on the surface of sand particles collected from the pyrolysis unit was determined by weighing the used sand before and after 3 hours of heating at 550 °C using a muffle furnace.

6.2.3 Pyrolysis-GC-MS

Pyrolysis-GC/MS (Py-GC/MS) was performed using a CDS Analytical Model 5200 Pyroprobe connected to an Agilent 7890 GC with an Agilent 5975C MS detector. Pyrolysis was run in trap mode without the use of a reactant gas and utilized a sorbent tube maintained at 325 °C containing Tenax. Pyrolysis was conducted at 480 °C (1000 °C/s heating rate) for 2 s under He using a 1 mg sample packed in a quartz cell and held in place using quartz wool. Each sample was heated to 100 °C in the pyroprobe for 10 s prior to analysis. The valve oven and transfer lines were each set at 325 °C. The column used in the GC was a DB1701 (60m × 0.25mm × 0.25 μm) and the temperature program was as follows: 45 °C for 3 min, followed by a ramp to 280 °C at 4 °C/min with a 10 min hold at the end. The flow rate was set to 1 mL/min using He as the carrier gas and an inlet split ratio of 90:1. The inlet and auxiliary lines were both maintained at 300 °C and the MS source was set to 69 eV. Py-GC/MS measurements were performed in triplicate for statistical purposes.

6.2.4 Bio-oil and Biochar Analysis

Bio-oil products from the spouted bed reactor were analyzed via GC-MS using an HP-88 column (30 m × 0.25 mm × 0.20 μm). This column, in comparison with DB-1 and DB-5 columns, provided the best resolution between peaks in each of the samples. The samples (oil fractions) were dissolved 1:100 in chloroform. The inlet was set at 325 °C and had a split ratio of 30:1, the auxiliary line was set to 325 °C, He was used as the carrier gas at 1 mL/min and the MS source was set to 69 eV. The temperature program was as follows: 50 °C for 1 min, ramp to 250 °C at 7 °C/min and hold for 5 min. Simulated distillation GC equipped with a DB-2887 column (ASTM D2887) was used to determine approximate boiling point distributions for the oil fractions (organic layer, not including water content). Given that hydrocarbon standards (C5-C44 linear alkanes) were used for calibration of the GC, whereas the bio-oils analyzed were rich in polar (N-

and O-containing) compounds, a series of heteroatom-containing compounds were also run, including pyridine, stearamide, octadecylamine, myristic acid, palmitic acid, stearic acid, methyl oleate and methyl stearate. In each case the boiling point determined by simulated distillation GC analysis agreed to within 20 °C of the literature value. The results obtained for the bio-oils are therefore considered to provide a fair indication of the actual boiling point ranges, although cannot be considered precise.

Ultimate analysis (ASTM D3176) using a LECO CHN-2000 analyzer was performed to determine C, H, N concentrations in both the oil and biochar (dry basis) fractions and an ELTRA CS-500 was used to determine sulfur content, while oxygen was determined by difference. Proximate analysis (particularly, ash composition) for oil and biochar was performed according to ASTM D3172 using a LECO TGA 601. The calorific content of each oil fraction was determined using a LECO AC500 according to ASTM D5865. The total acid number (ASTM D664) was also determined for the different oil fractions collected. FT-IR spectra of the oil fractions were collected over CaF_2 windows using a Nicolet 6700 FT-IR spectrometer. ^{13}C NMR spectra of several oil fractions were also collected using a Varian 400 MHz NMR spectrometer. Samples were dissolved in $CDCl_3$ and signals were referenced internally to the solvent peaks. SEM micrographs of the biochar were taken using a Hitachi S-4800 Scanning Electron Microscope operating at 15 kV. ICP-OES was used to determine the composition of various metals in the biochar.

6.3 Results and Discussion

6.3.1 Analysis of Feedstock

Ultimate and proximate analyses of the *Scenedesmus* sp. feedstock are summarized in Table 6.1. The amount of volatile matter contained in the feedstock provides information about the potential of liquid product formation. The amount of ash contained in this particular feedstock was found to be extremely high (35.2%). This can be explained by the presence of frustules from *Navicula* diatoms, which occur in the *Scenedesmus* as an invasive species (see section 6.3.2). The maximum liquid yield and ash content are important factors contributing toward the efficiency in the production of pyrolysis oil and in the types of compounds generated. The ash in the biomass may also influence the distribution of compounds seen in the oil product. Hence, these factors should be considered when selecting a feedstock for bio-oil production and in the use of the products formed.

Table 6.1. Ultimate and proximate analysis of *Scenedesmus* sp. feedstock.

Weight %								
C	H	N	O	S	Volatile	Moisture	Fixed C	Ash
32.1	4.8	5.3	22.1	0.5	59.7	2.9	2.1	35.2

This feedstock, like other algal species, also has a higher nitrogen content than typical lignocellulosic feedstocks due to the large amount of protein present in the algae. Therefore, bio-oil obtained from algae can be expected to contain higher concentrations of nitrogenous species than bio-oil obtained from feedstocks such as wood or switchgrass. The protein, glucose and lipid content of the algae are given in Table 6.2. These values are consistent with previously reported values for *Scenedesmus*.[2]

Table 6.2. Total protein, glucose and lipid content of *Scenedesmus* sp. feedstock.

Weight %		
Protein	Glucose	Lipids
27.8	7.8	11.5

6.3.2 Spouted Bed Pyrolysis Products

Fractions collected from the quenching coolers of the fast pyrolysis unit are defined such that C1 corresponds to the heaviest oil (highest condensing temperature) fraction collected and C4 corresponds to the lightest oil fraction (lowest condensing temperature not including the filter oil), where C2 and C3 are intermediate fractions. The C2-C4 and filter oil fractions were obtained as mobile, brown liquids and were analyzed as the primary bio-oil products from the pyrolysis process. C1 was an extremely viscous tar, constituting only 2% of the total oil recovered and hence was not analyzed. In addition, the reactor wall was scraped of oil and residual algae and this mass totaled 23.2 % of the total mass recovered. This fraction was not analyzed in detail due to the presence of unreacted algae and ash but was included as part of the calculation done to determine the percent yields of the fractions. The total oil yield was estimated at approximately 55 wt%, based on the yield of bio-oil fractions collected and the approximate amount of oil remaining on the reactor walls and piping. Note that this figure is based on the weight of feedstock, excluding its ash content.

Considering first the char product, the ratio of crude oil:char obtained was 3.76 by weight for the oil fractions collected. The char had low calorific content (4.6 MJ/kg) and contained 13.3 wt% volatile matter, while ultimate analysis showed it to contain 15.9 wt% carbon, together with small amounts of nitrogen (2.3 wt%), sulfur (0.8 wt%), and hydrogen (0.8 wt%). 75 wt% of the biochar mass was attributed to the presence of ash. SEM images (Figure 6.2) indicate that a significant portion of the ash content resulted from the presence of frustules derived from *Navicula* diatoms that were present in the algae feedstock as a contaminant. The presence of these organisms also explains the high ash content (35.2 wt%) in the original feedstock (see Table 6.1). The ash obtained from the biochar consisted of 49.5 wt% SiO_2, 4.1 wt% Fe_2O_3, and 11.0 wt% Al_2O_3 which is consistent with the presence of the silicate frustules.[28] The biochar ash also contained 10.7 wt% CaO, 1.6 wt% Na_2O, 5.9 wt% K_2O, 9.7 wt% P_2O_5, and 3.1 wt% SO_3 which were mainly associated with the *Scenedesmus* sp. (originating from the nutrients supplied to the algae feedstock).
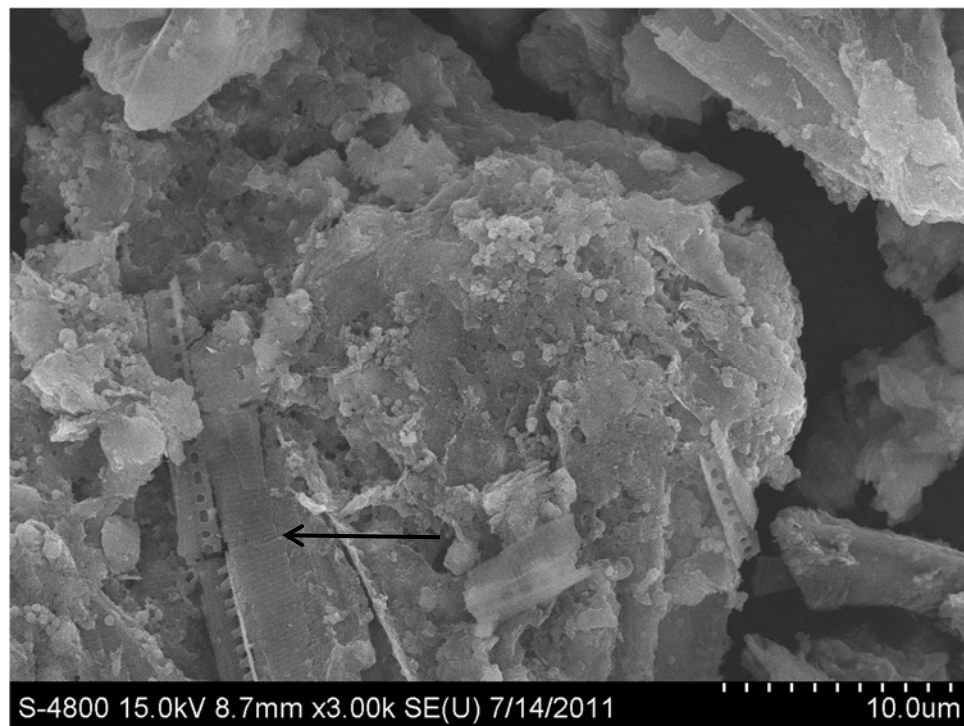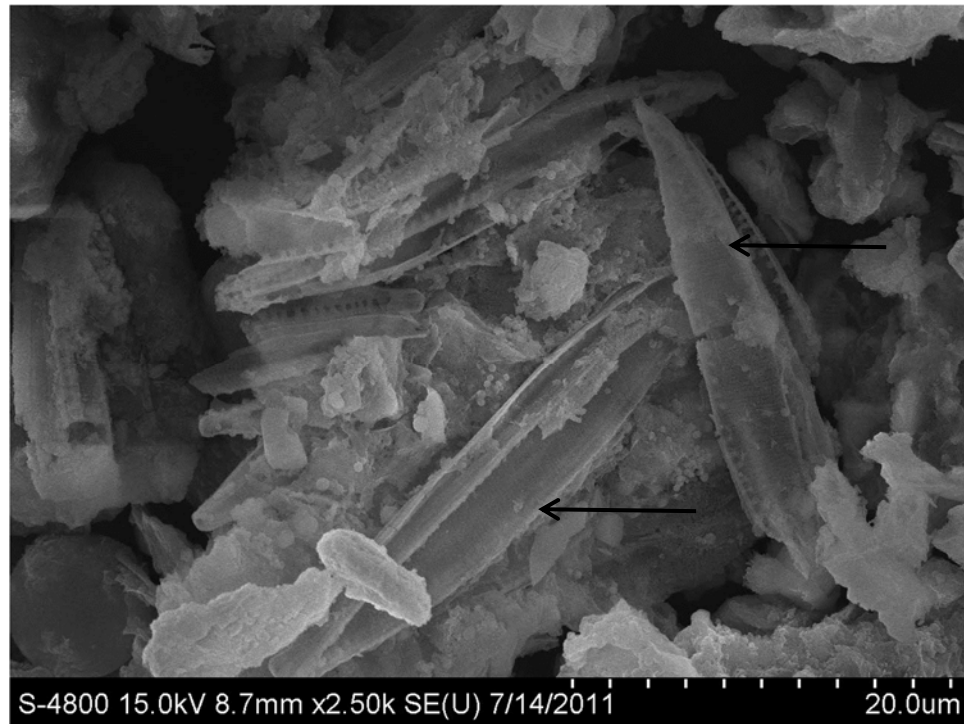
Figure 6.2. SEM micrographs of *Scenedesmus* sp. derived biochar showing presence of frustules.

Turning to the oil fractions, the filter oil constituted the largest percent of recovered oil product by mass (33.8% of the total), followed by the C3 oil fraction (28.5% of the total, see Table 6.3). The average total acid number for the oil products was 68 mg KOH/g, which is somewhat lower than typical bio-oil produced from wood pyrolysis.[10] The average calorific content and total acid number of the oil as a whole was calculated based on normalization of the mass of the different oil fractions.

Table 6.3. Product distributions for select oil fractions based on GC-MS analysis.

Compounds (Class of Compounds)	C2 (Area %)	C3 (Area %)	C4 (Area %)	Filter (Area %)
Alkanes	0.0	2.0	0.0	2.6
Alkenes	1.5	8.9	0.0	9.4
Fatty Oxygenates	21.0	12.1	0.0	32.3
Steroids	2.8	0.0	12.9	3.1
Aromatics	0.0	0.0	0.0	1.8
N-containing Compounds	18.7	70.4	86.2	21.7
Unidentified	56.0	6.7	1.0	29.1
Yield of oil fraction (% of total oil recovered)	3.1	28.5	11.4	33.8

Ultimate and proximate analysis showed the oil products to contain an average of 27.6 wt% oxygen, 51.9 wt% carbon, 9.0 wt% hydrogen and 8.6 wt% nitrogen (dry basis), the relatively high nitrogen content being a consequence of the high protein content of the algae. Figure 6.3 displays the results from ultimate and proximate analyses for the two most abundant oil fractions. It should be noted that the "moisture" content corresponds to compounds boiling around 100 °C, not just water, and "volatile" content includes "moisture" content and higher boiling point compounds. The average density of the oil was 1.1 g/mL, which is slightly lower than that of bio-oil derived from wood pyrolysis[10] but similar to values reported for pyrolysis oil derived from autotrophically grown algae.[18,19]
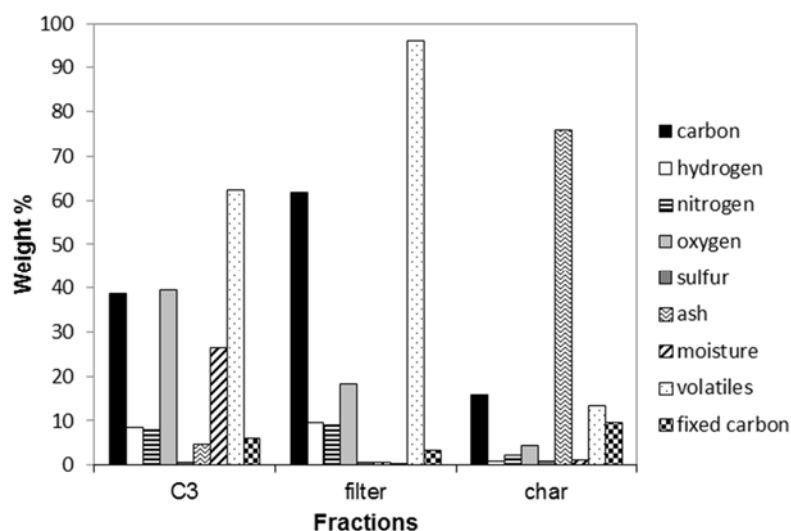
Figure 6.3. Ultimate and proximate analysis of select fractions obtained from *Scenedesmus* sp. pyrolysis in the spouted bed reactor.

The average calorific content of the oil was approximately 18.4 MJ/kg. This is comparable to bio-oil produced from the fast pyrolysis of wood[10] but is lower than the value of 30 MJ/kg reported by Miao and Wu[16] for pyrolysis oil obtained from fast pyrolysis of *Chlorella protothecoides* cultured autotrophically. This difference can be attributed to the lower oxygen content (19.43%) of the oil obtained by Miao and Wu (and correspondingly higher carbon and hydrogen contents) as compared to the oil produced in the current study. Additionally, there may also be differences in the water content of the bio-oils (the water content is not reported in references 15 or 16). The reason for these differences in bio-oil properties is not apparent, although we note that Babich *et al.*[21] reported an intermediate heating value of ~26 MJ/kg for bio-oil obtained from pyrolysis of *Chlorella* sp. at 450 °C.

Simulated distillation GC results, shown in Figure 6.4, indicated that each fraction contained a high proportion of components boiling in the heavy gas oil range (343 °C-524 °C). The lighter fractions also show a significant proportion of products that boil in the range typical of kerosene (204 °C-288 °C). GC-MS analysis of the oil fractions indicated the presence of nitrogenous and oxygenated compounds, such as amides and fatty acids, as well as a variety of hydrocarbons. Many of the compounds were branched or unsaturated as indicated by the C:H ratios and GC-MS results.
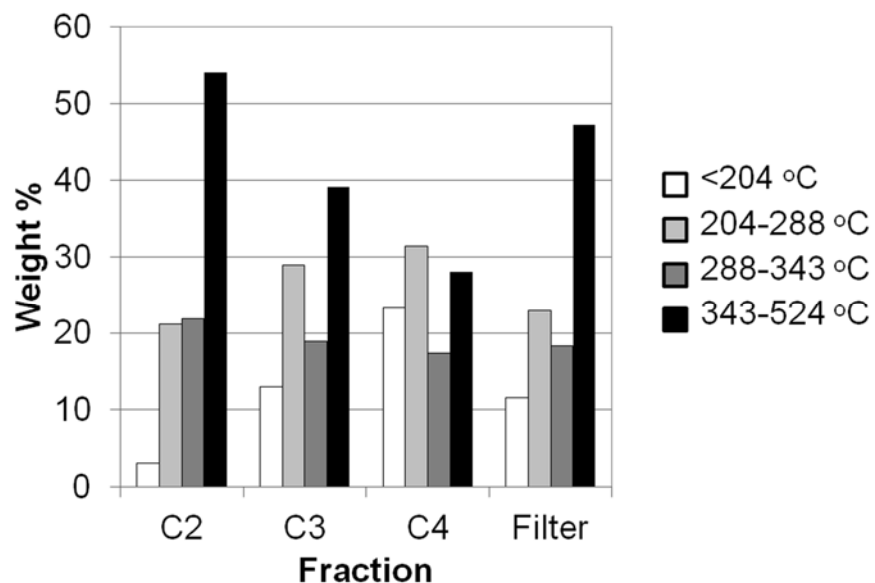
Figure 6.4. Simulated distillation GC results for select oil fractions.

The area % for the compounds identified for each oil fraction using GC-MS is summarized in Table 6.3 and select nitrogenous species detected in the bio-oil fractions are shown in Figure 6.5. Nitrogenous compounds identified include amines, amides, pyridines, pyrroles, pyrazoles, pyrazines, nitriles, imidazoles and indoles, although the majority of these compounds were amides. The amides varied in chain length ranging from acetamide to stearamide and also included cyclic amides such as 2-pyrrolidone (with these mentioned compounds being dominant). Cyclic amides may be formed from protein and amino acid intramolecular cyclization[29-34] whereas linear amides may be formed from primary protein decomposition or from amines in amino acids that reacted with carboxylic acids to produce amides and water (Figure 6.6). The presence of pyrroles can be attributed to the decomposition of amino acids such as glutamine present in proteins,[33] as well as decomposed chlorophyll in the algae feedstock.[35] Pyrazines, pyridines, piperidines and pyrazoles are also likely formed from protein decomposition and/or intramolecular cyclization. Additionally, pyrazines and other nitrogenous species may form from subsequent reactions of Amadori compounds generated by Maillard reactions.[20] Imidazoles may be formed from the decomposition of histidine amino acids present in proteins[32] and indoles may be produced from decomposed tryptophan amino acids.[30,32] Each of these compounds may be the result of primary or secondary reactions that occurred during pyrolysis or in the condensed oil phase.
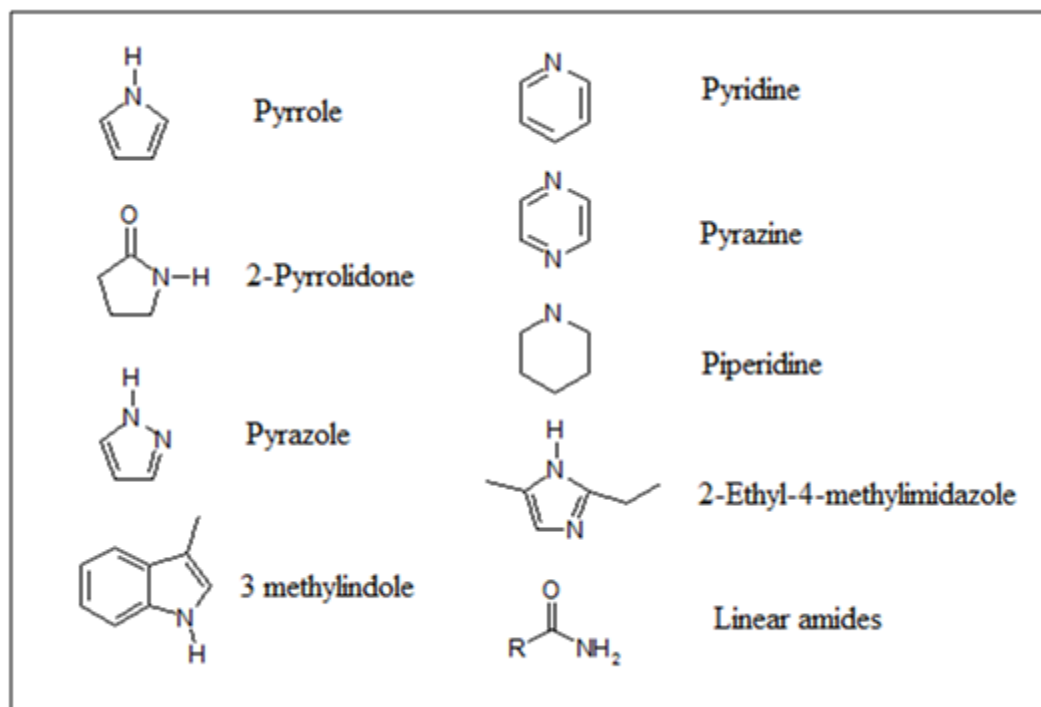
Figure 6.5. Select nitrogenous species detected in bio-oil fractions via GC-MS.

While the amount of nitrogenous compounds formed seems high, the results agree with elemental analysis. For example, if the average nitrogenous compound is compositionally similar to octanamide, then based on its empirical formula, a nitrogen content of 10 wt% would be expected. Since N-containing species constituted less than 100% of the various oil fractions, a nitrogen content of less than 10 wt% is to be expected.
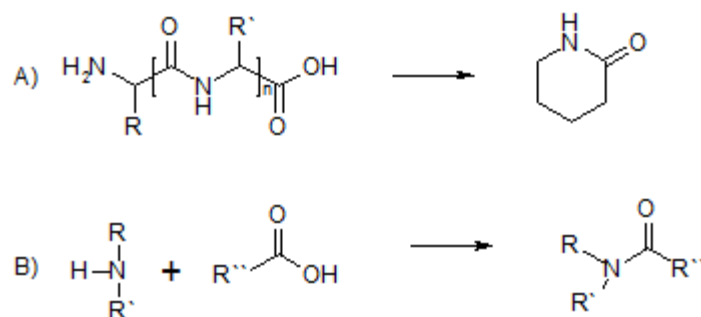
Figure 6.6. A) Intramolecular cyclization of proteins resulting in pyrrolidone structures. B) Carboxylic acids react with amines to produce linear amides.

Fatty oxygenates identified include aldehydes, ketones, acids, and alcohols with long carbon chains, including saturated and unsaturated, branched and linear isomers. Alkanes and alkenes in the products were identified in accordance with retention time calibrations and mass spectra analysis based on a NIST library. The majority of these hydrocarbon compounds were formed primarily from the pyrolysis of the lipid fraction (triglycerides and fatty acids) of the algae feedstock. Lipid pyrolysis mechanisms are complex and have been thoroughly investigated.[36-42] A simplified schematic of the pyrolysis of the triglycerides and fatty acids based on previous findings[36-42] is shown in Figure 6.7. Steroids and aromatic compounds such as phenols, naphthalene and toluene were also observed in the oil products, particularly in the filter oil.
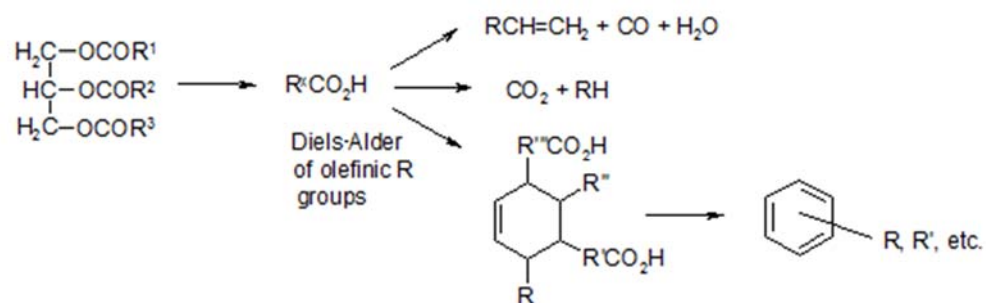
Figure 6.7. Production of saturated and unsaturated hydrocarbons, aromatic compounds, CO, and CO_2 from pyrolysis of triglycerides and fatty acids. Additional reactions ultimately lead to smaller chain hydrocarbons, as well as aldehydes and alcohols.[36-42]

FTIR spectra were similar for each of the oil fractions. Large, broad bands between 3200 cm^{-1} and 3600 cm^{-1} indicated the presence of water, alcohols, amides and amines. Strong bands between 2800 cm^{-1} and 2900 cm^{-1} resulted from aliphatic C-H stretching. Bands at 1660 cm^{-1} occurred in each spectrum and can be attributed to amide carbonyl stretching and/or C=C stretching. Medium-strength bands present at 1550 cm^{-1} indicated the presence of aromatic compounds. ^{13}C NMR spectra (not shown) of the filter oil and the C3 oil fraction contained peaks at 180 ppm, indicating the presence of carboxylic acids, while several peaks between 156 and 158 ppm were consistent with the presence of amides. There was also an abundance of peaks appearing between 120 and 140 ppm suggesting the presence of alkenes, aromatics and pyridine, while several peaks between 100 and 120 ppm indicated the presence of pyrazoles, pyrroles, and sugar pyrolysates such as furans.

The filter oil contained the most diverse range of compounds, whereas the C4 oil contained mostly water and nitrogen-containing molecules, particularly short-chain amides and cyclic nitrogenous species. The denser fractions and the filter oil contained a large amount of oxygenated compounds such as fatty acids and fatty alcohols. These fractions also contained the largest amount of alkanes, alkenes, and aromatic compounds. However, smaller chain acids, cyclic compounds, alcohols, and other products expected from the pyrolysis of carbohydrates and polysaccharides from the algae were not abundant in the oil fractions as indicated by GC-MS NIST library results. The distribution of the various species into each of the condensing train fractions corresponds to properties such as their condensing temperatures. Many higher boiling point compounds such as triglycerides and PAHs are not capable of being analyzed via GC-MS analysis. Hence, overall analysis of each separate fraction in solvent may not be a fair representation of the bio-oil as a whole. Therefore, a pyrolysis-GC-MS analysis was utilized to further elucidate the compounds produced from the pyrolysis of the microalgae. More importantly, pyrolysis-GC-MS provides the opportunity to analyze the composition of the initial pyrolysis vapor, as opposed to the condensed product which may contain the products of secondary reactions occurring in the liquid.

6.3.3 Pyrolysis-GC-MS

The pyrogram displayed in Figure 6.8 shows that pyrolysis of *Scenedesmus* sp. at 480 °C produces a significant amount of fatty oxygenates that appear at later retention times in the pyrogram, particularly beyond 28 min. These compounds, which include alcohols, ketones, acids and aldehydes, are derived predominantly from the pyrolysis of the fatty acids and triglycerides in the algae. Although many of these peaks could not be not unambiguously identified, the peak at 44.1 minutes corresponds to phytol, which would derive from chlorophyll.[35] The pyrogram also shows that a large amount of nitrogenous products are created; the majority of these products appear to be amines such as pyrroles and piperidines based on comparison of spectra with the NIST database, whereas the nitrogenous compounds from the spouted bed reactor appear to be mostly amides. The pyrolysis conditions may have been more severe in the spouted bed reactor such that the primary products underwent secondary reactions to produce the observed amides, or, more likely, secondary reactions may have occurred in the bio-oil (i.e., $RCOOH + RNH_2 \rightarrow RCONHR + H_2O$). Also, pyrazines were much more abundant in the bio-oil than in the products seen from the Py-GC/MS of the algae. Pyrazine production can occur as the result of a sequence of reactions following the Maillard reaction between sugars and proteins in the algae.[20] Since the pyrolysis vapors generated in the pyroprobe were quickly swept to the GC inlet they were not able to undergo many of the secondary reactions that may occur in condensed bio-oil to produce pyrazine derivatives.

The pyrogram also contains peaks corresponding to fatty olefins, paraffins, and aromatic compounds which are also likely produced from the pyrolysis of the lipid fraction of the algae (Figure 6.7). Carbohydrate pyrolysates such as butyrolactone and furan derivatives were observed in small quantities in the oil fractions from the spouted bed reactor but are more abundant in the pyrogram shown in Figure 6.8. This implies that they are primary pyrolysis products that can undergo secondary reactions, thereby explaining why there is a lower abundance of these compounds in the condensed pyrolysis oil.
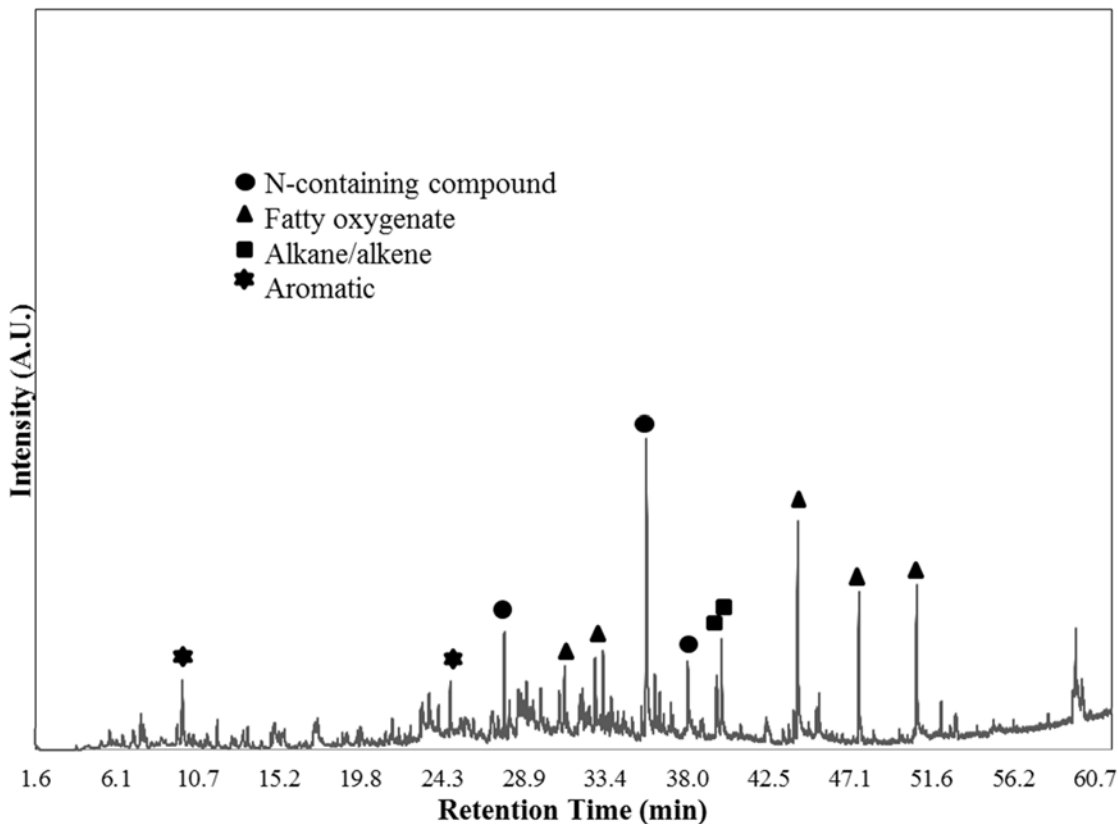
Figure 6.8. Pyrogram displaying products from *Scenedesmus* sp. pyrolysis in a pyroprobe at 480 °C.

The area percent of various types of compounds in the pyrogram are shown in Table 6.4. The majority of the peaks can be attributed to carbohydrate pyrolysates, fatty oxygenates, aromatics and nitrogen-containing compounds, with smaller amounts of alkanes and alkenes being present. The Py-GC/MS results for product distributions agree to a certain extent with the GC-MS results obtained from the bio-oil fractions when considering the weight distributions for each of the oil fractions. However, the Py-GC/MS analysis did not detect the presence of steroids which may have condensed in the transfer line prior to the GC inlet. In addition, GC-MS analysis of the oil fractions appeared to show higher percentages of nitrogen-containing compounds than the Py-GC/MS analysis because fewer of the fatty oxygenated hydrocarbons were detected. This is likely the result of secondary reactions that occurred during pyrolysis or in the oil during condensation. The Py-GC/MS analysis was also able to detect more carbohydrate pyrolysates that did not appear in GC-MS analysis of the bio-oil fractions. However, both techniques indicate that the

major components of pyrolysis oil produced from *Scenedesmus* algae are fatty oxygenated hydrocarbons and nitrogen-containing molecules such as amides and amines.

Table 6.4. Distribution of product types from *Scenedesmus* sp. pyrolysis in a pyroprobe at 480 °C.

Compounds	Area % (standard deviation)
Alkanes	2.4 (0.8)
Alkenes	2.1 (0.9)
Fatty oxygenates	23.7 (1.6)
Aromatics	8.9 (1.6)
N-containing compounds	14.3 (1.6)
Carbohydrate pyrolysates	8.6 (0.63)
Unidentified	40.0 (3.7)

6.4 Conclusions

Two reactor scales were utilized in order to compare and understand the origin and formation of products from fast pyrolysis of *Scenedesmus* algae. First, a technical, larger-scale production of bio-oil from the fast pyrolysis of a dried microalgae feedstock was investigated using a spouted bed reactor. Product analysis shows that the fractions of the bio-oil collected are, in certain respects, comparable to pyrolysis products from lignocellulosic feedstocks. Indeed, the overall heating value of the oil product is typical of lignocellulose-derived pyrolysis oil, although the average total acid number of the oil is lower than for bio-oil produced from wood pyrolysis. Furthermore, the bio-oil has a higher average nitrogen content due to the high protein content of the algae feedstock. Micro-scale Py-GC-MS was also used to study the pyrolysis of the dried *Scenedesmus* sp. in order to determine the composition of the primary pyrolysis products. Large amounts of fatty oxygenates and nitrogenous products were observed, while the Py-GC-MS was able to detect significant production of carbohydrate pyrolysates which were observed in only very minor amounts in the spouted bed pyrolysis oil fractions. Differences between the products generated from the different reactors are attributed mainly to secondary reactions that occurred either during pyrolysis in the spouted bed or in the oil during condensation.

Chapter 7. Concluding Remarks and Future Studies

The purpose of the research reported in this dissertation was to use Py-GC/MS to characterize the structure and composition of several types of biomass and extracted lignin based on the compounds the feedstocks generated upon pyrolysis. The pyrolysis of two lignin monomers, sinapyl and coniferyl alcohol, was also analyzed in order to understand the origin of lignin-based pyrolysates from lignin and lignocellulosic biomass. Fruit endocarp waste analyzed by Py-GC/MS included black walnut shell (*Juglans nigra*), coconut shell (*Cocos nucifera*), peach pit (*Prunus persica*) and olive pit (*Olea europaea*). Lignin was extracted from the endocarp samples using two techniques, sulfuric acid and formic acid, and was also analyzed by Py-GC/MS. Wild type and mutated sorghum of the Della variety and *Scenedesmus* sp. microalgae were analyzed for pyrolysate distributions as well. Other techniques, such as thermogravimetric analysis (TGA), nuclear magnetic resonance (NMR) spectroscopy and Fourier transform infrared spectroscopy (FTIR) were used to analyze the biomass samples.

Pyrolysis of sinapyl and coniferyl alcohol generated pyrolysates associated with each individual alcohol. Coniferyl alcohol generated pyrolysates with a guaiacyl moiety containing various groups at the *para* position of the aromatic ring. Sinapyl alcohol generated pyrolysates with a syringyl moiety containing various groups at the *para* position on the aromatic ring. There was a very low abundance of guaiacyl pyrolysates generated from demethoxylation of the sinapyl alcohol. Pyrolysis-GC/MS calibration lines were obtained by plotting S:G sum area % ratios from certain marker pyrolysates originating from sinapyl and coniferyl alcohol against the molar sinapyl:coniferyl alcohol ratio. Having the pyrolysate profiles of sinapyl alcohol, coniferyl alcohol, and various mixtures of the two made it possible to construct S:G ratio calibration lines using a variety of marker compounds from each alcohol. Different marker compounds may be needed for different types of biomass in order to calculate accurate S:G ratios. To validate the calibration, the S:G ratio of peach pit lignin was determined using Py-GC/MS and found to agree with the S:G ratio obtained from capillary electrophoresis of $KMnO_4$ oxidation products from the peach pit lignin.

Pyrolysis-GC/MS was used to analyze pyrolysates obtained from drupe endocarp waste including peach pits, coconut shells, olive pits and walnut shells and their respective formic acid and sulfuric acid extracted lignin and formic acid residue fractions. The formic acid treatment extracted only a fraction of the lignin present, as determined by the sulfuric acid technique (Klason lignin content). The pyrolysate distributions of lignins from different biomass types, extracted using the same formic acid procedure, revealed that the extraction technique doesn't

only yield lignin of particular structure or composition. The pyrolysates observed from each biomass type and its lignin fractions were found to be biomass dependent, but still differed slightly from biomass to each extracted lignin. These results indicate that the lignin may have changed during the extraction process and TGA indicated that the lignins decomposed at different temperatures and rates. Walnut shells and peach pits and their respective lignin fractions produced very few pyrolysates from sinapyl monomers whereas coconut shells and olive pits and their respective lignin fractions generated higher amounts of sinapyl-based pyrolysates. Coconut shell and the corresponding extracted lignins also generated large amounts of phenol upon pyrolysis, an observation unique to this biomass. HSQC NMR spectra of the formic acid-extracted lignins supported the Py-GC/MS data indicating the coconut shell and olive pit lignins contained more sinapyl monomers than the peach pit and walnut shell lignins. The HSQC spectra also revealed that the coconut shell lignin contained higher amounts of the coumaryl monomer than the other biomass, explaining the increased production of phenol during pyrolysis.

Wild type and mutated sorghum bicolor (L.) of the Della variety was also analyzed by Py-GC/MS. The mutant sorghum contained more lignin in the leaves and less lignin in the stems in comparison to the wild type biomass. However, pyrolysates generated from the mutants showed an increase in the amount of lignin-based pyrolysates and sinapyl-based pyrolysates from both stems and leaves in comparison to the wild type. The production of more lignin-based pyrolysates from the stems may be due to the presence of metals (ash) in the biomass influencing the amounts and types of pyrolysates generated. Additionally, thermogravimetric analysis (TGA) showed that the pyrolysis of the mutant stems left behind a greater percentage of nonvolatile residue than wild type, which may also explain the differences in the pyrolysate abundances observed. Overall, Py-GC/MS and thermogravimetric analysis of the wild type and mutant stems and leaves revealed differences in the structure and composition of the biomass and its subsequent decomposition in to other products upon pyrolysis.

Scenedesmus sp. microalgae were also analyzed by Py-GC/MS and pyrolysates were compared to those generated when the microalgae were pyrolyzed in a spouted fluidized bed pyrolysis unit. A large amount of fatty oxygenates originating from lipids present in the microalgae and nitrogenous products originating from the proteins were observed in the bio-oil fractions obtained from the fluidized bed pyrolysis unit. Py-GC-MS also observed fatty oxygenates and nitrogenous species from the microalgae feedstock. Additionally, Py-GC/MS was also able to detect significant production of carbohydrate pyrolysates, which were observed in only very minor amounts in the spouted bed pyrolysis oil fractions. Differences observed in the products generated

from the different reactors are attributed mainly to secondary reactions that occurred either during pyrolysis in the spouted bed or in the oil during condensation. Overall, Py-GC/MS provided a better understanding of the primary pyrolysates and the distribution of components present in the microalgae feedstock but still provided insight towards the types of compounds that can be generated on a larger scale pyrolysis unit.

Py-GC/MS was able to characterize the structure and composition of each biomass source analyzed according to unique pyrolysates generated. Lignin monomers were analyzed as models to validate the determination of certain monomers present in lignin in lignocellulosic biomass. The similarities and differences between micro-scale Py-GC/MS pyrolysates and those obtained from a larger fluidized bed unit have also been addressed. Py-GC/MS analysis of biomass and biomass constituents has been supported and validated by other techniques including TGA and NMR. However, interpretation of large data sets can be complicated and data obtained from the pyrolysis of biomass can be dependent on many variables, including the presence of metals and the formation of unanalyzable char fractions. Unlike many wet chemistry techniques though, Py-GC/MS allows for rapid analysis of microgram quantities of biomass samples, requires little sample preparation, does not require the use of hazardous materials and does not generate large amounts of wastes. In conclusion, Py-GC/MS is capable of rapidly analyzing biomass and its constituents in order to compare the structural variation of the components present in biomass. Py-GC/MS analysis provides information which is complimentary to other techniques used to analyze biomass and provides insight towards the kinds of chemicals capable of being generated by the thermal decomposition of biomass on larger scales.

There is still much to be learned about the structure, composition and pyrolysis of the biomass reported herein. Additional investigations varying the Py-GC/MS parameters, as well as those incorporating large scale pyrolysis units, wet chemistry techniques and spectroscopic analysis could be implemented in future studies. For example, solid-state NMR techniques or thioacidolysis methods may be useful for comparing the structure of the lignin present in the drupe endocarp to the sulfuric and formic acid-extracted lignins. Larger scale pyrolysis of the endocarp feedstocks would also be necessary to determine if they would generate bio-oil with improved properties (such as higher heating values) in comparison to other feedstocks such as switchgrass. Studies on the saccharification properties and sugar analysis of the sorghum mutants have already been performed, but further understanding of the structure of the lignin fraction and its potential utilization and thermal decomposition could be investigated. Overall, Py-GC/MS analysis has provided a means to compare biomass structures while simultaneously monitoring

141

their thermal degradation products rapidly. However, it is important to gain a more comprehensive understanding of the structure of biomass by the application of multiple analytical techniques and it is important to understand its potential applications through larger scale thermochemical conversion processes.

Appendix 1. List of Abbreviations

ASTM: Analytical Standard Test Method

ATR: Attenuated Total Reflection

CAD: Cinnamyl Alcohol Dehydrogenase

COMT: Caffeic Acid O-Methyl Transferase

DFRC: Derivatization Followed by Reductive Cleavage

DMSO: Dimethyl Sulfoxide

DTG: Derivative Thermogravimetric Analysis

E.I.A.: Energy Information Administration (USA)

EMS: Ethyl Methane Sulfonate

FTIR: Fourier Transform Infrared Spectroscopy

HHV: Higher Heating Value

HPLC: High Performance Liquid Chromatography

HSQC: Heteronuclear Single Quantum Coherence

LAP: Laboratory Analytical Protocol

LCC: Lignin Carbohydrate Complex

M1-M6: Marker Compound Group Numbers

MFC: Mass Flow Controller

ML or MWL: Milled Wood Lignin

NBO: Nitrobenzene Oxidation

NIST: National Institute of Standards and Technology

NMR: Nuclear Magnetic Resonance

NREL: National Renewable Energy Laboratory

PAH: Polycyclic Aromatic Hydrocarbon

Py-GC/MS: Pyrolysis-Gas Chromatography/Mass Spectrometry

RG: REDforGREEN Mutant Sorghum

SEM: Scanning Electron Microscopy

S:G or S/G: Sinapyl: Coniferyl Alcohol Ratio

TGA: Thermogravimetric Analysis

WT: Wild Type

Appendix 2. Supplementary Tables

Supplementary Table 4.1. Walnut shell pyrolysates for biomass and extracted lignin. Bold species are those that occur in highest abundance and standard deviations for pyrolysates from multiple lignin extractions and multiple analysis of biomass are provided for the most abundant species.

Compound Number	Retention Time	Compound	Whole Biomass Area %	Formic Acid Lignin Area %	Sulfuric Acid Lignin Area %
	6.50	2,3 butanedione	0.59	0.04	0.06
	7.12	benzene	0.00	0.03	0.12
1	**8.63**	**acetic acid**	**4.85** (+/-0.47)	0.10	0.09
	9.84	1-hydroxy-2-propanone	1.33	0.00	0.00
	10.12	toluene	0.19	0.58	0.22
	13.20	ethylbenzene	0.00	0.2	0.03
	13.43	xylene	0.00	0.07	0.16
	13.44	**acetic acid ethenyl ester**	**1.48** (+/- 0.09)	0.00	0.00
	14.90	styrene	0.00	0.11	0.02
2	**15.50**	**furfural**	**1.75** (+/- 0.06)	0.48	0.91
	17.67	2-methyl-2-cyclopenten-1-one	0.00	0.00	0.09
	19.80	**1,2-cyclopentanedione**	**1.62** (+/- 0.08)	0.01	0.03
	20.80	5-methyl-2-furancarboxaldehyde	0.00	0.03	0.19
	21.70	2(5H)-furanone	0.57	0.00	0.00
3	**22.80**	**4-hydroxy-5,6-dihydro-2H-pyran-2-one**	**1.92** (+/- 0.11)	0.20	0.07
	23.65	**2-hydroxy-3-methyl-2-cyclopenten-1-one**	**1.72** (+/- 0.07)	0.00	0.00
4	**24.71**	**phenol**	0.96	**3.25** (+/- 1.37)	**1.27** (+/- 0.41)
5	**25.35**	**2-methoxyphenol**	**5.06** (+/- 0.21)	**9.62** (+/- 2.61)	**4.58** (+/- 0.95)
	26.46	**2-methylphenol**	0.56	**1.80** (+/- 1.05)	**1.60** (+/- 0.65)
	27.00	2,6-dimethylphenol	0.00	0.23	0.36
	27.72	**4-methylphenol**	0.67	**2.89** (1.02)	**1.54** (+/- 0.38)
	27.80	3-methylphenol	0.61	0.96	0.71
	27.90	2-methoxy-3-methylphenol	0.23	0.79	0.93
6	**29.01**	**2-methoxy-4-methylphenol**	**3.87** (+/- 0.48)	**10.51** (+/-2.57)	**7.76** (+/-2.36)
	29.37	**2,4-dimethylphenol**	0.47	**2.00** (+/- 1.27)	**2.27** (+/- 0.90)
	29.81	3,4-dimethoxytoluene	0.11	0.24	0.02
	30.05	2,3,5-trimethylphenol	0.00	0.07	0.25
	30.78	4-ethylphenol	0.28	0.68	0.47
	32.31	**4-ethyl-2-methoxyphenol**	**1.56** (+/- 0.28)	**3.05** (+/- 0.65)	**2.41** (+/- 0.60)
	33.06	1,4:3,6-dianhydro-.alpha.-d-glucopyranose	0.41	0.00	0.0
	33.67	4-vinylphenol	1.20	1.30	0.40
7	**33.76**	**2-methoxy-4-vinylphenol**	**12.61** (+/- 0.23)	**10.59** (+/-1.39)	**3.65** (+/-0.15)
	34.55	**eugenol**	**2.80** (+/- 0.15)	**1.80** (+/- 0.58)	**0.34**
	34.70	2-methoxy-4-propylphenol	0.73	0.99	0.70
	35.39	1,2-benzenediol	0.00	0.52	1.50

Supplementary Table 4.1 (continued)

8	**35.48**	**2,6-dimethoxyphenol**	**2.71 (+/- 0.23)**	**3.82 (+/- 0.54)**	**3.22 (+/- 0.38)**
	36.31	**2-methoxy-4-(1-propenyl)phenol (Z)**	**2.33 (+/- 0.23)**	**2.03 (+/- 0.63)**	**1.41 (+/- 0.46)**
	37.63	4-(2-propenyl)phenol	1.04	0.86	1.12
	37.80	**4-methyl-1,2-benzenediol**	0.00	0.00	**1.53 (+/- 0.76)**
9	**37.90**	**2-methoxy-4-(1-propenyl)phenol (E)**	**12.50 (+/- 0.26)**	**6.73 (+/- 3.66)**	**4.35 (+/- 0.67)**
10	**38.30**	**4-methylsyringol**	1.16	**2.66 (+/- 0.72)**	**2.58 (+/- 0.50)**
11	**38.65**	**vanillin**	**3.54 (+/- 0.83)**	**3.47 (+/- 1.59)**	**4.25 (+/- 1.50)**
	40.48	4-ethylsyringol	0.71	0.33	0.68
	40.90	4-hydroxy-3-methoxybenzoic acid methyl ester	0.34	0.17	0.00
	41.05	4-Hydroxy-3-methoxyacetophenone	1.00	0.79	**1.71 (+/- 1.56)**
12	**42.15**	**4-vinylsyringol**	**1.57 (+/- 0.41)**	0.38	0.88
	42.56	1-(4-hydroxy-3-methoxyphenyl)acetone	0.81	0.98	0.89
	42.68	2,6-dimethoxy-4-(2-propenyl)phenol	0.41	0.20	0.52
	44.10	2,6-dimethoxy-4-(1-propenyl)phenol (Z)	0.00	0.00	0.28
	45.71	2,6-dimethoxy-4-(1-propenyl)phenol (E)	0.42	0.38	0.34
	47.03	4-hydroxy-3,5-dimethoxybenzaldehyde	0.06	0.50	0.00
	48.20	4-propylsyringol	0.00	0.00	0.00
	49.60	4-((1E)-3-Hydroxy-1-propenyl)-2-methoxyphenol T	0.33	0.00	0.00
	48.81	3,5-Dimethoxy-4-hydroxyacetophenone	0.10	0.12	0.00
	49.79	3-(4-hydroxy-3-methoxyphenyl)-2-propenal	0.15	0.00	0.00
		Sum identified compounds	78.37 (+/- 0.56)	76.56 (+/- 5.32)	56.51 (+/- 1.53)
		Sum lignin-based pyrolysates	61.61 (+/- 1.12)	75.70 (+/- 4.94)	55.07 (+/- 2.13)
		Sum sinapyl-based pyrolysates	7.14 (+/- 0.96)	8.39 (+/- 0.60)	8.50 (+/- 2.35)
		Sum coniferyl-based pyrolysates	47.61 (+/- 0.54)	50.73 (+/- 2.74)	32.05 (+/- 1.51)
		Sum area % S/G	0.15 (+/- 0.02)	0.17 (+/- 0.02)	0.27 (+/- 0.06)

Supplementary Table 4.2. Peach pit pyrolysates from biomass and lignin. Bold species are those that occur in highest abundance and standard deviations for pyrolysates from multiple lignin extractions and multiple analysis of biomass are provided for the most abundant species.

Compound Number	Retention Time	Compound	Whole Biomass Area %	Formic Acid Lignin Area %	Sulfuric Acid Lignin Area %
	6.50	2,3 butanedione	0.36	0.20	0.29
	7.12	benzene	0.00	0.00	0.07
1	**8.63**	**acetic acid**	**1.87 (+/- 0.66)**	0.92	0.14
	9.84	1-hydroxy-2-propanone	1.12	0.16	0.00
	10.12	toluene	0.39	0.15	0.49
	13.40	5-Hydroxymethyl-2[5H]-furanone	0.17	0.00	0.00
	13.43	xylene	0.00	0.08	0.29
	13.44	**acetic acid ethenyl ester**	**1.90 (+/- 0.06)**	0.00	0.00
	14.80	Propanoic acid, 2-oxo-, methyl ester	0.84	0.00	0.00
	14.90	styrene	0.00	0.00	0.31
2	**15.50**	**furfural**	**1.89 (+/- 0.21)**	1.35	1.20
	17.10	5-methyl-2-3h-furanone	0.15	0.00	0.00
	17.67	2-methyl-2-cyclopenten-1-one	0.00	0.00	0.17
	14.20	2-furanmethanol	0.10	0.00	0.00
	18.70	2-cyclopentene-1,4-dione	0.19	0.07	0.00
	19.80	1,2-cyclopentanedione	1.18	0.09	0.00
	20.80	5-methyl-2-furancarboxaldehyde	0.21	0.01	0.32
	20.87	3-methyl-2-cyclopenten-1-one	0.03	0.00	0.02
	21.70	2(5H)-furanone	0.66	0.04	0.00
3	**22.80**	**4-hydroxy-5,6-dihydro-2H-pyran-2-one**	**4.23 (+/- 0.34)**	1.41	0.00
	23.65	**2-hydroxy-3-methyl-2-cyclopenten-1-one**	**2.16 (+/- 0.27)**	0.00	0.12
4	24.71	**phenol**	0.74	0.77	**2.00 (+/- 0.60)**
5	**25.35**	**2-methoxyphenol**	**3.08 (+/- 0.38)**	**3.70 (+/- 0.05)**	**7.50 (+/- 1.81)**
	26.46	**2-methylphenol**	0.49	0.59	**2.67 (+/- 1.03)**
	27.72	**4-methylphenol**	1.20	0.67	**1.52 (+/- 0.36)**
	27.80	3-methylphenol	0.62	0.36	0.90
	27.90	**2-methoxy-3-methylphenol**	0.23	0.23	**1.74 (+/- 0.65)**
	28.20	5-Hydroxymethyldihydrofuran-2-one	1.28	0.00	0.00
6	**29.01**	**2-methoxy-4-methylphenol**	**4.89 (+/- 0.85)**	**5.63 (+/- 0.86)**	**10.09 (+/- 1.54)**
	29.37	**2,4-dimethylphenol**	0.87	0.90	**3.63 (+/- 1.24)**
	29.80	3,4-dimethoxytoluene	0.00	0.11	0.11
	30.05	2,3,5-trimethylphenol	0.00	0.17	0.59
	30.78	4-ethylphenol	0.27	0.19	0.65
	30.80	3,5-dimethylphenol	0.39	0.00	0.99
	32.20	**3-methyl-2,4(3H,5H)-Furandione**	**1.61 (+/- 0.16)**	0.00	0.00
	32.31	**4-ethyl-2-methoxyphenol**	**1.67 (+/- 0.04)**	1.32	**3.36 (+/- 0.87)**
	33.06	1,4:3,6-dianhydro-.alpha.-d-glucopyranose	0.16	0.00	0.00

Supplementary Table 4.2 (continued)

	33.67	4-vinylphenol	0.67	0.50	0.00
7	**33.76**	**2-methoxy-4-vinylphenol**	**10.35 (+/- 1.71)**	**4.67 (+/- 1.08)**	**3.23 (+/- 1.23)**
	34.55	**eugenol**	**2.77 (+/- 0.26)**	**2.01 (+/- 0.63)**	0.33
	34.70	2-methoxy-4-propylphenol	0.80	1.06	0.46
	35.39	1,2-Benzenediol	0.00	0.64	0.00
8	**35.48**	**2,6-dimethoxyphenol**	**2.51 (+/- 0.61)**	**4.71 (+/- 0.84)**	**3.60 (+/- 0.91)**
	36.31	**2-methoxy-4-(1-propenyl)phenol (Z)**	**2.12 (+/- 0.04)**	**2.21 (+/- 0.33)**	0.77
	37.63	4-(2-propenyl)phenol	0.35	0.77	0.00
9	**37.90**	**2-methoxy-4-(1-propenyl)phenol (E)**	**9.21 (+/- 1.97)**	**7.38 (+/- 0.97)**	**2.71 (+/- 1.40)**
10	**38.30**	**4-methylsyringol**	**2.96 (+/- 0.76)**	**6.11 (+/- 1.35)**	**2.69 (+/- 1.19)**
11	**38.65**	**vanillin**	**2.89 (+/- 1.80)**	**6.55 (+/-2.23)**	**2.82 (+/- 2.04)**
	40.48	4-ethylsyringol	0.45	1.15	0.57
	41.05	**4-Hydroxy-3-methoxyacetophenone**	0.00	**1.56 (+/- 0.95)**	1.08
12	**42.15**	**4-vinylsyringol**	0.60	**1.70 (+/- 0.94)**	0.43
	42.56	**1-(4-Hydroxy-3-methoxyphenyl)acetone**	0.22	**2.17 (+/- 1.37)**	0.41
	42.68	**2,6-dimethoxy-4-(2-propenyl)phenol**	0.30	**1.60 (+/- 0.92)**	0.17
	44.10	2,6-dimethoxy-4-(1-propenyl)phenol (Z)	0.00	0.73	0.08
	45.71	2,6-dimethoxy-4-(1-propenyl)phenol (E)	0.16	1.03	0.00
	47.03	4-hydroxy-3,5-dimethoxybenzaldehyde	0.22	0.28	0.00
	48.81	3,5-Dimethoxy-4-hydroxyacetophenone	0.09	0.12	0.00
	49.79	3-(4-hydroxy-3-methoxyphenyl)-2-propenal	0.43	0.00	0.00
	49.4	Sinapyl alcohol	0.28	0.00	0.00
		Sum identified compounds	72.30 (+/- 2.94)	66.07 (+/- 2.52)	58.69 (+/- 2.89)
		Sum lignin-based pyrolysates	52.19 (+/- 3.93)	61.82 (+/- 6.03)	56.43(+/- 2.25)
		Sum sinapyl-based pyrolysates	7.54 (+/- 1.43)	17.43 (+/- 5.08)	7.54 (+/- 2.57)
		Sum coniferyl-based pyrolysates	38.43 (+/- 3.77)	38.26 (+/- 1.87)	32.93 (+/- 1.01)
		Sum area % S/G	0.20 (+/- 0.05)	0.46 (+/- 0.12)	0.23 (+/- 0.07)

Supplementary Table 4.3. Coconut shell pyrolysates from biomass and extracted lignin. Bold species are those that occur in highest abundance and standard deviations for pyrolysates from multiple lignin extractions and multiple analysis of biomass are provided for the most abundant species.

Compound Number	Retention Time	Compound	Whole Biomass Area %	Formic Acid Lignin Area %	Sulfuric Acid Lignin Area %
	6.50	2,3 butanedione	0.44	0.26	0.06
	7.12	benzene	0.00	0.05	0.00
1	**8.63**	**acetic acid**	**4.68 (+/- 0.19)**	**1.36 (+/- 0.19)**	0.00
	9.84	1-hydroxy-2-propanone	0.93	0.09	0.00
	10.12	toluene	0.00	0.22	0.36
	13.20	ethylbenzene	0.00	0.04	0.00
	13.43	xylene	0.00	0.05	0.17
	13.44	acetic acid ethenyl ester	1.22	0.00	0.00
	14.90	styrene	0.00	0.00	0.00
2	**15.50**	**furfural**	**1.64 (+/- 0.04)**	**1.49 (+/- 0.45)**	1.24
	17.67	2-methyl-2-cyclopenten-1-one	0.00	0.00	0.06
	18.70	2-cyclopentene-1,4-dione	0.00	0.03	0.04
	19.80	1,2-cyclopentanedione	1.05	0.12	0.00
	20.80	5-methyl-2-furancarboxaldehyde	0.12	0.00	0.26
	20.87	3-methyl-2-cyclopenten-1-one	0.00	0.06	0.01
	21.70	2(5H)-furanone	0.47	0.00	0.00
3	**22.80**	**4-hydroxy-5,6-dihydro-2H-pyran-2-one**	**2.70 (+/- 0.11)**	1.15	0.02
	23.65	2-hydroxy-3-methyl-2-cyclopenten-1-one	1.16	0.00	0.00
4	**24.71**	**phenol**	**6.43 (+/- 0.34)**	**9.42 (+/- 2.69)**	**12.71 (+/-3.09)**
5	**25.35**	**2-methoxyphenol**	**2.33 (+/- 0.06)**	**4.26 (+/- 0.91)**	**3.27 (+/- 0.68)**
	26.46	**2-methylphenol**	0.47	1.33	**5.98 (+/- 2.88)**
	28.00	2,6-dimethylphenol	0.00	1.38	0.48
	27.72	**4-methylphenol**	0.36	0.58	**1.53 (+/- 0.47)**
	27.80	3-methylphenol	0.38	0.54	0.76
	27.90	**2-methoxy-3-methylphenol**	0.16	**4.88 (+/- 0.48)**	0.87
6	**29.01**	**2-methoxy-4-methylphenol**	**1.70 (+/- 0.06)**	0.95	**3.83 (+/- 0.53)**
	29.37	**2,4-dimethylphenol**	0.24	0.35	**1.72 (+/- 0.71)**
	30.05	2,3,5-trimethylphenol	0.00	0.12	0.25
	30.78	4-ethylphenol	0.00	0.39	0.31
	30.80	3,5-dimethylphenol	0.09	0.00	0.00
	32.31	**4-ethyl-2-methoxyphenol**	0.72	**1.78 (+/- 0.27)**	1.40
	33.06	1,4:3,6-dianhydro-.alpha.-d-glucopyranose	0.28	0.00	0.71
	33.67	4-vinylphenol	0.64	0.86	0.35
7	**33.76**	**2-methoxy-4-vinylphenol**	**7.23 (+/- 0.33)**	**5.67 (+/- 1.22)**	**3.14 (+/- 0.63)**
	34.55	eugenol	0.97	1.28	0.42
	34.70	2-methoxy-4-propylphenol	0.22	1.35	0.44

Supplementary Table 4.3 (continued)

8	**35.48**	**2,6-dimethoxyphenol**	**11.94 (+/- 0.28)**	**11.93 (+/-1.45)**	**9.16 (+/- 2.90)**
	36.31	**2-methoxy-4-(1-propenyl)phenol (Z)**	0.83	**1.62 (+/- 0.06)**	0.77
	37.63	4-(2-propenyl)phenol	0.50	0.69	0.00
9	**37.90**	**2-methoxy-4-(1-propenyl)phenol (E)**	**5.44 (+/- 0.01)**	**4.38 (+/- 1.01)**	**1.98 (+/- 0.71)**
10	**38.30**	**4-methylsyringol**	**5.62 (+/- 0.09)**	**8.14 (+/- 1.28)**	**9.09 (+/- 3.17)**
11	**38.65**	**vanillin**	**1.49 (+/- 0.20)**	**2.12 (+/- 1.42)**	**1.59 (+/- 0.95)**
	40.48	**4-ethylsyringol**	**1.89 (+/- 0.12)**	1.40	**2.07 (+/- 0.78)**
	40.90	4-hydroxy-3-methoxybenzoic acid methyl ester	0.25	0.07	0.18
	41.05	4-Hydroxy-3-methoxyacetophenone	0.73	0.17	0.11
12	**42.15**	**4-vinylsyringol**	**6.46 (+/- 0.34)**	1.17	1.36
	42.56	1-(4-Hydroxy-3-methoxyphenyl)acetone	0.49	0.67	0.00
	42.68	**2,6-dimethoxy-4-(2-propenyl)phenol**	**2.35 (+/- 0.36)**	0.92	0.44
	44.10	2,6-dimethoxy-4-(1-propenyl)phenol (Z)	1.00	0.16	0.11
	45.71	**2,6-dimethoxy-4-(1-propenyl)phenol (E)**	**3.89 (+/- 0.24)**	0.44	0.19
	47.03	4-hydroxy-3,5-dimethoxybenzaldehyde	0.44	0.16	0.00
	48.20	4-propylsyringol	0.00	0.00	0.07
	49.60	4-((1E)-3-Hydroxy-1-propenyl)-2-methoxyphenol T	0.41	0.00	0.00
	48.81	3,5-Dimethoxy-4-hydroxyacetophenone	0.00	0.14	0.05
	49.79	3-(4-hydroxy-3-methoxyphenyl)-2-propenal	0.22	0.00	0.00
		Sum identified compounds	81.11 (+/- 0.57)	74.24 (+/- 2.51)	67.56 (+/- 2.60)
		Sum lignin-based pyrolysates	66.03 (+/- 0.411	69.68 (+/- 3.06)	65.16 (+/- 2.80)
		Sum sinapyl-based pyrolysates	33.59 (+/- 0.29)	24.46 (+/- 0.60)	22.54 (+/- 8.03)
		Sum coniferyl-based pyrolysates	23.03 (+/- 0.31)	24.32 (+/- 3.34)	17.13 (+/- 2.99)
		Sum area % S/G	1.46 (+/- 0.03)	1.01 (+/- 0.15)	1.32 (+/- 0.33)

Supplementary Table 4.4. Olive pit pyrolysates from biomass and lignin. Bold species are those that occur in highest abundance and standard deviations for pyrolysates from multiple lignin extractions and multiple analysis of biomass are provided for the most abundant species.

Compound Number	Retention Time	Compound	Whole Biomass Area %	Formic Acid Lignin Area %	Sulfuric Acid Lignin Area %
	6.50	2,3 butanedione	0.62	0.19	0.00
	7.12	benzene	0.00	0.00	0.35
1	**8.63**	**acetic acid**	**4.66 (+/- 0.34)**	0.17	0.08
	9.84	**1-hydroxy-2-propanone**	**1.54 (+/- 0.04)**	0.06	0.00
	10.12	toluene	0.00	0.00	0.48
	13.20	ethylbenzene	0.00	0.25	0.00
	13.43	xylene	0.00	0.03	0.14
	13.44	**acetic acid ethenyl ester**	**1.62 (+/- 0.20)**	0.00	0.00
	14.90	styrene	0.00	0.03	0.15
2	**15.50**	**furfural**	**1.88 (+/- 0.10)**	1.36	0.88
	17.67	2-methyl-2-cyclopenten-1-one	0.00	0.04	0.10
	14.20	2-furanmethanol	0.30	0.00	0.00
	18.70	2-cyclopentene-1,4-dione	0.00	0.00	0.03
	19.80	1,2-cyclopentanedione	0.95	0.07	0.00
	20.80	5-methyl-2-furancarboxaldehyde	0.00	0.00	0.12
	20.87	3-methyl-2-cyclopenten-1-one	0.00	0.00	0.05
	21.70	2(5H)-furanone	0.51	0.00	0.00
3	**22.80**	**4-hydroxy-5,6-dihydro-2H-pyran-2-one**	**2.84 (+/- 0.13)**	0.36	0.11
	23.65	2-hydroxy-3-methyl-2-cyclopenten-1-one	1.44	0.00	0.00
4	24.71	phenol	0.48	0.48	0.57
5	**25.35**	**2-methoxyphenol**	**3.71 (+/- 0.46)**	**4.96 (+/- 1.22)**	**4.13 (+/- 0.78)**
	26.46	2-methylphenol	0.39	0.63	1.11
	27.00	2,6-dimethylphenol	0.00	0.00	0.00
	27.72	4-methylphenol	0.13	0.33	0.36
	27.80	3-methylphenol	0.44	0.37	0.48
	27.90	2-methoxy-3-methylphenol	0.14	0.39	1.07
	28.50	levoglucosenone	0.00	0.00	1.85
6	**29.01**	**2-methoxy-4-methylphenol**	**2.19 (+/- 0.09)**	**6.66 (+/- 1.17)**	**5.76 (+/- 1.53)**
	29.37	**2,4-dimethylphenol**	0.32	0.85	**1.68 (+/- 0.02)**
	29.80	3,4-dimethoxytoluene	0.06	0.11	0.00
	30.05	2,3,5-trimethylphenol	0.00	0.14	0.25
	30.78	4-ethylphenol	0.00	0.35	0.38
	30.80	3,5-dimethylphenol	0.13	0.34	0.73
	32.31	**4-ethyl-2-methoxyphenol**	0.85	**1.71 (+/- 0.46)**	**1.98 (+/- 0.46)**
	33.06	1,4:3,6-dianhydro-.alpha.-d-glucopyranose	0.45	0.00	1.08
	33.67	4-vinylphenol	0.20	0.00	0.10
7	**33.76**	**2-methoxy-4-vinylphenol**	**8.01 (+/- 0.56)**	**4.81 (+/- 0.79)**	**2.54 (+/- 0.31)**

Supplementary Table 4.4 (continued)

	34.55	eugenol	1.38	1.79 (+/- 0.13)	0.99
	34.70	2-methoxy-4-propylphenol	0.29	1.16	1.13
8	35.48	2,6-dimethoxyphenol	10.58 (+/- 0.42)	11.12 (+/- 2.74)	9.86 (+/- 1.26)
	36.31	2-methoxy-4-(1-propenyl)phenol (Z)	1.15	1.75 (+/- 0.29)	0.89
	37.63	4-(2-propenyl)phenol	0.00	0.00	0.00
9	37.90	2-methoxy-4-(1-propenyl)phenol (E)	8.11 (+/- 0.21)	6.06 (+/- 0.67)	2.79 (+/- 0.03)
10	38.30	4-methylsyringol	4.45 (+/- 0.33)	10.06 (+/- 0.90)	8.64 (+/- 1.71)
11	38.65	vanillin	2.30 (+/- 0.41)	4.35 (+/- 0.66)	2.64 (+/- 0.36)
	40.48	4-ethylsyringol	2.08 (+/- 0.03)	1.62(+/- 0.55)	1.52 (+/- 0.51)
	40.90	4-hydroxy-3-methoxybenzoic acid methyl ester	0.18	0.52	0.28
	41.05	4-Hydroxy-3-methoxyacetophenone	0.99	0.75	0.49
12	42.15	4-vinylsyringol	9.28 (+/- 0.67)	1.38	0.72
	42.56	1-(4-Hydroxy-3-methoxyphenyl)acetone	1.07	1.48	0.43
	42.68	2,6-dimethoxy-4-(2-propenyl)phenol	2.18 (+/- 0.10)	1.73 (+/- 1.10)	0.35
	44.10	2,6-dimethoxy-4-(1-propenyl)phenol (Z)	0.65	0.79	0.00
	45.71	2,6-dimethoxy-4-(1-propenyl)phenol (E)	2.19 (+/- 0.10)	0.56	0.11
	47.03	4-hydroxy-3,5-dimethoxybenzaldehyde	0.19	0.08	0.13
	49.60	4-((1E)-3-Hydroxy-1-propenyl)-2-methoxyphenol T	0.51	0.00	0.00
	48.81	3,5-Dimethoxy-4-hydroxyacetophenone	0.00	0.06	0.00
		Sum identified compounds	81.44 (+/- 0.95)	69.95 (+/- 4.82)	57.53 (+/- 1.58)
		Sum lignin-based pyrolysates	64.63 (+/- 0.46)	67.70 (+/- 4.29)	53.23(+/- 2.89)
		Sum sinapyl-based pyrolysates	31.60 (+/- 0.82)	27.40(+/- 1.84)	21.33 (+/- 2.99)
		Sum coniferyl-based pyrolysates	29.36 (+/- 0.61)	34.21 (+/- 4.70)	23.06 (+/- 1.77)
		Sum area % S/G	1.08 (+/- 0.04)	0.80 (+/- 0.12)	0.92 (+/- 0.16)

Supplementary Table 4.5. Pyrolysates obtained from the pyrolysis of endocarp pulp residues from formic acid extractions (extractions at 65 ^{0}C, 24 h).

Retention Time	Compound	Walnut shell residue	Coconut shell residue	Peach pit residue	Olive pit residue
6.30	2,3-butanedione	0.47	0.34	0.38	0.60
6.63	hydroxyacetaldehyde	0.03	0.00	0.00	0.00
7.62	formic acid	0.00	0.35	0.00	0.00
8.38	acetic acid	0.88	0.64	0.15	0.33
9.24	1-hydroxy-2-propanone	0.61	0.53	0.34	1.94
10.12	toluene	0.06	0.04	0.04	0.04
12.73	acetic acid methyl ester	0.93	0.46	0.44	0.54
14.36	propanal	0.30	0.20	0.00	0.00
14.80	propanoic acid, 2-oxo-, methyl ester	0.33	0.09	0.00	1.12
15.04	**furfural**	**2.02 (+/- 0.16)**	**1.58 (+/- 0.22)**	**1.70 (+/- 0.65)**	**2.58 (+/- 0.61)**
17.10	5-methyl-2-3h-furanone	0.12	0.11	0.00	0.00
17.50	1-(2-furanyl)-ethanone	0.00	0.00	0.00	0.14
18.30	2-cyclopentene-1,4-dione	0.15	0.04	0.08	0.17
19.00	4-hydroxydihydro-2(3H)-furanone	0.00	0.00	0.00	0.02
19.40	**1,2-cyclopentanedione**	0.81	0.76	0.54	**1.72 (+/- 0.55)**
20.18	2-Cyclohexen-1-ol	0.49	0.36	0.17	0.43
20.40	5-methyl-2-furancarboxaldehyde	0.21	0.23	0.12	0.53
20.87	3-methyl-2-cyclopenten-1-one	0.02	0.03	0.00	0.13
21.49	2(5H)-furanone	0.26	0.24	0.26	0.79
22.40	**4-hydroxy-5,6-dihydro-2H-pyran-2-one**	**2.84 (+/- 0.87)**	**1.84 (+/- 0.57)**	**1.40 (+/- 0.86)**	1.15
23.22	**2-hydroxy-3-methyl-2-cyclopenten-1-one**	0.48	0.83	0.47	**1.48 (+/- 0.60)**
24.42	**phenol**	0.51	**4.12 (+/- 0.87)**	0.34	0.67
25.00	**2-methoxyphenol**	**2.39 (+/- 0.19)**	**1.81 (+/- 0.44)**	**2.58 (+/- 0.57)**	**3.09 (+/- 0.20)**
26.18	2-methylphenol	0.42	0.49	0.40	0.34
26.69	2,6-dimethylphenol	0.27	0.00	0.23	0.00
26.90	2,5-furandicarboxaldehyde	0.51	0.35	0.37	0.26
27.30	4-methylphenol	0.50	0.15	0.19	0.09
27.40	3-methylphenol	0.00	0.14	0.23	0.24
27.50	2-methoxy-3-methylphenol	0.00	0.64	0.00	0.18
28.20	5-hydroxymethyldihydrofuran-2-one	0.00	0.19	0.50	0.26
28.33	levoglucosenone	0.00	0.00	0.00	0.70
29.01	**2-methoxy-4-methylphenol**	**3.88 (+/- 0.48)**	**2.04 (+/- 0.25)**	**4.29 (+/- 0.59)**	**1.50 (+/- 0.46)**
29.03	2,4-dimethylphenol	0.59	0.30	0.62	0.24
29.39	**3,5-dihydroxy-2-methyl-4H-pyran-4-one**	0.07	**2.14 (+/- 0.55)**	0.37	0.90
30.78	4-ethylphenol	0.08	0.11	0.00	0.00
32.31	4-ethyl-2-methoxyphenol	0.85	0.32	0.37	0.21

Supplementary Table 4.5 (continued)

32.20	**2,3-anhydro-d-mannosan**	0.86	0.65	0.95	**1.73 (+/- 0.16)**
32.73	**1,4:3,6-dianhydro-.alpha.-d-glucopyranose**	0.81	0.82	1.12	**2.14 (+/- 0.20)**
33.43	**2-methoxy-4-vinylphenol**	**5.34 (+/- 1.34)**	**4.06 (+/- 0.87)**	**3.94 (+/- 1.22)**	**1.83 (+/- 0.23)**
34.19	**eugenol**	**1.41 (+/- 0.09)**	0.61	**1.62 (+/- 0.81)**	0.41
34.28	2-methoxy-4-propylphenol	0.38	0.24	0.37	0.18
34.73	**5-(hydroxymethyl)furfural**	**2.65 (+/- 1.27)**	**3.66 (+/- 1.73)**	**1.30 (+/- 0.30)**	**7.53 (+/- 0.58)**
35.11	**2,6-dimethoxyphenol**	1.17	**4.74 (+/- 0.47)**	**1.49 (+/- 0.28)**	**3.58 (+/- 0.19)**
35.95	**2-methoxy-4-(1-propenyl)phenol (Z)**	**1.35 (+/- 0.09)**	0.94	1.08	0.65
36.95	**4-(2-propenyl)phenol**	**2.57 (+/- 1.64)**	0.00	0.00	0.00
37.56	**2-methoxy-4-(1-propenyl)phenol (E)**	**5.64 (+/- 1.21)**	**3.14 (+/- 0.55)**	**4.75 (+/- 0.76)**	**2.19 (+/- 0.29)**
37.94	**4-methylsyringol**	**1.65 (+/- 0.42)**	**6.41 (+/- 0.92)**	**1.99 (+/- 0.23)**	**1.99 (+/- 0.62)**
38.30	**vanillin**	**4.03 (+/- 0.28)**	**1.83 (+/- 0.34)**	**3.58 (+/- 0.69)**	**1.48 (+/- 0.28)**
40.00	**4-ethylsyringol**	**1.55 (+/- 0.38)**	0.78	1.19	0.60
40.50	4-hydroxy-3-methoxybenzoic acid methyl ester	0.43	0.25	0.37	0.37
40.67	**4-hydroxy-3-methoxyacetophenone**	**1.31 (+/- 1.04)**	0.68	**2.01 (+/- 0.32)**	0.95
41.80	**4-vinylsyringol**	**1.32 (+/- 0.44)**	**4.68 (+/- 0.13)**	**1.62 (+/- 0.21)**	**1.48 (+/- 0.34)**
42.13	**1-(4-hydroxy-3-methoxyphenyl)acetone**	**3.65 (+/- 0.69)**	**1.39 (+/- 0.21)**	**3.71 (+/- 1.05)**	**2.10 (+/- 0.71)**
42.33	**2,6-dimethoxy-4-(2-propenyl)phenol**	1.03	**2.85 (+/- 0.50)**	**1.30 (+/- 0.17)**	0.60
43.39	**4-((1E)-3-Hydroxy-1-propenyl)-2-methoxyphenol T**	**1.46 (+/- 0.09)**	0.53	**1.91 (+/- 0.18)**	0.60
43.77	**2,6-dimethoxy-4-(1-propenyl)phenol (Z)**	0.50	**1.36 (+/- 0.16)**	1.12	0.55
44.80	**1,6-anhydro-β- D-glucopyranose**	**2.47 (+/- 2.00)**	**1.51 (+/- 0.49)**	**3.62 (+/- 0.68)**	**3.02 (+/- 1.61)**
45.04	3-methoxy-2-naphthalenol	0.80	0.00	1.01	0.55
45.37	**2,6-dimethoxy-4-(1-propenyl)phenol (E)**	**1.52 (+/- 0.03)**	**5.25 (+/- 0.99)**	**2.77 (+/- 0.73)**	1.19
45.98	**4-hydroxy-3-methoxy-phenylacetylformic acid**	0.73	0.13	**1.58 (+/- 0.51)**	0.00
47.03	4-hydroxy-3,5-dimethoxybenzaldehyde	0.22	0.27	1.14	0.43
48.00	3,5-Dimethoxy-4-hydroxyacetophenone	0.08	0.13	0.42	0.03
48.97	3-(4-hydroxy-3-methoxyphenyl)-2-propenal	0.98	0.00	1.14	0.00
	Sum identified compounds	67.00 (+/- 5.08)	68.38 (+/- 1.68)	63.65 (+/- 3.16)	58.57 (+/- 1.22)
	Sum lignin-based pyrolysates	48.69 (+/- 1.19)	50.43 (+/- 3.60)	49.39 (+/- 0.27)	28.36 (+/- 4.97)
	Sum sinapyl-based pyrolysates	9.05 (+/- 1.90)	26.47 (+/- 2.11)	13.04 (+/- 0.73)	10.45 (+/- 1.74)
	Sum coniferyl-based pyrolysates	34.64 (+/- 1.36)	17.97 (+/- 1.39)	34.29 (+/- 0.74)	16.10 (+/- 3.17)
	Sum area % S/G	0.26 (+/- 0.05)	1.47 (+/- 0.02)	0.38 (+/- 0.01)	0.65 (+/- 0.02)

Appendix 3. Supplementary Figures

Supplementary Figure 4.1. Walnut shell formic acid lignin (red) and sulfuric acid lignin (purple) ATR IR spectra.
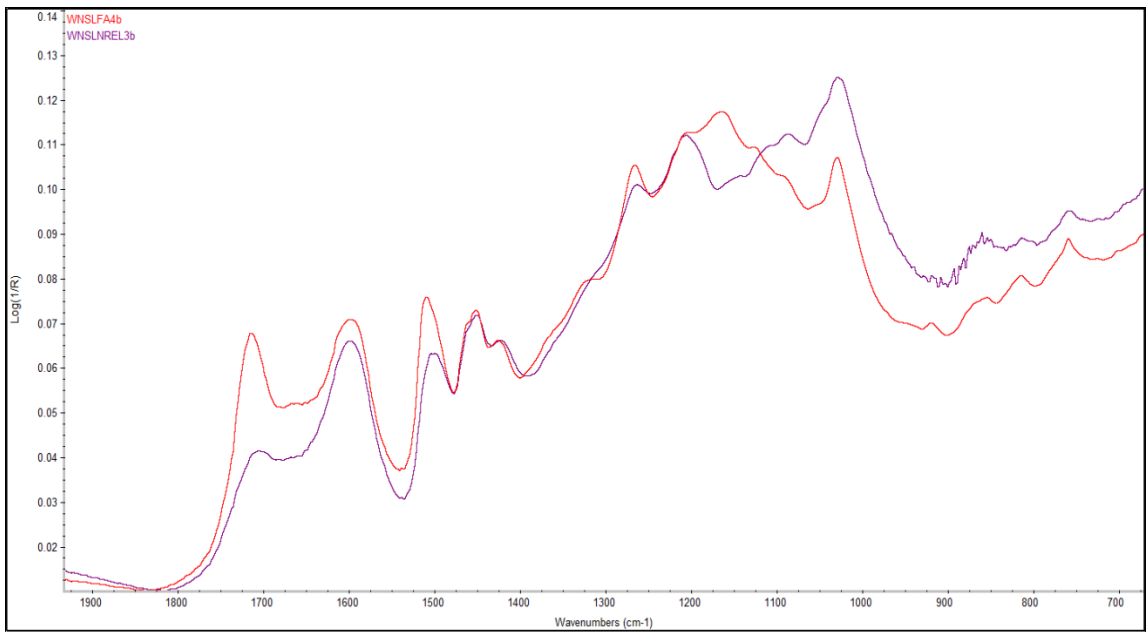
Supplementary Figure 4.2. Coconut shell formic acid lignin (red) and sulfuric acid lignin (purple) ATR IR spectra.
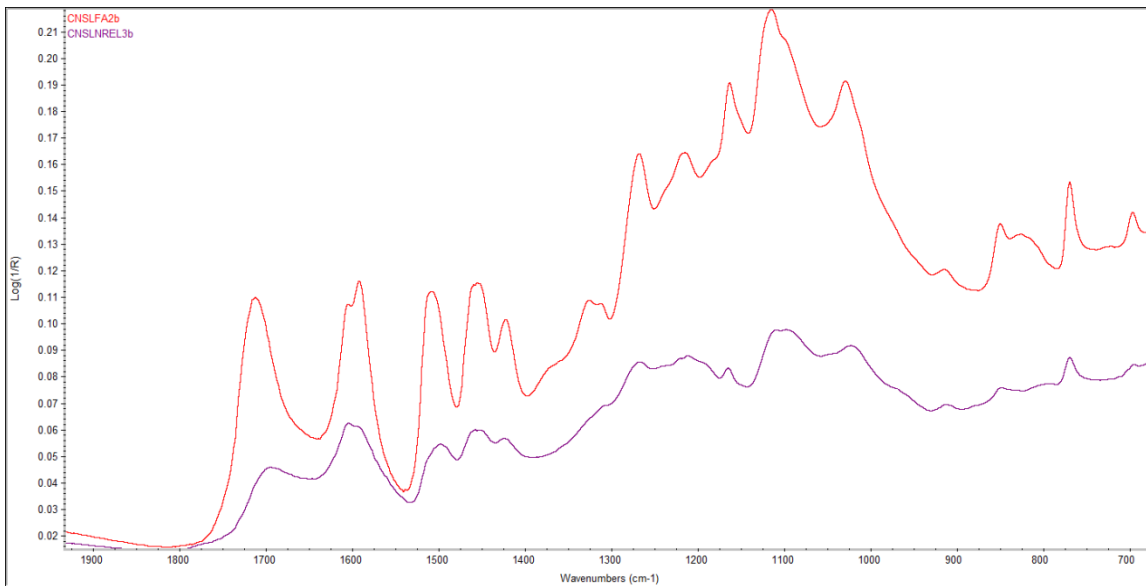
References

Chapter 1

1. Administration, U. S. E. I. International Energy Statistics: Total Primary Energy Consumption. http://www.eia.gov/cfapps/ipdbproject/iedindex3.cfm?tid=44&pid=44&aid=2&cid=regions&syid=2000&eyid=2011&unit=MBTUPP (accessed 5/15/13).
2. Administration, U. S. E. I. Frequently Asked Questions: How much energy is used to make plastic? http://www.eia.gov/tools/faqs/faq.cfm?id=34&t=6 (accessed May 22, 2013).
3. Crocker, M.; Andrews, R., Chapter 1 The Rationale for Biofuels. In *Thermochemical Conversion of Biomass to Liquid Fuels and Chemicals*, Crocker, M., Ed. The Royal Society of Chemistry: 2010; 1-25.
4. Montross, M.; Crofcheck, C., Chapter 2 Energy Crops for the Production of Biofuels. In *Thermochemical Conversion of Biomass to Liquid Fuels and Chemicals*, Crocker, M., Ed. The Royal Society of Chemistry: 2010; 26-45.
5. Brennan, L.; Owende, P., Biofuels from microalgae—A review of technologies for production, processing, and extractions of biofuels and co-products. *Renew. Sust. Energ Rev.* **2010,** *14*, 557-577.
6. Mata, T.; Martins, A.; Caetano, N., Microalgae for Biodiesel Production and other Applications: A Review. *Renew. Sust. Energ Rev.* **2010,** *14*, 217-232.
7. Bridgwater, A. V., Chapter 7 Fast Pyrolysis of Biomass for Energy and Fuels. In *Thermochemical Conversion of Biomass to Liquid Fuels and Chemicals*, Crocker, M., Ed. The Royal Society of Chemistry: 2010; 146-191.
8. Bridgwater, A.; Czernick, S.; Diebold, J.; Meier, D.; Oasmaa, A.; Peacocke, C.; Piskorz, J.; Radlein, D., *Fast Pyrolysis of Biomass: A Handbook*. CPL Scientific Publishing Services Limited: Newbury, United Kingdom, 2003; Vol. 1.
9. Czernik, S.; Bridgwater, A. V., Overview of Applications of Biomass Fast Pyrolysis Oil. *Energy Fuels* **2004,** *18*, 590-598.
10. Crocker, M., *Thermochemical Conversion of Biomass to Liquid Fuels and Chemicals*. RSC Publishing: Cambridge, United Kingdom, 2010.
11. Bird, M. I.; Wurster, C. M.; de Paula Silva, P. H.; Bass, A. M.; de Nys, R., Algal biochar – production and properties. *Bioresour. Technol.* **2011,** *102*, 1886-1891.
12. Wise, J.; Vietor, D.; Provin, T.; Capareda, S.; Munster, C.; Boateng, A., Mineral nutrient recovery from pyrolysis systems. *Environ. Prog. Sustain. Energy* **2012,** *31*, 251-255.
13. Mohan, D.; Pittman, C. U.; Steele, P. H., Pyrolysis of Wood/Biomass for Bio-oil: A Critical Review. *Energy Fuels* **2006,** *20*, 848-889.
14. Kingston, A., Pyrolysis Oil Premium Markets. In *CanBio Conference*, Quebec City, 2012.
15. Huber, G. W.; Iborra, S.; Corma, A., Synthesis of Transportation Fuels from Biomass: Chemistry, Catalysts, and Engineering. *Chem. Rev.* **2006**, 4044-4098.
16. Patwardhan, P. R.; Dalluge, D. L.; Shanks, B. L.; Brown, R. C., Distinguishing Primary and Secondary Reactions of Cellulose Pyrolysis. *Bioresour. Technol.* **2011,** *102*, 5265-5269.
17. Lin, Y.-C.; Cho, J.; Tompsett, G. A.; Westmoreland, P. R.; Huber, G. W., Kinetics and Mechanism of Cellulose Pyrolysis. *J. Phys. Chem. C* **2009,** *113*, 20097-20107.
18. Saiz-Jimenez, C.; De Leeuw, J. F., Lignin Pyrolysis Products: Their Structures and Their Significance as Biomarkers. *Adv. Org. Geochem.* **1985,** *10*, 869-876.

19. Saiz-Jimenez, C.; de Leeuw, J. W., Pyrolysis-gas chromatography-mass spectrometry of isolated, synthetic and degraded lignins. *Org. Geochem.* **1984,** *6*, 417-422.

20. Obst, J. R., Guaiacyl and Syringyl Lignin Composition in Hardwood Cell Components. *Holzforschung* **1982,** *36*, 143-152.

21. Santos, R. B.; Capanema, E. A.; Balakshin, M. Y.; Chang, H.-m.; Jameel, H., Lignin Structural Variation in Hardwood Species. *J. Agric. Food Chem.* **2012,** *60*, 4923-4930.

22. Miao, X.; Wu, Q.; Yang, C., Fast pyrolysis of microalgae to produce renewable fuels. *J. Anal. Appl. Pyrol.* **2004,** *71*, 855-863.

23. Miao, X.; Wu, Q., High yield bio-oil production from fast pyrolysis by metabolic controlling of Chlorella protothecoides. *J. Biotechnol.* **2004,** *110*, 85-93.

24. Du, Z.; Li, Y.; Wang, X.; Wan, Y.; Chen, Q.; Wang, C.; Lin, X.; Liu, Y.; Chen, P.; Ruan, R., Microwave-assisted pyrolysis of microalgae for biofuel production. *Bioresour. Technol.* **2011,** *102*, 4890-6.

25. Jena, U.; Das, K. C., Comparative Evaluation of Thermochemical Liquefaction and Pyrolysis for Bio-Oil Production from Microalgae. *Energy Fuels* **2011,** *25*, 5472-5482.

26. Peng, W.; Wu, Q.; Tu, P., Effects of temperature and holding time on production of renewable fuels from pyrolysis of Chlorella protothecoides. *J. Appl. Phycol.* **2000,** *12*, 147-152.

27. Brown, M. R., The amino-acid and sugar composition of 16 species of microalgae used in mariculture. *J. Exp. Mar. Biol. Ecol.* **1991,** *145*, 79-99.

28. Takeda, H., Cell wall sugars of some Scenedesmus species. *Phytochemistry* **1996,** *42*, 673-675.

29. Takeda, H., Sugar Composition of the Cell Wall and the Taxonomy of Chlorella (Chlorophyceae). *J. Phycol.* **1991,** *27*, 224-232.

30. Nichols, P.; Holman, R., Pyrolysis of saturated triglycerides. *Lipids* **1972,** *7*, 773-779.

31. Maher, K. D.; Bressler, D. C., Pyrolysis of triglyceride materials for the production of renewable fuels and chemicals. *Bioresour. Technol.* **2007,** *98*, 2351-2368.

32. Barupal, D.; Kind, T.; Kothari, S.; Lee, D.; Fiehn, O., Hydrocarbon phenotyping of algal species using pyrolysis-gas chromatography mass spectrometry. *BMC Biotechnol.* **2010,** *10*, 1-9.

33. Ratcliff, M. A.; Medley, E. E.; Simmonds, P. G., Pyrolysis of amino acids. Mechanistic considerations. *J. Org. Chem.* **1974,** *39*, 1481-1490.

34. Chiavari, G.; Galletti, G. C., Pyrolysis—gas chromatography/mass spectrometry of amino acids. *J. Anal. Appl. Pyrol.* **1992,** *24*, 123-137.

35. Shulman, G. P.; Simmonds, P. G., Thermal decomposition of aromatic and heteroaromatic amino-acids. *Chem. Comm. (London)* **1968**, 1040-1042.

36. Smith, W. T.; Harris, T. B.; Patterson, J. M., Pyrolysis of Soybean Protein and an Amino Acid Mixture Having the Same Amino Acid Composition. *J. Agric. Food Chem.* **1974,** *22*, 480-483.

37. Del Rio, J. C.; Gutierrez, A.; Martinez, A. T., Identifying acetylated lignin units in non-wood fibers using pyrolysis-gas chromatography/mass spectrometry. *Rapid Commun. Mass Sp.* **2004,** *18*, 1181-1185.

38. Ohra-aho, T.; Gomes, F. J. B.; Colodette, J. L.; Tamminen, T., S/G ratio and lignin structure among Eucalyptus hybrids determined by Py-GC/MS and nitrobenzene oxidation. *J. Anal. Appl. Pyrol.* **2013,** *101*, 166-171.

39. Sinha, S.; Jhalani, A.; Ravi, M. R.; Ray, A., Modelling of Pyrolysis in Wood: A Review. *J. Sol. Energy Soc. India* **2000,** *10*, 41-62.

40. Haas, T. J.; Nimlos, M. R.; Donohoe, B. S., Real-Time and Post-reaction Microscopic Structural Analysis of Biomass Undergoing Pyrolysis. *Energy Fuels* **2009,** *23*, 3810-3817.

41. Hu, J.; Shen, D.; Xiao, R.; Wu, S.; Zhang, H., Free-Radical Analysis on Thermochemical Transformation of Lignin to Phenolic Compounds. *Energy Fuels* **2013,** *27*, 285-293.

42. Britt, P. F.; Buchanan III, A. C.; Thomas, K. B.; Lee, S.-K., Pyrolysis mechanisms of lignin: surface-immobilized model compound investigation of acid-catalyzed and free-radical reaction pathways. *J. Anal. Appl. Pyrol.* **1995,** *33*, 1-19.

43. Patwardhan, P. R.; Satrio, J. A.; Brown, R. C.; Shanks, B. L., Product Distribution from Fast Pyrolysis of Glucose-based Carbohydrates. *J. Anal. Appl. Pyrol.* **2009,** *86*, 323-330.

44. Diebold, J. P. *A Review of the Chemical and Physical Mechanisms of the Storage Stability of Fast Pyrolysis Bio-oils*; National Renewable Energy Laboratory: Golden, Colorado, 2000.

45. Barreto, C. C. K.; Oliveira, C. C.; Souza, G. G.; Suarez, P. A. Z.; Rubim, J. C., Evaluation of the stability during storage of a diesel-like fuel obtained by the pyrolysis of soybean oil. *Biomass Bioenergy* **2012,** *37*, 42-48.

46. Mettler, M. S.; Mushrif, S. H.; Paulsen, A. D.; Javadekar, A. D.; Vlachos, D. G.; Dauenhauer, P. J., Revealing pyrolysis chemistry for biofuels production: Conversion of cellulose to furans and small oxygenates. *Energy Environ. Sci.* **2012,** *5*, 5414-5424.

47. Beste, A.; Buchanan, A. C., Role of Carbon–Carbon Phenyl Migration in the Pyrolysis Mechanism of β-O-4 Lignin Model Compounds: Phenethyl Phenyl Ether and α-Hydroxy Phenethyl Phenyl Ether. *J. Phys. Chem. A* **2012,** *116*, 12242-12248.

48. Poutsma, M. L., Fundamental reactions of free radicals relevant to pyrolysis reactions. *J. Anal. Appl. Pyrol.* **2000,** *54*, 5-35.

49. Evans, R. J.; Milne, T. A.; Soltys, M. N., Direct mass-spectrometric studies of the pyrolysis of carbonaceous fuels: III. Primary pyrolysis of lignin. *J. Anal. Appl. Pyrol.* **1986,** *9*, 207-236.

50. Kotake, T.; Kawamoto, H.; Saka, S., Pyrolysis reactions of coniferyl alcohol as a model of the primary structure formed during lignin pyrolysis. *J. Anal. Appl. Pyrol.* **2013**.

51. Faravelli, T.; Frassoldati, A.; Migliavacca, E. R., Detailed kinetic modeling of the thermal degradation of lignins. *Biomass Bioenergy* **2010,** *34*, 290-301.

52. Nunes, C. A.; Lima, C. F.; Barbosa, L. C. A.; Colodette, J. L.; Gouveia, A. F. G.; Silverio, F. O., Determination of *Eucalyptus* spp lignin S/G ratio: A comparison between methods. *Bioresour. Technol.* **2010,** *101*, 4056-4061.

53. Wang, S.; Wang, K.; Liu, Q.; Gu, Y.; Luo, Z.; Cen, K.; Fransson, T., Comparison of the Pyrolysis Behavior of Lignins from Different Tree Species. *Biotechnol. Adv.* **2009,** *27*, 562-567.

54. Butler, E.; Devlin, G.; Meier, D.; McDonnell, K., Characterisation of spruce, salix, miscanthus and wheat straw for pyrolysis applications. *Bioresour. Technol.*

55. Kim, J.-Y.; Oh, S.; Hwang, H.; Kim, U.-J.; Choi, J. W., Structural features and thermal degradation properties of various lignin macromolecules obtained from poplar wood (Populus albaglandulosa). *Polym. Degrad. Stabil.* **2013,** *98*, 1671-1678.

56. Rutkowski, P., Pyrolysis of cellulose, xylan and lignin with the K2CO3 and ZnCl2 addition for bio-oil production. *Fuel Proc. Technol.* **2011,** *92*, 517-522.

57. Lv, D.; Xu, M.; Liu, X.; Zhan, Z.; Li, Z.; Yao, H., Effect of cellulose, lignin, alkali and alkaline earth metallic species on biomass pyrolysis and gasification. *Fuel Proc. Technol.* **2010,** *91*, 903-909.

58. Hosoya, T.; Kawamoto, H.; Saka, S., Cellulose–hemicellulose and cellulose–lignin interactions in wood pyrolysis at gasification temperature. *J. Anal. Appl. Pyrol.* **2007,** *80*, 118-125.

59. Campanella, A.; Muncrief, R.; Harold, M. P.; Griffith, D. C.; Whitton, N. M.; Weber, R. S., Thermolysis of microalgae and duckweed in a CO2-swept fixed-bed reactor: Bio-oil yield and compositional effects. *Bioresour. Technol.* **2012,** *109*, 154-162.

60.   Burczyk, J.; Szkawran, H.; Zontek, I.; Czygan, F. C., Carotenoids in the outer cell-wall layer of Scenedesmus (Chlorophyceae). *Planta* **1981,** *151*, 247-250.

61.   Brown, T. M.; Duan, P.; Savage, P. E., Hydrothermal Liquefaction and Gasification of Nannochloropsis sp. *Energy Fuels* **2010,** *24*, 3639-3646.

62.   Del Rio, J. C.; Rencoret, J.; Prinsen, P.; Martinez, A. T.; Ralph, J.; Gutierrez, A., Structural Characterization of Wheat Straw Lignin as Revealed by Analytical Pyrolysis, 2D-NMR, and Reductive Cleavage Methods. *J. Agric. Food Chem.* **2012,** *60*, 5922-5935.

63.   Villaverde, J. J.; Li, J.; Ek, M.; Ligero, P.; de Vega, A., Native Lignin Structure of Miscanthus x giganteus and Its Changes during Acetic and Formic Acid Fractionation. *J. Agric. Food Chem.* **2009,** *57*, 6262-6270.

64.   Eom, I.-Y.; Kim, J.-Y.; Kim, T.-S.; Lee, S.-M.; Choi, D.; Choi, I.-G.; Choi, J.-W., Effect of Essential Inorganic Metals on Primary Thermal Degradation of Lignocellulosic Biomass. *Bioresour. Technol.* **2012,** *104*, 687-694.

65.   Fahmi, R.; Bridgwater, A. V.; Donnison, I.; Yates, N.; Jones, J. M., The Effect of Lignin and Inorganic Species in Biomass on Pyrolysis Oil Yields, Quality and Stability. *Fuel* **2007,** *87*, 1230-1240.

66.   Bridgeman, T. G.; Darvell, L. I.; Jones, J. M.; Williams, P. T.; Fahmi, R.; Bridgwater, A. V.; Barraclough, T.; Shield, I.; Yates, N.; Thain, S.; Donnison, I. S., Influence of Particle Size on the Analytical and Chemical Properties of Two Energy Crops. *Fuel* **2007,** *86*, 60-72.

67.   Patwardhan, P. R.; Brown, R. C.; Shanks, B. L., Understanding the Fast Pyrolysis of Lignin. *ChemSusChem* **2011,** *4*, 1629-1636.

68.   Faix, O.; Meier, D.; Fortmann, I., Pyrolysis-gas chromatography-mass spectrometry of two trimeric lignin model compounds with alkyl-aryl ether structure. *J. Anal. Appl. Pyrol.* **1988,** *14*, 135-148.

Chapter 2

1.   Montross, M.; Crofcheck, C., Chapter 2 Energy Crops for the Production of Biofuels. In Thermochemical Conversion of Biomass to Liquid Fuels and Chemicals, Crocker, M., Ed. The Royal Society of Chemistry: 2010; 26-45.

2.   Guha, S. K.; Kobayashi, H.; Fukuoka, A., Chapter 13 Conversion of Cellulose to Sugars. In Thermochemical Conversion of Biomass to Liquid Fuels and Chemicals, Crocker, M., Ed. The Royal Society of Chemistry: 2010; 344-364.

3.   McDonough, T. J., The Chemistry of Organosolv Delignification. Tappi J. 1993, 76, 186-193.

4.   Zhang, Y.; Culhaoglu, T.; Pollet, B.; Melin, C.; Denoue, D.; Barrière, Y.; Baumberger, S. P.; Méchin, V. r., Impact of Lignin Structure and Cell Wall Reticulation on Maize Cell Wall Degradability. J. Agric. Food Chem. 2011, 59, 10129-10135.

5.   Dien, B. S.; Miller, D. J.; Hector, R. E.; Dixon, R. A.; Chen, F.; McCaslin, M.; Reisen, P.; Sarath, G.; Cotta, M. A., Enhancing Alfalfa Conversion Efficiencies for Sugar Recover and Ethanol Production by Altering Lignin Composition. Bioresour. Technol. 2011, 102, 6479-6486.

6.   Akien, G.; Qi, L.; Horvath, I. T., Chapter 14 Conversion of Carbohydrates to Liquid Fuels. In Thermochemical Conversion of Biomass to Liquid Fuels and Chemicals, Crocker, M., Ed. The Royal Society of Chemistry: 2010; 365-381.

7.   Williams, P. J. l. B.; Laurens, L. M. L., Microalgae as biodiesel & biomass feedstocks: Review & analysis of the biochemistry, energetics & economics. Energy Environ. Sci. 2010, 3, 554-590.

8.   Mata, T. M.; Martins, A. A.; Caetano, N. S., Microalgae for biodiesel production and other applications: A review. Renew. Sust. Energ Rev. 2010, 14, 217-232.

9. Kamm, B.; Gerhardt, M.; Lei, Chapter 3 The Biorefinery Concept - Thermochemical Production of Building Blocks and Syngas. In Thermochemical Conversion of Biomass to Liquid Fuels and Chemicals, Crocker, M., Ed. The Royal Society of Chemistry: 2010; 46-66.

10. Crocker, M.; Andrews, R., Chapter 1 The Rationale for Biofuels. In Thermochemical Conversion of Biomass to Liquid Fuels and Chemicals, Crocker, M., Ed. The Royal Society of Chemistry: 2010; 1-25.

11. Mann, D., G.J.; Labbe, N.; Sykes, R. W.; Cracom, K.; Kline, L.; Swamidoss, I. M.; Burris, J. N.; Davis, M.; Stewart Jr., C. N., Rapid Assessmet of Lignin Content and Structure in Switchgrass (Panicum virgatum L.) Grown Under Different Environmental Conditions. BioEnerg. Res. 2009, 2, 246-256.

12. Zakzeski, J.; Bruijnincx, P. C. A.; Jongerius, A. L.; Weckhuysen, B. M., The Catalytic Valorization of Lignin for the Production of Renewable Chemicals. Chem. Rev. 2010, 110, 3552-3599.

13. Donald, D., Overview. In Lignin and Lignans, CRC Press: 2010; 1-10.

14. Obst, J. R., Guaiacyl and Syringyl Lignin Composition in Hardwood Cell Components. Holzforschung 1982, 36, 143-152.

15. Santos, R. B.; Capanema, E. A.; Balakshin, M. Y.; Chang, H.-m.; Jameel, H., Lignin Structural Variation in Hardwood Species. J. Agric. Food Chem. 2012, 60, 4923-4930.

16. Kim, H.; Ralph, J., Solution-state 2D NMR of ball-milled plant cell wall gels in DMSO-d6/pyridine-d5. Org. Biomol. Chem. 2010, 8, 576-591.

17. Martínez, Á. T.; Rencoret, J.; Marques, G.; Gutiérrez, A.; Ibarra, D.; Jiménez-Barbero, J.; del Río, J. C., Monolignol acylation and lignin structure in some nonwoody plants: A 2D NMR study. Phytochemistry 2008, 69, 2831-2843.

18. Del Rio, J. C.; Gutierrez, A.; Martinez, A. T., Identifying acetylated lignin units in non-wood fibers using pyrolysis-gas chromatography/mass spectrometry. Rapid Commun. Mass Sp. 2004, 18, 1181-1185.

19. Catherine, L., Determining Lignin Structure by Chemical Degradations. In Lignin and Lignans, CRC Press: 2010; 11-48.

20. Studer, M. H.; DeMartini, J. D.; Davis, M. F.; Sykes, R. W.; Davison, B.; Keller, M.; Tuskan, G. A.; Wyman, C. E., Lignin content in natural Populus variants affects sugar release. Proc. Natl. Acad. Sci. 2011.

21. Harris, D.; DeBolt, S., Sythesis, Regulation and Utilization of Lignocellulosic Biomass. Plant Biotechnol. J. 2010, 8, 244-262.

22. Demirbas, A., Relationships Between Heating Value and Lignin, Moisture, Ash and Extractive Contents of Biomass Fuels. Energ. Explor. Exploit. 2002, 20, 105-111.

23. Fahmi, R.; Bridgwater, A. V.; Donnison, I.; Yates, N.; Jones, J. M., The Effect of Lignin and Inorganic Species in Biomass on Pyrolysis Oil Yields, Quality and Stability. Fuel 2007, 87, 1230-1240.

24. Morton, S. A.; Morton, L. A., Chapter 12 Ionic Liquids for the Utilization of Lignocellulosics. In Thermochemical Conversion of Biomass to Liquid Fuels and Chemicals, Crocker, M., Ed. The Royal Society of Chemistry: 2010; 307-343.

25. Lawoko, M.; Henriksson, G.; Gellerstedt, G., Structural Differences between the Lignin−Carbohydrate Complexes Present in Wood and in Chemical Pulps. Biomacromolecules 2005, 6, 3467-3473.

26. Lawoko, M. Lignin Polysaccharide Networks in Softwood and Chemical Pulps: Characterisation, Structure and Reactivity. Doctoral Dissertation, Royal Institute of Technology, Stockholm, 2005.

27. Yuan, T.-Q.; Sun, S.-N.; Xu, F.; Sun, R.-c., Characterization of Lignin Structures and Lignin-Carbohydrate Complex (LCC) Linkages by Quantitative 13C and 2D HSQC NMR Spectroscopy. J. Agric. Food Chem. 2011, 59, 10604-10614.

28. Sluiter, A.; Hames, B.; Ruiz, R.; Scarlata, C.; Sluiter, J.; Templeton, D.; Crocker, D., Determination of Structural Carbohydrates and Lignin in Biomass. NREL Laboratory Analytical Procedure 2011.

29. DuBois, M.; Gilles, K. A.; Hamilton, J. K.; Rebers, P. A.; Smith, F., Colormetric Method for Determination of Sugars and Related Substances. Anal. Chem. 1956, 28, 350-356.

30. International, A., ASTM E1758 Standard Test Method for Determination of Carbohydrates in Biomass by High Performance Liquid Chromatography. West Conshohoken, PA, 2007.

31. International, A., ASTM Standard D1106-96: Standard Test Method for Acid-Insoluble Lignin in Wood. ASTM International 2007.

32. Greenhalf, C. E.; Nowakowski, D. J.; Harms, A. B.; Titiloye, J. O.; Bridgwater, A. V., A comparative study of straw, perennial grasses and hardwoods in terms of fast pyrolysis products. Fuel 2013, 108, 216-230.

33. Kim, J.-Y.; Oh, S.; Hwang, H.; Kim, U.-J.; Choi, J. W., Structural features and thermal degradation properties of various lignin macromolecules obtained from poplar wood (Populus albaglandulosa). Polym. Degrad. Stabil. 2013, 98, 1671-1678.

34. Brebu, M.; Tamminen, T.; Spiridon, I., Thermal degradation of various lignins by TG-MS/FTIR and Py-GC-MS. J. Anal. Appl. Pyrol.

35. Adachi, S.; Tanimoto, M.; Tanaka, M.; Matsuno, R., Kinetics of the alkaline nitrobenzene oxidation of lignin in rice straw. The Chem. Eng. J. 1992, 49, B17-B21.

36. Wang, S.; Wang, K.; Liu, Q.; Gu, Y.; Luo, Z.; Cen, K.; Fransson, T., Comparison of the Pyrolysis Behavior of Lignins from Different Tree Species. Biotechnol. Adv. 2009, 27, 562-567.

37. Javor, T.; Buchberger, W.; Faix, O., Capillary electrophoretic determination of lignin degradation products obtained by permanganate oxidation. Anal. Chim. Acta 2003, 484, 181-187.

38. Ziebell, A.; Gracom, K.; Katahira, R.; Chen, F.; Pu, Y.; Ragauskas, A.; Dixon, R. A.; Davis, M., Increase in 4-Coumaryl Alcohol Units during Lignification in Alfalfa (Medicago sativa) Alters the Extractability and Molecular Weight of Lignin. J. Biol. Chem. 2010, 285, 38961-38968.

39. Henriksson, G.; Li, J.; Zhang, L.; Lindstrom, M. E., Chapter 9 Lignin Utilization. In Thermochemical Conversion of Biomass to Liquid Fuels and Chemicals, Crocker, M., Ed. The Royal Society of Chemistry: 2010; 222-262.

40. Umesh, P. A.; Rajai, H. A., Vibrational Spectroscopy. In Lignin and Lignans, CRC Press: 2010; 103-136.

41. Janshekar, H.; Fiechter, A., Lignin: Biosynthesis, application and biodegradation. Adv. in Biochem. Eng. Biot. 1983, 27, 119-178.

42. Zhang, M.; Qi, W.; Liu, R.; Su, R.; Wu, S.; He, Z., Fractionating lignocellulose by formic acid: Characterization of major components. Biomass Bioenergy 2010, 34, 525-532.

43. Ralph, J.; Larry, L. L., NMR of Lignins. In Lignin and Lignans, CRC Press: 2010; 137-243.

44. Wen, J.-L.; Sun, S.-L.; Xue, B.-i.; Sun, R.-C., Recent Advances in Characterization of Lignin Polymer by Solution-State Nuclear Magnetic Resonance (NMR) Methodology. Materials 2013, 6, 359-391.

45. Kim, H.; Ralph, J.; Akiyama, T., Solution-state 2D NMR of Ball-milled Plant Cell Wall Gels in DMSO-d 6. BioEnerg. Res. 2008, 1, 56-66.

46. Bozell, J. J.; O'Lenick, C. J.; Warwick, S., Biomass Fractionation for the Biorefinery: Heteronuclear Multiple Quantum Coherence-Nuclear Magnetic Resonance Investigation of Lignin Isolated from Solvent Fractionation of Switchgrass. J. Agric. Food Chem. 2011, 59, 9232-9242.

47. Villaverde, J. J.; Li, J.; Ek, M.; Ligero, P.; de Vega, A., Native Lignin Structure of Miscanthus x giganteus and Its Changes during Acetic and Formic Acid Fractionation. J. Agric. Food Chem. 2009, 57, 6262-6270.

48. Pu, Y.; Chen, F.; Ziebell, A.; Davison, B.; Ragauskas, A., NMR Characterization of C3H and HCT Down-Regulated Alfalfa Lignin. BioEnerg. Res. 2009, 2, 198-208.

49. Rahimi, A.; Azarpira, A.; Kim, H.; Ralph, J.; Stahl, S. S., Chemoselective Metal-Free Aerobic Alcohol Oxidation in Lignin. J. Am. Chem. Soc. 2013, 135, 6415-6418.

50. LISPERGUER, J.; PEREZ, P.; URIZAR, S., Structure and Thermal Properties of Lignins: Characterization by Infrared Spectroscopy and Differential Scanning Calorimetry. J. Chil. Chem. Soc. 2009, 54, 460-463.

51. Murugan, P.; Mahinpey, N.; Johnson, K. E.; Wilson, M., Kinetics of the Pyrolysis of Lignin Using Thermogravimetric and Differential Scanning Calorimetry Methods. Energy Fuels 2008, 22, 2720-2724.

52. Baptista, C.; Robert, D.; Duarte, A. P., Relationship between lignin structure and delignification degree in Pinus pinaster kraft pulps. Bioresour. Technol. 2008, 99, 2349-2356.

53. Obst, J. R.; Kirk, T. K., Isolation of lignin. In Methods Enzymol., Willis A. Wood, S. T. K., Ed. Academic Press: 1988; Vol. Volume 161, 3-12.

54. Bauer, S.; Sorek, H.; Mitchell, V. D.; Ibáñez, A. B.; Wemmer, D. E., Characterization of Miscanthus giganteus Lignin Isolated by Ethanol Organosolv Process under Reflux Condition. J. Agric. Food Chem. 2012, 60, 8203-8212.

55. Chakar, F. S.; Ragauskas, A. J., Review of current and future softwood kraft lignin process chemistry. Ind. Crops Prod. 2004, 20, 131-141.

56. Dapía, S.; Santos, V.; Parajó, J. C., Study of formic acid as an agent for biomass fractionation. Biomass Bioenergy 2002, 22, 213-221.

57. Lieff, M.; Wright, G. F.; Hibbert, H., Studies on Lignin and Related Compounds. XL. The Extraction of Birch Lignin with Formic Acid. J. Am. Chem. Soc. 1939, 61, 1477-1482.

58. Li, M.-F.; Sun, S.-N.; Xu, F.; Sun, R.-C., Formic acid based organosolv pulping of bamboo (Phyllostachys acuta): Comparative characterization of the dissolved lignins with milled wood lignin. Chem. Eng. J. 2012, 179, 80-89.

59. Erismann, N. d. M.; Freer, J.; Baeza, J.; Durán, N., Organosolv pulping-VII: Delignification selectivity of formic acid pulping of Eucalyptus grandis. Bioresour. Technol. 1994, 47, 247-256.

60. Tu, Q.; Fu, S.; Zhan, H.; Chai, X.; Lucia, L. A., Kinetic Modeling of Formic Acid Pulping of Bagasse. J. Agric. Food Chem. 2008, 56, 3097-3101.

61. Zhao, X.; Liu, D., Fractionating pretreatment of sugarcane bagasse by aqueous formic acid with direct recycle of spent liquor to increase cellulose digestibility–the Formiline process. Bioresour. Technol. 2012, 117, 25-32.

62. Ferrer, A.; Vega, A.; Ligero, P.; Rodriguez, A., Pulping of Empty Fruit Bunches (EFB) from the Palm Oil Industry by Formic Acid. Bioresources 2011, 6, 4282-4301.

63. Wang, B.; Li, Y.; Wu, N.; Lan, C., CO2 bio-mitigation using microalga. Appl. Microbiol. Biotechnol. 2008, 79, 707-718.

64. Brennan, L.; Owende, P., Biofuels from microalgae—A review of technologies for production, processing, and extractions of biofuels and co-products. Renew. Sust. Energ Rev. 2010, 14, 557-577.

65. Mata, T.; Martins, A.; Caetano, N., Microalgae for Biodiesel Production and other Applications: A Review. Renew. Sust. Energ Rev. 2010, 14, 217-232.

66. Kumar, A.; Ergas, S.; Yuan, X.; Sahu, A.; Zhang, Q.; Dewulf, J.; Malcata, F. X.; van Langenhove, H., Enhanced CO2 fixation and biofuel production via microalgae: recent developments and future directions. Trends Biotechnol. 2010, 28, 371-380.

67. Miao, X.; Wu, Q.; Yang, C., Fast pyrolysis of microalgae to produce renewable fuels. J. Anal. Appl. Pyrol. 2004, 71, 855-863.

68. Miao, X.; Wu, Q., High yield bio-oil production from fast pyrolysis by metabolic controlling of Chlorella protothecoides. J. Biotechnol. 2004, 110, 85-93.

69. Barupal, D.; Kind, T.; Kothari, S.; Lee, D.; Fiehn, O., Hydrocarbon phenotyping of algal species using pyrolysis-gas chromatography mass spectrometry. BMC Biotechnol. 2010, 10, 1-9.

70. Brown, M. R., The amino-acid and sugar composition of 16 species of microalgae used in mariculture. J. Exp. Mar. Biol. Ecol. 1991, 145, 79-99.

71. Schnurr, P. J.; Espie, G. S.; Allen, D. G., Algae biofilm growth and the potential to stimulate lipid accumulation through nutrient starvation. Bioresour. Technol. 2013, 136, 337-344.

72. Zheng, G.; Li, C.; Guo, L.; Ruo, W.; Wang, S., Purification of Extracted Fatty Acids from the Microalgae Spirulina. J. Am. Oil Chem. Soc 2012, 89, 561-566.

73. Biller, P.; Riley, R.; Ross, A. B., Catalytic hydrothermal processing of microalgae: Decomposition and upgrading of lipids. Bioresour. Technol. 2011, 102, 4841-4848.

74. Bligh, E. G.; Dyer, W. J., A rapid method for total lipid extraction and purification. Can. J. Biochem. Physiol. 1959, 37, 911-917.

75. Bradford, M. M., A rapid and sensitive method for the quantitation of microgram quantities of protein utilizing the principle of protein-dye binding. Anal. Biochem. 1976, 72, 248-254.

76. Lowry, O. H.; Rosebrough, N. J.; Farr, A. L.; Randall, R. J., Protein Measurement with the Folin Phenol Reagent. J. Biol. Chem. 1951, 193, 265-275.

77. Safi, C.; Charton, M.; Pignolet, O.; Silvestre, F.; Vaca-Garcia, C.; Pontalier, P.-Y., Influence of microalgae cell wall characteristics on protein extractability and determination of nitrogen-to-protein conversion factors. J. Appl. Phycol. 2013, 25, 523-529.

78. Takeda, H., Cell wall sugars of some Scenedesmus species. Phytochemistry 1996, 42, 673-675.

79. Takeda, H., Sugar Composition of the Cell Wall and the Taxonomy of Chlorella (Chlorophyceae). J. Phycol. 1991, 27, 224-232.

80. Burczyk, J.; Szkawran, H.; Zontek, I.; Czygan, F. C., Carotenoids in the outer cell-wall layer of Scenedesmus (Chlorophyceae). Planta 1981, 151, 247-250.

81. van der Hage, E. R. E.; Mulder, M. M.; Boon, J. J., Structural characterization of lignin polymers by temperature-resolved in-source pyrolysis—mass spectrometry and Curie-point pyrolysis—gas chromatography/mass spectrometry. J. Anal. Appl. Pyrol. 1993, 25, 149-183.

82. Valdés, F.; Catalá, L.; Hernández, M. R.; García-Quesada, J. C.; Marcilla, A., Thermogravimetry and Py–GC/MS techniques as fast qualitative methods for comparing the biochemical composition of Nannochloropsis oculata samples obtained under different culture conditions. Bioresour. Technol. 2013, 131, 86-93.

83. Nunes, C. A.; Lima, C. F.; Barbosa, L. C. A.; Colodette, J. L.; Gouveia, A. F. G.; Silverio, F. O., Determination of Eucalyptus spp lignin S/G ratio: A comparison between methods. Bioresour. Technol. 2010, 101, 4056-4061.

84. Ohra-aho, T.; Gomes, F. J. B.; Colodette, J. L.; Tamminen, T., S/G ratio and lignin structure among Eucalyptus hybrids determined by Py-GC/MS and nitrobenzene oxidation. J. Anal. Appl. Pyrol. 2013, 101, 166-171.

85. Hodgson, E. M.; Nowakowski, D. J.; Shield, I.; Riche, A.; Bridgwater, A. V.; Clifton-Brown, J. C.; Donnison, I. S., Variation in Miscanthus chemical composition and implications for conversion by pyrolysis and thermo-chemical bio-refining for fuels and chemicals. Bioresour. Technol. 2011, 102, 3411-3418.

162

86.   Boateng, A. A.; Hicks, K. B.; Vogel, K. P., Pyrolysis of Switchgrass (Panicum virgatum) Harvested at Several Stages of Maturity. J. Anal. Appl. Pyrol. 2006, 75, 55-64.

87.   Del Rio, J. C.; Rencoret, J.; Prinsen, P.; Martinez, A. T.; Ralph, J.; Gutierrez, A., Structural Characterization of Wheat Straw Lignin as Revealed by Analytical Pyrolysis, 2D-NMR, and Reductive Cleavage Methods. J. Agric. Food Chem. 2012, 60, 5922-5935.

88.   Boateng, A. A.; Anderson, W. F.; Phillips, J. G., Bermudagrass for Biofuels: Effect of Two Genotypes on Pyrolysis Product Yield. Energy Fuels 2007, 21, 1183-1187.

89.   Azeez, A. M.; Meier, D.; Odermatt, J. r.; Willner, T., Fast Pyrolysis of African and European Lignocellulosic Biomasses Using Py-GC/MS and Fluidized Bed Reactor. Energy Fuels 2010, 24, 2078-2085.

90.   Qiang, L.; Wen-zhi, L.; Dong, Z.; Xi-feng, Z., Analytical pyrolysis–gas chromatography/mass spectrometry (Py–GC/MS) of sawdust with Al/SBA-15 catalysts. J. Anal. Appl. Pyrol. 2009, 84, 131-138.

91.   Lu, Q.; Tang, Z.; Zhang, Y.; Zhu, X.-f., Catalytic Upgrading of Biomass Fast Pyrolysis Vapors with Pd/SBA-15 Catalysts. Ind. Eng. Chem. Res. 2010, 49, 2573-2580.

92.   Fahmi, R.; Bridgwater, A. V.; Darvell, L. I.; Jones, J. M.; Yates, N.; Thain, S.; Donnison, I. S., The Effect of Alkali Metals on Combustion and Pyrolysis of Lolium and Festuca grasses, Switchgrass and Willow. Fuel 2007, 86, 1560-1569.

93.   Bridgeman, T. G.; Darvell, L. I.; Jones, J. M.; Williams, P. T.; Fahmi, R.; Bridgwater, A. V.; Barraclough, T.; Shield, I.; Yates, N.; Thain, S.; Donnison, I. S., Influence of Particle Size on the Analytical and Chemical Properties of Two Energy Crops. Fuel 2007, 86, 60-72.

94.   Eom, I.-Y.; Kim, J.-Y.; Kim, T.-S.; Lee, S.-M.; Choi, D.; Choi, I.-G.; Choi, J.-W., Effect of Essential Inorganic Metals on Primary Thermal Degradation of Lignocellulosic Biomass. Bioresour. Technol. 2012, 104, 687-694.

95.   Lima, C. F.; Barbosa, L. C. A.; Marcelo, C. R.; Silverio, F. O.; Colodette, J. L., Comparison Between Analytical Pyrolysis and Nitrobenzene Oxidation for Determination of Syringyl/Guaiacyl Ratio in Eucalyptus spp. . Bioresources 2008, 3, 701-712.

96.   Patwardhan, P. R.; Dalluge, D. L.; Shanks, B. L.; Brown, R. C., Distinguishing Primary and Secondary Reactions of Cellulose Pyrolysis. Bioresour. Technol. 2011, 102, 5265-5269.

97.   Patwardhan, P. R.; Satrio, J. A.; Brown, R. C.; Shanks, B. H., Product distribution from fast pyrolysis of glucose-based carbohydrates. J. Anal. Appl. Pyrol. 2009, 86, 323-330.

98.   Lin, Y.-C.; Cho, J.; Tompsett, G. A.; Westmoreland, P. R.; Huber, G. W., Kinetics and Mechanism of Cellulose Pyrolysis. J. Phys. Chem. C 2009, 113, 20097-20107.

99.   Jiang, G.; Nowakowski, D. J.; Bridgwater, A. V., Effect of the Temperature on the Composition of Lignin Pyrolysis Products. Energy Fuels 2010, 24, 4470-4475.

100.   Patwardhan, P. R.; Brown, R. C.; Shanks, B. H., Understanding the Fast Pyrolysis of Lignin. ChemSusChem 2011, 4, 1629-1636.

101.   Saiz-Jimenez, C.; De Leeuw, J. F., Lignin Pyrolysis Products: Their Structures and Their Significance as Biomarkers. Adv. Org. Geochem. 1985, 10, 869-876.

102.   Hu, J.; Shen, D.; Xiao, R.; Wu, S.; Zhang, H., Free-Radical Analysis on Thermochemical Transformation of Lignin to Phenolic Compounds. Energy Fuels 2013, 27, 285-293.

103.   Kotake, T.; Kawamoto, H.; Saka, S., Pyrolysis reactions of coniferyl alcohol as a model of the primary structure formed during lignin pyrolysis. J. Anal. Appl. Pyrol. 2013.

104.   Faix, O.; Meier, D.; Fortmann, I., Pyrolysis-gas chromatography-mass spectrometry of two trimeric lignin model compounds with alkyl-aryl ether structure. J. Anal. Appl. Pyrol. 1988, 14, 135-148.

105.   Drage, T. C.; Vane, C. H.; Abbott, G. D., The closed system pyrolysis of β-O-4 lignin substructure model compounds. Org. Geochem. 2002, 33, 1523-1531.

106. Saiz-Jimenez, C.; de Leeuw, J. W., Pyrolysis-gas chromatography-mass spectrometry of isolated, synthetic and degraded lignins. Org. Geochem. 1984, 6, 417-422.

107. Shin, E.-J.; Nimlos, M. R.; Evans, R. J., A study of the mechanisms of vanillin pyrolysis by mass spectrometry and multivariate analysis. Fuel 2001, 80, 1689-1696.

108. Friderichsen, A. V.; Shin, E.-J.; Evans, R. J.; Nimlos, M. R.; Dayton, D. C.; Ellison, G. B., The pyrolysis of anisole (C6H5OCH3) using a hyperthermal nozzle. Fuel 2001, 80, 1747-1755.

109. Li, G.; Zhou, Y.; Ji, F.; Liu, Y.; Adhikari, B.; Tian, L.; Ma, Z.; Dong, R., Yield and Characteristics of Pyrolysis Products Obtained from Schizochytrium limacinum under Different Temperature Regimes. Energies 2013, 6, 3339-3352.

Chapter 3

1. Harman-Ware, A. E.; Crocker, M.; Kaur, A. P.; Meier, M. S.; Kato, D.; Lynn, B., Pyrolysis–GC/MS of sinapyl and coniferyl alcohol. *J. Anal. Appl. Pyrol.* **2013,** *99*, 161-169.

2. Zakzeski, J.; Bruijnincx, P. C. A.; Jongerius, A. L.; Weckhuysen, B. M., The Catalytic Valorization of Lignin for the Production of Renewable Chemicals. *Chem. Rev.* **2010,** *110*, 3552-3599.

3. Brown, R. C., *Biorenewable Resources: Engineering New Products from Agriculture*. Iowa, 2003.

4. Adler, E., Lignin chemistry—past, present and future. *Wood Sci. Technol.* **1977,** *11*, 169-218.

5. Mann, D., G.J.; Labbe, N.; Sykes, R. W.; Cracom, K.; Kline, L.; Swamidoss, I. M.; Burris, J. N.; Davis, M.; Stewart Jr., C. N., Rapid Assessmet of Lignin Content and Structure in Switchgrass (*Panicum virgatum* L.) Grown Under Different Environmental Conditions. *BioEnerg. Res.* **2009,** *2*, 246-256.

6. Obst, J. R., Guaiacyl and Syringyl Lignin Composition in Hardwood Cell Components. *Holzforschung* **1982,** *36*, 143-152.

7. Dien, B. S.; Miller, D. J.; Hector, R. E.; Dixon, R. A.; Chen, F.; McCaslin, M.; Reisen, P.; Sarath, G.; Cotta, M. A., Enhancing Alfalfa Conversion Efficiencies for Sugar Recover and Ethanol Production by Altering Lignin Composition. *Bioresour. Technol.* **2011,** *102*, 6479-6486.

8. Zhang, Y.-H. P.; Ding, S.-Y.; Mielenz, J. R.; Cui, J.-B.; Elander, R. T.; Laser, M.; Himmel, M. E.; McMillan, J. R.; Lynd, L. R., Fractionating recalcitrant lignocellulose at modest reaction conditions. *Biotechnol. Bioeng.* **2007,** *97*, 214-223.

9. Wang, S.; Wang, K.; Liu, Q.; Gu, Y.; Luo, Z.; Cen, K.; Fransson, T., Comparison of the Pyrolysis Behavior of Lignins from Different Tree Species. *Biotechnol. Adv.* **2009,** *27*, 562-567.

10. Fahmi, R.; Bridgwater, A. V.; Donnison, I.; Yates, N.; Jones, J. M., The Effect of Lignin and Inorganic Species in Biomass on Pyrolysis Oil Yields, Quality and Stability. *Fuel* **2007,** *87*, 1230-1240.

11. Adachi, S.; Tanimoto, M.; Tanaka, M.; Matsuno, R., Kinetics of the alkaline nitrobenzene oxidation of lignin in rice straw. *The Chem. Eng. J.* **1992,** *49*, B17-B21.

12. Nunes, C. A.; Lima, C. F.; Barbosa, L. C. A.; Colodette, J. L.; Gouveia, A. F. G.; Silverio, F. O., Determination of *Eucalyptus* spp lignin S/G ratio: A comparison between methods. *Bioresour. Technol.* **2010,** *101*, 4056-4061.

13. Lima, C. F.; Barbosa, L. C. A.; Marcelo, C. R.; Silverio, F. O.; Colodette, J. L., Comparison Between Analytical Pyrolysis and Nitrobenzene Oxidation for

Determination of Syringyl/Guaiacyl Ratio in Eucalyptus spp. . *Bioresources* **2008,** *3*, 701-712.

14. Bose, S. K.; Francis, R. C.; Govender, M.; Bush, T.; Spark, A., Lignin content versus syringyl to guaiacyl ratio amongst poplars. *Bioresour. Technol.* **2009,** *100*, 1628-1633.

15. Billa, E.; Tollier, M.-T.; Monties, B., Characterisation of the Monomeric Composition ofin situWheat Straw Lignins by Alkaline Nitrobenzene Oxidation: Effect of Temperature and Reaction Time. *J. Sci. Food Agric.* **1996,** *72*, 250-256.

16. Reeves Iii, J. B.; Galletti, G. C., Nitrobenzene oxidation vs. pyrolysis—gas chromatography/mass spectrometry as a means to determine lignin composition. *J. Anal. Appl. Pyrol.* **1993,** *25*, 195-207.

17. Saiz-Jimenez, C.; De Leeuw, J. F., Lignin Pyrolysis Products: Their Structures and Their Significance as Biomarkers. *Adv. Org. Geochem.* **1985,** *10*, 869-876.

18. del Rio, J. C.; Martinez, A. T.; Gutierrez, A., Presence of 5-hydroxyguaiacyl units as native lignin constituents in plants as seen by Py-GC/MS. *J. Anal. Appl. Pyrol.* **2007,** *79*, 33-38.

19. Mendu, V.; Harman-Ware, A. E.; Crocker, M.; Jae, J.; Stork, J.; Morton, S.; Placido, A., Identification and thermochemical analysis of high-lignin feedstocks for biofuel and biochemical production. *Biotechnol. Biofuels* **2011,** *4*.

20. van der Hage, E. R. E.; Mulder, M. M.; Boon, J. J., Structural characterization of lignin polymers by temperature-resolved in-source pyrolysis—mass spectrometry and Curie-point pyrolysis—gas chromatography/mass spectrometry. *J. Anal. Appl. Pyrol.* **1993,** *25*, 149-183.

21. Britt, P. F.; Buchanan III, A. C.; Thomas, K. B.; Lee, S.-K., Pyrolysis mechanisms of lignin: surface-immobilized model compound investigation of acid-catalyzed and free-radical reaction pathways. *J. Anal. Appl. Pyrol.* **1995,** *33*, 1-19.

22. Faix, O.; Meier, D.; Fortmann, I., Pyrolysis-gas chromatography-mass spectrometry of two trimeric lignin model compounds with alkyl-aryl ether structure. *J. Anal. Appl. Pyrol.* **1988,** *14*, 135-148.

23. Yang, H.; Yan, R.; Chen, H.; Lee, D. H.; Zheng, C., Characteristics of hemicellulose, cellulose and lignin pyrolysis. *Fuel* **2007,** *86*, 1781-1788.

24. Pandey, M. P.; Kim, C. S., Lignin Depolymerization and Conversion: A Review of Thermochemical Methods. *Chem. Eng. Technol.* **2011,** *34*, 29-41.

25. Shen, D. K.; Gu, S.; Luo, K. H.; Wang, S. R.; Fang, M. X., The Pyrolytic Degredation of Wood-derived Lignin from the Pulping Process. *Bioresour. Technol.* **2010,** *101*, 6136-6146.

26. Nakamura, T.; Kawamoto, H.; Saka, S., Pyrolysis behavior of Japanese cedar wood lignin studied with various model dimers. *J. Anal. Appl. Pyrol.* **2008,** *81*, 173-182.

27. Kawamoto, H.; Horigoshi, S.; Saka, S., Effects of side-chain hydroxyl groups on pyrolytic β-ether cleavage of phenolic lignin model dimer. *J. Wood Sci.* **2007,** *53*, 268-271.

28. Kawamoto, H.; Horigoshi, S.; Saka, S., Pyrolysis reactions of various lignin model dimers. *J. Wood Sci.* **2007,** *53*, 168-174.

29. Drage, T. C.; Vane, C. H.; Abbott, G. D., The closed system pyrolysis of β-O-4 lignin substructure model compounds. *Org. Geochem.* **2002,** *33*, 1523-1531.

30. Saiz-Jimenez, C.; de Leeuw, J. W., Pyrolysis-gas chromatography-mass spectrometry of isolated, synthetic and degraded lignins. *Org. Geochem.* **1984,** *6*, 417-422.

31. Izumi, A.; Kuroda, K.-i., Pyrolysis-mass spectrometry analysis of dehydrogenation lignin polymers with various syringyl/guaiacyl ratios. *Rapid Commun. Mass Sp.* **1997,** *11*, 1709-1715.

32. Asmadi, M.; Kawamoto, H.; Saka, S., The effects of combining guaiacol and syringol on their pyrolysis. *Holzforschung* **2012,** *66*, 323.

33. Gellerstedt, G.; Lindfors, E.-L., Structural Changes in Lignin During Kraft Pulping. *Holzforschung* **1984,** *38*, 151.

34. Bridgeman, T. G.; Darvell, L. I.; Jones, J. M.; Williams, P. T.; Fahmi, R.; Bridgwater, A. V.; Barraclough, T.; Shield, I.; Yates, N.; Thain, S.; Donnison, I. S., Influence of Particle Size on the Analytical and Chemical Properties of Two Energy Crops. *Fuel* **2007,** *86*, 60-72.

35. Eom, I.-Y.; Kim, J.-Y.; Kim, T.-S.; Lee, S.-M.; Choi, D.; Choi, I.-G.; Choi, J.-W., Effect of Essential Inorganic Metals on Primary Thermal Degradation of Lignocellulosic Biomass. *Bioresour. Technol.* **2012,** *104*, 687-694.

Chapter 4

1. Zakzeski, J.; Bruijnincx, P. C. A.; Jongerius, A. L.; Weckhuysen, B. M., The Catalytic Valorization of Lignin for the Production of Renewable Chemicals. *Chem. Rev.* **2010,** *110*, 3552-3599.

2. Mohan, D.; Pittman, C. U.; Steele, P. H., Pyrolysis of Wood/Biomass for Bio-oil: A Critical Review. *Energy Fuels* **2006,** *20*, 848-889.

3. Pandey, M. P.; Kim, C. S., Lignin Depolymerization and Conversion: A Review of Thermochemical Methods. *Chem. Eng. Technol.* **2011,** *34*, 29-41.

4. Azadi, P.; Inderwildi, O. R.; Farnood, R.; King, D. A., Liquid fuels, hydrogen and chemicals from lignin: A critical review. *Renew. Sust. Energ Rev.* **2013,** *21*, 506-523.

5. Pasangulapati, V.; Ramachandriya, K. D.; Kumar, A.; Wilkins, M. R.; Jones, C. L.; Huhnke, R. L., Effects of cellulose, hemicellulose and lignin on thermochemical conversion characteristics of the selected biomass. *Bioresour. Technol.* **2012,** *114*, 663-669.

6. Neves, D.; Thunman, H.; Matos, A.; Tarelho, L.; Gómez-Barea, A., Characterization and prediction of biomass pyrolysis products. *Prog. Energ. Combust.* **2011,** *37*, 611-630.

7. Bahng, M.-K.; Mukarakate, C.; Robichaud, D. J.; Nimlos, M. R., Current technologies for analysis of biomass thermochemical processing: A review. *Anal. Chim. Acta* **2009,** *651*, 117-138.

8. Jiang, G.; Nowakowski, D. J.; Bridgwater, A. V., Effect of the Temperature on the Composition of Lignin Pyrolysis Products. *Energy Fuels* **2010,** *24*, 4470-4475.

9. Patwardhan, P. R.; Brown, R. C.; Shanks, B. H., Understanding the Fast Pyrolysis of Lignin. *ChemSusChem* **2011,** *4*, 1629-1636.

10. Jegers, H. E.; Klein, M. T., Primary and secondary lignin pyrolysis reaction pathways. *Ind. Eng. Chem. Process Des. Dev.* **1985,** *24*, 173-183.

11. Shen, D. K.; Gu, S.; Luo, K. H.; Wang, S. R.; Fang, M. X., The Pyrolytic Degradation of Wood-derived Lignin from the Pulping Process. *Bioresour. Technol.* **2010,** *101*, 6136-6146.

12. Miao, X.; Wu, Q., High yield bio-oil production from fast pyrolysis by metabolic controlling of Chlorella protothecoides. *J. Biotechnol.* **2004,** *110*, 85-93.

13. Nunes, C. A.; Lima, C. F.; Barbosa, L. C. A.; Colodette, J. L.; Gouveia, A. F. G.; Silverio, F. O., Determination of *Eucalyptus* spp lignin S/G ratio: A comparison between methods. *Bioresour. Technol.* **2010,** *101*, 4056-4061.

14. Demirbas, A., Relationships Between Heating Value and Lignin, Moisture, Ash and Extractive Contents of Biomass Fuels. *Energ. Explor. Exploit.* **2002,** *20*, 105-111.

15. Mendu, V.; Shearin, T.; Campbell, J. E.; Stork, J.; Jae, J.; Crocker, M.; Huber, G.; DeBolt, S., Global bioenergy potential from high-lignin agricultural residue. *Proc. Natl. Acad. Sci.* **2012,** *109*, 4014-4019.

16. McDonough, T. J., The Chemistry of Organosolv Delignification. *Tappi J.* **1993,** *76*, 186-193.

17. Baptista, C.; Robert, D.; Duarte, A. P., Relationship between lignin structure and delignification degree in Pinus pinaster kraft pulps. *Bioresour. Technol.* **2008,** *99*, 2349-2356.

18. Dapía, S.; Santos, V.; Parajó, J. C., Study of formic acid as an agent for biomass fractionation. *Biomass Bioenergy* **2002,** *22*, 213-221.

19. Tu, Q.; Fu, S.; Zhan, H.; Chai, X.; Lucia, L. A., Kinetic Modeling of Formic Acid Pulping of Bagasse. *J. Agric. Food Chem.* **2008,** *56*, 3097-3101.

20. Zhang, M.; Qi, W.; Liu, R.; Su, R.; Wu, S.; He, Z., Fractionating lignocellulose by formic acid: Characterization of major components. *Biomass Bioenergy* **2010,** *34*, 525-532.

21. Erismann, N. d. M.; Freer, J.; Baeza, J.; Durán, N., Organosolv pulping-VII: Delignification selectivity of formic acid pulping of Eucalyptus grandis. *Bioresour. Technol.* **1994,** *47*, 247-256.

22. Lieff, M.; Wright, G. F.; Hibbert, H., Studies on Lignin and Related Compounds. XL. The Extraction of Birch Lignin with Formic Acid. *J. Am. Chem. Soc.* **1939,** *61*, 1477-1482.

23. Villaverde, J. J.; Li, J.; Ek, M.; Ligero, P.; de Vega, A., Native Lignin Structure of Miscanthus x giganteus and Its Changes during Acetic and Formic Acid Fractionation. *J. Agric. Food Chem.* **2009,** *57*, 6262-6270.

24. Mendu, V.; Harman-Ware, A. E.; Crocker, M.; Jae, J.; Stork, J.; Morton, S.; Placido, A., Identification and thermochemical analysis of high-lignin feedstocks for biofuel and biochemical production. *Biotechnol. Biofuels* **2011,** *4*.

25. Harman-Ware, A. E.; Crocker, M.; Kaur, A. P.; Meier, M. S.; Kato, D.; Lynn, B., Pyrolysis–GC/MS of sinapyl and coniferyl alcohol. *J. Anal. Appl. Pyrol.* **2013,** *99*, 161-169.

26. Hodgson, E. M.; Nowakowski, D. J.; Shield, I.; Riche, A.; Bridgwater, A. V.; Clifton-Brown, J. C.; Donnison, I. S., Variation in *Miscanthus* chemical composition and implications for conversion by pyrolysis and thermo-chemical bio-refining for fuels and chemicals. *Bioresour. Technol.* **2011,** *102*, 3411-3418.

27. Rencoret, J.; Ralph, J.; Marques, G.; Gutiérrez, A.; Martínez, Á. T.; del Río, J. C., Structural Characterization of Lignin Isolated from Coconut (Cocos nucifera) Coir Fibers. *J. Agric. Food Chem.* **2013,** *61*, 2434-2445.

28. Rodríguez, G.; Lama, A.; Rodríguez, R.; Jiménez, A.; Guillén, R.; Fernández-Bolaños, J., Olive stone an attractive source of bioactive and valuable compounds. *Bioresour. Technol.* **2008,** *99*, 5261-5269.

29. Siengchum, T.; Isenberg, M.; Chuang, S. S. C., Fast pyrolysis of coconut biomass – An FTIR study. *Fuel* **2013,** *105*, 559-565.

30. Tsamba, A. J.; Yang, W.; Blasiak, W., Pyrolysis characteristics and global kinetics of coconut and cashew nut shells. *Fuel Proc. Technol.* **2006,** *87*, 523-530.

31. Demirbas, A., Effect of temperature on pyrolysis products from four nut shells. *J. Anal. Appl. Pyrol.* **2006,** *76*, 285-289.

32. Sluiter, A.; Hames, B.; Ruiz, R.; Scarlata, C.; Sluiter, J.; Templeton, D.; Crocker, D., Determination of Structural Carbohydrates and Lignin in Biomass. *NREL Laboratory Analytical Procedure* **2011**.

33. International, A., ASTM Standard D1106-96: Standard Test Method for Acid-Insoluble Lignin in Wood. *ASTM International* **2007**.

34. Del Rio, J. C.; Gutierrez, A.; Martinez, A. T., Identifying acetylated lignin units in non-wood fibers using pyrolysis-gas chromatography/mass spectrometry. *Rapid Commun. Mass Sp.* **2004,** *18*, 1181-1185.

35.	Lin, Y.-C.; Cho, J.; Tompsett, G. A.; Westmoreland, P. R.; Huber, G. W., Kinetics and Mechanism of Cellulose Pyrolysis. *J. Phys. Chem. C* **2009,** *113*, 20097-20107.

36.	Friderichsen, A. V.; Shin, E.-J.; Evans, R. J.; Nimlos, M. R.; Dayton, D. C.; Ellison, G. B., The pyrolysis of anisole (C6H5OCH3) using a hyperthermal nozzle. *Fuel* **2001,** *80*, 1747-1755.

37.	Shin, E.-J.; Nimlos, M. R.; Evans, R. J., A study of the mechanisms of vanillin pyrolysis by mass spectrometry and multivariate analysis. *Fuel* **2001,** *80*, 1689-1696.

38.	Drage, T. C.; Vane, C. H.; Abbott, G. D., The closed system pyrolysis of β-O-4 lignin substructure model compounds. *Org. Geochem.* **2002,** *33*, 1523-1531.

39.	Britt, P. F.; Buchanan III, A. C.; Thomas, K. B.; Lee, S.-K., Pyrolysis mechanisms of lignin: surface-immobilized model compound investigation of acid-catalyzed and free-radical reaction pathways. *J. Anal. Appl. Pyrol.* **1995,** *33*, 1-19.

40.	Faravelli, T.; Frassoldati, A.; Migliavacca, E. R., Detailed kinetic modeling of the thermal degradation of lignins. *Biomass Bioenergy* **2010,** *34*, 290-301.

41.	Amen-Chen, C.; Pakdel, H.; Roy, C., Production of monomeric phenols by thermochemical conversion of biomass: a review. *Bioresour. Technol.* **2001,** *79*, 277-299.

42.	Wang, S.; Wang, K.; Liu, Q.; Gu, Y.; Luo, Z.; Cen, K.; Fransson, T., Comparison of the Pyrolysis Behavior of Lignins from Different Tree Species. *Biotechnol. Adv.* **2009,** *27*, 562-567.

43.	Hu, J.; Shen, D.; Xiao, R.; Wu, S.; Zhang, H., Free-Radical Analysis on Thermochemical Transformation of Lignin to Phenolic Compounds. *Energy Fuels* **2013,** *27*, 285-293.

44.	Bozell, J. J.; O'Lenick, C. J.; Warwick, S., Biomass Fractionation for the Biorefinery: Heteronuclear Multiple Quantum Coherence-Nuclear Magnetic Resonance Investigation of Lignin Isolated from Solvent Fractionation of Switchgrass. *J. Agric. Food Chem.* **2011,** *59*, 9232-9242.

45.	Bauer, S.; Sorek, H.; Mitchell, V. D.; Ibáñez, A. B.; Wemmer, D. E., Characterization of Miscanthus giganteus Lignin Isolated by Ethanol Organosolv Process under Reflux Condition. *J. Agric. Food Chem.* **2012,** *60*, 8203-8212.

46.	Varhegyi, G., Aims and methods in non-isothermal reaction kinetics. *J. Anal. Appl. Pyrol.* **2007,** *79*, 278-288.

47.	Varhegyi, G.; Bobaly, B.; Jakab, E.; Chen, H., Thermogravimetric Study of Biomass Pyrolysis Kinetics. A Distributed Activation Energy Model with Prediction Tests. *Energy Fuels* **2011,** *25*, 24-32.

48.	Haykiri-Acma, H.; Yaman, S.; Kucukbayrak, S., Comparison of the thermal reactivities of isolated lignin and holocellulose during pyrolysis. *Fuel Proc. Technol.* **2010,** *91*, 759-764.

49.	Obst, J. R., Guaiacyl and Syringyl Lignin Composition in Hardwood Cell Components. *Holzforschung* **1982,** *36*, 143-152.

50.	Lan, W.; Liu, C.-F.; Sun, R.-C., Fractionation of Bagasse into Cellulose, Hemicelluloses, and Lignin with Ionic Liquid Treatment followed by Alkaline Extraction. *J. Agric. Food Chem.* **2011,** *59*, 8691-8701.

51.	Del Rio, J. C.; Rencoret, J.; Prinsen, P.; Martinez, A. T.; Ralph, J.; Gutierrez, A., Structural Characterization of Wheat Straw Lignin as Revealed by Analytical Pyrolysis, 2D-NMR, and Reductive Cleavage Methods. *J. Agric. Food Chem.* **2012,** *60*, 5922-5935.

52.	Yuan, T.-Q.; Sun, S.-N.; Xu, F.; Sun, R.-c., Characterization of Lignin Structures and Lignin-Carbohydrate Complex (LCC) Linkages by Quantitative ^{13}C and 2D HSQC NMR Spectroscopy. *J. Agric. Food Chem.* **2011,** *59*, 10604-10614.

53.	Pu, Y.; Chen, F.; Ziebell, A.; Davison, B.; Ragauskas, A., NMR Characterization of C3H and HCT Down-Regulated Alfalfa Lignin. *BioEnerg. Res.* **2009,** *2*, 198-208.

54.	Ralph, J.; Larry, L. L., NMR of Lignins. In *Lignin and Lignans*, CRC Press: 2010; 137-243.

Chapter 5

1.   Huber, G. W.; Iborra, S.; Corma, A., Synthesis of Transportation Fuels from Biomass: Chemistry, Catalysts, and Engineering. *Chem. Rev.* **2006**, 4044-4098.
2.   Harris, D.; DeBolt, S., Sythesis, Regulation and Utilization of Lignocellulosic Biomass. *Plant Biotechnol. J.* **2010,** *8*, 244-262.
3.   Dien, B. S.; Miller, D. J.; Hector, R. E.; Dixon, R. A.; Chen, F.; McCaslin, M.; Reisen, P.; Sarath, G.; Cotta, M. A., Enhancing Alfalfa Conversion Efficiencies for Sugar Recover and Ethanol Production by Altering Lignin Composition. *Bioresour. Technol.* **2011,** *102*, 6479-6486.
4.   Simmons, B. A.; Loque, D.; Ralph, J., Advances in Modifying Lignin for Enhanced Biofuel Production. *Curr. Opin. Biotechnol.* **2010,** *13*, 313-320.
5.   Boateng, A. A.; Hicks, K. B.; Vogel, K. P., Pyrolysis of Switchgrass (*Panicum virgatum*) Harvested at Several Stages of Maturity. *J. Anal. Appl. Pyrol.* **2006,** *75*, 55-64.
6.   Boateng, A. A.; Anderson, W. F.; Phillips, J. G., Bermudagrass for Biofuels: Effect of Two Genotypes on Pyrolysis Product Yield. *Energy Fuels* **2007,** *21*, 1183-1187.
7.   Mann, D., G.J.; Labbe, N.; Sykes, R. W.; Cracom, K.; Kline, L.; Swamidoss, I. M.; Burris, J. N.; Davis, M.; Stewart Jr., C. N., Rapid Assessmet of Lignin Content and Structure in Switchgrass (*Panicum virgatum* L.) Grown Under Different Environmental Conditions. *BioEnerg. Res.* **2009,** *2*, 246-256.
8.   Hodgson, E. M.; Nowakowski, D. J.; Shield, I.; Riche, A.; Bridgwater, A. V.; Clifton-Brown, J. C.; Donnison, I. S., Variation in *Miscanthus* chemical composition and implications for conversion by pyrolysis and thermo-chemical bio-refining for fuels and chemicals. *Bioresour. Technol.* **2011,** *102*, 3411-3418.
9.   Harris, D.; Stork, J.; DeBolt, S., Genetic modification in cellulose-synthase reduces crystallinity and improves biochemical conversion to fermentable sugar. *GCB Bioenergy* **2009,** *1*, 51-61.
10.   Zhang, Y.; Culhaoglu, T.; Pollet, B.; Melin, C.; Denoue, D.; Barrière, Y.; Baumberger, S.; Méchin, V., Impact of Lignin Structure and Cell Wall Reticulation on Maize Cell Wall Degradability. *J. Agric. Food Chem.* **2011,** *59*, 10129-10135.
11.   Fahmi, R.; Bridgwater, A. V.; Donnison, I.; Yates, N.; Jones, J. M., The Effect of Lignin and Inorganic Species in Biomass on Pyrolysis Oil Yields, Quality and Stability. *Fuel* **2007,** *87*, 1230-1240.
12.   Demirbas, A., Relationships Between Heating Value and Lignin, Moisture, Ash and Extractive Contents of Biomass Fuels. *Energ. Explor. Exploit.* **2002,** *20*, 105-111.
13.   Bout, S.; Vermerris, W., A candidate-gene approach to clone the sorghum Brown midrib gene encoding caffeic acid O-methyltransferase. *Mol. Genet. Genomics* **2003,** *269*, 205-214.
14.   Saballos, A.; Vermerris, W.; Rivera, L.; Ejeta, G., Allelic Association, Chemical Characterization and Saccharification Properties of brown midrib Mutants of Sorghum (Sorghum bicolor (L.) Moench). *BioEnerg. Res.* **2008,** *1*, 193-204.
15.   Sattler, S. E.; Saathoff, A. J.; Haas, E. J.; Palmer, N. A.; Funnell-Harris, D. L.; Sarath, G.; Pedersen, J. F., A Nonsense Mutation in a Cinnamyl Alcohol Dehydrogenase Gene is Responsible for the Sorghum *brown midrib6* Phenotype. *Plant Physiol.* **2009,** *150*, 584-595.

16.   Mohan, D.; Pittman, C. U.; Steele, P. H., Pyrolysis of Wood/Biomass for Bio-oil: A Critical Review. *Energy Fuels* **2006,** *20*, 848-889.

17.   del Rio, J. C.; Martinez, A. T.; Gutierrez, A., Presence of 5-hydroxyguaiacyl units as native lignin constituents in plants as seen by Py-GC/MS. *J. Anal. Appl. Pyrol.* **2007,** *79*, 33-38.

18.   Del Rio, J. C.; Gutierrez, A.; Martinez, A. T., Identifying acetylated lignin units in non-wood fibers using pyrolysis-gas chromatography/mass spectrometry. *Rapid Commun. Mass Sp.* **2004,** *18*, 1181-1185.

19.   Del Rio, J. C.; Rencoret, J.; Prinsen, P.; Martinez, A. T.; Ralph, J.; Gutierrez, A., Structural Characterization of Wheat Straw Lignin as Revealed by Analytical Pyrolysis, 2D-NMR, and Reductive Cleavage Methods. *J. Agric. Food Chem.* **2012,** *60*, 5922-5935.

20.   Shen, D. K.; Gu, S.; Luo, K. H.; Wang, S. R.; Fang, M. X., The Pyrolytic Degredation of Wood-derived Lignin from the Pulping Process. *Bioresour. Technol.* **2010,** *101*, 6136-6146.

21.   Bridgeman, T. G.; Darvell, L. I.; Jones, J. M.; Williams, P. T.; Fahmi, R.; Bridgwater, A. V.; Barraclough, T.; Shield, I.; Yates, N.; Thain, S.; Donnison, I. S., Influence of Particle Size on the Analytical and Chemical Properties of Two Energy Crops. *Fuel* **2007,** *86*, 60-72.

22.   Fahmi, R.; Bridgwater, A. V.; Darvell, L. I.; Jones, J. M.; Yates, N.; Thain, S.; Donnison, I. S., The Effect of Alkali Metals on Combustion and Pyrolysis of Lolium and *Festuca* grasses, Switchgrass and Willow. *Fuel* **2007,** *86*, 1560-1569.

23.   Patwardhan, P. R.; Brown, R. C.; Shanks, B. L., Understanding the Fast Pyrolysis of Lignin. *ChemSusChem* **2011,** *4*, 1629-1636.

24.   Patwardhan, P. R.; Dalluge, D. L.; Shanks, B. L.; Brown, R. C., Distinguishing Primary and Secondary Reactions of Cellulose Pyrolysis. *Bioresour. Technol.* **2011,** *102*, 5265-5269.

25.   Patwardhan, P. R.; Satrio, J. A.; Brown, R. C.; Shanks, B. L., Product Distribution from Fast Pyrolysis of Glucose-based Carbohydrates. *J. Anal. Appl. Pyrol.* **2009,** *86*, 323-330.

26.   Nunes, C. A.; Lima, C. F.; Barbosa, L. C. A.; Colodette, J. L.; Gouveia, A. F. G.; Silverio, F. O., Determination of *Eucalyptus* spp lignin S/G ratio: A comparison between methods. *Bioresour. Technol.* **2010,** *101*, 4056-4061.

27.   Eom, I.-Y.; Kim, J.-Y.; Kim, T.-S.; Lee, S.-M.; Choi, D.; Choi, I.-G.; Choi, J.-W., Effect of Essential Inorganic Metals on Primary Thermal Degradation of Lignocellulosic Biomass. *Bioresour. Technol.* **2012,** *104*, 687-694.

28.   Jiang, G.; Nowakowski, D. J.; Bridgwater, A. V., Effect of the Temperature on the Composition of Lignin Pyrolysis Products. *Energy Fuels* **2010,** *24*, 4470-4475.

29.   Mendu, V.; Harman-Ware, A. E.; Crocker, M.; Jae, J.; Stork, J.; Morton, S.; Placido, A., Identification and thermochemical analysis of high-lignin feedstocks for biofuel and biochemical production. *Biotechnol. Biofuels* **2011,** *4*.

30.   Varhegyi, G.; Bobaly, B.; Jakab, E.; Chen, H., Thermogravimetric Study of Biomass Pyrolysis Kinetics. A Distributed Activation Energy Model with Prediction Tests. *Energy Fuels* **2011,** *25*, 24-32.

31.   Wang, S.; Wang, K.; Liu, Q.; Gu, Y.; Luo, Z.; Cen, K.; Fransson, T., Comparison of the Pyrolysis Behavior of Lignins from Different Tree Species. *Biotechnol. Adv.* **2009,** *27*, 562-567.

32.   Lin, Y.-C.; Cho, J.; Tompsett, G. A.; Westmoreland, P. R.; Huber, G. W., Kinetics and Mechanism of Cellulose Pyrolysis. *J. Phys. Chem. C* **2009,** *113*, 20097-20107.

33.   Mendu, V.; Shearin, T.; Campbell, J. E.; Stork, J.; Jae, J.; Crocker, M.; Huber, G.; DeBolt, S., Global bioenergy potential from high-lignin agricultural residue. *Proc. Natl. Acad. Sci.* **2012,** *109*, 4014-4019.

34. Petti, C.; Harman-Ware, A. E.; Tateno, M.; Kushwaha, R.; Shearer, A.; Downie, A. B.; Crocker, M.; DeBolt, S., Sorghum mutant RG displays antithetic leaf shoot lignin accumulation resulting in improved stem saccharification properties *Biotechnol. Biofuels* **2013,** *6*.

35. Sluiter, A.; Hames, B.; Ruiz, R.; Scarlata, C.; Sluiter, J.; Templeton, D.; Crocker, D., Determination of Structural Carbohydrates and Lignin in Biomass. *NREL Laboratory Analytical Procedure* **2011**.

Chapter 6.

1. Harman-Ware, A. E.; Morgan, T.; Wilson, M.; Crocker, M.; Zhang, J.; Liu, K.; Stork, J.; DeBolt, S., Microalgae as a renewable fuel source: Fast pyrolysis of *Scenedesmus* sp. *Renew. Energ.* **2013,** *60*, 625-632.

2. Mata, T. M.; Martins, A. A.; Caetano, N. S., Microalgae for biodiesel production and other applications: A review. *Renew. Sust. Energ Rev.* **2010,** *14*, 217-232.

3. Zhang, H. L.; Baeyens, J.; Tan, T. W., Mixing phenomena in a large-scale fermenter of starch to bio-ethanol. *Energy* **2012,** *48*, 380-391.

4. Zhang, H. L.; Baeyens, J.; Tan, T. W., The bubble-induced mixing in starch-to-ethanol fermenters. *Chem. Eng. Res. Des.* **2012,** *90*, 2122-2128.

5. Tran, N. H.; Bartlett, J. R.; Kannangara, G. S. K.; Milev, A. S.; Volk, H.; Wilson, M. A., Catalytic upgrading of biorefinery oil from micro-algae. *Fuel* **2010,** *89*, 265-274.

6. Biller, P.; Riley, R.; Ross, A. B., Catalytic hydrothermal processing of microalgae: Decomposition and upgrading of lipids. *Bioresour. Technol.* **2011,** *102*, 4841-4848.

7. Wang, B.; Li, Y.; Wu, N.; Lan, C., CO_2 bio-mitigation using microalga. *Appl. Microbiol. Biotechnol.* **2008,** *79*, 707-718.

8. Brennan, L.; Owende, P., Biofuels from microalgae—A review of technologies for production, processing, and extractions of biofuels and co-products. *Renew. Sust. Energ Rev.* **2010,** *14*, 557-577.

9. Williams, P. J. B.; Laurens, L. M. L., Microalgae as biodiesel & biomass feedstocks: Review & analysis of the biochemistry, energetics & economics. *Energy Environ. Sci.* **2010,** *3*, 554-590.

10. Mohan, D.; Pittman, C. U.; Steele, P. H., Pyrolysis of Wood/Biomass for Bio-oil: A Critical Review. *Energy Fuels* **2006,** *20*, 848-889.

11. Van de Velden, M.; Baeyens, J.; Brems, A.; Janssens, B.; Dewil, R., Experimentals, kinetics and endothermicity of the biomass pyrolysis reaction. *Renew. Energ.* **2010,** *35*, 232-242.

12. Van de Velden, M.; Baeyens, J.; Boukis, I., Modeling CFB biomass pyrolysis reactors. *Biomass Bioenergy* **2008,** *32*, 128-139.

13. Lehmann, J.; Gaunt, J.; Rondon, M., Bio-char Sequestration in Terrestrial Ecosystems – A Review. *Mitig. Adapt. Strat. Gl.* **2006,** *11*, 395-419.

14. *Biochar for Environmental Management*. earthscan: Sterling, VA, 2009.

15. Thies, J. E.; Rillig, M. C., Characteristics of Biochar: Biological Properties. In *Biochar for Environmental Management*, Lehmann, J.; Joseph, S., Eds. Earthscan: Virginia, 2009.

16. Peng, W.; Wu, Q.; Tu, P., Effects of temperature and holding time on production of renewable fuels from pyrolysis of Chlorella protothecoides. *J. Appl. Phycol.* **2000,** *12*, 147-152.

17. Wu, Q.; Zhang, B.; Grant, N., High yield of hydrocarbon gases resulting from pyrolysis of yellow heterotrophic and bacterially degradedChlorella protothecoides. *J. Appl. Phycol.* **1996,** *8*, 181-184.

18. Miao, X.; Wu, Q., High yield bio-oil production from fast pyrolysis by metabolic controlling of Chlorella protothecoides. *J. Biotechnol.* **2004,** *110*, 85-93.

19.   Miao, X.; Wu, Q.; Yang, C., Fast pyrolysis of microalgae to produce renewable fuels. *J. Anal. Appl. Pyrol.* **2004,** *71*, 855-863.

20.   Campanella, A.; Muncrief, R.; Harold, M. P.; Griffith, D. C.; Whitton, N. M.; Weber, R. S., Thermolysis of microalgae and duckweed in a CO2-swept fixed-bed reactor: Bio-oil yield and compositional effects. *Bioresour. Technol.* **2012,** *109*, 154-162.

21.   Babich, I. V.; van der Hulst, M.; Lefferts, L.; Moulijn, J. A.; O'Connor, P.; Seshan, K., Catalytic pyrolysis of microalgae to high-quality liquid bio-fuels. *Biomass Bioenergy* **2011,** *35*, 3199-3207.

22.   Du, Z.; Li, Y.; Wang, X.; Wan, Y.; Chen, Q.; Wang, C.; Lin, X.; Liu, Y.; Chen, P.; Ruan, R., Microwave-assisted pyrolysis of microalgae for biofuel production. *Bioresour. Technol.* **2011,** *102*, 4890-6.

23.   Pan, P.; Hu, C.; Yang, W.; Li, Y.; Dong, L.; Zhu, L.; Tong, D.; Qing, R.; Fan, Y., The direct pyrolysis and catalytic pyrolysis of Nannochloropsis sp. residue for renewable bio-oils. *Bioresour. Technol.* **2010,** *101*, 4593-4599.

24.   Ware, L.; Morgan, T.; Wilson, M.; Mohapatra, S.; Crocker, M.; Zhang, J.; Liu, K.; Stork, J.; DeBolt, S., Fast Pyrolysis of Scenedesmus algae. In *Abstr. Pap. Am. Chem. S.*, 2011; Vol. 242, p 152.

25.   Bradford, M. M., A rapid and sensitive method for the quantitation of microgram quantities of protein utilizing the principle of protein-dye binding. *Anal. Biochem.* **1976,** *72*, 248-254.

26.   Updegraff, D. M., Semimicro determination of cellulose inbiological materials. *Anal. Biochem.* **1969,** *32*, 420-424.

27.   Bligh, E. G.; Dyer, W. J., A rapid method for total lipid extraction and purification. *Can. J. Biochem. Physiol.* **1959,** *37*, 911-917.

28.   Badaut, D.; Risacher, F., Authigenic smectite on diatom frustules in Bolivian saline lakes. *Geochim. Cosmochim. Acta* **1983,** *47*, 363-375.

29.   Smith, W. T.; Harris, T. B.; Patterson, J. M., Pyrolysis of Soybean Protein and an Amino Acid Mixture Having the Same Amino Acid Composition. *J. Agric. Food Chem.* **1974,** *22*, 480-483.

30.   Tsuge, S.; Matsubara, H., High Resolution Pyrolysis-Gas Chromatography of Proteins and Related Materials. *J. Anal. Appl. Pyrol.* **1985,** *8*, 49-64.

31.   Boon, J. J., Amino Acid Sequence Information in Proteins and Complex Proteinaceous Material Revealed by Pyrolysis-Capillary Gas Chromatograph-Low and High Resolution Mass Spectrometry. *J. Anal. Appl. Pyrol.* **1987,** *11*, 313-327.

32.   Shulman, G. P.; Simmonds, P. G., Thermal decomposition of aromatic and heteroaromatic amino-acids. *Chem. Comm. (London)* **1968**, 1040-1042.

33.   Chiavari, G.; Galletti, G. C., Pyrolysis—gas chromatography/mass spectrometry of amino acids. *J. Anal. Appl. Pyrol.* **1992,** *24*, 123-137.

34.   Ratcliff, M. A.; Medley, E. E.; Simmonds, P. G., Pyrolysis of amino acids. Mechanistic considerations. *J. Org. Chem.* **1974,** *39*, 1481-1490.

35.   Brown, T. M.; Duan, P.; Savage, P. E., Hydrothermal Liquefaction and Gasification of Nannochloropsis sp. *Energy Fuels* **2010,** *24*, 3639-3646.

36.   Alencar, J. W.; Alves, P. B.; Craveiro, A. A., Pyrolysis of tropical vegetable oils. *J. Agric. Food Chem.* **1983,** *31*, 1268-1270.

37.   Chang, C.-C.; Wan, S.-W., China's Motor Fuels from Tung Oil. *Ind. Eng. Chem.* **1947,** *39*, 1543-1548.

38.   Kitamura, K., Studies of the pyrolysis of triglycerides. *Bull. Chem. Soc. Jpn.* **1971,** *44*, 1606-1609.

39.   Nawar, W. W., Thermal degradation of lipids. *J. Agric. Food Chem.* **1969,** *17*, 18-21.

40.   Nichols, P.; Holman, R., Pyrolysis of saturated triglycerides. *Lipids* **1972,** *7*, 773-779.

41.   Schwab, A. W.; Dykstra, G. J.; Selke, E.; Sorenson, S. C.; Pryde, E. H., Diesel fuel from thermal decomposition of soybean oil. *J. Am. Oil Chem. Soc.* **1988,** *65*, 1781-1786.

42.   Idem, R. O.; Katikaneni, S. P. R.; Bakhshi, N. N., Thermal Cracking of Canola Oil: Reaction Products in the Presence and Absence of Steam. *Energy Fuels* **1996,** *10*, 1150-1162.

Anne Elizabeth Ware

Personal Information
Place of birth: Bluefield, WV U.S.A.

Education
Concord University
Athens, WV U.S.A.
Bachelor of Science Degree in Chemistry (2009)

University of Kentucky
Center for Applied Energy Research/Department of Chemistry
Lexington, KY U.S.A.
Doctoral studies (2009-2013)
Advisor: Dr. Mark Crocker, Co-advisor: Dr. John Selegue

Awards and Scholarships
Max Steckler Fellowship 2009-2013

University of Kentucky Teaching Assistantship 2009

University of Kentucky Center for Applied Energy Research
Research Assistantship 2010-2013

University of Kentucky
Chemistry Department Outstanding Graduate Student Research Award 2012

Publications

Carloalberto Petti, Anne E. Harman-Ware, Mizuki Tateno, Rekha Kushwaha, Andrew Shearer, A. Bruce Downie, Mark Crocker, Seth DeBolt. Sorghum mutant RG displays antithetic leaf shoot lignin accumulation resulting in improved stem saccharification. properties Biotechnology for Biofuels 6:146, 2013.

Anne E. Harman-Ware, Tonya Morgan, Michael Wilson, Mark Crocker, Jun Zhang, Kunlei Liu, Jozsef Stork, Seth DeBolt. Microalgae as a renewable fuel source: Fast pyrolysis of *Scenedesmus* sp. Renewable Energy 60, 625-632, 2013.

Anne E. Harman-Ware, Mark Crocker, Aman Preet Kaur, Mark S. Meier, Dawn Kato, Bert Lynn. Pyrolysis-GC/MS of Sinapyl and Coniferyl Alcohol. Journal of Analytical and Applied Pyrolysis 99, 161-169, 2012.

Tonya Morgan, Eduardo Santillan-Jimenez, Anne E. Harman-Ware, Yaying Ji, Daniel Grubb, Mark Crocker. Catalytic Deoxygenation of Triglycerides to Hydrocarbons Over Supported Nickel Catalysts. Chemical Engineering Journal 189-190, 346-355, 2012.

Venugopal Mendu, Anne E. Harman-Ware, Mark Crocker, Jungho Jae, Jozsef Stork, Samuel Morton, Andrew Placido, George Huber and Seth DeBolt. Identification and thermochemical analysis of high lignin feedstocks for biofuel and bio-chemical production. Biotechnology for Biofuels 4:43, 2011.

Conference Proceedings
Renewable Energy and Energy Efficiency Workshop Louisville, KY 2013
Poster Session "Pyrolysis-GC/MS Characterization of Bioenergy Crops" -1st place prize

ACS Fall Conference Philadelphia, PA 2012
Presentation: Hydrocarbons from Biomass Division: "Pyrolysis-GC/MS Characterization of Biomass"

NSF EFRI Awardees Conference Washington, D.C. 2012
Poster Session: "Hydrocarbons from Biomass: Lignin Deconstruction for the Production of Liquid Fuels"

University of Kentucky Naff Symposium Lexington, KY 2012
Poster Session: "Pyrolysis-GC/MS Characterization of Biomass" -2nd place prize

ACS Fall Conference Denver, CO 2011
Poster Session: Fuel Division: "Fast Pyrolysis of Scenedesmus Algae"